Canada

Fisheries and Oceans
Pêches et Océans

Canadian Journal of Fisheries and Aquatic Sciences

Journal canadien des sciences halieutiques et aquatiques

Fisheries and Oceans | Pêches et Océans

Information and Publications Branch | Direction de l'information et des publications

Ottawa K1A 0E6

The *Canadian Journal of Fisheries and Aquatic Sciences* has been published continuously since 1901, previously as *Contributions to Canadian Biology* 1901–25, *Contributions to Canadian Biology and Fisheries* 1926–34, *Journal of the Biological Board of Canada* 1934–37, and *Journal of the Fisheries Research Board of Canada* 1938–79.

Editorial policy

The *Journal* publishes original research articles and notes, critical reviews, Perspectives (essays of opinion or hypothesis), comments, and book reviews. Papers may concern cells, organisms, populations, ecosystems, or processes that affect aquatic production systems, and they should lead to identifiable conclusions or synthesis, which variously may amplify, modify, question, or redirect accumulated knowledge embodied in contemporary perceptions of a particular state of fisheries and aquatic sciences. They should demonstrate clearly a contribution to knowledge beyond the confirmatory state. Originality should relate to more than the particular (a certain year, place, taxon, or chemical compound) such that existing understanding is reformulated or extended.

It would assist the Editors if prospective authors identified briefly by covering letter (a) aspects of their papers that meet the foregoing objectives, (b) potential referees, and (c) other manuscripts contemplated or in press containing the same or similar information.

Submissions in English or French are acceptable. The information must be original, that is, not copyrighted, published, or submitted elsewhere except in abstract form or unless by written consent of the Editor. The *Journal* accepts no responsibility for statements made by contributors. The use of proprietary names does not imply endorsement of the product or company.

A charge is made for manuscripts published. When submitting a manuscript, an author must state that the charge will be accepted.

Guides

Guides for authors and typists appear in the first issue of each volume and are available free from the *Journal*.

Subscriptions

The *Journal* is issued monthly to form annual volumes of twelve numbers and Supplements. Orders and inquiries regarding subscriptions must be sent directly to Supply and Services Canada, Ottawa, Ontario, Canada K1A 0S9. Prepayment is required in Canadian funds to the order of "The Receiver General for Canada."

Microfilm

Issues from 1934 through the current volume can be purchased on 16- or 35-mm microfilm. Photocopies of individual articles or issues can be purchased from Xerox University Microfilms, 300 North Zeeb Road, Ann Arbor, Michigan 48106, USA.

Design: Ludvic Saleh & Associates, Ottawa

Conception graphique: Ludvic Saleh & Associates, Ottawa

Publié sans interruption depuis 1901, le *Journal canadien des sciences halieutiques et aquatiques* a paru sous plusieurs titres : *Contributions to Canadian Biology* 1901–25, *Contributions to Canadian Biology and Fisheries* 1926–34, *Journal of the Biological Board of Canada* 1934–37 et *Journal de l'office des recherches sur les pêcheries du Canada* 1938–79.

Politique de rédaction

Le *Journal* publie des articles et des notes fondés sur une recherche originale, des critiques, des essais portant sur une opinion ou une hypothèse (Perspectives), des commentaires et des comptes rendus de livres. Les textes peuvent avoir trait aux cellules, aux organismes, aux populations, aux écosystèmes ou aux processus qui influencent les systèmes de production aquatique. Ils doivent aboutir à des conclusions ou synthèses précises qui, de diverses façons, peuvent accroître, modifier, remettre en question ou réorienter le bagage actuel des connaissances et perceptions dans une discipline donnée des sciences aquatiques. Ils doivent clairement démontrer qu'ils contribuent aux connaissances en faisant plus que corroborer des faits. L'originalité doit dépasser le caractère particulier (une année, un endroit, un taxon ou un composé chimique donné) et tenir à une épuration ou à une reformulation des connaissances actuelles.

Les auteurs éventuels aideraient les rédacteurs s'ils identifiaient brièvement, dans une lettre d'accompagnement (a) les aspects de leurs textes qui répondent particulièrement aux objectifs indiqués ci-dessus, (b) des arbitres possibles et (c) d'autres manuscrits envisagés ou sous presse, dont la teneur est identique ou se rapproche de celui qui est soumis.

Les contributions peuvent être en anglais ou en français. Elles doivent être originales, c.-à-d. qu'elles ne doivent pas avoir fait l'objet d'un copyright, avoir été publiées ou soumises ailleurs, sauf sous forme abrégée ou avec le consentement du rédacteur. Le *Journal* décline toute responsabilité quant aux énoncés des contributeurs. L'utilisation des noms de marques de commerce ne signifie aucunement une sanction du produit en question ou de la compagnie qui le fabrique.

Les manuscrits acceptés sont sujets à des frais de publication. Quant un auteur présente un texte, il doit préciser que ces frais seront acceptés. On trouvera dans une récente livraison du *Journal* les taux par page en vigueur.

Guides

Le guide des auteurs et celui des secrétaires d'auteurs paraissent dans la première livraison de chaque volume et sont disponibles gratuitement du *Journal*.

Abonnement

Le *Journal* paraît tous les mois, formant ainsi un volume de douze numéros et Supplements par année. On est prié d'adresser directement commandes et demande de renseignements relatifs à l'abonnement à Approvisionnements et Services Canada, Ottawa (Ontario), Canada K1A 0S9. Les paiements doivent être faits à l'avance en devises canadiennes, à l'ordre du « Receveur général du Canada ».

Microfilms

On peut acheter sur microfilms de 16 ou 35 mm tous les numéros publiés depuis 1934. Des photocopies d'articles ou de numéros individuels sont aussi en vente auprès de Xerox University Microfilms, 300 North Zeeb Road, Ann Arbor, Michigan 48106, É.-U.

Canadian Journal of Fisheries and Aquatic Sciences

Journal canadien des sciences halieutiques et aquatiques

Volume 43, No. 9, September 1986 | **Volume 43, n° 9, septembre 1986**

Information and Publications Branch / Direction de l'information et des publications

J. Watson, Ph.D.	*Director and Editor-in-Chief / Directeur et rédacteur en chef*
Johanna M. Reinhart, M.Sc.	*Deputy Director and Editor / Sous-directrice et rédactrice*
D. G. Cook, Ph.D. / Lorraine C. Smith, Ph.D.	*Assistant Editors / Rédacteurs adjoints*
J. Camp / G. J. Neville / P. M. Burke / M. L. Gilbert	*Editorial and Publishing Services / Services de rédaction et d'edition*

Editorial Board / Conseil de rédaction

L. Legendre	*Université Laval*	(1983–1986)
M. Sinclair	*Department of Fisheries and Oceans, Halifax*	(1983–1986)
C. J. Walters	*University of British Columbia*	(1983–1986)
C. M. Wood	*McMaster University*	(1983–1986)
P. J. Dillon	*Ontario Ministry of the Environment*	(1984–1987)
M. C. Healey	*Department of Fisheries and Oceans, Nanaimo*	(1984–1987)
J. J. Magnuson	*University of Wisconsin*	(1984–1987)
J. Sprague	*University of Guelph*	(1984–1987)
L. M. Dickie	*Department of Fisheries and Oceans, Dartmouth*	(1985–1988)
J. J. Dodson	*Université Laval*	(1985–1988)
S. J. Smith	*Department of Fisheries and Oceans, Dartmouth*	(1985–1988)
A. P. Zimmerman	*University of Toronto*	(1985–1988)

Editorial Office:
Department of Fisheries and Oceans
Communications Directorate
Information and Publications Branch
Centennial Towers
200 Kent Street
Ottawa, Canada K1A 0E6

Bureau de rédaction :
Ministère des Pêches et des Océans
Direction générale des communications
Direction de l'information et des publications
Les Tours Centennial
200, rue Kent
Ottawa, Canada K1A 0E6

The *Journal* is abstracted or indexed in: / Le *Journal* est résumé ou signalé dans :

Aquatic Sciences and Fisheries Abstracts, Biological Abstracts, Chemical Abstracts, Current Awareness in Biological Sciences, Current Contents, FAO Freshwater and Aquaculture Contents Tables, FAO Marine Science Contents Tables, and Science Citation Index

A General Multivariate Dose–Response Model

J. Schnute and J. O. T. Jensen

Department of Fisheries and Oceans, Pacific Biological Station, Nanaimo, B.C. V9R 5K6

Schnute, J., and J. O. T. Jensen. 1986. A general multivariate dose–response model. Can. J. Fish. Aquat. Sci. 43: 1684–1693.

This paper presents a general model for describing and predicting biological response to environmental factors. The theory embraces concepts and models used in earlier studies of the effects of toxicity on fish, and it extends these ideas in several directions. It can include an arbitrary number of factors, either detrimental or beneficial to the organism. Also, its statistical formulation allows (1) hypothesis testing to determine the relative importance of various factors and (2) calculation of critical factor levels that (with prescribed confidence) assure a community response no worse than a specified level. Our model is based on earlier work by Schnute and McKinnell, and, like theirs, its parameters have biologically meaningful interpretations. Our discussion includes an explanation of how the model relates specifically to toxicity studies. In a companion paper (Can. J. Fish. Aquat. Sci. 43: 1694–1709), we use our model to investigate salmonid response to gas supersaturation and ancillary factors.

Les auteurs présentent un modèle général de description et de prévision de la réponse biologique à des facteurs environnementaux. La théorie englobe des concepts et des modèles utilisés au cours d'études antérieures portant sur les effets de la toxicité chez le poisson et les développent dans plusieurs directions. Le modèle peut comprendre un nombre arbitraire de facteurs à effets nocifs ou utiles pour l'organisme. Sa formulation statistique permet aussi 1) d'effectuer un test d'hypothèse visant à déterminer l'importance relative de divers facteurs et 2) de calculer des niveaux critiques (à un niveau de confiance établi) garantissant que la réponse d'une communauté ne sera pas inférieure à un niveau déjà précisé. Le modèle repose sur des travaux antérieurement effectués par Schnute et McKinnell et, comme pour ces travaux, ses paramètres autorisent des interprétations biologiquement significatives. Les auteurs traitent de la façon dont le modèle peut être spécifiquement appliqué à des études de toxicité. Ils traitent aussi dans une publication connexe (Can. J. Fish. Aquat. Sci. 43: 1694–1709) de l'application du modèle à la réponse de salmonidés à une sursaturation gazeuse et à d'autres facteurs connexes.

Received November 8, 1985
Accepted May 6, 1986
(J8560)

Reçu le 8 novembre 1985
Accepté le 6 mai 1986

A biologist concerned with pollution invariably faces the problem of describing community response to toxicant levels. For example, a common measure of response is the exposure time to 50% mortality (ET50). Typical questions to be resolved include the following: (1) What toxic level causes the response to drop below a prescribed threshhold? (2) What is the combined effect of several toxicants? (3) Are toxic effects altered by changes in environmental variables, such as temperature? (4) Does toxicity depend on characteristics of the organism, such as animal size?

The resolution of such problems requires a model relating the response y to various factors $x_1, x_2, \ldots$. These factors may represent toxicant levels, environmental variables, organism characteristics, and so on. For example, if y represents ET50 and x measures a lethal toxicant concentration, then y is a decreasing function of x; that is, the greater the toxic level x, the shorter the time y required for half the population to die. Three equations used historically to describe this relationship are

$$(1.1) \quad \log y = a - b \log x,$$

implicit in Sprague (1969) and Knittel et al. (1980),

$$(1.2) \quad y = -c \log (a - bx^{-1}),$$

proposed by Zitko (1979, 1982), and

$$(1.3) \quad (y - a)(x - b)^c = d,$$

suggested in a diverse literature, including Wuhrmann and Woker (1950), Wuhrmann (1952), and Warren and Doudoroff (1971). In (1.1)–(1.3), a, b, c, and d represent constants, not necessarily comparable among the equations. These equations exhibit certain similarities; for example, (1.3) includes a log–log relationship like (1.1) as a special case.

The main feature of models (1.1)–(1.3) is that they describe a monotonic (increasing or decreasing) relationship between x and y. Notice that, depending on the signs of the constants, equations (1.1)–(1.3) allow for a factor that either favors or inhibits the response; that is, increasing x must cause y either to decrease or to increase steadily. This paper presents a model that preserves this general idea, but extends it in several directions. First, our model can include an arbitrary number of factors. Second, the possible relationships between any one factor x and y can be enumerated precisely. For example, a factor may favor y up to a certain level at which the beneficial gain stops; or it may cause y to decrease, but not below a minimum value. A full set of 16 possibilities is presented later. Third, the model parameters allow for a quick judgement as to the relative importance of the factors. Fourth, the model is rendered statistical, so that hypothesis tests can be used to assess the importance of factors and to add or remove them in a manner analogous to stepwise regression. Finally, all necessary equations for confidence levels are derived so that, for example, one can answer the following question: At what level of factor x is it 95% certain that the response y will be greater than some prescribed response y_0?

The model proposed here is based on earlier work by Schnute and McKinnell (1984). They were concerned with an optimal (minimum or maximum) response for some set of factor levels, whereas the model here is simpler, since it is monotone in the factors. All that is required for the simplification is to drop the quadratic terms in transformed values of the factors. The purpose of this paper is to explain the significance of the model in the context of dose−response relationships, to improve Schnute and McKinnell's (1984) analysis of the various cases of the model, and to derive the confidence level formulas required for finding toxicity tolerance limits.

In a companion paper (Jensen et al. 1986), we apply our model to literature data on salmonid response to gas supersaturation and associated ancillary factors. We also describe techniques of exploratory data analysis for making a preliminary assessment of the model's suitability.

The Model

To state the model precisely, let y be the response to the m factors $x_1, \ldots, x_m$. Let u_i and U_i be typical low and high values, respectively, for the factors x_i $(i = 1, \ldots, m)$; similarly, let v and V be typical low and high values of the response y. Then the model considered here is defined by the following three equations:

$$\text{(2.1)} \qquad \eta = p + \sum_{i=1}^{m} q_i \xi_i$$

$$\text{(2.2*)} \qquad \xi_i = (2x_i^{\alpha_i} - U_i^{\alpha_i} - u_i^{\alpha_i})/(U_i^{\alpha_i} - u_i^{\alpha_i})$$

$$\text{(2.3*)} \qquad \eta = (2y^{\gamma} - V^{\gamma} - v^{\gamma})/(V^{\gamma} - v^{\gamma}).$$

In (2.2) and (2.3), the values $u_1, \ldots, u_m, U_1, \ldots, U_m, v$, and V are prescribed in advance by the user to conform to reasonable limits for the data. Thus, these are presumed to be *known* quantities, in contrast with the $2m + 2$ unknown parameters: $m + 1$ coefficients $p, q_1, \ldots, q_m$, and $m + 1$ exponents $\alpha_1, \ldots, \alpha_m, \gamma$. The new variables ξ_i and η are dimensionless counterparts of the original x_i and y, respectively, scaled between -1 and 1 for typical low and high values of the original variables. The model itself, equation (2.1), defines a linear relationship between η and ξ_i, that is, between the transformed value of the response and transformed values of the factors. As described in the introduction, this is the special case of Schnute and McKinnell's (1984) response surface obtained by setting the quadratic coefficients (labelled r_{ij} by Schnute and McKinnell) equal to 0.

To see precisely how the model (2.1)−(2.3) defines the response in terms of the factors, consider the back-transformed version of (2.3),

$$\text{(2.4*)} \qquad y = \left[\frac{V^{\gamma} + v^{\gamma} + (V^{\gamma} - v^{\gamma})\eta}{2}\right]^{1/\gamma},$$

which expresses y in terms of η. Given the factors x_i $(i = 1, \ldots, m)$, one can compute the transforms ξ_i $(i = 1, \ldots, m)$ from (2.2). These, in turn, determine η from (2.1), and η determines y from the back-transform (2.4). Incidentally, it may happen that the quantity in square parentheses in (2.4) is negative, so that y is not defined. Although this indicates factor levels outside the range of model validity, it is convenient numerically to adopt the convention in (2.4) that

$$y = -(-Q)^{1/\gamma}$$

when $Q < 0$, where Q is the quantity in square parentheses. This convention avoids computing errors and yet indicates invalid y values by reporting $y < 0$.

The model coefficients p and q_i $(i = 1, \ldots, m)$ typically have magnitude around 1, since they relate quantities in (2.1) with this order of magnitude. If any q_i is small, then the corresponding x_i has little influence on y within the range of the data. An increase in x_i causes y to increase or decrease when $q_i > 0$ or $q_i < 0$, respectively. The exponents γ and α_i $(i = 1, \ldots, m)$ relate to the nonlinear nature of the response. The factor x_i has greatest influence on y at low levels of x_i when $\alpha_i < 1$ and high levels of x_i when $\alpha_i > 1$. Similarly, the combined effect of all factors is most influential at low values of y when $\gamma > 1$ and high values of y when $\gamma < 1$.

Notice that the model includes two parameters for each factor x_i: the coefficient q_i (associated with the factor's influence) and the exponent α_i (associated with a transformation to account for nonlinearity). In this sense, the model is parsimonious. When $\alpha_i = 1$, the model is linear in x_i, and q_i is the usual regression coefficient. Obviously, it is impossible to include a factor without introducing a coefficient like q_i. In the present context we also need a second parameter, like α_i, to account for an unknown nonlinear effect on the response. The reason for the rather complex formulation (2.1)−(2.3), involving the specified quantities u_i, U_i, v, and V, is that the resulting parameters q_i and α_i tend to be statistically independent in practice. Thus, for example, it may turn out that (for some i) q_i is well determined, although α_i is not. If so, we can say with some confidence that the factor x_i is influential, but we are less certain about the appropriate transformation to account for nonlinearity. Our companion paper (Jensen et al. 1986) illustrates this possibility.

The present paper follows a convention adopted by Schnute and McKinnel (1984) that equations such as (2.2) and (2.3) with continuous extensions to zero exponents are marked with an asterisk. For example, as γ tends to 0 in (2.3), the transformation takes the limiting form

$$\text{(2.5)} \qquad \eta = \frac{\log\,[y^2/(Vv)]}{\log\,(V/v)}.$$

Thus, the case $\gamma = 0$ essentially corresponds to a log transform of y. It is particularly interesting to compare the cases $\gamma = 1$ and $\gamma = 0$. When $\gamma = 1$, the factors x_i (through their transforms ξ_i) influence y additively in (2.1). By contrast, when $\gamma = 0$, the factors influence $\log y$ additively; that is, they influence the response y itself multiplicatively.

In many applications, y represents ET50, the exposure time to 50% mortality. The response $y = \infty$, if it can be extrapolated from the data, holds particular interest because it implies that the organisms do not die; that is, the corresponding factor levels are not lethal. When $\gamma < 0$, the model admits this possibility. As above, let Q represent the quantity in square brackets in (2.4). Notice that, with $\gamma < 0$, y becomes increasingly large as Q becomes smaller. Finally, $y = \infty$ when $Q = 0$, that is, when

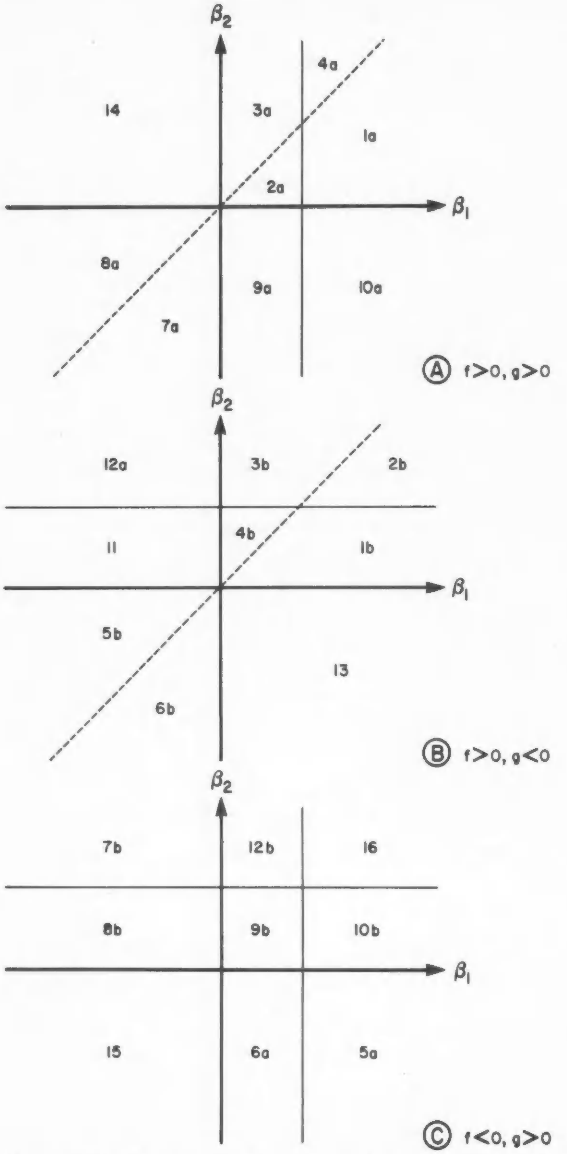

FIG. 1. Regions in the space of parameters (f, g, β_1, β_2) for equation (2.9). In panels A and B the broken line is characterized by $\beta_1 = \beta_2$. In panels A and C the lines parallel to the β_2-axis have $\beta_1 = 1$, and in panels B and C the lines parallel to the β_1-axis have $\beta_2 = 1$. The values of β_1 and β_2, together with the signs of f and g, determine a particular region 1a, 1b, 2a, 2b, . . . , 16. This region, in turn, determines a curve type from Fig. 2 and 3.

$$\eta = \frac{v^\gamma + V^\gamma}{v^\gamma - V^\gamma}. \tag{2.6}$$

Combining (2.1) and (2.6) gives the condition

$$p + \sum_{i=1}^{m} q_i \xi_i = \frac{v^\gamma + V^\gamma}{v^\gamma - V^\gamma} \tag{2.7}$$

on the factors x_i, through their transforms ξ_i. Thus, when $\gamma < 0$, (2.7) defines the boundary where $y = \infty$. In the present context, the factors theoretically cause mortality on one side of this boundary and are not lethal on the other side. In particular, with only one factor ($m = 1$), it follows from (2.7) and (2.2) that the level of x_1 where $y = \infty$ is given by

$$x = \left[\frac{u^\alpha + U^\alpha}{2} - \frac{U^\alpha - u^\alpha}{2q(V^\gamma - v^\gamma)} \times [(1+p)V^\gamma + (1-p)v^\gamma]\right]^{1/\alpha} \tag{2.8}$$

where subscripts "1" have been dropped throughout.

To understand the geometric significance of the model (2.1)−(2.3), it is useful to consider the equation

$$z_2^{\beta_2} = f z_1^{\beta_1} + g, \tag{2.9}$$

which involves two variables z_1 and z_2, two exponents β_1 and β_2, and two coefficients f and g. Depending on the values of f, g, β_1, and β_2, the graph of z_2 versus z_1 in (2.9) can take various forms. Since both z_1 and z_2 must be positive, it follows that f and g cannot both be negative. This leaves three possible cases: (A) $f > 0$ and $g > 0$, (B) $f > 0$ and $g < 0$, and (C) $f < 0$ and $g > 0$. To determine the shape of a curve (2.9), it is enough to know only the exponents β_1 and β_2 and the case (A), (B), or (C). Figures 1, 2, and 3 present the possible shapes systematically. First, from Fig. 1, the case and the exponents determine a particular region in the $\beta_1\beta_2$ plane, labelled 1a, 1b, 2a, etc. The label then determines a curve type in Fig. 2 or 3, where the letter "a" or "b" typically distinguishes two possible intercepts of the curve. Mathematical proofs underlying Fig. 1, 2, and 3 are given in Appendix A. These results correspond to earlier work by Schnute and McKinnell (1984), but the formulation here differs from theirs and is more convenient to apply, particularly in the present context.

Several general features of the curve shapes have particular interest. To give the ideas a specific context, suppose that z_2 is the exposure time to 50% mortality (ET50) in the presence of a factor z_1. Then, significant features of Fig. 1, 2, and 3 include the following.

(1) The curves either increase (types 1−8, Fig. 2) or decrease (types 9−16, Fig. 3) steadily as functions of z_1. A curve increases when $\beta_1\beta_2 f > 0$ and decreases when $\beta_1\beta_2 f < 0$. Thus, the sign of $\beta_1\beta_2 f$ (+ or −, respectively) determines whether the factor z_1 is favorable or detrimental to survival.

(2) Curves in case (A) are defined for all values of z_1 and yet do not take all possible values of z_2. Type 9a illustrates this feature; here, there is a finite time to mortality, such as a natural life span, even when z_1 is absent ($z_1 = 0$); but as the detrimental factor z_1 increases, this time is reduced almost to 0 (immediate death). Type 1a exhibits a similar feature when z_1 is favorable. Again, there is a finite time to mortality when $z_1 = 0$, but this is increased at an accelerating rate as z_1 increases.

(3) Curves in case (B) are defined only for some values of z_1 and yet take all possible values of z_2. For example, consider type 13. Here, as in the discussion leading to (2.8), there is a critical level of z_1 below which mortality does not occur. Above this level, the time to mortality decreases steadily as z_1 increases, until death is almost immediate. Types 5b and 6b illustrate a related feature when z_1 is favorable. In these cases, there is instant death ($z_2 = 0$) when z_1 is absent ($z_1 = 0$); as z_1 increases, z_2 increases rapidly until, at a critical value of z_1, there is no further mortality. Thus, in types 5b and 6b, z_1 might

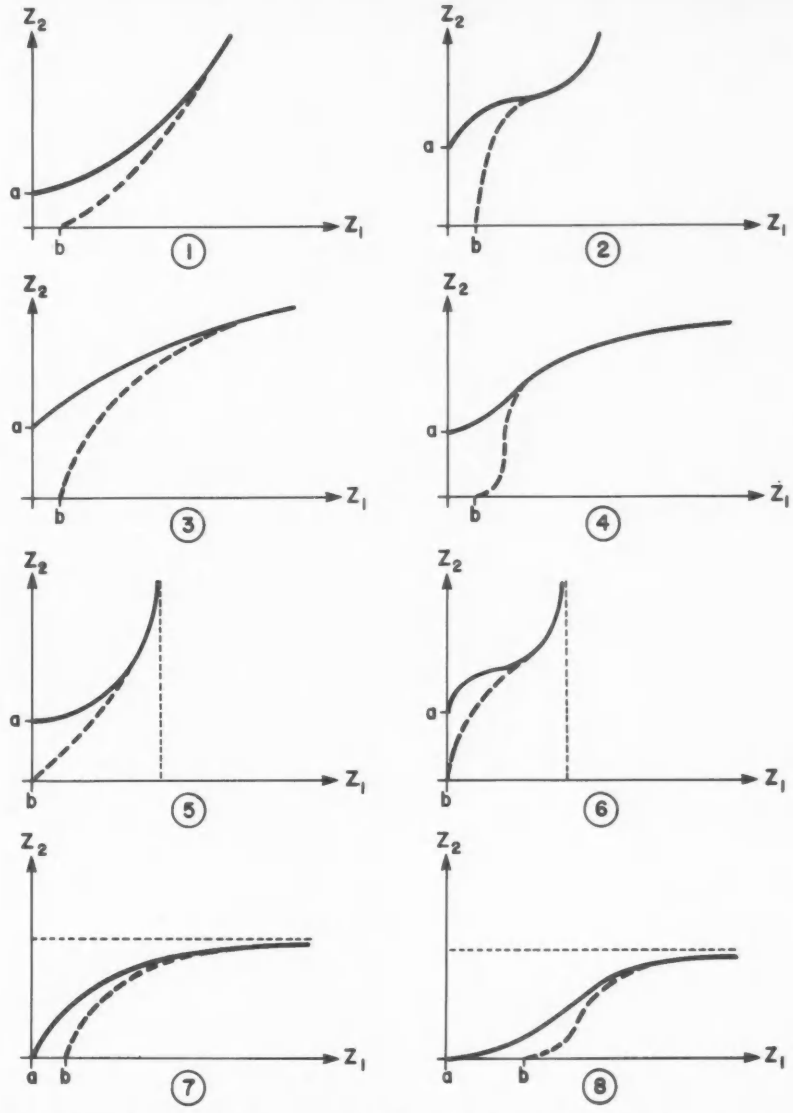

FIG. 2. Curve types determined by equation (2.9) when $\beta_1 \beta_2 f > 0$. These have the common feature that z_2 is an increasing function of z_1. The particular type 1a, 1b, 2a, 2b, . . . , 8 corresponds to the region in Fig. 1 indicated by the parameters in (2.9).

represent availability of a nutrient: a certain amount is essential for life, but beyond a threshold where the requirement is saturated, no more is necessary.

(4) Curves in case (C) are defined for only some values of z_1 and take only some values of z_2. Type 15 illustrates this possibility. Here, as in type 13, there is a critical level of z_1 below which mortality does not occur. Above this level, the time to mortality decreases, but only down to a finite limit, as z_1 increases.

(5) Curves may or may not have inflection points. For example, compare 3a and 4a. In 3a, z_1 has a steadily decelerating favorable influence on z_2, while in 4a, the effect of z_1 accelerates at first and then ultimately decelerates. Mathematical formulas for inflection points, when they exist, are given in Appendix A.

The above examples are based on interpreting (2.9) as a dose−response relationship. Of course, (2.9) has many other possible biological interpretations. For example, the reader might relate types 7 and 8 to animal growth with an asymptotic size limit. In the present context, these same curve types might indicate a favorable factor z_1 which cannot, however, increase the time to mortality z_2 beyond some ultimate limit, such as a natural life span.

The curves (2.9) relate to the model (2.1)−(2.3) in at least two ways. First, they represent the response y when there is only one factor x_1. In this case, (2.9) applies with $z_1 = x_1$,

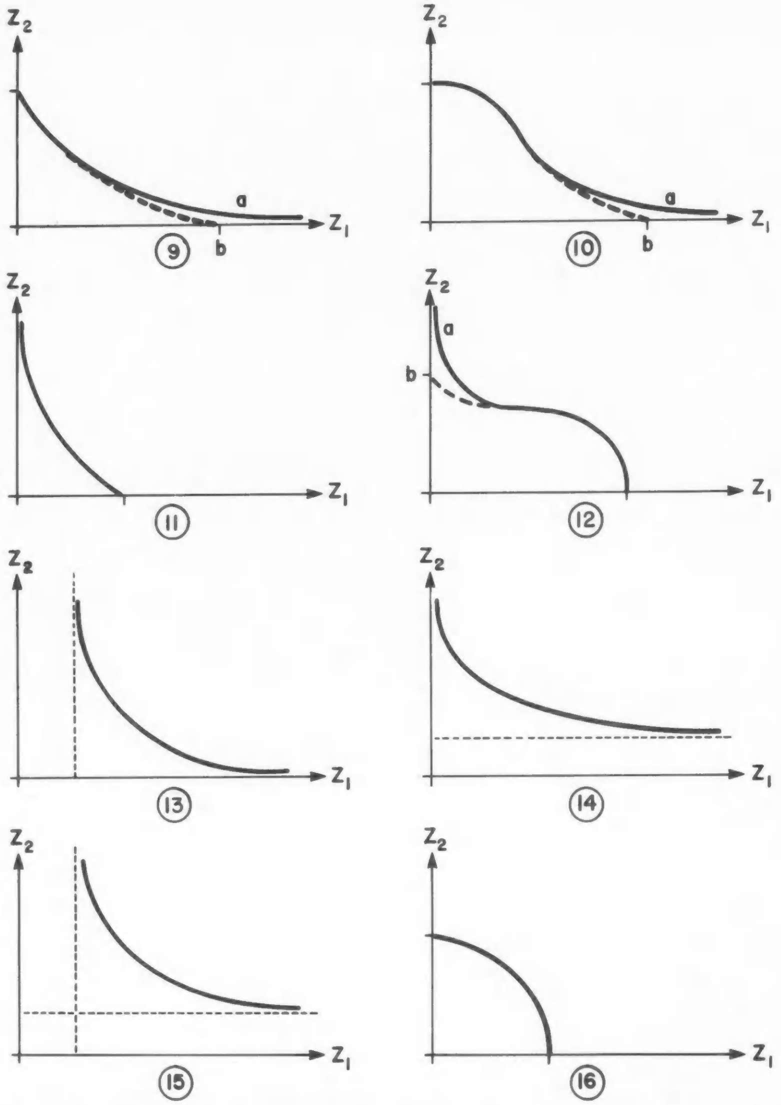

FIG. 3. Curve types determined by equation (2.9) when $\beta_1 \beta_2 f < 0$. These have the common feature that z_2 is a decreasing function of z_1. The particular type 9a, 9b, 10a, 10b, . . . , 16 corresponds to the region in Fig. 1 indicated by the parameters in (2.9).

$z_2 = y$, $\beta_1 = \alpha_1$, $\beta_2 = \gamma$, and f and g given sequentially by

$$f = q_1(V^\gamma - v^\gamma)/(U_1^{\alpha_1} - u_1^{\alpha_1}) \tag{2.10}$$

$$g = \tfrac{1}{2}[(1 + p)V^\gamma + (1 - p)v^\gamma - f(U_1^{\alpha_1} + u_1^{\alpha_1})]. \tag{2.11}$$

Second, the curves (2.9) also represent a contour of (2.1)–(2.3) when there are two factors ($m = 2$). Let y_0 be the value of y on a particular contour, and let η_0 be the corresponding value of η from (2.3). Then, the contour is described by (2.9) with $z_i = x_i$ $(i = 1,2)$, $\beta_1 = \alpha_i$ $(i = 1,2)$, and f and g given sequentially by

$$f = -(q_1/q_2)\,(U_2^{\alpha_2} - u_2^{\alpha_2})/(U_1^{\alpha_1} - u_1^{\alpha_1}) \tag{2.12}$$

$$g = \tfrac{1}{2}\left[\frac{\eta_0 - p}{q_2}(U_2^{\alpha_2} - u_2^{\alpha_2}) + f(U_1^{\alpha_1} + u_1^{\alpha_1}) + (U_2^{\alpha_2} + u_2^{\alpha_2})\right]. \tag{2.13}$$

More generally, (2.9) can represent the general case of m factors either as (1) the response function when all factors but one are fixed or (2) a response contour when both y and all factors but two are fixed.

We can compare our model to the following generalization of (1.3):

$$(2.14) \qquad \log (y - a) = \log d - \sum_{i=1}^{m} c_i \log (x_i - b_i).$$

Like ours, model (2.14) involves $2m + 2$ parameters: $a_1, \ldots, a_m, b_1, \ldots, b_m, c$ and d. When $c_i > 0$ in (2.14), a and b_i correspond to asymptotic values for the response y and the factor x_i. Curve type 15 (Fig. 3) shows that our model also allows for such asymptotes without imposing the requirement in (2.14) that the variables are log transformed. For example, (2.14) allows *only* a multiplicative effect of the factors, while our model includes the case ($\gamma = 1$) that factors influence the response additively. Our philosophy is to allow the data to speak for themselves in selecting the appropriate transformation.

The model (2.1)−(2.3) is designed primarily for a response y which, like ET50, can take arbitrary positive values from 0 to ∞. Sometimes, however, bioassay involves studying the fraction y of organisms that survive a prescribed set of deleterious conditions. In such cases, the response y is necessarily restricted to lie between 0 and 1. The transformation (2.3) may then be inappropriate, and a better choice might be

$$(2.15^*) \qquad \eta = \frac{\log \{(y^\gamma - 1)^2 / [(V^\gamma - 1)(v^\gamma - 1)]\}}{\log \{(V^\gamma - 1)/(v^\gamma - 1)\}}$$

where v and V (typical low and high values of y) are restricted to lie between 0 and 1. The transformation (2.15), originally suggested by Schnute and McKinnell (1984), generalizes the logistic transform commonly applied in bioassay. When $\gamma = -1$, (2.15) is logistic and, consequently, symmetric with respect to the inflection point at $y = 0.5$. The extra parameter γ in (2.15) allows for asymmetry around the inflection point. The inverse of this transform is

$$(2.16^*) \; y = [1 - \operatorname{sign}(\gamma) |1 - V^\gamma|^{(1+\eta)/2} \times |1 - v^\gamma|^{(1-\eta)/2}]^{1/\gamma}.$$

Thus, (2.15)−(2.16) can be regarded as counterparts to (2.3)−(2.4) when the response y is restricted to the range 0 to 1. In this sense, the classical theory of logistic bioassay can readily be generalized along the lines developed here by using the model (2.1), (2.2), and (2.15) in place of (2.1)−(2.3). Because we are concerned primarily with responses y, like ET50, that can take arbitrary positive values, we restrict our mathematical development to the model (2.1)−(2.3).

Likelihood and Hypothesis Tests

Biological data, of course, never precisely conform to the model (2.1)−(2.3). Schnute and McKinnell (1984) described a systematic way to introduce statistical error. This section summarizes their results as applied to the model here. Suppose that there are n data points with the observed response $\hat{y}_j$ corresponding to the factor vector

$$(3.1) \qquad \boldsymbol{X}_j = (x_{1j}, x_{2j}, \ldots, x_{mj})$$

where $j = 1, \ldots, n$. Let $\hat{\eta}_j$ be the transformed value of $\hat{y}_j$ from (2.3); similarly, let η_j and y_j be model predictions from the factor vector $\boldsymbol{X}_j$. Then the error assumption is that

$$(3.2) \qquad \hat{\eta}_j = \eta_j + \sigma \epsilon_j$$

where σ is the standard deviation of $\hat{\eta}_j$ and the model errors $\epsilon_1, \ldots, \epsilon_n$ are independent and normal with mean 0 and variance 1. From (3.2), it can be shown that the error in $\hat{y}$ depends on γ; for example, the error is normal when $\gamma = 1$ and lognormal when $\gamma = 0$.

The model (2.1)−(2.3) involves the parameter vector

$$(3.3) \qquad \boldsymbol{\theta} = (p, q_1, \ldots, q_m, \alpha_1, \ldots, \alpha_m, \gamma)$$

of coefficients and exponents, and the prediction $y_j(\boldsymbol{\theta})$ at $\boldsymbol{X}_j$ depends on $\boldsymbol{\theta}$. Schnute and McKinnell (1984) showed that the maximum likelihood estimate $\hat{\boldsymbol{\theta}}$ for $\boldsymbol{\theta}$ can be obtained by minimizing the function

$$(3.4^*) \qquad A(\boldsymbol{\theta}) = \sum_{j=1}^{n} \left[\frac{\hat{y}_j^{\gamma} - y_j(\boldsymbol{\theta})^{\gamma}}{\gamma Y^{\gamma - 1}} \right]^2$$

where Y is the geometric mean of the observed responses, that is,

$$Y = \left[\prod_{j=1}^{n} \hat{y}_j \right]^{1/n}$$

Once $\hat{\boldsymbol{\theta}}$ is known, then a bias-corrected likelihood estimate for σ turns out to be determined by

$$(3.5^*) \qquad \hat{\sigma}^2 = \frac{1}{n - k} \sum_{j=1}^{n} \left[\frac{\hat{y}_j^{\hat{\gamma}} - y_j(\hat{\boldsymbol{\theta}})^{\hat{\gamma}}}{V^{\hat{\gamma}} - v^{\hat{\gamma}}} \right]^2$$

where k is the number of parameters that have been estimated. Schnute and McKinnell (1984) described an efficient method for minimizing $A(\boldsymbol{\theta})$ to obtain $\hat{\boldsymbol{\theta}}$ (see also Mittertreiner and Schnute 1985, p. 54).

We frequently must ask whether or not the addition or removal of a factor is statistically significant in determining the response. Essentially, this question amounts to a hypothesis test on $\boldsymbol{\theta}$. For example, if $m = 3$ and the third factor x_3 is unimportant, then we should not be able to reject the hypothesis $q_3 = 0$ against the alternative $q_3 \neq 0$. In general, suppose that $\boldsymbol{\theta}$ is written in two parts:

$$\boldsymbol{\theta} = (\boldsymbol{\theta}_k, \boldsymbol{\theta}_l)$$

where $\boldsymbol{\theta}_k$ and $\boldsymbol{\theta}_l$ have k and l components, respectively. Suppose we wish to test the null hypothesis

$$H_0\text{: } \boldsymbol{\theta}_k = \boldsymbol{\theta}_k^*$$

with prescribed $\boldsymbol{\theta}_k^*$ against the alternative

$$H_1\text{: } \boldsymbol{\theta}_k \neq \boldsymbol{\theta}_k^*.$$

Let A_0 and A_1 represent the minima of A under H_0 and H_1, respectively. Then, if H_0 is true, the statistic

$$(3.6) \qquad B = \frac{n - k - l}{k} \, \frac{A_0 - A_1}{A_1}$$

is approximately F-distributed with k and $n - k - l$ df. Thus if B exceeds, say, the upper 95% point for F, then H_0 can be rejected with 95% confidence. This test is approximate, in general, because the model involves some parameters (namely the exponents) nonlinearly. Consequently, the test should be regarded informally, more as a guide for understanding than a rigorous statement of statistical probabilities.

Variances and Confidence Limits

A full application of the model (2.1)−(2.3) typically involves finding confidence intervals for the parameter estimates and model predictions. For example, suppose that y represents ET50 and $\boldsymbol{X}$ represents a vector of toxicant concentrations. Let $y(\boldsymbol{X})$ denote the model's predicted ET50 based on the value of

$\boldsymbol{X}$. An actual measured response $\hat{y}$ in the presence of toxicity levels $\boldsymbol{X}$ will typically be either higher or lower than this prediction. The biologist is particularly concerned with instances when the observed $\hat{y}$ is less than the predicted $y(\boldsymbol{X})$; that is, the observed survival time to 50% mortality is shorter than predicted. It is clearly important to be able to compute a lower limit $y'(\boldsymbol{X})$ such that, given $\boldsymbol{X}$, an observed $\hat{y}$ is guaranteed to be higher than $y'(\boldsymbol{X})$ at least, say, 95% of the time. In fact, it could be argued that the lower limit $y'(\boldsymbol{X})$ is actually more important than the prediction $y(\boldsymbol{X})$ for the purposes of environmental management.

The calculations required to find a confidence limit like $y'(\boldsymbol{X})$ are somewhat extensive and require a suitable notation. Consistent with (3.3), let $\boldsymbol{\theta}$ be the parameter vector

$$(4.1) \qquad \boldsymbol{\theta} = (\theta_1, \ldots, \theta_{2m+2})$$

where

$$\theta_1 = p$$

$$\theta_{i+1} = q_i;\ i = 1, \ldots, m$$

$$\theta_{i+m+1} = \alpha_i;\ i = 1, \ldots, m$$

$$\theta_{2m+2} = \gamma.$$

Define the function

$$(4.2) \qquad F(\boldsymbol{X}, y, \boldsymbol{\theta}) = \eta - \sum_{i=1}^{m} q_i \xi_i$$

where, as usual in this paper,

$$\boldsymbol{X} = (x_1, \ldots, x_m)$$

is a vector of factors with the transformed coordinates ξ_i from (2.2) and y is a response with the transformed value η from (2.3). Then, the model (2.1)−(2.3) simply boils down to the assertion that

$$(4.3) \qquad F(\boldsymbol{X}, y, \boldsymbol{\theta}) = 0.$$

The derivatives of F with respect to the parameters are required for calculating variances. For $k = 1, \ldots, 2m + 2$, define

$$(4.4) \qquad G_k = \partial F / \partial \theta_k.$$

Then, it turns out that

$$(4.5) \qquad G_1 = -1$$

$$(4.6) \qquad G_{2m+2} = \frac{2y^{\gamma} \log y - (1 + \eta) V^{\gamma} \log V - (1 - \eta) v^{\gamma} \log v}{V^{\gamma} - v^{\gamma}}$$

and, for $i = 1, \ldots, m$,

$$(4.7) \qquad G_{i+1} = -\xi_i$$

$$(4.8) \qquad G_{i+m+1} = -q_i \frac{2x_i^{\alpha_i} \log x_i - (1 + \xi_i) U_i^{\alpha_i} \log U_i - (1 - \xi_i) u_i^{\alpha_i} \log u_i}{U_i^{\alpha_i} - u_1^{\alpha_1}}$$

Conceptually, each derivative G_k is a function of $\boldsymbol{X}$, y, and $\boldsymbol{\theta}$:

$$G_k = G_k(\boldsymbol{X}, y, \boldsymbol{\theta}),$$

although typically a derivative depends on only one or two coordinates of the vectors $\boldsymbol{X}$ and $\boldsymbol{\theta}$. For example, G_{i+m+1} depends only on x_i, q_i, and α_i. Incidentally, notice that η and ξ_i in (4.6)−(4.8) refer to the usual transforms computed from y, γ, x_i, and α_i.

As in the preceding section, suppose that n observations $(\boldsymbol{X}_j, \hat{y}_j)$, $j = 1, \ldots, n$, have been made and that $\hat{\boldsymbol{\theta}}$ is the estimated parameter vector for these data. Then define

$$(4.9) \qquad H_{kl} = \sum_{j=1}^{n} G_k(\boldsymbol{X}_j, \hat{y}_j, \hat{\boldsymbol{\theta}})\, G_l(\boldsymbol{X}_j, \hat{y}_j, \hat{\boldsymbol{\theta}})$$

for $k = 1, \ldots, N$ and $l = 1, \ldots, N$, where

$$N = 2m + 2$$

is the number of parameters (the dimension of $\boldsymbol{\theta}$). Also, let

$$(4.10) \qquad S = \sum_{j=1}^{n} [F(\boldsymbol{X}_j, \hat{y}_j, \hat{\boldsymbol{\theta}})]^2.$$

Then the elements H_{kl} define a symmetric matrix $\boldsymbol{H}$ from which the matrix

$$(4.11) \qquad \boldsymbol{C} = \frac{S}{n - N} \boldsymbol{H}^{-1}$$

can be defined, where $\boldsymbol{H}^{-1}$ represents the matrix inverse of $\boldsymbol{H}$.

It turns out that $\boldsymbol{C}$ is an estimate of the covariance matrix for the components of the estimated parameter vector $\hat{\boldsymbol{\theta}}$; that is, if C_{kl} is a component of $\boldsymbol{C}$, then it is approximately true that

$$(4.12) \qquad \mathrm{Cov}(\hat{\theta}_k, \hat{\theta}_l) = C_{kl}.$$

From a practical point of view, uncertainty in the model's parameters is perhaps less important than uncertainty in its predictions. To describe the error in prediction, we first need a notation that distinguishes several related quantities. As above, let $\hat{\boldsymbol{\theta}}$ be the parameter vector estimated from a data set. This differs, in general, from the unknown true parameter vector $\boldsymbol{\theta}^*$. Suppose that a factor vector $\boldsymbol{X}$ is given. Define

$$\tilde{y} = \tilde{y}(\boldsymbol{X}, \hat{\boldsymbol{\theta}})$$

to be the predicted response to $\boldsymbol{X}$ based on the parameter estimate $\hat{\boldsymbol{\theta}}$. Similarly, let

$$y^* = y^*(\boldsymbol{X}, \boldsymbol{\theta}^*)$$

be the correct prediction based on the true parameter vector $\boldsymbol{\theta}^*$. Finally, let

$$\hat{y} = \hat{y}(\boldsymbol{X}, \boldsymbol{\theta}^*, \epsilon)$$

denote a new observed response associated with the factor level $\boldsymbol{X}$, the true parameter vector $\boldsymbol{\theta}^*$, and a random error ϵ as in (3.2). Notice that $\tilde{y}$, y^*, and $\hat{y}$ are all different, in general. The known prediction $\tilde{y}$ differs from the unknown true prediction y^* due to the error in the parameter estimate $\boldsymbol{\theta}$. The observation

$\hat{y}$ differs from the known prediction $\tilde{y}$ because, first, $\tilde{y}$ contains the error due to the estimate $\hat{\boldsymbol{\theta}}$ just described and, second, $\hat{y}$ includes the random error ϵ.

To quantify these errors, define the following two functions of $\boldsymbol{X}$:

$$(4.13) \qquad D(\boldsymbol{X}) = \sum_{k=1}^{m} \sum_{l=1}^{m} G_k(\boldsymbol{X}, \tilde{y}, \hat{\boldsymbol{\theta}})\, G_l(\boldsymbol{X}, \tilde{y}, \hat{\boldsymbol{\theta}})\, C_{kl}$$

$$(4.14) \qquad E(\boldsymbol{X}) = D(\boldsymbol{X}) + \frac{S}{n - N}.$$

Then it is approximately true that

$$(4.15) \qquad \frac{2(y^{*\hat{\gamma}} - \tilde{y}^{\hat{\gamma}})}{\sqrt{D(\boldsymbol{X})}\,(V^{\hat{\gamma}} - v^{\hat{\gamma}})} \sim t(n - N)$$

$$(4.16) \qquad \frac{2(\hat{y}^{\hat{\gamma}} - \tilde{y}^{\hat{\gamma}})}{\sqrt{E(\boldsymbol{X})}\,(V^{\hat{\gamma}} - v^{\hat{\gamma}})} \sim t(n - N)$$

where $\hat{\gamma}$ is the estimate for γ (a component of $\hat{\boldsymbol{\theta}}$) and $t(n - N)$ is Student's t-distribution with $n - N$ df. The quantities $D(\boldsymbol{X})$ and $E(\boldsymbol{X})$ in (4.13)–(4.16) correspond essentially to variances associated with $\tilde{y}$ and $\hat{y}$, respectively. In (4.14), $E(\boldsymbol{X})$ is expressed as the sum of two terms. These correspond to the two sources of error in $\hat{y}$ cited above.

The distributions (4.15) and (4.16) can be used to obtain either one-sided or two-sided confidence intervals for the various quantities in question. In the present context, one-sided intervals are the most useful, since, for example, it is a low value of ET50 that is problematic. If π is a probability level (such as 95%), let $T(\pi, n - N)$ represent the upper π-level point of the t-distribution with $n - N$ df. Then, (4.15) and (4.16) can be used to show that the following inequalities hold with probability π:

$$(4.17) \qquad y^* > [\tilde{y}^{\hat{\gamma}} - \tfrac{1}{2}\sqrt{D(\boldsymbol{X})}\,(V^{\hat{\gamma}} - v^{\hat{\gamma}})\,T(\pi, n - N)]^{1/\hat{\gamma}}$$

$$(4.18) \qquad \hat{y} > [\tilde{y}^{\hat{\gamma}} - \tfrac{1}{2}\sqrt{E(\boldsymbol{X})}\,(V^{\hat{\gamma}} - v^{\hat{\gamma}})\,T(\pi, n - N)]^{1/\hat{\gamma}}.$$

The inequality (4.17) gives a lower limit for the true prediction y^*, that is, for the response surface itself. Similarly, (4.18) gives a lower limit for a new observation $\hat{y}$. From (4.14) it follows that

$$E(\boldsymbol{X}) > D(\boldsymbol{X});$$

consequently, the limit defined by (4.18) lies below that defined in (4.17). Again, this relates to the two sources of error in $\hat{y}$.

The right-hand member of (4.18) is the limit $y'(\boldsymbol{X})$ described in the first paragraph of this section. In the particular case where there is only one factor x_1, (4.18) can be written as

$$(4.19) \qquad \hat{y} > y'(x_1),$$

an inequality that holds with probability π. If a minimum tolerable response $\hat{y}_{\min}$ is *prescribed*, then the equation

$$(4.20) \qquad \hat{y}_{\min} = y'(x_1)$$

can be solved numerically (although not analytically) for x_1. This gives a factor level x_1 which, at confidence level π, will yield a response at least as high as the prescribed $\hat{y}_{\min}$. Determining such a factor level is ultimately the purpose of many toxicology studies.

The formulas for variance and confidence in this section are all approximate, based on approximations commonly used in nonlinear regression problems. In this case, there is one point of departure from the conventional theory. Here, there is an unknown parameter (namely γ) associated with the response y, along with other parameters associated with the factor vector $\boldsymbol{X}$. This point is discussed in mathematical detail in Appendix B, which contains brief proofs of the results presented above.

The equations here, although perhaps mathematically complicated, have been written to allow straighforward programming on a computer. First, the functions F and G_k ($k = 1, \ldots, N$) are defined by (4.2)–(4.8). Second, after the estimate $\hat{\boldsymbol{\theta}}$ is found for a given data set, the matrix $\boldsymbol{H}$, the sum S, and the matrix $\boldsymbol{C}$ can be computed from (4.9)–(4.11). Notice that these quantities are determined completely from the data. Third, given $\hat{\boldsymbol{\theta}}$, S, and $\boldsymbol{C}$, the functions $D(\boldsymbol{X})$ and $E(\boldsymbol{X})$ are defined by (4.13) and (4.14). Notice in particular that $\tilde{y}$ in (4.13) is itself a function of $\boldsymbol{X}$. Finally, lower limits for the true prediction y^* and a new observation $\hat{y}$ at $\boldsymbol{X}$ can be calculated from (4.17) and (4.18). These depend on $\boldsymbol{X}$, just as the familiar confidence curve for an ordinary y-on-x regression line typically lies further from the line as x moves away from the region where data are available. We illustrate all these ideas in a companion paper (Jensen et al. 1986) that gives the complete analysis of a particular data set.

Acknowledgements

We were led to this work by Dr. D. F. Alderdice who explained to us the significance of the problem, provided useful historical references, and made helpful suggestions for improving the manuscript. We are grateful for his valuable contribution.

References

JENSEN, J. O. T., J. SCHNUTE, AND D. F. ALDERDICE. 1986. Assessing juvenile salmonid response to gas supersaturation using a general multivariate dose–response model. Can. J. Fish. Aquat. Sci. 43: 1694–1709.

KENDALL, M., AND A. STUART. 1979. The advanced theory of statistics. Vol. 2: Inference and relationship. 4th ed. Macmillan, New York, NY. 748 p.

KNITTEL, M., G. CHAPMAN, AND R. GARTON. 1980. Effects of hydrostatic pressure on steelhead survival in air-supersaturated water. Trans. Am. Fish. Soc. 109: 755–759.

MITTERTREINER, A. C., AND J. SCHNUTE. 1985. SIMPLEX: a manual and software package for easy nonlinear parameter estimation and interpretation in fishery research. Can. Tech. Rep. Fish. Aquat. Sci. 1384: 90 p.

SCHNUTE, J., AND S. MCKINNELL. 1984. A biologically meaningful approach to response surface analysis. Can. J. Fish. Aquat. Sci. 41: 936–953.

SPRAGUE, J. 1969. Measurement of pollutant toxicity to fish. Part I. Bioassay methods for acute toxicity. Water Res. 3: 793–821.

WARREN, C., AND P. DOUDOROFF. 1971. Biology and water pollution control. W. B. Saunders Co., Toronto, Ont. 434 p.

WURHMANN, K. 1952. Sur quelques principes de la toxicologie du poisson. Bulletin du Centre belge d'Etude et de Documentation des Eaux, n° 15. 12 p. (Transl. by D. Alderdice. 1959. Fish. Res. Board Can. Transl. Ser. No. 243: 19 p.)

WUHRMANN, K., AND H. WOKER. 1950. Die Giftigkeit von Phenol für verschiedene Fischarten. Schweiz. Z. Hydrol. 12: 271–287.

ZITKO, V. 1979. An equation of lethality curves in tests with aquatic fauna. Chemosphere 8: 47–51.

1982. LETCUR, the lethality curve program. Can. Tech. Rep. Fish. Aquat. Sci. 1134: 10 p.

Appendix A. Derivation of Fig. 1, 2, and 3

The following equivalences are immediate from (2.9):

$$(\text{A.1}) \qquad z_1^{\beta_1} = 0 \Leftrightarrow z_2^{\beta_2} = g$$

$$(\text{A.2}) \qquad z_2^{\beta_2} = 0 \Leftrightarrow z_1^{\beta_1} = -g/f.$$

These potentially determine intercepts and asymptotes. For example, if $g > 0$, then (A.1) determines a z_2-intercept ($z_1 = 0$) when $\beta_1 > 0$ and a z_2-asymptote ($z_1 = \infty$) when $\beta_1 < 0$. Also, if (2.9) has an inflection point, then its coordinates $z_i^*(i = 1,2)$ turn out to be given by

$$\text{(A.3)}\qquad z_1^{*\beta_1} = \frac{g(1-\beta_1)\beta_2}{f(\beta_1-\beta_2)}$$

$$\text{(A.4)}\qquad z_2^{*\beta_2} = \frac{g(1-\beta_2)\beta_1}{(\beta_1-\beta_2)}.$$

Finally, first and second derivatives of z_2 in (2.9) can be written in the forms

$$\text{(A.5)}\qquad \frac{dz_2}{dz_1} = \frac{f\beta_1}{\beta_2}\, z_1^{\beta_1 - 1}\, z_2^{1-\beta_2}$$

$$\text{(A.6)}\qquad \frac{d^2z_2}{dz_1^2} = \frac{1}{z_2}\left(\frac{dz_2}{dz_1}\right)^2 \frac{\beta_1-\beta_2}{\beta_1}\left[1-(z_1^*/z_1)^{\beta_1}\right].$$

Notice that (A.6) involves z_1^* raised to the power β_1. This quantity can be calculated from (A.3), even if the left side of (A.3) is negative and z_1^* itself fails to exist.

From (A.1)−(A.4), the existence of intercepts, asymptotes, and inflection points depends on the signs of the seven quantities

$$\text{(A.7)}\qquad \beta_1,\ \beta_2,\ 1-\beta_1,\ 1-\beta_2,\ \beta_1-\beta_2,\ f,\ g.$$

Furthermore, since z_1 and z_2 both must be positive, the slope (A.5) and acceleration (A.6) also depend on these signs. The first five quantities (A.7) are zero on the various lines drawn in Fig. 1, where each single panel involves only four lines. The last two quantities (f and g) determine a particular panel, (A), (B), or (C). Thus, any region in Fig. 1 is uniquely determined by the quantities (A.7). For example, the region 2a in panel (A) is determined by the condition that all quantities are positive. Region 1a is determined by the sequence of signs

$$+,\ +,\ -,\ \pm,\ +,\ +,\ +,$$

where the ± indicates that the sign of $1 - \beta_2$ is irrelevant.

Using region 2a (all signs +) as an example, it follows from (A.1) that there is a z_2-intercept; but, from (A.2), there is no z_1-intercept, since $-g/f < 0$. Similarly, from (A.3) and (A.4), there is an inflection point. From (A.5), the curve slopes upward, and from (A.6), it is convex down for z_1 below the inflection point and convex up for z_1 above it. These properties precisely define the curve 2a in Fig. 2. Proofs for all remaining curves are similar.

Appendix B. Proofs of the Variance Formulas

Using notation developed in the paper, the model can be written in the form

$$\text{(B.1)}\qquad F(X, \hat{y}, \boldsymbol{\theta}^*) = \sigma\epsilon$$

where $\hat{y}$ is an observation, $\boldsymbol{\theta}^*$ is the true (unknown) parameter vector, and ϵ is normal with mean 0 and variance 1. Let $(X_j, y_j), j = 1, \ldots, n$, be a data set with the associated parameter estimate $\hat{\boldsymbol{\theta}}$. Define the following functions of $\boldsymbol{\theta}$:

$$\text{(B.2)}\qquad F_j(\boldsymbol{\theta}) = F(X_j, \hat{y}_j, \boldsymbol{\theta})$$

$$\text{(B.3)}\qquad f_j(\boldsymbol{\theta}) = \frac{\partial F}{\partial y}(X_j, \hat{y}_j, \boldsymbol{\theta})$$

for $j = 1, \ldots, n$. Then the likelihood function for the data is

$$\text{(B.4)}\qquad L = (2\pi)^{-n/2}\,\sigma^{-n} \prod_{j=1}^{n} f_j \exp\left[-\frac{1}{2}\sigma^{-2}\sum_{j=1}^{n} F_j^2\right].$$

The product Π in (B.4) is a Jacobian required to convert the normal likelihood for ϵ into a likelihood for an observation $\hat{y}$. Let

$$\lambda = -\log L - (n/2)\log(2\pi)$$

represent the negative log likelihood, except for a constant. Then

$$\text{(B.5)}\qquad \lambda(\boldsymbol{\theta}) = n \log \sigma + (\sigma^{-2}/2)\, S(\boldsymbol{\theta}) - R(\boldsymbol{\theta})$$

where

$$\text{(B.6)}\qquad S(\boldsymbol{\theta}) = \sum_{j=1}^{n} [F_j(\boldsymbol{\theta})]^2$$

$$\text{(B.7)}\qquad R(\boldsymbol{\theta}) = \sum_{j=1}^{n} \log[f_j(\boldsymbol{\theta})].$$

In a conventional least squares problem, the quantities f_j and R do not depend on $\boldsymbol{\theta}$; consequently, the term R in (B.5) is a constant.

From the general theory of likelihood (Kendall and Stuart 1979, p. 59), if $\boldsymbol{C}$ is the covariance matrix of parameter estimates, then the approximation

$$\text{(B.8)}\qquad (C^{-1})_{kl} \simeq \frac{\partial^2\lambda}{\partial\theta_k\partial\theta_l}(\hat{\boldsymbol{\theta}})$$

is valid for large sample sizes. From (B.5) it follows that

$$\text{(B.9)}\qquad \frac{\partial^2\lambda}{\partial\theta_k\partial\theta_l} = \sigma^{-2}\sum_{j=1}^{n}\frac{\partial F_j}{\partial\theta_k}\frac{\partial F_j}{\partial\theta_l} + \sigma^{-2}\sum_{j=1}^{n} F_j\frac{\partial^2 F_j}{\partial\theta_k\partial\theta_l} - \frac{\partial^2 R}{\partial\theta_k\partial\theta_l}.$$

If σ is small and expressions in (B.9) are evaluated at $\hat{\boldsymbol{\theta}}$, then it follows from (B.1) that $F_j = 0(\sigma)$ and $R = 0(1)$, so that the three terms on the right-hand side of (B.9) have orders of magnitude $0(\sigma^{-2})$, $0(\sigma^{-1})$, and $0(1)$, respectively. Keeping only the dominant term of order $0(\sigma^{-2})$ gives, from (B.8) and (B.9),

$$\text{(B.10)}\qquad (C^{-1})_{kl} \simeq \sigma^{-2}\sum_{j=1}^{n}\frac{\partial F_j}{\partial\theta_k}(\hat{\boldsymbol{\theta}})\,\frac{\partial F_j}{\partial\theta_l}(\hat{\boldsymbol{\theta}}).$$

Also, from (3.5) and (4.10), an unbiased estimate for σ^2 is

$$\text{(B.11)}\qquad \hat{\sigma}^2 \doteq \frac{S}{n-N}.$$

Combining (B.10) and (B.11) gives (4.11) and (4.12).

To obtain a lower limit for the unknown true prediction y^*, consider the Taylor expansion

$$\text{(B.12)}\qquad F(X, y^*, \hat{\boldsymbol{\theta}}) \simeq F(X, y^*, \boldsymbol{\theta}^*) + \sum_{k=1}^{N}\frac{\partial F}{\partial\theta_k}(X, y^*, \boldsymbol{\theta}^*)\,(\hat{\theta}_k - \theta_k^*).$$

Notice, however, that $F(X, y^*, \hat{\boldsymbol{\theta}}^*) = 0$ by definition of $\boldsymbol{\theta}^*$. Consequently, since the estimate $\hat{\boldsymbol{\theta}}$ is asymptotically multinormal, it follows that the statistic $F(X, y^*, \hat{\boldsymbol{\theta}})$ is asymptotically normal with mean 0 and variance given approximately by

$$\text{(B.13)}\quad \operatorname{Var}[F(\boldsymbol{X},y^*,\hat{\boldsymbol{\theta}})] \simeq \sum_{k=1}^{N}\sum_{l=1}^{N} \frac{\partial F}{\partial \theta_k}(\boldsymbol{X},\hat{y},\hat{\boldsymbol{\theta}}) \times \frac{\partial F}{\partial \theta_l}(\boldsymbol{X},\hat{y},\hat{\boldsymbol{\theta}})\, C_{kl}.$$

In passing from (B.12) to (B.13), we use the fact that

$$\text{(B.14)}\quad \frac{\partial F}{\partial \theta_k}(\boldsymbol{X},y^*,\hat{\boldsymbol{\theta}}^*) \simeq \frac{\partial F}{\partial \theta_k}(\boldsymbol{X},\hat{y},\hat{\boldsymbol{\theta}})$$

to within $0(\sigma)$, since both $y^* - \hat{y}$ and $\boldsymbol{\theta}^* - \hat{\boldsymbol{\theta}}$ are $0(\sigma)$. A short calculation shows that

$$\text{(B.15)}\quad F(\boldsymbol{X},y^*,\hat{\boldsymbol{\theta}}) = F(\boldsymbol{X},y^*,\hat{\boldsymbol{\theta}}) - F(\boldsymbol{X},\tilde{y},\hat{\boldsymbol{\theta}}) = \frac{2(y^{*\hat{\gamma}} - \tilde{y}^{\hat{\gamma}})}{V^{\hat{\gamma}} - v^{\hat{\gamma}}},$$

since $F(\boldsymbol{X},\tilde{y},\hat{\boldsymbol{\theta}}) = 0$ by definition of $\tilde{y}$. Dividing the normal statistic (B.15) by its estimated standard deviation from (B.13) gives the t-statistic (4.15). Details of this argument follow from linearization and an application of the usual theory for normal variables. The distribution (4.15) implies the lower limit for y^* given in (4.17).

To obtain a lower limit for a new observation $\hat{y}$, consider the expansion

$$\begin{aligned}\text{(B.16)}\quad F(\boldsymbol{X},\hat{y},\hat{\boldsymbol{\theta}}) &= [F(\boldsymbol{X},\hat{y},\hat{\boldsymbol{\theta}}) - F(\boldsymbol{X},\hat{y},\boldsymbol{\theta}^*)] + F(\boldsymbol{X},\hat{y},\boldsymbol{\theta}^*)\\ &\simeq \sum_{k=1}^{N} \frac{\partial F}{\partial \theta_k}(\boldsymbol{X},\hat{y},\boldsymbol{\theta}^*)\,(\hat{\theta}_k - \theta_k^*) + \sigma\epsilon\\ &\simeq \sum_{k=1}^{N} \frac{\partial F}{\partial \theta_k}(\boldsymbol{X},y^*,\boldsymbol{\theta}^*)\,(\hat{\theta}_k - \theta_k^*) + \sigma\epsilon\\ &\simeq F(\boldsymbol{X},y^*,\hat{\boldsymbol{\theta}}) + \sigma\epsilon.\end{aligned}$$

Line 2 of (B.16) is simply a Taylor expansion combined with (B.1), line 3 is based on the fact that $\hat{y} - y^* = 0(\sigma)$, and line 4 follows from (B.12). Notice that the two variates summed in the final line are independent. The first, $F(\boldsymbol{X},y^*,\hat{y})$, depends only on past data, and the second, $\sigma\epsilon$, depends only on the random error ϵ in the new data observation $\hat{y}$. Consequently,

$$\text{(B.17)}\quad \operatorname{Var}[F(\boldsymbol{X},\hat{y},\hat{\boldsymbol{\theta}})] \simeq \operatorname{Var}[F(\boldsymbol{X},y^*,\hat{\boldsymbol{\theta}})] + \sigma^2.$$

Also, a short calculation similar to (B.15) shows that

$$\text{(B.18)}\quad F(\boldsymbol{X},\hat{y},\hat{\boldsymbol{\theta}}) = \frac{2(\hat{y}^{\hat{\gamma}} - \tilde{y}^{\hat{\gamma}})}{V^{\hat{\gamma}} - v^{\hat{\gamma}}}.$$

Just as (B.13) and (B.15) lead to the t-statistic (4.15), so (B.17) and (B.18) lead to the t-statistic (4.16), from which the lower limit (4.18) for $\hat{y}$ follows. This completes the proof of all variance formulas and confidence limits in that section.

Assessing Juvenile Salmonid Response to Gas Supersaturation Using a General Multivariate Dose–Response Model

J. O. T. Jensen, J. Schnute, and D. F. Alderdice

Department of Fisheries and Oceans, Pacific Biological Station, Nanaimo, B.C. V9R 5K6

Jensen, J. O. T., J. Schnute, and D. F. Alderdice. 1986. Assessing juvenile salmonid response to gas supersaturation using a general multivariate dose–response model. Can. J. Fish. Aquat. Sci. 43: 1694–1709.

Based on data compiled from the literature, we investigate the effects of excess total gas pressure (TGP%) on juvenile salmonids (chinook, *Oncorhynchus tshawytscha*; coho, *O. kisutch*; sockeye, *O. nerka*; and steelhead, *Salmo gairdneri*). Our study relates exposure time to 50% mortality (ET50) to TGP%, component levels of dissolved oxygen (O_2%) and nitrogen (N_2%), water depth, temperature, barometric pressure (BP), and fish size. We employ a new device, called a tabular histogram, for exploratory data analysis. We also formulate and test statistical hypotheses by applying the general multivariate dose–response model described in a companion paper (Can. J. Fish. Aquat. Sci. 43: 1684–1693). When modeled in response to TGP%, ET50 follows a typical exponential dose–response relationship. Based on our full data set, two ancillary factors, water depth and fish length, significantly improve the model's ability to explain variations in ET50. Furthermore, based on a smaller subset of the data, either of the factors O_2% or N_2% also improve the model fit significantly. For 50-d exposures, apparently "safe" levels of TGP% range from 103.8 to 114.8%, depending on associated factor levels of water depth and fish size.

À partir de données tirées des publications, les auteurs ont étudié les effets d'une pression gazeuse totale excessive (PGT, %) sur des salmonidés juvéniles (saumons quinnat, *Oncorhynchus tshawytscha*, coho, *O. kisutch*, rouge, *O. nerka* et truite arc-en-ciel, *Salmo gairdneri*). Ils ont mis en relation la durée d'exposition correspondant à une mortalité de 50 % (DE50) avec la PGT, les concentrations en oxygène (O_2, %) et en azote (N_2, %) dissous, la profondeur de l'eau, la température, la pression barométrique (PB) et la taille des poissons. Ils ont fait appel à une nouvelle approche, un histogramme tabulaire, pour l'analyse exploratoire des données et formulé des hypothèses qui ont fait l'objet d'un test statistique de par l'application du modèle général à variables multiples dose–réponse décrit dans une communication connexe (Can. J. Fish. Aquat. Sci. 43 : 1684–1694). La DE50 présentait une relation dose–réponse exponentielle type quand elle était modélisée en réponse à la PGT. L'utilisation de deux facteurs connexes, la profondeur de l'eau et la longueur des poissons, a permis d'accroître de façon appréciable la capacité du modèle à expliquer les variations de DE50 lorsqu'il était appliqué à l'ensemble des données. L'utilisation des teneurs en O_2 ou N_2 permettait aussi d'accroître de façon appréciable l'ajustement du modèle appliqué à un sous-ensemble des données. Dans le cas d'expositions de 50 jours, les valeurs de PGT « sécuritaires » variaient de 103,8 à 114,8 %, tout dépendant de l'importance des facteurs connexes associés, la profondeur de l'eau et la taille des poissons.

Received November 8, 1985
Accepted May 6, 1986
(J8561)

Reçu le 8 novembre 1985
Accepté le 6 mai 1986

When exposed to water supersaturated with atmospheric gases, fish can develop a problem commonly called "gas bubble disease." The cause is not pathogenic, but physical, resulting from pressure disequilibrium between liquid and gas phases. Hence, "gas bubble trauma" may be a more appropriate phrase (Fidler 1984). At equilibrium the total gas pressure (TGP, millimetres of mercury, where 1 mmHg = 133.3 Pa), defined as the sum of partial pressures of all dissolved gases, equals the barometric pressure (BP, millimetres of mercury). If the differential pressure

$$(1.1)\quad \Delta P = \mathrm{TGP} - \mathrm{BP}$$

is positive, then the water is supersaturated, and gases tend to come out of solution. Aquatic organisms in such an environment can develop gas bubbles or emboli in their organs, tissues, and vascular systems. Such effects were described in the early 1900s (Gorham 1900; Marsh and Gorham 1905). These authors found gas bubbles externally in the fins, along the lateral line, and in the lining of the mouth. Internally they also found bubbles behind the eye, causing exopthalmia or "pop-eye," and within the blood vessels. Vascular bubbles varied in size; they may block vessels, or in extreme cases block blood flow through the heart, resulting in blood stasis and death.

For about half a century subsequent to these early studies, elevated TGP levels ($\Delta P > 0$) were considered to be minor problems, caused either by faulty pumps or water-intake pipes in man-made fish-rearing facilities or by unusual occurrences of photosynthetic activity creating water supersaturated with high levels of oxygen. Then, in the 1960s, serious gas supersaturation events were recognized in the Columbia and Snake rivers, resulting from the operation of numerous hydroelectric dams. Initially, the problem was assumed to be one of nitrogen supersaturation. By the 1970s, however, it became increasingly clear that gas bubble trauma resulted from supersaturation by all atmospheric gases, rather than just nitrogen alone. Investigations were conducted to determine the lethal and sublethal responses of migrating adult and juvenile salmonids. These, and related studies, are described in reviews by Harvey (1975) and Weitkamp and Katz (1980), and also in the compilation by Fickeisen and Schneider (1976).

Although much effort went into quantifying biological responses to supersaturation, published information in the 1960s and early 1970s suffered from an incomplete understanding of the physical laws governing gas solubilities. For example, various studies have reported on oxygen alone, on nitrogen (more precisely, combined nitrogen and argon) alone, or on TGP alone with no information on the proportions of dissolved gases. In addition, problems arose from difficulties of measurement and analysis and from nonstandard ways of reporting TGP.

Measurement of TGP prior to the early 1970s required measuring each component gas in solution. While this was not a problem for oxygen, nitrogen could be measured only by the tedious manometric method of Van Slyke (1927) or by laboratory use of a gas chromatograph (D'Aoust and Clark 1980). In 1971 a very simple membrane-diffusion method was developed for measuring TGP. The instrument, the "Weiss saturometer" (Colt 1983) and several later models called "tensionometers and gasometers" (D'Aoust et al. 1976; Bouck 1982), consists of gas-permeable silicone rubber tubing connected to a pressure-sensing device. The tubing, although impermeable to liquids, allows passage of gases and water vapour until pressure equilibrium between the inside and the outside of the tubing is achieved. The result is a direct measure of ΔP, the driving force required for bubble growth. Harvey (1975) and Colt (1983) gave excellent discussions on the principal factors and physical laws that govern dissolved gases in water. In addition, Colt (1983) proposed standards for computation and reporting of gas supersaturation in freshwater and seawater. These landmark papers make clear the necessity of obtaining measurements not only of TGP, but also BP, oxygen (or the oxygen/nitrogen ratio), water temperature, salinity (if applicable), and water depth. Only by considering all of these factors can one understand fully whether or not fish may be subjected to gas disequilibrium and develop gas bubble trauma.

Total gas pressure traditionally has been reported as a percentage of complete saturation, based on the equation

$$(1.2)\quad \mathrm{TGP\%} = 100\,(\mathrm{BP} + \Delta P)/\mathrm{BP}$$

where ΔP either is measured directly with a tensionometer or is computed indirectly by adding the measured partial pressures of component gases, including water vapour. In (1.2), BP typically is much larger than ΔP, so that moderate changes in BP result in relatively small alterations in TGP%. For example, suppose that $\Delta P = 76$ mmHg, and consider the difference in TGP% between two sites at different altitudes (AL, metres), one at sea level (20°C) and the other at 1500 m. Then BP, 760 mmHg at sea level, is reduced to 638 mmHg using the equation (Colt 1980)

$$(1.3)\quad \log(\mathrm{BP}) = 2.8808 - (\mathrm{AL}/19748.2).$$

Consequently, TGP%, which is 110% at sea level, is increased to 112% at 1500 m.

Another pressure component, hydrostatic pressure, may have a more dramatic effect on TGP%. In (1.2), both BP and ΔP are normally taken to be pressures at the water surface. Indeed, the membrane-diffusion method measures the surface ΔP, regardless of the depth of the probe, since the membrane essentially blocks water pressure from the sensing device. However, bubble growth is dependent on differential pressure at a given depth. The total pressure (TP, millimetres of mercury) at depth D (metres) is (Colt 1983)

$$(1.4)\quad \mathrm{TP} = \mathrm{BP} + 73.56\rho D$$

where ρ (grams per cubic centimetre) is the water density and 73.56 is the conversion factor from metric pressure to millimetres of mercury. (Essentially, a column of about 74 mmHg will balance a 1-m column of water.) Assuming uniform mixing of water and gas from the surface to depth D, this corrected TP should be used instead of BP in the denominator of (1.2). Thus, TGP% becomes a function of D:

$$(1.5)\quad \mathrm{TGP\%}(D) = 100\,(\mathrm{BP} + \Delta P)/(\mathrm{BP} + 73.56\rho D).$$

At 20°C, ρ is 0.9982 g/cm^3 for freshwater. Therefore, at a BP of 760 mmHg, a depth D of 1 m, and a measured surface ΔP of 76 mmHg, TGP% is 100.3%. In other words, in a uniform water column with TGP% = 110% at the surface, gas bubble growth cannot occur at a depth of 1 m. In general, each metre of water depth compensates approximately for a 10% increase in TGP%.

Two important considerations follow from the knowledge that hydrostatic pressure can have a pronounced effect on bubble growth. First, many investigators have tested fish in tanks or water columns 0.6 m or more in depth, without noting at what depth the fish resided. Consequently, TGP% levels may be reported with large errors related to the depths of enclosures employed. Second, salmonids may be able to detect and avoid lethal TGP% levels by swimming to a greater depth. Weitkamp and Katz (1980) suggested that insufficient evidence exists to draw useful conclusions on this issue. Recent data (M. Shrimpton, University of British Columbia, Vancouver, B.C., pers. comm.) affirm the fact that young salmon indeed move to greater depths in the water column at TGP levels greater than 100% saturation. However, the question of whether these fish detect excess total gas pressure or respond to the symptoms of gas bubble trauma remains unanswered.

The main objective for much experimentation since the 1960s has been to determine safe TGP% levels for salmonids migrating through the Columbia and Snake rivers and, more recently, for salmonids held in shallow hatchery incubation and rearing environments. The sources of high TGP% in the former case have been numerous dams, creating TGP% levels of 120% or greater by entraining air in the plunge of water over spillways. In hatcheries, TGP% levels from 102 to 110% may occur naturally or be produced by heating or mechanical entrainment of air (e.g. from the use of aspirators or faulty pumps).

A recent examination of the literature (Alderdice and Jensen 1985) has suggested a division of mortality responses into two categories, chronic and acute, resulting from extravascular and intravascular bubble growth, respectively. Thus, the relationship between mortality and TGP% may exhibit two phases, each associated with different etiologies and rate processes. Indeed, such a compound relationship was described by Bengtsson (1974) for the response of the minnow *Phoxinus*

TABLE 1. Source authors and record frequencies for data sets 1 and 2.

Source	No. of records Set 1	Set 2
Meekin and Turner 1974	15	15
Dawley and Ebel 1975	4	4
Nebeker et al. 1979	121	35
Rucker 1975b	12	12
Blahm et al. 1975	1	1
Stroud and Nebeker 1976	1	0
Nebeker et al. 1976	14	14
Nebeker and Brett 1976	3	0
Total	171	81

phoxinus to zinc. A boundary between chronic and acute gas bubble trauma appears to lie in the TGP% range between 108 and 110%. Practical experience in the two major problem situations, below dams and within hatcheries, seems to bear out this distinction. The levels of TGP% encountered below dams often are acutely lethal, causing bubble growth in the blood circulatory system and other tissues. In hatcheries the TGP% levels, being much lower, are not rapidly lethal but can cause chronic low-level mortality in salmonid larvae and juveniles (Harvey and Cooper 1962; Wedemeyer et al. 1976; Wright and McLean 1985).

Various agencies have recommended safe levels of TGP%, below which aquatic species are not expected to be adversely affected, ranging from 105% in Oregon to 110% in Washington and Idaho (Weitkamp and Katz 1980). Ebel et al. (1979), in reviewing the most recent Environmental Protection Agency criteria, indicated that dissolved gas criteria could be established at either 110, 115, or 120%. It is not surprising that such a range in dissolved gas criteria can exist, given the variety of test conditions used in examining response to TGP.

The difficulties in measurement and the problems of nonstandard reporting may account for some of this variability. However, the main difficulty in interpreting biological response to gas supersaturation is the fact that ancillary factors also appear to have strong influences. We have discussed how two ancillary factors, barometric pressure and water depth, influence the computed TGP%. The modifying influences of high temperature (Ebel et al. 1971; Nebeker et al. 1979) and oxygen/nitrogen ratios (Rucker 1975a; Nebeker and Brett 1976; Nebeker et al. 1979) have also been demonstrated. Possible influences of species, life stage, and fish size were discussed by Weitkamp and Katz (1980). Hence, it seems reasonable to establish dissolved gas criteria by modeling lethal responses not only to TGP%, but also to ancillary factors when such information is available.

The objective of this paper is to model exposure times necessary to cause 50% mortality (ET50, hours) in a salmonid population exposed to levels of TGP% higher than 100% (i.e. dissolved gas supersaturation). In a separate report (Jensen et al. 1985), literature data have been compiled to obtain, where possible, information on species, life stage, fish size (length and weight), water temperature, barometric pressure, water depth, percentage mortality, exposure time, and the proportions of dissolved gases. The present paper investigates these data, first, with a simple exploratory device defined as a "tabular histogram." Then the data are modeled in stepwise fashion using a general multivariate dose−response model described in the companion paper by Schnute and Jensen (1986). Finally, we employ the models that best explain ET50 to estimate safe levels of gas supersaturation.

Exploratory Data Analysis

The literature search for quantitative data on salmonid mortality response to excess gas pressure yielded 621 records from 23 publications. These and two subsets of the data have been compiled elsewhere (Jensen et al. 1985). Our analysis here is confined to the two data subsets, which we refer to as data sets 1 and 2 (Table 1). Each contains information on ET50 among juvenile salmonids exposed to excess gas pressure, together with information on various ancillary variables. Data set 1, comprising 171 records, includes the ancillary variables water depth, temperature, fish length, barometric pressure, and fish species. Data set 2 consists of 81 records from data set 1 for which ancillary information on oxygen and nitrogen levels is also available.

Before describing the data sets in detail, it is necessary to clarify the meanings of four quantities related to gas pressure. The first, TGP%, has already been discussed. Within both data sets, this is reported as the *surface* gas saturation level, given by (1.2) or (1.5) with $D = 0$. Any depth effect is considered separately by admitting water depth as an ancillary variable. The second quantity, $O_2\%$, is the percentage saturation of oxygen at the surface in relation to the equlibrium level of dissolved oxygen associated with normal air. Similarly, the third quantity, $N_2\%$, is the percentage saturation of combined nitrogen and argon in relation to equilibrium with normal air. Due to the relative amounts of oxygen and nitrogen in normal air, the quantities TGP%, $O_2\%$, and $N_2\%$ are connected approximately by the relationship

$$(2.1) \quad \text{TGP\%} = (0.21)\ O_2\% + (0.79)\ N_2\%.$$

A more precise version of (2.1) is well known in the literature (e.g. Colt 1983, table 1); however, (2.1) reflects the precision available in the literature data used here. Finally, the fourth quantity, the oxygen/nitrogen ratio (ONR), is defined by

$$(2.2) \quad \text{ONR} = O_2\%/N_2\%.$$

Notice that the four quantities TGP%, $O_2\%$, $N_2\%$, and ONR are constrained by the two equations (2.1) and (2.2). Thus, any two of these quantities determine the other two.

Tables 2 and 3 summarize the information in data sets 1 and 2, respectively. They include the mean, minimum, and maximum for each variable. Furthermore, to represent the distribution of each variable, the tables include a simple graphic device that we call a "tabular histogram." We use this name because the device contains the essential information in a histogram and yet fits easily in a table. To be more precise, Tables 2 and 3 include a 10-cell one-dimensional tabular histogram for each variable, where the cells are defined by dividing the interval between the variable's minimum and maximum value into 10 equal intervals. A histogram consists of the symbols "1" through "9", "*", and ".", where the symbol for each cell represents the cell frequency on a scale from 1 to 9. In particular, the cell with the largest number of observations (the "maximum cell count" in Tables 2 and 3) is always coded "9". To enhance the histogram's visual impact, cells with only 0 or 1 observation are considered special cases and designated with a "." or "*", respectively.

TABLE 2. Descriptive statistics for data set 1 (171 records), including means, minima, maxima, and tabular histograms with maximum cell counts. The histograms represent cell counts on a scale of "1" to "9". The symbols "." and "*" represent the particular instances of 0 and 1 records, respectively.

Variable and code description	Mean	Minimum	Maximum	Histogram	Max. cell count
y ET50 (h)	139.3	1.5	1182.0	932111...*	109
ln y ln (ET 50)	4.02	0.41	7.07	3322496751	39
x_1 TGP % (%)	122.6	111.0	141.4	1489.23.22	55
x_2 Depth (m)	0.54	0.14	1.00	21...9...*	144
x_3 Temperature (°C)	13.1	8.0	20.0	3139252.31	60
x_4 Fish length (mm)	119.8	45.0	209.0	31898392*3	36
x_5 BP (mmHg)	755.6	736.0	761.6	3.....3992	64
Species[a]	—	1	4	4..3..5..9	81

[a] 1 = chinook, 2 = coho, 3 = sockeye, 4 = steelhead.

TABLE 3. Descriptive statistics for data set 2 (81 records), including means, minima, maxima, and tabular histograms with maximum cell counts. The histograms represent cell counts on a scale of "1" to "9". The symbols "." and "*" represent the particular instances of 0 and 1 records, respectively.

Variable and code description	Mean	Minimum	Maximum	Histogram	Max. cell count
y ET 50 (h)	79.8	1.5	1182.0	91*1**...*	67
ln y ln (ET50)	3.06	0.41	7.07	8844496221	16
x_1 TGP% (%)	126.2	111.0	141.4	3179.67.45	18
x_2 Depth (m)	0.47	0.14	1.00	41...9...*	54
x_3 Temperature (°C)	12.8	8.3	16.0	*..49.3.33	35
x_4 Fish length (mm)	112.5	45.0	150.0	121612*1*9	35
x_5 BP (mmHg)	753.8	736.0	760.0	3......3.9	52
x_6 O_2% (%)	117.2	40.5	307.9	239511****	37
x_7 N_2% (%)	128.3	97.3	163.9	1*29843111	26
x_8 ONR	0.94	0.25	3.16	14911.*.**	47
Species[a]	—	1	4	4..3..4..9	38

[a] 1 = chinook, 2 = coho, 3 = sockeye, 4 = steelhead.

In data set 1 (Table 2) notice that the response variable y (ET50) ranges from 1.5 to 1182 h with most of the data skewed towards low values of y (i.e. rapidly lethal responses). The log-transformed responses, in comparison, are more uniformly distributed. The major explanator, TGP% (x_1), ranges from 111.0 to 141.4% with little information at low levels. In fact, there are only six records with TGP% below 115%. Most tests (144 records) were performed with a water depth (x_2) of 0.6 m. A reasonable range of depths is available, however, between 0.1 and 0.3 m, although this is not evident in the tabular histogram. Water temperatures (x_3) and fish lengths (x_4) are fairly evenly distributed over their ranges. Levels of BP (x_5) are skewed towards the maximum value. The narrow range of BP levels available in the literature data makes it unlikely that a significant BP effect can be proved from these data. Four salmonid species are represented, including 28 chinook (*Oncorhynchus tshawytscha*), 23 coho (*O. kisutch*), 39 sockeye (*O. nerka*) and 81 steelhead (*Salmo gairdneri*) records.

In data set 2 (Table 3) the distribution of y (ET50) differs little from the distribution in data set 1,the range remaining the same with most of the data skewed toward small values of y. Similarly, the ranges of x_1 (TGP%), x_2 (depth), and x_5 (BP) are essentially unchanged, with points removed primarily from the middle of each range. By contrast, x_3 (temperature) and x_4 (fish length) have reduced ranges, due primarily to the loss of points with high values of x_3 and x_4. Data set 2 also includes the three variables O_2% (x_6), N_2% (x_7), and ONR (x_8) discussed earlier. Most oxygen levels lie between 80 and 140%, and nitrogen levels are concentrated between 120 and 140%. Although ONR ranges from 0.25 to 3.16, roughly 80% of the records in this data set have ONR values close to 1.0. The species in data set 2 appear in nearly the same proportions as in data set 1, as evidenced by the fact that the two tabular histograms are almost identical. Explicitly, data set 2 includes 16 chinook, 13 coho, 14 sockeye, and 38 steelhead records.

To explore possible interactions between the main explanator x_1 (TGP%) and the ancillary variables (x_2-x_8), Tables 4 and 5 present a series of two-dimensional (9 × 9) tabular histograms for data sets 1 and 2, respectively. These histograms represent record frequencies and scaled response plots of y (ET50) and ln y for each combination of x_1 plus one of the variables x_2-x_8. The frequency histograms follow the notation (using "1" through "9", "*", and ".") described earlier for one-dimensional histograms. A cell in a two-dimensional histogram is a rectangle of values for x_1 and x_i, with $i = 2, \ldots, 8$. On the horizontal axis, values x_1 are divided into nine equal intervals between the minimum and maximum for x_1. Similarly, on the vertical axis, values of x_i ($i > 1$) are divided into nine equal intervals between the minimum and maximum for x_i. This gives a total of 81 (9 × 9) rectangular cells for the histogram. The character shown in any cell position represents the number of data points available within that cell. One can inspect the

TABLE 4. Two-dimensional (9 × 9) tabular histograms for data set 1. The table represents the five possible factor pairs with x_1 (TGP%) as the first factor. In each plot, x_1 increases from left to right, and the second factor increases from bottom to top. Histograms for data frequency, mean response y (ET50), and mean ln y are shown. The range of values for each factor is shown in Table 2. Other ranges are indicated below. See the text for an explanation of the histogram symbols.

	Data frequency	Plot of y	Plot of ln y
x_2 (depth)	*........	9........	9........
Max. cell count = 46	....	....	....
Min. $y = 3$	....	....	....
Max. $y = 1182$	....	....	....
Min. ln $y = 0.83$	.66921322	.32111111	.77533211
Max. ln $y = 7.07$	....	....	....
	....	....	....
	1......	41.1.....	84.3.....
	2121.....	2221.....	7665.....
x_3 (temp.)	...3.....	...1.....	...6.....
Max. cell count = 11	.373.....	.221.....	.774.....
Min. $y = 3$	...8.2...	...1.1...	...5.3...
Max. $y = 1182$	*579.*1..	4231.11..	8675.54..
Min. ln $y = 0.83$	.28......	.22......	.66......
Max. ln $y = 7.07$	.9398.878	.3211.111	.8753.211
	5..8.....	2..1.....	7..5.....
	.**3.....	.411.....	.855.....
	77.....	9321.....	9875.....
x_4 (length)	.*14.....	.611.....	.966.....
Max. cell count = 16	..*......	..1......	..6......
Min. $y = 3$	..13.....	..22.....	..76.....
Max $y = 777$	....5.555	....1.111	....3.211
Min. ln $y = 0.83$	*198.....	6131.....	9585.....
Max. ln $y = 6.50$	1765.....	2531.....	6975.....
	*718.21..	2221.11..	7776.34..
	14.1.....	45.1.....	88.5.....
	1.31.....	9.32.....	9.77.....
x_5 (BP)	...4.....	...1.....	...5.....
Max. cell count = 28	163*3.333	93211.111	97733.211
Min. $y = 3$	.597.....	.431.....	.876.....
Max. $y = 834$	.**4.21..	.611.11..	.956.34..
Min. ln $y = 0.83$	....	....	....
Max. ln $y = 6.63$	....	....	....
	....	....	....
	....	....	....
	2..3.....	3..1.....	7..6.....
Species no.[a]	4*9564.444	95211.111	98753.211
Max. cell count = 21	3.447.21..	.961.11..	.986.44..
Min. $y = 3$	2.163.....	.342.....	.786.....
Max. $y = 486$	13*27.....	7152.....	8586.....
Min. ln $y = 0.83$			
Max. ln $y = 6.19$			

[a] 1 = chinook, 2 = coho, 3 = sockeye, 4 = steelhead.

frequency histograms to detect weaknesses in the data, that is, factor values for which no information is available. These appear as periods ("."). Conversely, a "9" in the frequency histogram indicates that numerous records (up to the maximum cell count indicated) are available in that cell.

The response histograms in Tables 4 and 5 represent y and ln y as functions of two variables, x_1 and x_i with $i > 1$. Like the corresponding frequency histograms, the response histograms involve 81 cells in x_1 and x_i. When there are no data in a cell, each type of histogram indicates this with the symbol ".". When data are available, the response histogram uses the symbols "1" to "9" to represent the *mean* response (mean y or mean ln y) within the cell on a scale of 1 to 9. Notice that, when a cell contains more than one data point, the value of the response in that cell is potentially ambiguous; the mean value within a cell serves as a compromise. It may happen that the maximum value of the response is not the maximum cell average, because the maximum value may occur in a cell where lower responses are also observed. Similar remarks apply to the minimum. Thus, Tables 4 and 5 show for each histogram

TABLE 5. Two-dimensional (9 × 9) tabular histograms for data subset 2. The table represents the seven possible factor pairs with x_1 (TGP%) as the first factor. In each plot, x_1 increases frm left to right, and the second factor increases from bottom to top. Histograms for data frequency, mean response y (ET50), and mean ln y are shown. The range of values for each factor (minimum and maximum) is shown in Table 3. Other ranges are indicated below. See the text for an explanation of the histogram symbols.

	Data frequency	Plot of y	Plot of ln y
x_2 (depth)	*........	9........	9........
Max. cell count = 13	....	....	....
Min. $y = 3$	....	....	....
Max. $y = 1182$	....	....	....
Min. ln $y = 0.83$	...973867	...111111	...533211
Max. ln $y = 7.07$	....	....	....
	....	....	....
	1......	41.1.....	84.3.....
	4273.....	2221.....	7665.....
x_3 (temp.)	...6.3...	...1.1...	...5.3...
Max. cell count = 9	*2.3.*2..	41.1.11..	84.5.54..
Min. $y = 3$	..39.....	.22......	.66......
Max. $y = 1182$	....	....	....
Min. ln $y = 0.83$	....9.989	....1.111	....3.211
Max. ln $y = 7.07$	6..9.....	2..1.....	7..5.....
	....	....	....
	....	....	....
	*........	9........	9........
x_4 (length)	....9.989	....1.111	....3.211
Max. cell count = 9	*........	6........	9........
Min. $y = 3$	.2.*.....	.1.1.....	.5.3.....
Max $y = 1182$	....	....	....
Min. ln $y = 0.83$	2.24.....	2.11.....	6.65.....
Max. ln $y = 7.07$	2329.42..	3221.11..	8776.34..
	...2.....	...1.....	...5.....
	2.4......	9.2......	9.7......
	*.*2.....	5.82.....	9.97.....
x_5 (BP)	259*9.989	92211.111	96733.211
Max. cell count = 9	....	....	....
Min. $y = 3$	...8.42..	...1.11..	...6.34..
Max. $y = 834$	....	....	....
Min. ln $y = 0.83$	....	....	....
Max. ln $y = 6.63$	....	....	....
	....	....	....
	....	....	....
	6..9.....	3..1.....	7..6.....
x_6 (O_2%)	........*	1	2
Max. cell count = 14	.......*.	.......1.	.......2.
Min. $y = 2$	........*	1	2
Max. $y = 1182$	........*	1	1
Min. ln $y = 0.41$	.....****	1111	5211
Max. ln $y = 7.07$	..*...221	..2...111	..7...211
	3493231	912111111	967543311
	5.*32.*.*	2.111.1.1	7.652.2.1
	..*.*.***	..1.1.111	..6.2.211
x_7 (N_2%)	.......**	11	11
Max. cell count = 14	......*.1	......1.1	......2.1
Min. $y = 2$	....*..1*	....1..11	....2..11
Max. $y = 834$	..*31.12*	..111.111	..663.211
Min. ln $y = 0.41$	..*.325**	..1.11111	..6.43311
Max. ln $y = 6.63$	4349*.*.*	32311.1.1	76764.2.1
	1....*..*	9....1..1	9....5..2
	..*......	..3......	..8......
	.......**	11	22

TABLE 5. (*Concluded*)

	Data frequency	Plot of y	Plot of $\ln y$
x_8 (ONR)	........*	1	2
Max. cell count = 13	.......*.	.......1.	.......2.
Min. y = 2	....	....	....
Max. y = 1182	........*	1	2
Min. $\ln y$ = 0.41	.....*..*	.....1..1	.....5..1
Max. $\ln y$ = 7.07	..*...***	..2...111	..7...211
	*.4942521	9.2111111	9.7543311
	54.*2.111	21.11.111	76.52.211
	..13*.***	..111.111	..652.211
Species no.[a]	4**.*9.989	91.11.111	95.63.211
Max. cell count = 9	3...8.42..	...2.11..	...6.44..
Min. y = 3	2.39*.....	.341.....	.775.....
Max. y = 486	17*.8.....	71.2.....	85.6.....
Min. $\ln y$ = 0.83			
Max. $\ln y$ = 6.19			

[a] 1 = chinook, 2 = coho, 3 = sockeye, 4 = steelhead.

the minimum and maximum cell mean values of the response. The symbols "1" to "9" represent the response scaled between these two values.

The combined information in the frequency and response histograms indicates both (1) uncertainty in the data, based on record frequency, and (2) trends (if any) in response to factor pairs. For example, if the response plot shows a "9" where the frequency plot shows "*", then the response appears high in that cell, although it is based on only one data point. Similarly, a response of "5" with a corresponding frequency of "9" indicates a midlevel response based on many data points. If a series of four adjacent cells show response values of "1", "3", "5", and "6", then this suggests an increasing trend. To the extent that trends exist, they are usually more evident in the plot of $\ln y$, rather than the plot of y.

The most obvious feature of the data presented in Tables 4 and 5 is the uneven distribution of records over the full range of each factor pair. In no case is there a full representation of observations at the minima and maxima of the factor ranges. Furthermore, in several cases, very large areas exist where no information is available. For example, in both tables the frequency histogram for TGP% (x_1) and depth (x_2) indicates that most of the records occur at about 0.6 m and at 0.1−0.3 m, with only a single record at 1.0 m. Furthermore, high levels of TGP% occur in the data only when the depth is about 0.6 m.

In spite of the weaknesses of the data, several possible relationships can be seen in the response plots of Tables 4 and 5. The response to TGP% (x_1), the main explanator, is consistent; that is, both y and $\ln y$ are high for low values of x_1 (near the left of each response plot) and low for high values of x_1. In plain terms, fish live longer with lower levels of gas supersaturation. To see if an ancillary factor ($x_2 - x_8$) modifies the effect of TGP% (x_1), it is necessary to look for trends within individual columns (i.e. fixed levels of x_1) of the response plots. In particular, we note the following apparent effects of ancillary factors.

(1) In general, fish appear to live longer at greater depths. This is indicated by larger values of y and $\ln y$ at higher positions in the first and second columns of the x_1x_2-plots in Table 4. The limited available data, however, make this a somewhat tenuous conclusion, particularly since the large value of y at a depth of 1.0 m is based on only one observation.

(2) The effect of temperature is quite variable; however, the first and second columns of the x_1x_3-plot for $\ln y$ in Table 4 suggest that fish might live longer at lower temperatures.

(3) The response to fish size is extremely variable. The x_1x_4-plot for $\ln y$ in Table 5 gives some hint that smaller fish live longer.

(4) The response to BP (x_5) is too variable to indicate a trend.

(5) The x_1x_6-plot for $\ln y$ in Table 5 shows rather convincingly that, for a given level of TGP%, fish live longer when the O_2% component is higher.

(6) The x_1x_7-plot for $\ln y$ in Table 5 reinforces the previous conclusion. Fish appear to live longer when the N_2% component is lower.

(7) The x_1x_8-plot for $\ln y$ in Table 5 is consistent with the previous two conclusions; that is, fish live longest when ONR is largest. Incidentally, it is not surprising that conclusions 5, 6, and 7 are redundant, since any pair of the variables x_1, x_6, x_7, and x_8 determines the other two, as explained earlier in connection with (2.1) and (2.2).

(8) The response plots for species in Tables 4 and 5 illustrate the differences in data frequencies, with steelhead data available over the largest range of TGP% and coho data over the smallest range. No clear species response is indicated, although Table 4 might suggest that sockeye (species 3) are the most resistant to lethal effects of gas supersaturation.

Figures 1 and 2 show plots of ET50 (y) versus TGP% (x_1) for data sets 1 and 2, respectively. These suggest that ET50 decays exponentially as TGP% increases, a possibility we explore further in the analysis to follow. However, the figures also exhibit considerable data scatter, perhaps due to biological variability and/or the effect of ancillary factors. Notice that no data points lie below $x_1 = 111\%$. Furthermore, a large number of points are lost from data set 1 (Fig. 1) by the requirement in data set 2 (Fig. 2) that records should include information on O_2% and N_2%.

Modeling

The preceding exploratory data analysis shows that ET50 (y) exhibits the strongest relationship to TGP% (x_1) among the factors considered here. There is some evidence that

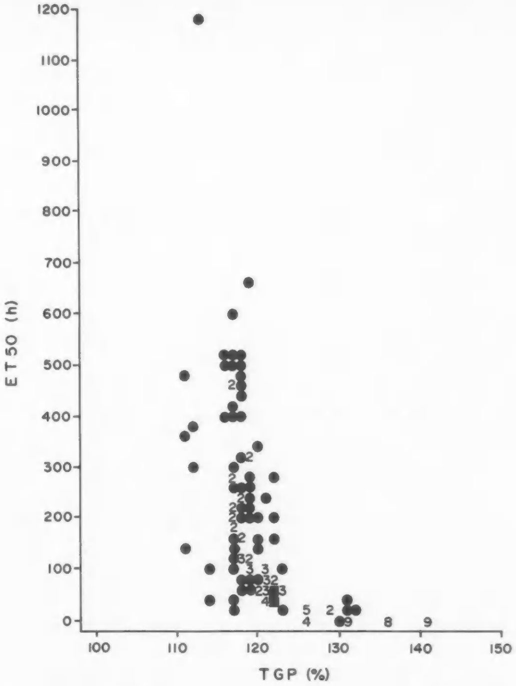

FIG. 1. ET50 plotted against TGP% for data set 1. Records are indicated by a circle, or by the number of points (up to 9) in one location, or by a square for 10 or more points in one location.

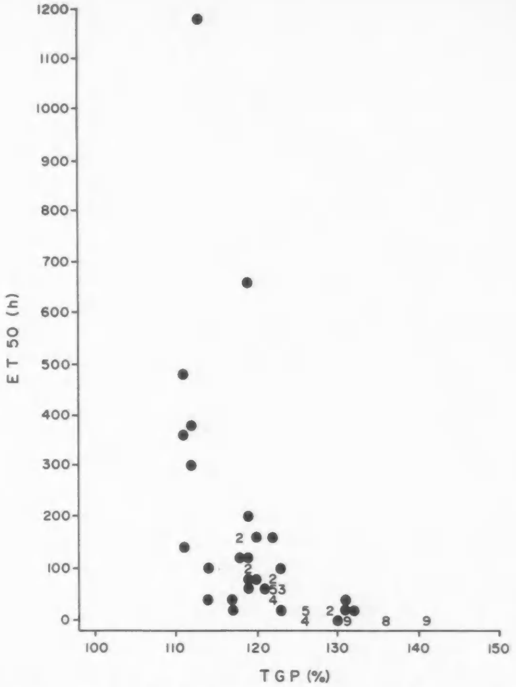

FIG. 2. ET50 plotted against TGP% for data set 2. Records are indicated by a circle, or by the number of points (up to 9) in one location.

other factors, such as depth (x_2), temperature (x_3), fish size (x_4), and component gas levels (x_6, x_7, x_8), may modify the ET50 response to TGP%. To identify such relationships and test their statistical significance, we apply the general multivariate dose−response model described in the companion paper by Schnute and Jensen (1986). We refer to equations from that paper by denoting them here in square parentheses; for example, [1.1] refers to the first equation in that paper, as distinguished from the first equation (1.1) here.

The model itself is given by equations [2.1]−[2.3]. It includes m factors ($x_1, \ldots, x_m$), a single response (y), and $2m + 2$ parameters: $m + 1$ coefficients ($p, q_1, \ldots, q_m$) and $m + 1$ exponents ($\alpha_1, \ldots, \alpha_m, \gamma$). A particular coefficient q_i indicates the strength of relationship between the factor x_i and the response y. The exponent α_i determines a suitable scaling of x_i, and similarly, γ determines a scaling of y. Together, the coefficients and exponents determine 1 of 16 possible characteristic relationships (described by Schnute and Jensen 1986) between x_i and y. To apply the model [2.1]−[2.3], we must choose typical low and high values for the variables (u_i and U_i for x_i, and v and V for y). For data sets 1 and 2, respectively, these are taken simply to be the minimum and maximum values given in Tables 2 and 3. For example, $v = 1.5$ h and $V = 1182$ h in the model for both data sets.

We employed the simplex search method (Mittertreiner and Schnute 1985) to obtain parameter estimates for 18 dose−response models (Table 6), where each model is distinguished by a data set and a particular choice of factors used to explain ET50. Models 1−11 pertain to data set 1. Of all available factors, it turns out that TGP% best explains ET50. Consequently, model 1 includes only this single factor, and models 2−5 include this factor in combination with one ancillary variable. The best second factor turns out to be depth, and models 6−8 are three-factor models that include TGP% and depth, along with one of the remaining ancillary variables. Similarly, models 9 and 10 are four-factor models that include the previous best three factors. Finally, model 11 is a complete five-factor model. These models progress according to a bottom-up (as opposed to top-down) philosophy: we add factors as they improve the previous best fit.

Models 12−18 pertain to data set 2. The first, model 12, includes only TGP%. The remaining models include ancillary factors related to the extra information in data set 2 on components of dissolved gases. As described earlier, any two of the four factors TGP%, O_2%, N_2%, and ONR determine the other two. Models 13−18 include the six possible choices of factor pairs from this list. No other factor combinations were attempted for data set 2, since ancillary variables such as depth and length are better represented within data set 1.

Tables 7 and 8 can be used to assess how well the various models fit the data. Table 7 lists estimated standard deviations for the model parameter estimates in Table 6, based on [4.13] and [4.14]. Table 8 shows the results of significance tests, based on [3.6], to assess whether or not adding ancillary variables improves the model fit. Furthermore, the distributions [4.15] and [4.16] can be used to calculate one-sided and two-sided confidence intervals for both model predictions y^* and new observations of $\hat{y}$ of ET50. In particular, [4.16] is used to compute the confidence bands shown in Fig. 3. Finally, given some minimum tolerable ET50 ($\hat{y}_{\min}$), [4.20] can be solved

TABLE 6. Parameter estimates for models generated using data sets 1 and 2. Each model is characterized by the data set number and by the factors considered. The symbol "+" or "−" indicates whether a factor is included or excluded, respectively, from a given model.

Model No.	Data set	Factor[a] 1 2 3 4 5 6 7 8	α_1	α_2	α_3	α_4	α_5	α_6	α_7	α_8	γ	p	q_1	q_2	q_3	q_4	q_5	q_6	q_7	q_8
1	1	+−−−−−−−	−0.4								−0.074	0.00	−0.99							
2	1	++−−−−−−	−1.2	1.8							−0.054	0.09	−1.02	0.21						
3	1	+−+−−−−−	−0.4		−8.8						−0.069	0.06	−0.98		−0.08					
4	1	+−−+−−−−	−0.5			−7.2					−0.067	0.20	−0.98			−0.20				
5	1	+−−−+−−−	−0.6				2.1				−0.068	−0.01	−1.00				0.04			
6	1	+++−−−−−	−1.2	1.8	0.5						−0.053	−0.08	−1.03	0.21	−0.01					
7	1	++−+−−−−	−1.5	1.0		−3.6					−0.041	0.29	−1.01	0.24		−0.30				
8	1	++−−+−−−	−1.2	1.8			7.2				−0.054	0.08	−1.03	0.21			0.01			
9	1	++++−−−−	−1.5	1.0	6.8	−3.6					−0.041	0.29	−1.01	0.24	0.00	−0.30				
10	1	++−++−−−	−1.7	0.9		−3.2	2.2				−0.032	0.26	−1.01	0.23		−0.31	0.05			
11	1	+++++−−−	−1.5	0.9	−12.9	−2.9	6.4				−0.037	0.28	−1.00	0.22	−0.05	−0.30	0.05			
12	2	+−−−−−−−	0.6								−0.115	−0.05	−0.89							
13	2	+−−−−+−−	1.8					1.2			−0.170	0.14	−1.00					0.36		
14	2	+−−−−−+−	2.1						−1.6		−0.172	0.04	−0.82						−0.36	
15	2	+−−−−−−+	1.7							0.8	−0.172	0.14	−0.97							0.37
16	2	−−−−−++−						1.2	−0.1		−0.160	−0.68						−1.58	−1.79	
17	2	−−−−−+−+						0.3		0.1	−0.163	−0.59						−8.31		8.57
18	2	−−−−−−++							−0.8	0.9	−0.136	−0.71							−2.17	−1.98

[a] 1 = TGP%, 2 = depth, 3 = temperature, 4 = length, 5 = BP, 6 = O_2%, 7 = N_2%, 8 = ONR.

numerically to obtain (one-sided) tolerance limits for TGP% (x_1). Table 9 presents such results for models found to be significant, based on tolerance limits of ET50 set at both 50 and 20 d.

Before discussing specific models, we make the following general observations about the parameter estimates (Table 6) and their standard deviations (Table 7).

(1) As anticipated by Schnute and Jensen (1986), most coefficients (p, q_1) have magnitude 1 or less. Since the magnitude of q_i reflects the importance of factor i, Table 6 immediately suggests that the most important factor is x_1, TGP%.

(2) Estimates of the coefficients are reasonably stable, regardless of which ancillary factors are included in the model. For example, inspection of the appropriate columns in Table 6 shows that p and $q_1 - q_5$ are similar for all models (1−11) of data set 1. Hence, the apparent importance of any factor is somewhat independent of the other factors considered in the model.

(3) Table 7 shows a similar stability in the standard deviations for the coefficient estimates.

(4) Tables 6 and 7 together can be used to suggest for any particular factor i whether $q_i > 0$, $q_i < 0$, or $q_i = 0$, that is, whether an increase in x_i tends to increase, decrease, or have no effect on the response y. For example, q_1 is typically near -1 with a standard deviation less than 0.1. Consequently, we can say with some certainty that $q_1 < 0$; that is, an increase in TGP% reduces ET50, as indicated earlier by our exploratory data analysis. Similarly, q_2 is roughly 0.2 with a standard deviation around 0.1. This suggests that depth has a positive influence on ET50; that is, a greater depth leads to higher ET50, again consistent with our exploratory data analysis. In contrast with q_1 and q_2, q_5 is roughly 0.05 with a standard deviation of 0.4. Thus, we cannot eliminate the possibility that $q_5 = 0$, that is, that BP has no influence on ET50.

(5) Estimates of the exponents α_i are less constant from model to model than estimates of the coefficients. This suggests that the influence of a factor x_i (indicated by q_i) is better defined than its transform (indicated by α_i). For example, notice that α_3 varies from -12.9 to 6.8 in Table 6 with standard deviation as high as 410 in Table 7. The fact that α_3 is ill-determined is not surprising, however, in view of the fact that q_3 (by the reasoning in point 4 above) is essentially 0. In general, if a factor has no effect in the model, its transformation is irrelevant. This is evident in [2.1]−[2.3], since, if $q_i = 0$ for some i, then the parameter α_i no longer enters the model. By contrast with α_3, α_1 is better determined (since $q_1 \neq 0$), although the standard deviation of α_1 in Table 7 is typically of the same magnitude as the estimate for α_1 in Table 6.

(6) In contrast with the exponents α_i, the exponent γ for the dependent variable ET50 is relatively constant from model to model. Furthermore, γ has much smaller standard deviations than the other exponents. For data set 1, γ is essentially 0, corresponding to the log transform [2.5]. Hence, it appears that ET50 follows a typical exponential pattern in response to TGP%.

Results

This section gives a detailed discussion of the various models considered for data sets 1 and 2. We use the larger data set 1 to draw inferences on the factors TGP% (x_1), depth (x_2), temperature (x_3), length (x_4), and BP (x_5). The smaller data set 2 is used only for inferences on the possible combined effects of

TABLE 7. Standard deviations of parameter estimates for models listed in Table 6.

Model No.	Data set	α_1	α_2	α_3	α_4	α_5	α_6	α_7	α_8	γ	p	q_1	q_2	q_3	q_4	q_5	q_6	q_7	q_8
1	1	1.0								0.005	0.10	0.07							
2	1	1.0	1.2							0.005	0.11	0.08	0.10						
3	1	1.4		10						0.051	0.08	0.04		0.05					
4	1	1.4			5.1					0.050	0.10	0.04			0.08				
5	1	1.5				2				0.053	0.06	0.04				0.04			
6	1	1.0	1.2	50						0.005	0.12	0.09	0.11	0.03					
7	1	1.4	1.2		1.3					0.052	0.13	0.04	0.09		0.07				
8	1	1.4	1.3			1681				0.054	0.11	0.04	0.10			0.04			
9	1	9.9	1.2	410	1.3					0.004	0.14	0.09	0.09	0.04	0.07				
10	1	1.4	1.3		1.1	155				0.054	0.13	0.04	0.09		0.07	0.04			
11	1	1.5	1.4	258	1.0	164				0.055	0.13	0.04	0.10	0.05	0.07	0.04			
12	2	1.9								0.080	0.07	0.05							
13	2	1.8					0.7			0.082	0.12	0.05					0.09		
14	2	2.0						2.7		0.078	0.12	0.05						0.08	
15	2	1.8							0.5	0.081	0.13	0.05							0.09
16	2						0.2	0.8		0.054	0.10						0.11	0.10	
17	2						0.1		0.1	0.053	0.11						0.44		0.46
18	2							0.8	0.2	0.055	0.10							0.12	0.14

the factors related to components of dissolved gases, namely, TGP% (x_1), O_2% (x_6), N_2% (x_7), and ONR (x_8). To implement the stepwise philosophy that guides our approach to each data set, we measure statistical significance with the statistic B in [3.6]. Theoretical problems with stepwise regression are well known. As Kendall and Stuart (1979, p. 358) pointed out,[1] background knowledge usually plays an important role in the selection of predictor variables. Particularly since the F-distribution of B in [3.6] is only approximate for our nonlinear model, we take a somewhat informal approach, guided by our exploratory data analysis. In Table 8, we report not only the results of each hypothesis test, but also the probability level (P-level) of B in [3.6], given that the null hypothesis is true. Thus, a small P-level favors rejecting the null hypothesis.

Data Set 1

Model 1

This model predicts ET50 exclusively from TGP% (x_1) and exhibits a typical dose−response relationship (Fig. 3). Both two-sided and one-sided confidence bands indicate a large area of uncertainty around the predicted ET50 curve at TGP% levels lower than about 125%. This uncertainty, a result of the scatter of points shown in Fig. 1, probably is due mainly to a combination of biological variability and measurement errors. However, the data were obtained under various experimental conditions (i.e. various levels of ancillary factors) and with various species. Therefore, models that include ancillary factors in addition to TGP% may explain more of the variability than model 1, and thus be more useful in predicting salmonid mortality in response to gas supersaturation.

TABLE 8. Minimum A-values (in units of 10^3) and significance tests for the 18 models listed in Table 6. The symbol "+" or "−" indicates whether a factor is included or excluded, respectively, from a model. Asterisks in the final column indicate significant improvements in fit due to adding the ancillary variables (*significant at 10% level, **significant at 5% level, ***significant at 1% level).

Model No.	Data set	Factor[a] 1 2 3 4 5 6 7 8	Min. A	H_0	H_1	P-level
1	1	+−−−−−−−	1020			
2	1	++−−−−−−	942	1	2	0.010**
3	1	+−+−−−−−	1000	1	3	0.511
4	1	+−−+−−−−	973	1	4	0.098*
5	1	+−−−+−−−	1010	1	5	0.802
6	1	+++−−−−−	942	2	6	1.000
7	1	++−+−−−−	832	2	7	0.002***
8	1	++−−+−−−	942	2	8	1.000
9	1	++++−−−−	832	7	9	1.000
10	1	++−++−−−	822	7	10	0.981
11	1	+++++−−−	818	10	11	1.000
12	2	+−−−−−−−	70			
13	2	+−−−−+−−	56	12	13	0.002***
14	2	+−−−−−+−	54	12	14	0.001***
15	2	+−−−−−−+	56	12	15	0.001***
16	2	−−−−−++−	50			
17	2	−−−−−+−+	51			
18	2	−−−−−−++	51			

[a] 1 = TGP%, 2 = depth, 3 = temperature, 4 = length, 5 = BP, 6 = O_2%, 7 = N_2%, 8 = ONR.

Model 2

Including water depth (x_2) as a second explanator of ET50 significantly (Table 8) reduces the minimum A-value. Furthermore, as discussed earlier in connection with Table 6 and 7, $q_2 > 0$; that is, fish live longer when greater water depth is available. A plot of ET50 contours (Fig. 4) in response to TGP% and depth illustrates both the exponential response of ET50 to TGP% (since the distance between ET50 contours

---

[1] These authors are concerned with theoretical problems in the theory of stepwise regression. They conclude that "Fortunately for human impatience, life has a habit of being less complicated than it need be, and we usually escape the worst possible consequences of simplifying procedures for the selection of 'predictor' variables; we usually have enough background knowledge, even in new fields, to help us avoid the more egregious oversights, but the theoretical problem remains."

TABLE 9. TGP% levels associated with ET50 set at 50 and 20 d. The two columns in each case give values of TGP% computed from the model and from a (one-sided) lower 95% confidence limit for the model, respectively. Each row in the table applies to a specified model (1, 2, 4, 7, 12, or 15) with various specified levels of ancillary factors (depth, length, and ONR).

					ET50 = 50 d		ET50 = 20 d	
Model No.	Data set	Depth (m)	Length (mm)	ONR	Model	Lower limit	Model	Lower limit
1	1	—	—	—	110.9	104.4	114.0	108.0
2	1	0.1	—	—	109.8	105.3	112.7	108.4
2	1	1.0	—	—	114.8	109.1	117.9	112.1
4	1	—	200	—	110.6	105.4	113.8	109.0
4	1	—	65	—	111.0	105.9	114.2	109.4
4	1	—	45	—	116.0	109.7	119.4	113.3
7	1	0.1	200	—	108.1	103.8	111.6	106.8
7	1	0.1	45	—	114.8	109.9	118.1	113.2
7	1	1.0	200	—	113.7	108.3	117.0	111.4
7	1	1.0	45	—	121.3	114.8	125.1	118.4
12	2	—	—	—	108.2	—[a]	111.6	101.2
15	2	—	—	0.5	107.7	—[a]	110.7	102.5
15	2	—	—	0.8	109.2	—[a]	112.2	104.2
15	2	—	—	1.0	110.2	—[a]	113.1	105.2
15	2	—	—	1.2	111.1	—[a]	114.0	106.0
15	2	—	—	2.0	114.4	—[a]	117.3	108.0

[a] The computed value is less than 100% in these cases.

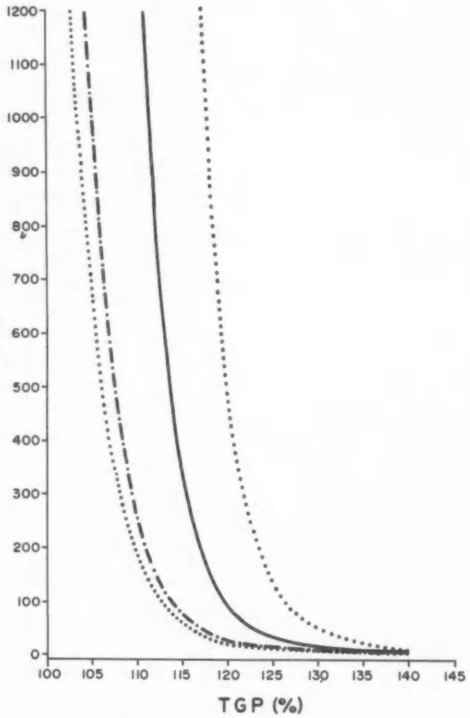

FIG. 3. Predicted ET50 (solid line) with two-sided (dotted lines) and one-sided (dash-dotted line) 95% confidence intervals, calculated using model 1.

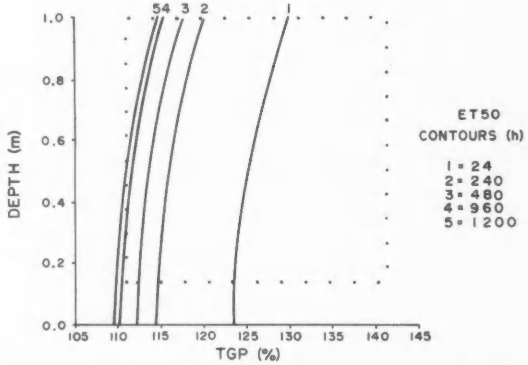

FIG. 4. ET50 contours in response to TGP% (x_1) and water depth (x_2), calculated from model 2. Dotted lines indicate the data window for x_1 and x_2: u_1, U_1, u_2 and U_2.

becomes smaller at lower levels of TGP%) and the beneficial effect of greater available depths (since ET50 contours bend to the right with increasing depth). Thus, for the range of depth (0.1−1.0 m) modeled, fish appear to use a significant portion of the water column available to them, thereby finding protection against gas supersaturation. Notice that we draw this inference by including depth as a second explanator of ET50, rather than simply by correcting TGP% for the water depth as in (1.5). M. Shrimpton (pers. comm.) has found that the modal depth of juvenile coho salmon in a 3-m water column varies with TGP%. At low levels of gas supersaturation, the modal depth is below the compensation depth, so that fish appear to obtain protection for themselves when swimming in deep water. However, at TGP% levels higher than 112%, the modal

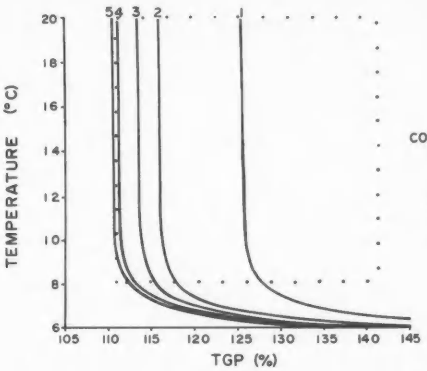

FIG. 5. ET50 contours in response to TGP% (x_1) and temperature (x_3), calculated from model 3. Dotted lines indicate the data window for x_1 and x_3: u_1, U_1, u_3, and U_3.

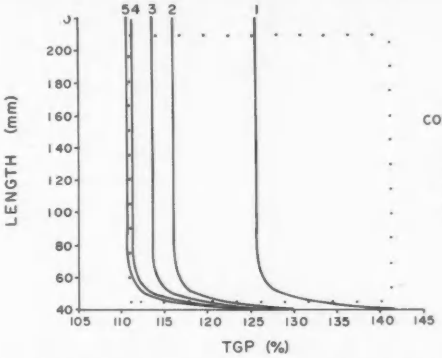

FIG. 6. ET50 contours in response to TGP% (x_1) and fish length (x_4), calculated from model 4. Dotted lines indicate the data window for x_1 and x_4: u_1, U_1, u_4, and U_4.

depth rises above the compensation depth. In such cases, overinflated swim bladders may prevent fish from obtaining the benefits of greater depths.

Model 3

Temperature (x_3) does not significantly modify the ET50 response to TGP% (Table 8). This is consistent with the earlier discussion of Tables 6 and 7 in which it is shown that q_3 cannot be distinguished from 0 statistically. Figure 5 suggests that, at temperatures less than 10°C, fish live longer when subjected to lethal levels of gas supersaturation, although the effect must be recognized as perhaps statistically spurious. It has been conjectured that low temperature may have beneficial effects due to an increase in blood viscosity and a resulting increase in blood pressure that could inhibit bubble growth in the fishes' vascular system (L. Fidler, Department of Zoology, University of British Columbia, Vancouver, B.C., pers. comm.). Notice that, for temperatures from 10 to 20°C, the ET50 contours are nearly vertical in Fig. 5, indicating no effect of temperature on fish mortality. We suspect that if data were available for higher temperatures (above 20°C), the ET50 contours would probably begin to curve to the left as the upper lethal limit for temperature is approached. However, at present there is not enough information to allow us to speculate further about the possible interaction of temperature and TGP%.

Model 4

Fish length (x_4), as an ancillary factor to TGP%, appears marginally to improve the model fit (Table 8). The estimate for q_4 (−0.20, Table 6) indicates more rapid mortality (smaller ET50) for larger fish at a given lethal level of TGP%. This is illustrated in Fig. 6. Notice, however, that the modifying effect of fish size is present only between about 45 and 80 mm, with the ET50 contours bending sharply to the right. A possible explanation for this effect may be that larger fish would be more likely to possess numerous irregularities and discontinuities (i.e. bubble nucleation sites) of the inner walls of their blood vessels (L. Fidler, pers. comm.). Hence, gas bubbles would be more likely to form in larger fish, resulting in greater susceptibility to gas supersaturation. At present, this conclusion is tenuous and speculative, and may be based more on a poor data distribution in data set 1, which deals only with juvenile salmonids. Indeed, the tabular histograms (Tables 4 and 5) indicate that the interaction between TGP% and length is not very consistent, with large values of scaled ET50 occurring at both low and high levels of length. This could reflect a real phenomenon, based on different sensitivities of the fish at different life stages. If so, then our model would be inappropriate for a wider range of lengths, since it assumes a monotonic relation between the factors and the response. The more general model of Schnute and McKinnell (1984) could then be applied, but we do not explore this possibility here.

Model 5

Of the four factors $x_2 - x_5$ considered as ancillary factors to TGP% (x_1), BP (x_5), has the least significant modifying effect on fish mortality. The *P*-level associated with the test of model 5 versus model 1 is 1.0, an extreme indication that the null hypothesis (model 1) should not be rejected. Also, as discussed earlier in connection with Tables 6 and 7, the estimate for q_5 in model 5 is essentially 0. This lack of significance in BP is not surprising, given the limited available range of data (736−762 mmHg, Table 2). Since the measurement of TGP% automatically accounts for the atmospheric pressure at the water surface, one might expect BP to be a significant second factor if the real driving force for bubble formation is ΔP, rather than TGP%. More precisely, it follows from (1.2) that

$$\Delta P = \left[\frac{\text{TGP\%}}{100} - 1\right] \text{BP}$$

so that ΔP is directly proportional to BP for a fixed TGP%. We do not recommend ignoring BP in fish-rearing systems. For example, a rapid reduction in atmospheric pressure due to the movement of a storm front may put fish in jeopardy by causing TGP% (or ΔP) to shift past a critical point. In practice, then, the lowest possible BP values must be considered when determining the highest values of TGP% that may occur.

Models 6−8

These are three-factor models to be compared with model 2, the most successful two-factor model. Only one, model 7, gives a significant improvement (Table 8). This result is consistent with the models considered so far. We have already observed that depth (x_2) and length (x_3) individually are the most significant second factors; apparently, these two factors combined also improve the model's predictions. Furthermore, the estimates for q_2 (0.10 in model 2 and 0.09 in model 7) and q_4 (0.08 in model 4 and 0.07 in model 7) are remarkably con-

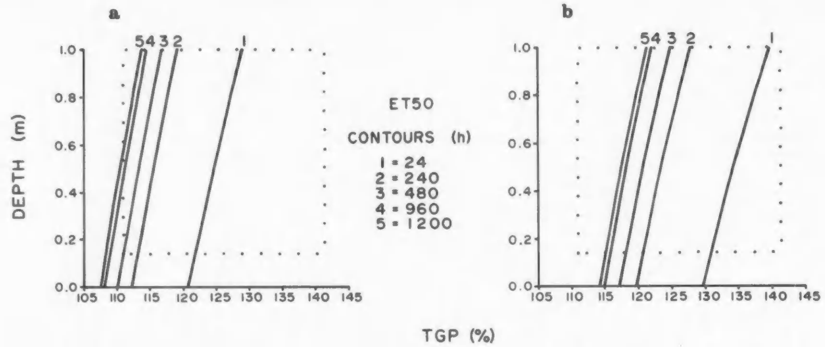

FIG. 7. ET50 contours from model 7 for fish length (x_2) set at (a) 200 mm and (b) 45 mm. In each panel, ET50 is represented as a function of TGP% (x_1) and depth (x_2). Dotted lines indicate the data window for x_1 and x_2.

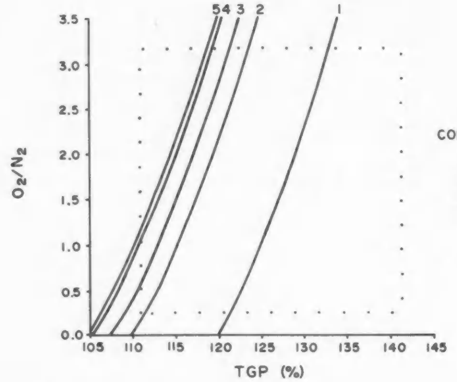

FIG. 8. ET50 contours in response to TGP% (x_1) and ONR (x_8), calculated from model 15. Dotted lines indicate the data window for x_1 and x_8.

sistent. Figure 7 illustrates the predictions of ET50 from model 7 based on TGP%, depth, and length. The figure shows TGP%-depth contours of ET50 for two lengths, 200 mm (Fig. 7a) and 45 mm (Fig. 7b). Each panel is similar to Fig. 4 (for model 2), but the contours in Fig. 7a are shifted to the right of those in Fig. 7b, thus illustrating that shorter fish tend to live longer.

Models 9–11

These correspond to attempts to extend model 7 (the most successful so far) to four-factor or five-factor models. In each case the resulting *P*-level is nearly 1.0; that is, no significant improvement is achieved. This reinforces what we might anticipate from the simpler two-factor models 2–5; temperature (x_3) and BP (x_5) are not proved to be useful ancillary factors.

Data Set 2

Model 12

This model is identical to model 1, except that it is based on the smaller data set 2, which includes information on component gases. Parameter estimates and their standard deviations for the two models are similar, except for α_1, as shown in the extract below from Tables 6 and 7:

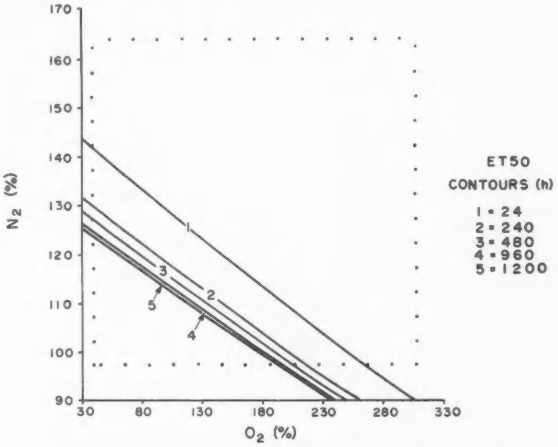

FIG. 9. ET50 contours in response to O_2% (x_6) and N_2% (x_7), calculated from model 16. Dotted lines indicate the data window for x_6 and x_7.

	Estimate		Standard deviation	
Parameter	Model 1	Model 12	Model 1	Model 12
p	0.00	−0.05	0.10	0.07
q_1	−0.99	−0.89	0.07	0.05
α_1	−0.4	0.6	1.0	1.9
γ	−0.074	−0.115	0.005	0.080

The standard deviations indicate that all changes in the estimates are not significant. The estimated coefficients (p, q_1) have similar standard deviations for both models; however, the estimated exponents for model 12 have notably larger standard deviations, indicating a loss of information in the smaller data set 2.

Models 13–15

These include the three gas component measurements O_2% (x_6), N_2% (x_7), and ONR (x_8) as ancillary factors to TGP%. In each case, the additional variable is highly significant, although the *A*-value in Table 8 indicates that model 14

(TGP% and N_2%) gives the best fit by a slight margin. Notice in Tables 6 and 7 that q_6, q_7, and q_8 all have nearly the same magnitude and standard deviation, thus confirming that each of these factors has roughly the same significance as an ancillary variable. Furthermore, q_6 and q_8 are both positive, while q_7 is negative. These results consistently indicate that at a higher component level of O_2% (or, equivalently, a lower level of N_2%), fish live longer when exposed to a prescribed lethal TGP% level. Figure 8 illustrates this by showing contours of ET50 in relation to TGP% and ONR from model 15. The contours slant to the right with a slight upward curvature, indicating a longer survival time (greater ET50) at higher ONR levels. However, as the level of ONR increases, the beneficial effect decreases, suggesting the existence of a critical upper limit for O_2%. This possibility may be important in fish culture operations that attempt to increase production by employing oxygen-supersaturated rearing environments without increasing rearing space or water flow.

Models 16−18

Theoretically, any two of the factors TGP%, O_2%, N_2%, and ONR should determine the other two. There are six possible such factor pairs, three of which are considered in models 13−15. The remaining models 16−18 consider the other three pairs, namely those involving O_2%, N_2%, and ONR. Curiously, these models, which exclude TGP%, give *A*-values (in the range 50 000 to 51 000) that are distinctly lower than the *A*-values for models 13−15 (in the range 54 000 to 56 000). Since all models 13−18 have the same number (six) of parameters, this suggests that those excluding TGP% are preferable, perhaps because the data are better known for O_2% and N_2% than for TGP%. Greater uncertainty in TGP% measurements is possible because the absolute accuracy for tensionometers is less than that for method of determining O_2% and N_2%. Figure 9 illustrates ET50 contours in response to O_2% and N_2%, according to model 16. The leftward slant of the contours indicates that, if one wishes to retain a constant ET50, then O_2% must be decreased when N_2% is increased, and vice versa.

Criteria for Safe Exposure

Our discussion so far pertains to finding those factors most influential on the ET50 response. It remains to specify critical safe levels for the influential factors. One approach to determining a critical value for a single factor x, discussed by Schnute and Jensen (1986), is to calculate from [2.8] the x-value associated with the response $y = \infty$. For example, consider model 1, where x is TGP%. It turns out from [2.8] that the critical level of TGP%, where ET50 = ∞, is 78.9%. This is well below the obvious safe limit at around 100%. A poor estimate for the critical value of x in this case is not surprising, since our data set contains too few observations at low values of TGP% to determine accurately the location of the asymptote where ET50 = ∞. Thus, an attempt to find a safe level by this method is necessarily an extrapolation. Furthermore, the method has the more serious flaw that it fails to take account of the model's statistical nature.

A better approach to the problem of finding critical levels is discussed by Schnute and Jensen (1986) in connection with formulas for confidence intervals around the response surface. This method begins by prescribing (1) a minimum tolerable response ($\hat{y}_{\min}$), such as a value of ET50 set at 50 d, and (2) a confidence level, such as 95%. Then, for any of the models 1−18 a critical value of x_1 (TGP%) can be determined, given the values of the remaining ancillary factors. This critical value has the property that when x_1 is at that level or lower, ET50 is guaranteed with 95% confidence to be at least as high as the prescribed minimum. The critical x_1 can be calculated by solving [4.20] numerically. Notice that this method, unlike the asymptote method, takes account of the fact that y is not precisely determined by the specified factors. Thus, we use a *confidence limit* for the model, rather than the model iself, in finding safe factor levels.

Table 9 presents the results of calculating critical TGP% levels by this method for two prescribed levels of ET50. These two exposure times, 50 and 20 d, are chosen as potentially representative of resident and migratory fish, respectively. The table shows the value of TGP% calculated both from the model and from the formula [4.20] for the model's lower 95% confidence limit. For example, suppose that one wishes to estimate a safe level for salmonid juveniles based on model 1 using the single factor TGP%. Then, for a 50-d exposure, one can be 95% confident that, at levels of 104.4 TGP% or less, 50% of the fish will live. Similarly, for 20-d exposures, at TGP% of 108.0 or less, 50% survival can be expected with 95% confidence. However, since the data considered here have not been obtained under identical experimental conditions, it may be misleading to determine critical levels using model 1, which ignores the influence of the associated ancillary variables.

To investigate the influence of ancillary factors, Table 9 shows similar calculations for various multifactor models (2, 4, 7, and 15) shown significant in Table 8. In each case, TGP% levels from the model and its lower 95% confidence limit are calculated at fixed levels of the ancillary factors. For the models of data set 1 (models 2, 4, and 7), critical TGP% levels for 50-d exposure range from 103.8 to 114.8%, depending on the levels of ancillary factors. Similarly, the critical levels for 20-d exposure range from 106.8 to 118.4%. These results suggest that there is no single safe level of gas supersaturation for salmonid juveniles, but rather a series of criteria dependent on associated depth and fish size. Models of data set 2 indicate a similar conclusion with regard to ancillary variables related to component gases. However, the smaller data set leads to greater uncertainty in the model's predictions. Indeed, the uncertainty is so great that we cannot calculate critical TGP% levels for a 50-d exposure time, even when values of ancillary variables are prescribed. Table 9 does illustrate from model 15 the significance of the ancillary factor ONR on critical TGP% levels for 20-d exposure. These range from 102.5 to 108.0%. Notice, however, that 108.0% is the critical TGP% level for 20-d exposure based on model 1 (data set 1) without considering ancillary factors. Consequently, data set 2 is inadequate to improve our knowledge of critical levels for TGP%, except to indicate that component gas levels play an influential role in the calculation.

The lowest level of TGP% available in both data sets is 111%. This occurs at two data points from Meekin and Turner (1974) (see also Jensen et al. 1985, p. 29 and 33), where the recorded values of ET50 are 144 and 360 h. Notice that these values of ET50 are both below the minimum of 20 d (480 h) considered in Table 9. Furthermore, most of the critical TGP% levels cited in Table 9 are below the observed minimum of

111%. Thus, these criteria are extrapolations from the data. This conclusion relates to our earlier discussion of two phases of mortality, chronic and acute, based on different etiologies and rate processes, with a TGP% boundary between them around 108−110%. Consequently, the criteria in Table 9 are extrapolations into the chronic range from data in the acute range. If indeed the rate processes differ in these two ranges, then we must interpret our conclusions with particular caution. An analysis based on data in the chronic range might give TGP% criteria different from those obtained here. Nevertheless, a recent study by Wright and McLean (1985) at low TGP% levels appears to support the criteria in Table 9, when ancillary variables in their study are taken into account. An exact comparison between their work and our model is not possible because (consistent with normal hatchery conditions) TGP% levels varied both temporally and spatially within the test tank. For further discussion of the possible implications of chronic and acute mortality, see Alderdice and Jensen (1985).

Conclusions

This paper is only one step in a proper assessment of salmonid response to gas supersaturation. We have used literature data to obtain indications of important ancillary factors and their influence in setting safe criteria. Unfortunately, the lack of comprehensive data prevents us from making statements with adequate precision. We conclude that TGP%, together with the ancillary factors water depth and fish size, affects the survival of fish populations. Furthermore, it appears that the components of dissolved gases significantly alter mortality due to excess gas pressure. However, an assessment of *safe* criteria requires data at low levels of excess TGP%, and these are notably absent in the literature cited in Table 1, where the lowest available level is 111% (Tables 2 and 3). In addition, to discern the importance of ancillary factors, these need to be incorporated into a proper experimental design. The conclusions from data sets 1 and 2 illustrate this principle. It is clear from data set 2 that gas components are important ancillary variables. Nevertheless, the lack of component data leaves us unable to improve our estimate of safe criteria available from the larger data set 1 without component information.

It is important to note in Table 9 that the determination of a safe level depends on the definition of "safe." We have selected exposure times of 50 and 20 d as examples, but these may be quite inappropriate in particular situations. Furthermore, this entire exercise is devoted to the response ET50. Critics often point out that mortality is a rather gross measure of safety. This paper and its companion (Schnute and Jensen 1986) describe a methodology for assessing biological response to variables such as TGP% and other factors. The particular choice of response and the setting of a safe level are matters for careful consideration. We have specifically demonstrated that the conclusions depend on these choices.

This paper appears to suggest that certain factors, such as temperature and barometric pressure, have no influence ancillary to gas supersaturation. It should be emphasized that this is probably due to a limited range of available data. Furthermore, we have not explored species differences here. These are only a few of many possible extensions to our work. Our tabular histograms (Tables 4 and 5) illustrate large gaps in the historical data records. Future work could profitably explore these possibilities, with an experimental design guided by our conclusions.

In summary, the determination of a safe level of TGP% depends on (1) the definition of "safe," (2) associated levels of various ancillary factors, and (3) more extensive data than are currently available in the literature. Given such information, the methodology here can be used to estimate safe criteria. This conclusion may seem equivocal to the reader who seeks a definitive acceptable level of gas supersaturation. We can attempt to define such a quantity here, but we must again emphasize the fact that our conclusions are based on extrapolations from data in the acute mortality range for TGP% to criteria in the chronic range. The worst case recorded in Table 9 (model 7 with the shallowest depth and largest fish) gives a TGP% level of 103.8% to guarantee with 95% confidence that it will take at least 50 d for half the population to die. In our view, this conservative TGP% criterion is the best possible until better data become available, especially data in the chronic range for TGP%, and more precise criteria of safety are defined.

Acknowledgements

We thank N. Hally for his part in organizing and compiling the data records into computer files. We are also indebted to S. McKinnell and M. Marshall for developing the computer software for the model parameter search and surface plots, respectively. Finally, we thank L. Fidler and M. Shrimpton, Department of Zoology, U.B.C., for their comments regarding bubble nucleation sites and fish distribution in the water column.

References

ALDERDICE, D. F., AND J. O. T. JENSEN. 1985. Assessment of the influence of gas supersaturation on salmonids in the Nechako River in relation to Kemano Completion. Can. Tech. Rep. Fish. Aquat. Sci. 1386: 48 p.

BENGTSSON, B. E. 1974. The effects of zinc on the mortality and reproduction of the minnow, *Phoxinus phoxinus*. Arch. Environ. Contam. Toxicol. 2: 342−355.

BLAHM, T. H., R. J. MCCONNELL, AND G. R. SNYDER. 1975. Effect of gas super-saturated Columbia River water on survival of juvenile chinook and coho salmon. NOAA Tech. Rep. NMFS SSRF-688: 9 p.

BOUCK, G. R. 1982. Gasometer: an inexpensive device for continuous monitoring of dissolved gases and supersaturation. Trans. Am. Fish. Soc. 111: 505−516.

COLT, J. 1980. The computation of dissolved gas levels as a function of temperature, salinity, and pressure. Department of Civil Engineering, University of California, Davis, CA.

1983. The computation and reporting of dissolved gas levels. Water Res. 17: 841−849.

D'AOUST, B. G., AND M. J. R. CLARK. 1980. Analysis of supersaturated air in natural water and reservoirs. Trans. Am. Fish. Soc. 109: 708−724.

D'AOUST, B. G., R. WHITE, AND H. SEIBOLD. 1976. An electronic monitor for total dissolved gas pressure, p. 106−110. *In* D. H. Fickeisen and M. J. Schneider [ed.] Gas bubble disease. Technical Information Center, Energy Research and Development Administration, Oak Ridge, TN.

DAWLEY, E. M., AND W. J. EBEL. 1975. Effects of various concentrations of dissolved atmospheric gas on juvenile chinook salmon and steelhead trout. U.S. Fish. Bull. 73: 787−796.

EBEL, W. J., K. T. BEININGEN, G. R. BOUCK, W. R. PENROSE, AND D. E. WEITKAMP. 1979. Gases, total dissolved, p. 113−118. *In* R. V. Thurston, R. C. Russo, C. M. Fetterolf Jr., T. A. Edsall, and Y. M. Barber Jr. [ed.] A review of the EPA Red Book: quality criteria for water. Water Quality Section, American Fisheries Society, 5410 Grosvenor, Bethesda, MD.

EBEL, W. J., E. M. DAWLEY, AND B. H. MONK. 1971. Thermal tolerance of juvenile Pacific salmon and steelhead trout in relation to supersaturation of nitrogen gas. U.S. Fish. Bull. 69: 833−843.

FICKEISEN, D. H., AND M. J. SCHNEIDER [ED.] 1976. Gas bubble disease. CONF-741033. Technical Information Center, Energy Research and Development Administration, Oak Ridge, TN. 123 p.

FIDLER, L. 1984. A study of biophysical phenomena associated with gas bubble trauma in fishes. 133 p. (Available from Department of Fisheries and Oceans, Vancouver, B.C.)

GORHAM, F. P. 1900. Some physiological effects of reduced pressure on fish. J. Boston Soc. Med. 3: 33−37.

HARVEY, H. H. 1975. Gas disease in fishes — a review, p. 450−485. *In* W. A. Adams [ed.] Chemistry and physics in aqueous gas solutions. The Electrochemical Society, Princeton, NJ.

HARVEY, H. H., AND A. C. COOPER. 1962. Origin and treatment of a supersaturated river water. Prog. Rep. No. 9, Int. Pac. Salmon Fish. Comm. 19 p.

JENSEN, J. O. T., A. N. HALLY, AND J. SCHNUTE. 1985. Literature data on salmonid response to gas supersaturation and ancillary factors. Can. Data Rep. Fish. Aquat. Sci. 501: 35 p.

KENDALL, M., AND A. STUART. 1979. The advanced theory of statistics. Vol. 2: Inference and relationship. 4th ed. Macmillan, New York, NY. 748 p.

MARSH, M. C., AND F.P. GORHAM. 1905. The gas disease in fishes. Rep. U.S. Bur. Fish.: 343−376.

MEEKIN, T. K., AND B. K. TURNER. 1974. Tolerance of salmonid eggs, juveniles, and squawfish to supersaturated nitrogen. Wash. Dep. Fish. Tech. Rep. 12: 78−126.

MITTERTREINER, A. C., AND J. SCHNUTE. 1985. SIMPLEX: a manual and software package for easy nonlinear parameter estimation and interpretation in fishery research. Can. Tech. Rep. Fish. Aquat. Sci. 1384: 90 p.

NEBEKER, A. V., G. R. BOUCK, AND D. G. STEVENS. 1976. Carbon dioxide and oxygen−nitrogen ratios as factors affecting salmon survival in air-supersaturated water. Trans. Am. Fish. Soc. 105: 425−429.

NEBEKER, A. V., AND J. R. BRETT. 1976. Effects of air-supersaturated water on survival of Pacific salmon and steelhead smolts. Trans. Am. Fish. Soc. 105: 338−342.

NEBEKER, A. V., A. K. HAUCK, AND F. D. BAKER. 1979. Temperature and oxygen−nitrogen gas ratios affect fish survival in air-supersaturated water. Water Res. 13: 299−303.

RUCKER, R. R. 1975a. Gas bubble disease mortalities of coho salmon, *Oncorhynchus kisutch*, in water with constant total gas pressure and different oxygen-nirogen ratios. Natl. Mar. Fish. Serv. Seattle Fish Bull. 73(4): 915−918.

1975b. Excess nitrogen gas in water not a cause of coagulated yolk disease in chinook salmon. Prog. Fish-Cult. 37: 101−102.

SCHNUTE, J., AND J. O. T. JENSEN. 1986. A general multivariate dose−response model. Can. J. Fish. Aquat. Sci. 43: 1684−1693.

SCHNUTE, J., AND S. MCKINNELL. 1984. A biologically meaningful approach to response surface analysis. Can. J. Fish. Aquat. Sci. 41: 936−953.

STROUD, R. K., AND A. V. NEBEKER. 1976. A study of the pathogenesis of gas bubble disease in steelhead trout, p. 66−71. *In* D. H. Fickeisen and M. J. Schneider [ed.] Gas bubble disease. Technical Information Center, Energy Research and Development Administration, Oak Ridge, TN.

VAN SLYKE, D. D. 1927. Note on a portable form of manometric gas apparatus and on certain points in the technique of its use. J. Biol. Chem. 73: 121−126.

WEDEMEYER, G. A., F. P. MEYER, AND L. SMITH. 1976. Diseases of fishes Book 5: Environmental stress and fish disease. T. F. H. Publications, Inc. Ltd. Jersey City, NJ. 192 p.

WEITKAMP, D. E., AND M. KATZ. 1980. A review of dissolved gas supersaturation literature. Trans. Am. Fish. Soc. 109: 659−702.

WRIGHT, P. B., AND W. E. MCLEAN. 1985. The effects of aeration on the rearing of summer chinook fry (*Oncorhynchus tshawytscha*) at the Puntledge hatchery. Can. Tech. Rep. Fish. Aquat. Sci. 1390: 59 p.

Functional Maturity and Terminal Molt of Male Snow Crab, *Chionoecetes opilio*

Gérard Y. Conan and Michel Comeau

Department of Fisheries and Oceans, Fisheries Research Branch, Gulf Region, Marine Biology Research Center at the University of Moncton, Moncton, N.B. E1A 3E9

Conan, G. Y., and M. Comeau. 1986. Functional maturity and terminal molt of male snow crab, *Chionoecetes opilio*. Can. J. Fish. Aquat. Sci. 43: 1710–1719.

Bivariate and multivariate analyses of allometric relationships between chela size and carapace size of snow crab, *Chionoecetes opilio*, show that mature males are recognizable by morphometry. The most simple procedure is to plot logarithms of chela height (C_h) against logarithms of carapace width (L_c). Data from mature and immature males fit into two distinct ellipses with parallel major axes. The discriminant function $Y = -0.78893 \log_e L_c + 0.614488 \log_e C_h + 1.76051$ will assign individuals to the correct groups in 99% of cases (for mature males: $Y > 0$). Spermatophores are present in the vasa deferentia of all males larger than 60 mm L_c. The molt to morphometric maturity occurs later at L_c sizes ranging from 60 to 120 mm; it is identified as final. Only morphometrically mature males larger than 96 mm L_c have been observed to mate efficiently with multiparous females in intermolt and be functionally mature. In the catch, as many as 40% of males larger than the minimal legal size of 95 mm can be immature.

L'analyse bivariée et multivariée des relations d'allométrie entre la taille de la pince et la taille de la carapace du crabe des neiges, *Chionoecetes opilio*, permet d'identifier aisément par morphométrie les mâles matures. Une méthode simple consiste à porter graphiquement les logarithmes des hauteurs de pinces (C_h) en fonction de ceux des largeurs de carapace (L_c). Suivant l'état de maturité, les données s'aggroupent en deux ellipses d'axes majeurs parallèles. La fonction discriminante $Y = -0.78893 \log_e L_c + 0.614488 \log_e C_h + 1.76051$ permet d'identifier des individus dans 99% des cas (pour les mâles matures : $Y > 0$). Des spermatophores sont présents dans les canaux déférents des mâles de taille L_c supérieure à 60 mm. La maturité morphométrique apparaît après une mue terminale qui s'effectue entre L_c = 60 et 120 mm. Seuls les mâles morphométriquement matures de taille L_c supérieure à 95 mm s'accouplent efficacement avec des femelles multipares en intermue et sont fonctionnellement matures. Jusqu'à 40% des mâles capturés, dont la taille L_c est supérieure à la taille minimale légale de 95 mm sont immatures.

Received November 5, 1985
Accepted May 8, 1986
(J8554)

Reçu le 5 novembre 1985
Accepté le 8 mai 1986

The snow crab, *Chionoecetes opilio* (Brachyura, Majidae), is one of the most valuable species harvested in Atlantic Canada. Only males are commercially exploited by the fishery, and a minimum legal size of 95 mm carapace (cephalothorax) width (L_c) has been enforced since 1973. This size is the smallest acceptable by processors for mechanized meat extraction. Male snow crab are generally believed to mature and mate before they reach 95 mm L_c (Powles 1968; Watson 1970). Watson (1970) concluded that male snow crabs reach maturity between 51 and 72 mm L_c. Since 1970 it has frequently been assumed that the snow crab stocks were protected from recruitment overexploitation because females were not harvested and because all males were thought to mature and have the opportunity to mate before they reached the minimum legal size.

Teissier (1933, 1935) and Hartnoll (1963) have shown that male majid crabs show a differentiation of the chelae, a change in allometry, when they reach maturity. When the logarithms of chelae measurements are plotted against the logarithms of some standard measurements of carapace size, this results in three segments of straight lines. The first segment, for small crabs, is characteristic of the "prepubertal" stage; it leads, without discontinuity, to an angular point marking a transition. The prepubertal molt leads to the second segment which is characteristic of the pubertal stage. The third segment is parallel to the second, but shifted in ordinate. The discontinuity between the second segment and the third is caused by the pubertal molt or molt to maturity during which the chelae increase considerably in volume in one abrupt step. The molt to maturity may occur over a large range of carapace size. In many species of majid crab, large immature males may be two to three times larger than the smallest mature ones. The molt to maturity is believed to be the last one, the "final" or "terminal molt," in most species.

Powles (1968), Watson (1970), and Coulombe et al. (1985) have observed such a differentiation in the claw of *C. opilio* at maturity. The overlap of the immature/mature carapace size reported by Watson (1970) is short. In contrast, Powles (1968) and Coulombe et al. (1985) observed a wider overlap of carapace sizes, suggesting that immature crabs could be found in the commercial catch at sizes greater than 95 mm L_c. However, Coulombe et al. (1985) questioned whether these morphometrically "immature" crabs larger than 95 mm L_c were actually functionally immature.

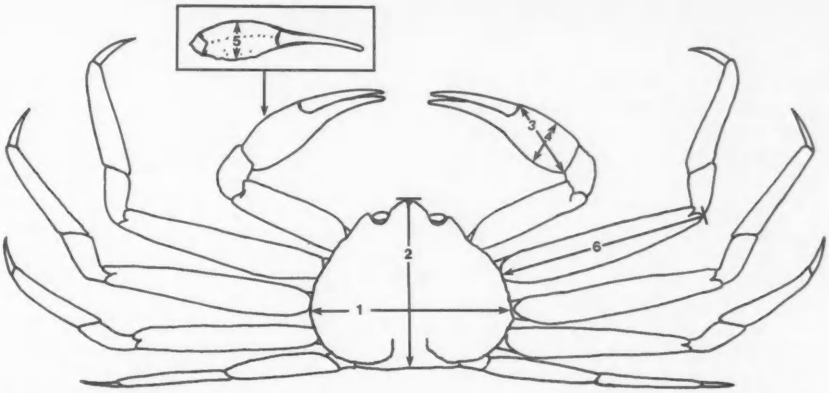

FIG. 1. Standard measurements taken on male snow crab: 1, cephalothorax length; 2, cephalothorax width; 3, chela length; 4, chela height; 5, chela width; 6, 2nd pereiopod meropodite length. Dorsal view of chela is shown in rectangle.

Somerton (1980) developed a tool for estimating the size of sexual maturity in crabs. His technique is based on a computer algorithm for iteratively fitting two regressions lines starting simultaneously from the two extremities of the range of observations. However, Somerton's technique was not designed to respond to the goal of precisely attributing individual observations to the mature versus immature subgroups. Somerton (1981) later mentioned that in *Chionoecetes* it is difficult to distinguish by simple means mature males from immature ones on the basis of allometry alone.

We have analyzed morphometric data on maturity of male snow crabs and compared these results with observations on the presence of spermatozoa in the vasa deferentia and observations on functional maturity made on mating pairs in their natural habitat and in an aquarium. Our goal was to develop a simple nondestructive tool to allow efficient discrimination of mature males from immature ones for fishery management surveys. We analyzed the discriminant value of several standard measurements made on the chela and the carapace for identification of mature and immature individuals. We first used multivariate tools allowing for synergic discriminatory effects of several standard measurements. The multivariate approach also allowed identification of the two most efficient parameters for a simple bivariate discrimination tool. We attempted to develop a technique based on Fisher's discriminant function to efficiently assign individuals to either of the two categories by a criterion of highest probability.

To verify the existence of a terminal molt at the onset of maturity, we thereon applied the discriminant function for identifying mature males in the catch. We checked for the occurrence of molting within the group of mature males by aquarium and field experiments.

Materials and Methods

Sea Sampling

Male snow crabs were collected by trawling. Previous authors (e.g. Watson 1970) have used trapping to collect large animals and beam trawling to collect small- and medium-sized ones. We used a Bay of Biscay *Nephrops* otter trawl with a 25-m opening designed for capturing semiburied crustacean species. The *Nephrops* trawl catches snow crabs of a wide range of sizes efficiently. We believe that it is less selective for immature and recently molted crabs than traps. Conan and Maynard (1986) have shown by underwater television that small crabs tend to bury themselves in soft bottom sediment. The trawling was conducted over the summer of 1984 in Baie des Chaleurs and over the snow crab fishing grounds in the southwest Gulf of St. Lawrence.

A sample of mating snow crab pairs was collected by SCUBA divers (G. Y. Conan and R. W. Elner, DFO, Biological Station, St. Andrews, N.B.) in Bonne Bay (Newfoundland) during May 1984 at depths of 20−35 m during the spring inshore mating migration described by Hooper (1986) and Taylor et al. (1985). An additional sample of commercial sized crabs was obtained from Baie de Chaleurs using standard commercial traps.

Aquarium Experiment

During April 1985, 18 males of 66−116 mm L_c were selected for sizes within and above the range of maturity differentiation described by Watson (1970) as 51−72 mm L_c. The males were placed in an 18-m^3 tank holding 17 multiparous females, i.e. females having already mated and spawned at least once (Paul 1984). Six females bore bright orange, freshly layed eggs and 11 females bore older eggs showing conspicuous eye spots. The bottom of the tank was covered with small gravel and large rocks as observed on natural mating grounds in Bonne Bay. The temperature ranged from 2 to 3°C and the salinity was 32. Observations on mating behavior were made on a 24-h basis over a period of 14 d. An underwater video camera ("Subsea" system) and a recorder were used for continuous observations. Male crabs were measured for biometric characterstics, and at the end of the experiment their vasa deferentia were dissected for identification of spermatophores.

In a long-term rearing experiment, 110 morphometrically mature males and 24 morphometrically immature ones of the same size range were kept for 10 mo from November 1984 to September 1985, through the period of "white" crabs (i.e. molting) in the commercial catch. The crabs were monitored for occurrence of molts.

Biological Analysis of Data

Biometric measurements were made to the nearest millimetre using a modified vernier caliper (Watson and Wells 1970). Six standard measurements were taken on snow crabs as indicated in Fig. 1.

All males in the aquarium experiment and a subsample of males from the sea sampling were used for direct reading of physiological maturity: a smear of the vasa deferentia was examined at low magnification for the presence of spermatophores under a light transmission microscope (Powles 1968).

For reading the molt stages we have used the simple technique described by Drach and Tchernigovtzeff (1967), and successfully adapted to snow crabs by Moriyasu and Mallet (1986). The endite of the second maxilliped is removed in vivo using a pair of forceps and is observed in transmitted light under a low-resolution microscope. The presence/absence and morphology of developing setae inside the old tegument allow easy and accurate identification of molters (A stage) postmolts (B), intermolts (C), and premolts (D). The operation is harmless for the crab.

Statistical Analysis of Data

We used a principal component analysis (PCA) on log transformations of the measurements to identify which variables (measurements) were redundant and could be discarded and which variables were the most representative of the size factor and of the sexual differentiation factor (Conan et al. 1985). A log transform is used to linearize the allometric data:

$$C_w = a(w)L_c^{b(w)}$$

which becomes

$$\log_e C_w = \log_e a(w) + b(w) \log_e L_c$$

where C_w = chela width, L_c = carapace width, a and b are parameters, and w is the index for width. The transformation normalizes the dispersion of points around the linear regression lines and stabilizes the variances of the dispersion of points along the regression lines. These conditions are required by the PCA.

The graphics output of the PCA is set as described by Lebart et al. (1979). The data are centered and reduced. The observations are projected onto the planes defined by the principal components taken two at a time. The variables are also projected onto the plane, as vectors of unit length. A circle of radius 1 (unity) is centered on the origin of axes, and it represents the maximal extent of the vectors if they are fully defined within the plane considered. Dummy observations (observations that do not take part in the computation of the PCA, but are projected onto the planes) may be used for identifying locations within the swarms of data points. In this application, we used as dummy observations sets of measurements made on males in mating couples observed in the wild.

We further proceeded from the output of the PCA with a bivariate discriminant analysis for observations made on the two variables chosen for best sharing two properties: (1) identified in the PCA as being suitable for discriminating mature from immature individuals (i.e. best representing the sexual differentiation factor versus the growth factor) and (2) most suitable for practical measurements. Fisher's bivariate discriminant analysis can be visualized as an orthogonal (rectangular) projection of the data points from the plot of chela sizes versus carapace width onto a line perpendicular to the line discriminating (separating) most adequately the two swarms of points to be contrasted. The new coordinates of the data points read along the perpendicular are called discriminant scores. An implicit a priori condition is that the variance and the covariances between variables (here, chela size and carapace width) be the same for the two swarms contrasted (Cooley and Lohnes 1971). We compared the variance/covariance matrices by a test described in Morrison (1976). The sets of data points that are contrasted must be identified before the analysis. The output is (1) a linear function allowing "recognition" of individuals in further analysis, (2) an estimate of the variance of coordinates on the orthogonal projection (discriminant scores) allowing calculation by *t* test of the cumulative probability for any individual to pertain to either group, and (3) an estimate of the probability of misclassification in future analysis, based on the overlap of the two distributions on the orthogonal projection.

TABLE 1. Percentage of variance explained by the principal components analysis for observations from Baie des Chaleurs ($N = 217$).

Axis	Percentage of variance
1	98.05
2	1.14
3	0.55
4	0.13
5	0.11
6	0.03

We also used a more traditional tool, the Powles (1968) index of morphometric maturity, in which the chela length is multiplied by the claw width. The index is plotted against carapace width on a log − log scale for identification of immature versus mature males. It can be shown that if the relationships between chela width (C_w) and cephalothorax width (L_c) and claw height (C_h) and L_c are allometric, then the relationship between the index $C_w \cdot C_h$ and L_c is also allometric:

$$C_w = a(w)L_c^{b(w)}$$

$$C_h = a(h)L_c^{b(h)}$$

$$I = C_w \cdot C_h = a(w) \cdot a(h) \cdot L_c^{b(w) + b(h)}$$

$$I = aL_c^b.$$

The justification for a composite index using the product of two measurements would be to reduce multivariate data to a simple bivariate case without restricting the information to bivariate measurements.

We set confidence limits on observed proportions of molters for checking how substantial was their presence within categories. Confidence limits on non-zero proportions are set by reading isopleths for the binomial distribution (Dixon and Massey 1957). Confidence limits on observed null proportions are set by assuming a Poisson distribution for occurrence of rare events:

$$p(x) = \frac{e^m m^x}{x!}$$

where p is the probability of x occurrences in the sample and m is the mean number of occurrences in a distribution of samples of given size n within the population. At the $p = 0.05$ level, a zero observation is obtained when m approximates 3, and the proportion of events (individuals of given category) within the population is

$$P = \frac{m}{n}.$$

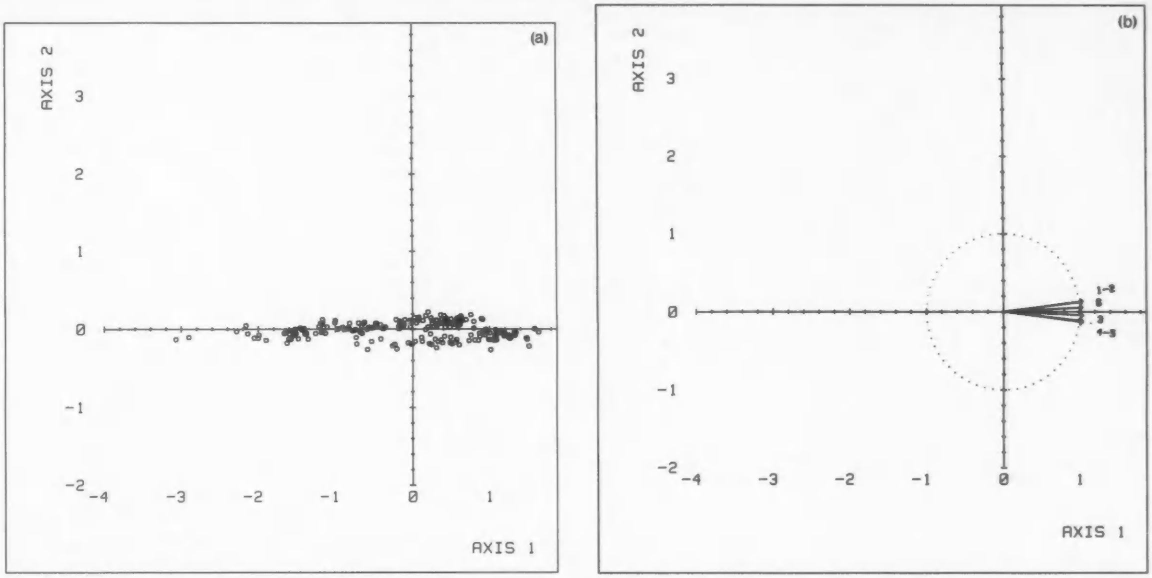

FIG. 2. Principal component analysis on six variables (carapace length, carapace width, chela length, chela height, chela width, and 2nd pereiopode meropodite length. (a) Representation of observations ($N = 217$). Two discrete swarms of points elongated along axis 1 are attributed to immature males (positive direction of axis 2) and mature males (negative direction of axis 2). (b) Representation of the variables as vectors (1, carapace width; 2, carapace length; 3, chela length; 4, chela height; 5, chela width; 6, 2nd pereiopode meropodite length). Variables 1 and 2 are redundant, as are variables 4 and 5. Variables 1 and 2 are orientated along the major axis of the ellipses and represent a size factor. Variables 4 and 5 are the most efficient in discriminating the two swarms of points and are correlated with a sexual differentiation factor.

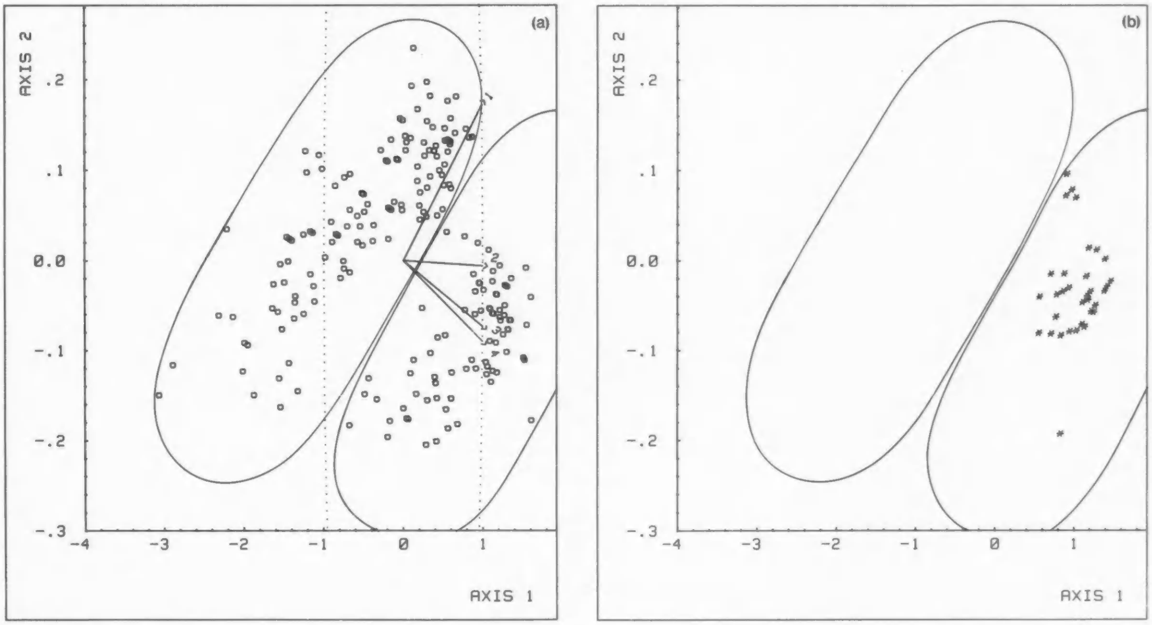

FIG. 3. Principal component analysis on four variables (1, carapace width; 2, chela length; 3, chela height; 4, chela width). (a) Simultaneous magnified representation of the variable as vectors and of the observations ($N = 217$). Variables 1 and 2 are parallel to the major axis of the swarms of points and represent a size factor. Variables 3 and 4 are the most efficient in discriminating the two swarms of points and are correlated with a sexual differentiation factor. (b) Numbers represent the projection of dummy observations: measurements taken on males from mating pairs from Bonne Bay. The arbitrarily drawn contours outline the location of observations from Baie des Chaleurs. The dummy observations fit into the contour of the lower swarm of points, and are therefore identified as representing mature animals.

TABLE 2. Correlations between variables and principal axes of the principal components analysis for observations from Baie des Chaleurs ($N = 217$).

Axis	Carapace		Chela			2nd pereiopode meropodite length
	Width	Length	Length	Height	Width	
1	0.990443	0.989806	0.995751	0.99678	0.988837	0.985572
2	0.123476	0.126781	0.04683	0.11891	0.13429	0.050159
3	−0.05236	−0.05686	−0.01163	−0.02131	−0.01857	0.0161517
4	0.010479	0.0099	−0.07745	0.013512	0.036758	0.007312
5	0.000775	−0.00045	0.012826	−0.06157	0.049822	−0.00138
6	−0.03059	0.029059	−0.00008	−0.00023	−0.000492	0.000604

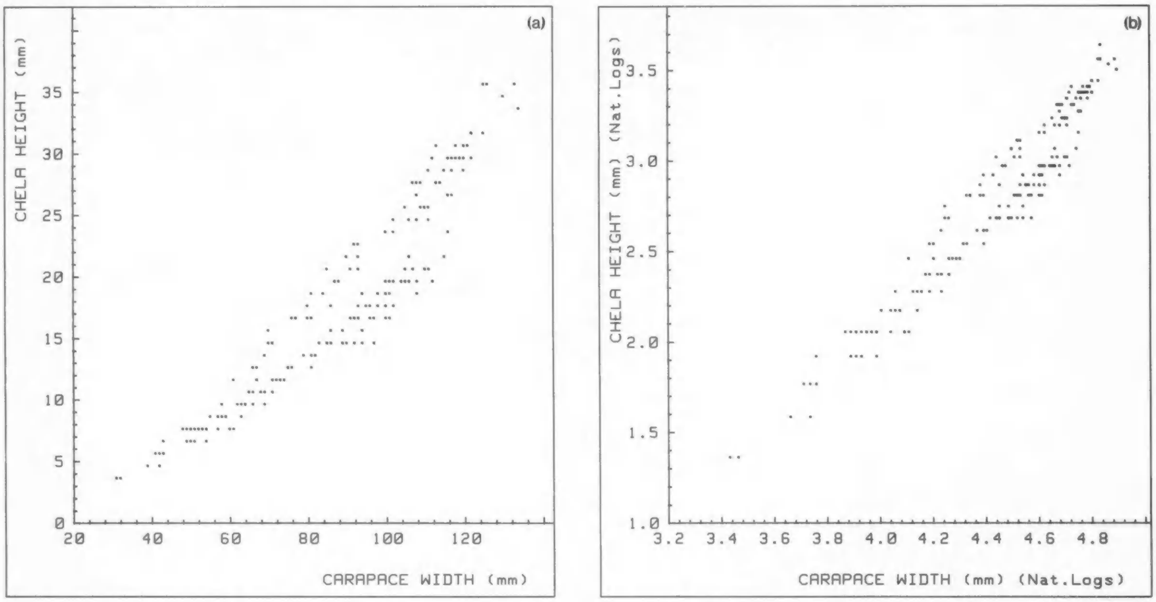

FIG. 4. Relationship between chela height and carapace width for male snow crabs from Baie des Chaleurs. (a) Linear scale ($N = 217$); (b) logarithmic scale ($N = 217$).

All statistical procedures were conducted on an HP 9845B computer using custom designed programs. The programming technique for the discriminant analysis can be found in Davies (1971).

Results

Component one explains most of the variance in the PCA (98%) (Table 1). Component two explains only 1.14% of the variance, about twice as much as component three. Therefore, for further graphic analysis in the PCA we proceeded only with projections in the plane defined by the first and second components. On the projection of the observations (Fig. 2a), two swarms of points are elongated at a slight angle with the first axis. On the projection of the variables (Fig. 2b), all variables appear to be almost entirely defined within the plane: the plane will suffice for graphic analysis. Variables 1 and 2 overlap and are redundant; one measurement of either carapace width or length would be sufficient. Variables 1 and 2 have the same orientation as the major axes of the swarms of points; they efficiently represent the growth factor. Variables 4 and 5 (chela height, chela width) are highly correlated between themselves and define the most open angles with variables 1 and 2 (less correlated); variables 4 and 5 are almost redundant and they are the most efficient to discriminate the two swarms of points by representing the sexual differentiation factor. This graphic analysis is confirmed in Fig. 3a where observations and variables are represented simultaneously on a magnified non-isotropic scale.

When the data from Bonne Bay (independent measurements made on males from mating couples in their natural environment) are projected as dummy observations in Fig. 3b, the points are accurately positioned within the contours defined by the lower swarm; we therefore identify this swarm as data points representing functional adults.

Carapace width and chela height were selected as the most suitable variables for a bivariate analysis because (1) they appeared to efficiently represent, respectively (Table 2), the size (major axis of swarms of points) and the sexual differentiation and (2) they are easy to measure. Graphs of chela height versus carapace width for Baie des Chaleurs data are presented on an arithmetic scale in Fig. 4a and on a logarithmic scale in Fig. 4b.

The two swarms of points are conspicuous on both graphs. The logarithmic transformation linearizes the shape of the swarms and stabilizes the variance. The relationships between chela height and carapace width are therefore typically allometric. The two swarms in Fig. 4b could be circumbscribed in two elongated ellipses with parallel major axes. The swarms widely overlap in abscissa and ordinate. The major axes apparently differ in ordinate intercept but not in slope. There is no conspicuous angular point suggesting a prepubertal molt along the swarm of immature points.

A graph of the Powles index versus carapace size on a logarithmic scale provided identical results, and did not allow better discrimination between swarms of points. For this set of data the Powles index, as compared with a simple bivariate plot, does not enhance visual discrimination between the swarm of points because the chela length and width measurements are highly correlated and carry almost redundant information (Fig. 2b).

The points pertaining to either of the mature/immature groups identified on the PCA plots for Baie des Chaleurs data were processed in a bivariate discriminant analysis which was 99% efficient in allocating points to the right groups, although the variance/covariance matrices for the two sets of points were significantly different at the 0.01 level. We generalized the discriminant analysis to 784 data points from the whole southwest Gulf of St. Lawrence (Fig. 5) in order to develop a discriminant function representative for the whole fishery. The data points had previously been attributed to immature/mature groups by graphic PCA. The resolution of the cutting line statistically fitted by the analysis remained good although the variance along the Y and X variables increased due to slight local variations in allometry (Fig. 6a). Morphometrically immature males ranged in size from 31 to 120 mm L_c and morphometrically mature males from 52 to 137 mm L_c. The histograms of the discriminant scores (orthogonal projection of the points on either side of the cutting line onto a perpendicular) slightly overlap, possibly due to initial a priori misclassification of a few points (Fig. 6b) in the graphic PCA. However, the analysis forecasts that 99% of the observations will be correctly assigned to either group (Table 3) when the discriminant function $Y = -0.7889259 \log_e L_c + 0.6144883 \log_e C_h + 1.7605142$ is used. If $Y < 0$, the individual is immature; if $Y > 0$, the individual is mature. Alternatively, the function $C_h = 0.015554\, L_c^{1.5787}$ can be plotted on graph paper. All points of chela height versus carapace width plotted below this line will identify immature individuals, and all points above the line will identify mature ones. The probability for an individual to pertain to either group can be calculated as follows:

immatures: $Z = (S - 244.5752)/4.6488$

matures: $Z = (S - 222.9641)/4.6488$

where Z is a standard normal deviate and S is the discriminant score where

$$S = 104.7737 \log_e L_c - 81.6074 \log_e C_h.$$

The two-tailed cumulative probability can be read from tables of the standard normal deviate. The variance/covariance matrices for the two sets of points were significantly different at the 0.01 level. Results of discriminant analysis for alternative measurements used as standards by other authors are presented in Table 3 as a reference for analysing data sets defined by different measurements (Powles 1968; Watson 1970).

TABLE 3. Discriminant functions allowing identification of morphometrically mature versus immature males as a function of carapace width (L_c), chela height (C_h), chela length (C_l), and chela width (C_w).

Discriminant functions (immature: $Y < 0$; mature: $Y > 0$)	% assigned to right group	Normal deviate indicating probability for an individual to pertain to either group	
		Immatures	Matures
$Y = -0.7915457 \log_e L_c + 0.6111111 \log_e C_l + 1.3591466$	99.1	$Z = (136.7477 \log_e L_c - 105.5755 \log_e C_l - 245.9584)/4.730$	$Z = (136.7477 \log_e L_c - 105.5755 \log_e C_l - 223.5834)/4.730$
$Y = -0.7889259 \log_e L_c + 0.6144883 \log_e C_h + 1.7605142$	99.0	$Z = (104.7737 \log_e L_c - 81.6074 \log_e C_h - 244.5752)/4.6488$	$Z = (104.7737 \log_e L_c - 81.6074 \log_e C_h - 222.9641)/4.6488$
$Y = -0.802818 \log_e L_c + 0.5962242 \log_e C_w + 1.9761339$	98.9	$Z = (93.4585 \log_e L_c - 69.4083 \log_e C_w - 240.4603)/4.5715$	$Z = (93.4585 \log_e L_c - 69.4083 \log_e C_w - 219.5614)/4.5715$

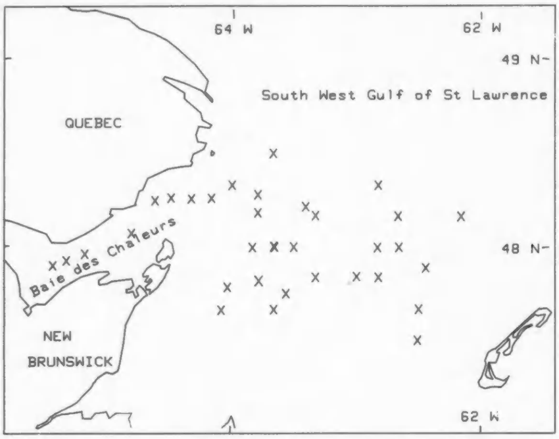

FIG. 5. Geographic location of sampling sites in Baie des Chaleurs and southwest Gulf of St. Lawrence.

An additional minimal size constraint increases the efficiency of the discrimination. In Fig. 6a, it appears that the swarm of points representing immatures is slightly curved. This results in a few points towards the lower range of sizes being located above the discriminant line and therefore classified erroneously as pertaining to mature animals. To avoid this artefact, we suggest identifying all males smaller than 50 mm L_c as immature.

The discriminant function was used for identifying morphometrically mature males in the sea sampling data and the aquarium experiment. All morphometrically mature males bore spermatophores in their vasa deferentia, but the smaller ones (below 95 mm) bore many more spermatophores than the larger ones, except in Bonne Bay. Small morphometrically mature males identified as "pygmies" by fishermen usually bore highly turgescent vasa deferentia, also found in some large males from couples collected by diving in Bonne Bay. All males larger than 60 mm bore spermatophores independent of their morphometric state of maturity.

In the aquarium experiment, 12 males were morphometrically mature, ranging in size from 74 to 116 mm L_c, and 6 were morphometrically immature, ranging in size from 66 to 98 mm L_c. All males bore spermatophores. Complete mating behavioral sequences (Watson 1970, 1972) were observed for three couples of morphometrically mature males and hard-shell females, immediately after hatching of an old brood and prior to extrusion of the new brood. None of the females molted. Seven morphometrically mature males initiated mating behavior with hard-shell females but were disturbed by bachelors. Two morphometrically mature and six morphometrically immature males did not initiate any mating behavior. The morphometrically immature males retreated to remote locations of the aquarium and displayed a hiding behavior by picking a stone and putting it on top of their carapace. Morphometrically mature males initiated mating behavior (precopulatory embrace) with five of six females bearing orange, recently spawned eggs, but the embrace never lasted more than 30 min and copulation was never achieved.

Of the 110 morphometrically mature males maintained in the aquarium from November to September, none molted. At a 95% probability level we may therefore assume that no more than 2.7% may have molted under similar conditions. Meanwhile, 16 of 24 morphometrically immature ones molted, which yields confidence limits at the 95% level of 46−85% for molting incidence within the immature group under similar conditions.

Of 260 morphometrically mature males sampled from the catch in *Nephrops* trawls from July to December at depths ranging from 40 to 160 m and of 110 males caught in traps, no individuals were ever found in a premolt "D" or molt "A" stage. At the 95% level we may therefore assume that no more than 0.8% of morphometrically mature males in the wild initiate molting. Premolt and molting immatures are frequently found in trawl catches.

Discussion

Identification of Morphometrically Mature Males

The bivariate discriminant function developed for logarithms of carapace width and chela height allows efficient identification of morphometric maturity of males. The variance/covariance matrices of the mature and immature swarms of points significantly differed, but the discriminant analysis was robust enough to provide accurate results. Bivariate discriminant analyses on logarithms of chela length and chela width versus carapace width provide very similar results, and the associated discriminant functions (Table 3) may also be used, although in our experience precise measurements are more difficult to take.

The discriminant function appears to be efficient for data originating from a geographic area as wide as the southwest Gulf of St. Lawrence (Fig. 5). It may be robust enough to allow discrimination in most other geographic stocks, although some geographic variation in allometry may be anticipated (Davidson et al 1985).

Precise measures are required with a modified caliper such as that described by Watson and Wells (1970); otherwise, the variances of the variables increase and the tool may lose considerable discriminative power. Coulombe et al. (1985), for instance, concluded that the immatures could not be distinguished easily from the mature individuals by morphometry; however, the dispersion of the sets of points they provided was much greater than ours, and they used as an equation for the cutting line a constant ratio between claw size and carapace width for the slope and a zero value for the elevation (Watson 1970). Even for field identification this approach is incompatible with an allometric relationship between variables. For field identification we would suggest a more rigorous approach: a simple arithmetic plot of chela height (C_h) versus carapace width (L_c) and check for location above (mature) or below (immature) the predrawn curve $C_h = 0.01555\ L_c^{1.5787}$ obtained from the equation of the cutting line in the discriminant analysis. If the measurements are precise enough, 99% of the identifications will be accurate.

Morphometric versus Functional Maturity

The equivalence of the presence of spermatophores in the vasa deferentia and morphometric maturity, defined by a change of allometry in the chela size versus carapace width, was questioned, with reason, by Coulombe et al. (1985). Watson (1970) apparently found that all males bearing spermatophores were also morphometrically mature; this was in an

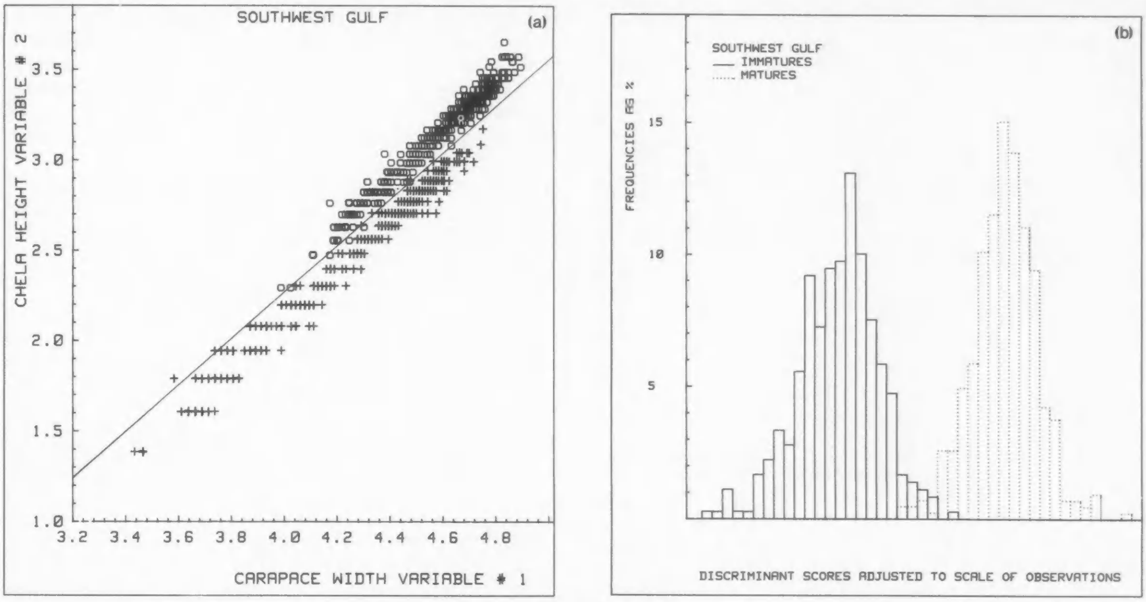

FIG. 6. Discriminant analysis of observations from southwest Gulf of St. Lawrence. (a) Representation of the cutting line separating the two swarms of points. The discrimination is about 100% efficient (○ = mature males, + = immature males). $N = 784$. (b) Histograms of discriminant scores (projection of points on a line perpendicular to the cutting line). There is very little overlap. The discrimination is about 100% efficient. $N = 784$.

early stage of exploitation of the fishery. Our data provide different information. In the subsamples of dissected males we occasionally found morphometrically mature individuals with few spermatophores in the vasa deferentia, while all morphometrically immature males larger than 60 mm L_c already bore spermatophores.

Our observations made while SCUBA diving in Bonne Bay and during aquarium experiments provide a biological interpretation for the differentiation of the claw of males at maturity. We observed that males carry the females for up to 3 wk before mating. The female, which is much smaller than the male, is held facing her mate. The chela of the male firmly grasps two to three legs along one side of the female. There is strong competition between males in mating pairs and numerous aggressive bachelors at this time. The female is carried in one claw extended outwards high above ground while fencing takes place with the other claw extended outwards in the opposite direction. If we compare the position of the dummy observations representing males collected in the field during the act of mating (Fig. 3b) with the contours of the volume defining the swarms of points of the morphometrically mature and immature animals collected by trawling (Fig. 3a), we may observe that all functionally mature animals are confined towards the larger carapace sizes within the swarm. Some functionally mature animals, however, have small chelae which position them close to the immature swarm. The dummy observations in the PCA indicate that the size factor modeled by the carapace size of the male is probably of great advantage in this competition. However, the contribution of the sexual differentiation factor modeling differentiation of secondary sexual characters is a prerequisite. The differentiation of the chela in mature males as a secondary sexual character is probably functionally justified by the mating embrace behavior. However, the size of the claw does not seem to provide an advantage in the competition between males. As shown by our data, males with a chela at the smallest portion of the range but of otherwise large body are successful in achieving precopulatory embrace and most likely in mating.

It used to be assumed that all males larger than the minimum commercial size of 95 mm L_c reached functional maturity at sizes ranging from 51 to 72 mm L_c, grew, and had the chance to mate at least once before being captured. This assumption is usually made after referring to Watson (1970), but is challenged by two of our observations:

(1) Morphometrically immature individuals can be found up to a size of 120 mm L_c. In certain samples, up to 40% of the males larger than 95 mm L_c may be immature. In the aquarium experiment, none of the morphometrically immature males that bore spermatophores and were as large or larger than active morphometrically mature males initiated any precopulatory behavior.

(2) Our data show that morphometrically and physiologically mature males as small as 60 mm L_c can be captured by trawling. However, we have no indication that these crabs are functionally mature, i.e. able to carry females during the long precopulatory embraced phase and copulate. The smallest male in copulating pairs found in Bonne Bay had a carapace width of 96 mm. Similar size for onset of functional maturity has also been reported by Paul et al. (1983) for the closely related species *C. bairdi*. Small mature males called "pygmies" by the fishermen usually have their vasa deferentia loaded with spermatophores, while larger ones reveal much smaller quantities of genital products. The production of spermatophores seems to be a continuous process with continuous accumulation prior to mating. The vasa deferentia of pygmy males appear never to be emptied by mating. There is no indication that the pygmies

do efficiently contribute to mating and reproduction.

In heavily harvested stocks (southwest Gulf of St. Lawrence), large morphometrically mature males above commercial size frequently bear few spermatophores; this was never observed in lightly exploited stocks such as Bonne Bay and never reported in old records from the southwest Gulf (Powles 1968). We believe that in heavily exploited stocks the proportion of males caught as soon as they reach morphometric maturity becomes very high. Little time, if any, is given to the functionally mature males for accumulating spermatophores and efficiently mating.

A New Interpretation of the Life Cycle of *C. opilio*

Our biological observations and our morphometric analysis bring new interpretations of the life cycle of *C. opilio*. The mating pattern we observed is similar to that described by Paul (1984) for *C. bairdi*. We definitely observed morphometrically mature males mating with hard-shell multiparous females immediately after hatching of the previous brood and without any sign of molting. We believe that previous observations by Watson (1970, 1972) of females molting prior to mating actually recorded mating of primiparous (virgin) females. This is an exceptional event which occurs during the terminal molt to maturity of the female. Mating of hard-shell males and multiparous females is the common rule in the wild.

It was previously believed (Watson 1970) that (1) male *C. opilio* simultaneously reached morphometric maturity (differentiation of the claw) and gonad maturity (production of spermatophores), (2) all males were mature beyond a critical carapace width of 60 mm, and (3) they kept on growing beyond the molt to maturity. We suggest that production of spermatophores is already initiated for most males when they reach 60 mm L_c but that the "true" functional maturity is eventually reached much later. A special molt, which coincides with the differentiation of the claw for grabbing the female, is required. This morphometric maturity is reached around 60 mm by very few individuals and can be delayed to sizes of up to 120 mm L_c (Fig. 4b). Such individuals are functionally immature, do not even demonstrate behavioral precopulatory sequences, and actually tend to hide under stones in an aquarium when mating activity is taking place, although they all carry spermatophores in their vasa deferentia. Such life history patterns are the common rule among majid crabs (Hartnoll 1963 for review), and so far the genus *Chionoecetes* was considered an exception. We also believe that among morphometrically mature animals only the larger ones (approximately 95 mm and more) are functionally mature, i.e. apt to grab a female, carry it around (precopulatory embrace), and mate. This agrees with independent observations made by Taylor et al. (1985) although their interpretation of the facts differs.

The twofold range of sizes (60−120 mm) over which morphometric maturity is reached is not exceptional; ranges as wide as three- to four-fold have been described in other species of majid crabs. The molt to morphometric maturity in majid crabs of other genera is always described as the last molt or terminal molt.

The size difference between larger morphometrically immature males and larger morphometrically mature ones in our data is 120−130 mm L_c (Fig. 4b) and can easily be covered over one molt to maturity. The wider gap sometimes reported between these sizes and attributed to growth is most likely a sampling artifact. Some types of gear such as traps or trawls which do not rake the sediment efficiently enough do not capture large morphometrically immature males which tend to conceal themselves more than the mature ones, as shown by the aquarium experiments, or do not appear on the mating grounds, as shown by Bonne Bay diving observations. The *Nephrops* trawl allowed us to catch a more representative sample of the population.

Our tank-rearing observations and molt stage identifications do confirm that morphometrically mature males extremely seldom, if ever, molt. We never observed molting of morphometrically mature males while morphometrically immature ones of the same size range molted. We never found morphometrically mature males in premolt stages, while morphometrically immature males in premolt stages were common in the *Nephrops* trawl catch. We strongly suspect that the common assumption that male *C. opilio* keep growing after the molt to morphometric maturity is an illusion resulting from incorrect identification of morphometrically mature individuals.

Implications for Fisheries Management

As suggested by Comeau (1985), one practical consequence of this peculiar life history is that the legal size of 95 mm does not "protect" the fecundity of the stock. Many male snow crabs are caught by the fishery before they mature at sizes ranging up to 120 mm. Further, there is no evidence that sublegal morphometrically mature males can efficiently mate in their natural environment with multiparous females. Such males have been described to mate with primiparous females in an aquarium (Watson 1970), but no mating involving primiparous females has been observed by us in the wild, and it is likely to be a very rare event. This situation is not necessarily critical; most species start to be harvested before maturity. However, one must be aware that the reproductive potential of a harvested snow crab stock will not remain as high as in a virgin stock even if the fishery is restricted to males and if these males all have a carapace width larger than a minimal legal size of 95 mm. The proper legal size for avoiding the capture of mature males would be 120 mm, but this would not allow for a harvested biomass sufficient to sustain a fishery.

Another practical consequence is that a minimal legal size is not an efficient tool for achieving the best yield per recruit. The harvestable stock comprises two types of individuals within most of the size range: immature males that grow and mature ones that have stopped growing. At an early state of exploitation, most individuals captured in the southern Gulf of St. Lawrence were mature ones accumulated over many years. As the fishery developed, old mature males tended to be fished out. The proportion of "whites" (animals recently molted to maturity) increased. The proportion of immatures about to reach maturity also increased within the catch. In terms of yield per recruit, all individuals that stop growing should be immediately harvested. This cannot be efficiently regulated by size because (1) the terminal molt is reached by different individuals at any of the sizes harvestable, (2) recently molted individuals are of poor commercial quality, and (3) individuals that stopped growing below the legal minimum size are not harvested and will never contribute to yield.

To protect fecundity of the stock and to achieve maximal yield per recruit, a selective gear catching only mature animals should be designed. This goal is not impossible; we have observed in an aquarium and in situ by diving that mature and immature crabs display different behavioral patterns and segregate. Several leads are presently being studied.

Acknowledgments

We wish to thank Dr. R. W. Elner and Dr. P. Lawton, Biological Station, St. Andrews, for reviewing and constructively criticizing our manuscript.

References

COMEAU, M. 1985. Détermination de la maturité sexuelle par morphométrie chez le crabe des neiges *Chionoecetes opilio*. CAFSAC Res. Doc. 85/81.

CONAN, G. Y., M. COMEAU, AND M. MORIYASU. 1985. Functional maturity of male American lobsters, *Homarus americanus*. ICES Shellfish Comm. C.M. 1985/K:29.

CONAN, G. Y., AND D. R. MAYNARD. 1986. Estimates of snow crab (*Chionoecetes opilio*) abundance by underwater television. J. Appl. Ichthyol. (In press).

COOLEY, W. W., AND P. R. LOHNES. 1971. Multivariate data analysis. John Wiley & Sons, New York, NY. 364 p.

COULOMBE, F., J. C. BRETHES, R. BOUCHARD, AND G. DESROSIERS. 1985. Ségrégation édaphique et bathymétrique chez le crabe des neiges, *Chionoecetes opilio* (O. Fabr.), dans le sud-ouest du golfe du Saint Laurent. Can. J. Fish. Aquat. Sci. 42: 169−180.

DAVIDSON, K., J. C. ROFF, AND R. W. ELNER. 1985. Morphological, electrophoretic, and fecundity characteristics of Atlantic snow crab, *Chionoecetes opilio*, and implications for fisheries management. Can. J. Fish. Aquat. Sci. 42: 474−482.

DAVIES, R. G. 1971. Computer programming in quantitative biology. Academic Press, London. 492 p.

DIXON, W. J., AND F. J. MASSEY. 1957. Introduction to statistical analysis. McGraw-Hill, New York, NY. 638 p.

DRACH, P., AND C. TCHERNIGOVTZEFF. 1967. Sur la méthode de détermination des stades d'intermue et son application générale aux crustacés. Vie Milieu Ser. A Biol. Mar. 18: 595−610.

HARTNOLL, R. G. 1963. The biology of Manx spider crabs. Proc. Zool. Soc. Lond. 141: 423−496.

HOOPER, R. G. 1986. A spring breeding migration of the snow crab (*Chionoecetes opilio*) into shallow water in Newfoundland. Crustaceana. (In press)

LEBART, L., A. MORINEAU, AND J. P. FENELON. 1979. Traitement des données statistiques, méthodes et programmes, Dunod, Paris. 513 p.

MORIYASU, M., AND P. MALLET. 1986. Reading molt stages of the snow crab (*Chionoecetes opilio*) by observation of maxilla. J. Crust. Biol. (In press)

MORRISON, D. F. 1976. Multivariate statistical methods. McGraw-Hill, New York, NY. 415 p.

PAUL, A. J. 1984. Mating frequency and viability of stored sperm in the tanner crab *Chionoecetes bairdi* (*Decapoda, Majidae*). J. Crust. Biol. 4(3): 375−381.

PAUL, A. J., A. E. ADAMS, J. M. PAUL, H. M. FEDER, AND W. E. DONALDSON. 1983. Some aspects of reproductive biology of the crab *Chionoecetes bairdi*. Univ. Alaska, Alaska Sea Grant Rep. 83−1, IMS Rep. 82−4: 32 p.

POWLES, H. 1968. Distribution and biology of the spider crab *Chionoecetes opilio* in the Madgalen Shallows, Gulf of St. Lawrence. Fish. Res. Board Can. MS Rep. Ser. 997: 106 p.

SOMERTON, D. A. 1980. A computer technique for estimating the size of sexual maturity in crabs. Can. J. Fish. Aquat. Sci. 37: 1488−1494.

1981. Regional variation in the size of maturity of two species of tanner crab (*Chionoecetes bairdi* and *C. opilio*) in the eastern Bering Sea, and its use in defining management subareas. Can. J. Fish. Aquat. Sci. 38: 163−174.

TAYLOR, D. M., R. G. HOOPER, AND G. P. ENNIS. 1985. Biological aspects of the spring breeding migration of snow crabs, *Chionoecetes opilio* in Bonne Bay, Newfoundland (Canada). Fish. Bull. 83(4): 707−711.

TEISSIER, G. 1933. Etude de la croissance de quelques variants sexuels chez *Macropodia rostrata* L. Bull. Biol. France Belg. 67: 401−444.

1935. Croissance des variants sexuels chez *Maïa squinado* L. Trav. Stat. Biol. Roscoff 13: 93−130.

WATSON, J. 1970. Maturity, mating, and egg laying in the spider crab, *Chionoecetes opilio*. J. Fish. Res. Board Can. 27: 1607−1616.

1972. Mating behavior in the spider crab, *Chionoecetes opilio*. J. Fish. Res. Board Can. 29: 447−449.

WATSON, J., AND P. G. WELLS. 1970. A gauge for carapace measurements of crabs. J. Fish. Res. Board Can. 27: 1158−1161.

Food Limitation of Larval Dragonflies: A Field Test of Spacing Behaviour

Robert L. Baker

Department of Zoology, University of Toronto, Erindale Campus, Mississauga, Ont. L5L 1C6

Baker, R. L. 1986. Food limitation of larval dragonflies: a field test of spacing behaviour. Can. J. Fish. Aquat. Sci. 43: 1720–1725.

Density-dependent growth and survival of larval odonates may result from some larvae excluding others from profitable hunting sites. This hypothesis predicts that both degree and variation in food limitation should increase with population density; it also suggests that large larvae should show less food limitation than small larvae. I tested these predictions by analyzing food limitation, determined by mass of fecal pellets, and population density of larval *Ischnura verticalis* and *Enallagma ebrium* from a pond in southern Ontario. When data from all sampling days were combined, population densities of both species were negatively correlated with gut fullness but there was no correspondence between population density and gut fullness measured at different sites on any given day. Also, there was no correlation between population density and variation in food limitation and there was no evidence that small larvae suffered a greater degree of food limitation than larger larvae. A lack of discrete and persistent prey patches and/or low larval population densities may account for the lack of evidence that larvae are excluded from patches of prey.

Les taux de croissance et de survie dépendants de la densité des larves d'odonates peuvent s'expliquer par le fait que certaines larves en excluent d'autres de lieux de chasse profitables. Selon cette hypothèse, le degré et la variation de la limitation alimentaire devraient s'accroître avec la densité de la population et les grosses larves devraient subir une limitation alimentaire moins importante que les petites. J'ai testé ces prévisions en analysant la limitation alimentaire, déterminée par la masse des pastilles fécales, et la densité de population de larves de *Ischnura verticalis* et *Enallagma ebrium* habitant un étang du sud de l'Ontario. Les densités de population des deux espèces étaient négativement corrélées avec le contenu stomacal lorsqu'on utilisait l'ensemble des données de tous les jours d'échantillonnage, mais cette corrélation était absente aux divers sites si l'on utilisait les données d'un seul jour. Il y avait aussi absence de corrélation entre la densité de population et la variation de la limitation alimentaire et aucun indice n'indiquait que les petites larves souffraient plus du manque de nourriture que les grosses larves. L'absence de plages discrètes et persistantes de proies et/ou les faibles densités des populations larvaires peuvent expliquer l'absence d'indices de l'exclusion de larves des plages de proies.

Received December 19, 1985
Accepted April 28, 1986
(J8617)

Reçu le 19 décembre 1985
Accepté le 28 avril 1986

Recent laboratory studies suggest that several species of aquatic insects engage in some form of spacing behaviour (Baker 1981; Hildrew and Townsend 1980; Wiley and Kohler 1984) and several authors have suggested these behavioural interactions may account for observed changes in individual growth rates and local population densities (Macan 1977; McAuliffe 1984; Wiley and Kohler 1984). Unfortunately it is often difficult to assess the importance of these behavioural interactions because it is often difficult to determine if, and how often, interactions occur in the field.

Growth and behaviour of larval odonates provide a good example of this problem. Under laboratory conditions, individuals of some species remain near profitable hunting sites and exclude conspecifics (Baker 1981, 1983), and under field conditions, increases in population density can reduce individual growth rates and survival (Benke 1978; Johnson et al. 1984; Johnson et al. 1985; Morin 1984; Pierce et al. 1985). Although exclusion of larvae from food could account for density-dependent growth, there is no evidence that exclusion is important in the field. It may be that prey are fairly evenly distributed in the field, and thus, exclusion of larvae from particular areas will have little influence on feeding, growth, or survival. Also, even if food is patchy, the number of patches may not be limiting. In this paper, I test for evidence of spacing behaviour in field populations of odonates by analyzing aspects of food limitation.

The hypothesis that exclusion of some larvae occurs in the field predicts a positive relationship between population density and food limitation. When densities are high, a greater proportion of the population should be excluded from the limited number of hunting sites. The hypothesis also predicts a positive correlation between density and variation in food limitation; when animals are rare, all should be able to find feeding sites, but when numerous, some animals should find sites while others are excluded. Finally, the hypothesis predicts that small, subordinate larvae should show a greater degree of food limitation than large larvae because they are more likely to be excluded from feeding areas (Baker 1980). Differences in food limitation should be greatest when population densities are highest.

I tested these predictions by analyzing food limitation and densities of larval *Ischnura verticalis* (Say) and *Enallagma ebrium* (Hagen) populations from a pond in southern Ontario.

Materials and Methods

Study Area

The pond on the Erindale Campus of the University of Toronto in the City of Mississauga was dug in 1968 and has a surface area of 0.62 ha with a mean depth of 1 m. At depths less than 1 m the bottom is almost entirely covered in aquatic vegetation.

Three sampling stations were used, station 1 near the north shore was almost entirely covered with *Myriophyllum spicatum*. Station 2 near the east shore was also dominated by *Myriophyllum*. Large amounts of allochthonous material were also collected at this station. Station 3 near the south shore was covered in approximately equal amounts of *Elodea canadensis* and *Myriophyllum*.

Ice-off occurred in mid-April 1983 and 1984. Mean water temperature ranged from 22 to 26°C during summer months, but a gradual decline began in mid-September 1983 and late August 1984. The pond froze over in mid-December 1983 and early January 1985. Temperatures at the three stations were similar.

At least four species of fish were present in the pond: goldfish, *Carassius auratus*; carp, *Cyprinus carpio*; brown bullhead, *Ictalurus nebulosus;* and largemouth bass, *Micropterous salmoides*.

Population Densities of Odonates and Prey

I sampled the pond twice in August 1983 and then monthly from September to November 1983 and from May to September 1984. On each sampling day I took six samples from each station; two samples were taken from each depth of approximately 10, 30, and 60 cm. I sampled with a "drop box" (Benke and Benke 1975) 75 cm high and 30 cm square. I pushed the open end of the box into the mud and removed all the vegetation with a grapple; I then used a hand net (mesh opening 500 μm) to collect animals not collected with the vegetation. I chose to work with mesh openings of 500 μm because, although some small prey could pass through the net, meshes of smaller openings were quickly clogged with sediments and I was concerned that the backpressure would reduce my efficiency of capturing odonates. I used the net until only fine sediment remained. Samples were preserved in the field with formalin (1983) or 95% ethanol (1984).

Odonates were picked from samples by hand. Each sample was sieved through meshes of 16.0 mm, 1.0 mm, and 500 μm to rid them of fine sediment. Material remaining on the 16.0-mm screen, after being picked free of odonates, was air dried to a constant weight and weighed to the nearest 0.01 g to estimate the abundance of substrate of zygopteran larvae.

Larvae of *I. verticalis* and *E. ebrium* were classified into the four developmental stages described by Baker (1986a), with stage 1 being the smallest and stage 4 the largest. Very small larvae (head width smaller than 0.6 mm) could not be identified to species and were excluded from analysis.

Prey population densities were estimated from subsamples of the original samples. Material retained by the 1.0-mm and 500-μm screens was spread evenly over the bottom of large tubs and subsampled by delimiting one quarter of the bottom with a plastic frame made to fit a corner of the tub. The material was removed with a large-bore pipet and sorted under a dissecting microscope. I considered all chironomids, Cladocera, ostracods, and copepods as prey, since they were frequently seen in the odonate's fecal pellets. Oligochaetes and mayflies (*Caenis*) were common in the samples but I did not consider them as prey because they were not seen in the fecal pellets. Oligochaetes and *Caenis* may have escaped detection by the odonates by remaining on or near the sediments which were avoided by the odonates. Dip net samples taken from the vegetation, but above the sediments, rarely collected any oligochaetes or *Caenis*.

Food Limitation

Food limitation was estimated using a modified version of the technique developed by Folsom and Collins (1982) and Thompson (1982). On the day before each sampling day, I used a dip net (mesh size 500 μm) to collect larvae from each station. I collected larvae from all depths by sweeping the net in a wide arc from the shore towards the centre of the pond and then back again. I emptied the contents of the net into white enamel pans and immediately transferred individual larvae to small plastic vials filled with clean, dechlorinated water. Larvae were returned to the laboratory and kept in the vials for 48 h, during which time they defecated. I collected fecal pellets 24 and 48 h after larvae were collected and transferred them to small metal dishes. Pellets were dried at 50°C for 5 d and then weighed to the nearest microgram on an electrobalance.

Folsom and Collins (1982) developed a food limitation index by subtracting the $\log_{10}$ (mass of pellets) produced by larvae collected in the field from a predicted maximum value based on pellets produced by larvae fed ad libitum in the laboratory. Thompson (1982) also used pellets from larvae fed ad libitum in the laboratory to predict maximum pellet mass. Unfortunately, this method can lead to questionable estimates of food limitation because mass of pellets produced by larvae fed ad libitum in the laboratory is dependent on the type of food offered (Baker 1986b). In an effort to avoid this problem, I estimated food limitation by comparing the mass of pellets produced by larvae collected in the field with a predicted maximum pellet mass estimated from the heaviest pellets produced by the field collected animals.

Plots of the pellet mass of larvae collected in the field showed a wide range for any given head width (Fig. 1 and 2). However, despite this variability there is a distinct upper border of points on both figures. That the border shows an apparently linear relationship with head width suggests that it represents the maximum pellet mass for larvae of a given head width. Both Folsom and Collins (1982) and Thompson (1982) reported linear relationships between log (pellet mass) and head width for *Anax junius* and *Ischnura elegans*, respectively. In addition, the border corresponds well with the pellet mass of larvae (indicated by stars on Fig. 1 and 2) given ad libitum feedings of worms in the laboratory (R. L. Baker, unpubl. data). These points suggest that the upper border of points on Fig. 1 and 2 represents a good estimate of maximum pellet mass. Thus, I estimated food limitation by calculating the gut fullness for each larva collected in the pond by dividing its pellet mass by the value of the line fitted by eye to the upper border of points. Comparison of gut fullness of larvae in different stages could be affected by the slope of the line, but the

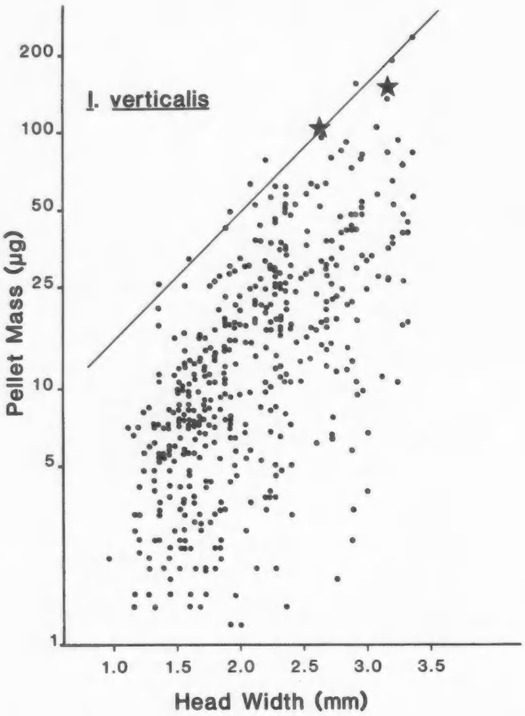

FIG. 1. Relationship between head width and dry mass of fecal pellets of *I. verticalis* larvae collected from the field. Stars represent mean pellet mass of larvae fed worms ad libitum in the laboratory plotted against the midpoint of that instar's range in head width. The line, fitted by eye, represents maximum pellet mass used in calculation of gut fullness.

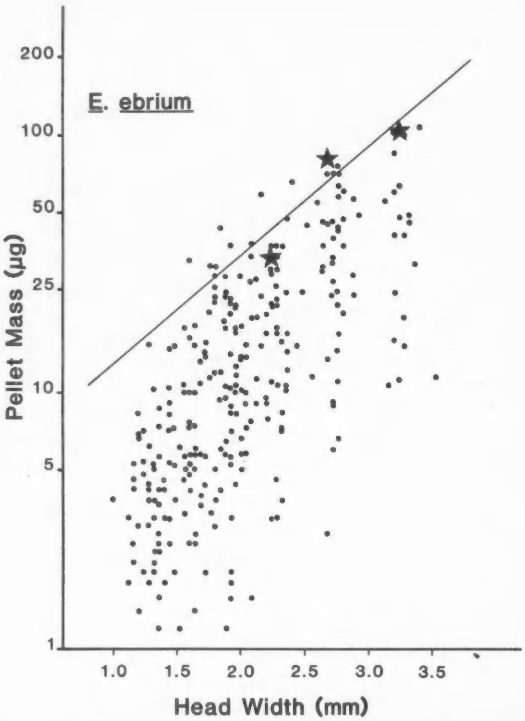

FIG. 2. Relationship between head width and dry mass of fecal pellets of *E. ebrium* larvae collected from the field. Symbols as in Fig. 1.

TABLE 1. Partial correlation coefficients and significance levels for correlation analysis between gut fullness and odonate density with effects of the two food types held constant (density expressed as no. $\cdot$ m^{-2} or no. $\cdot$ g $substrate^{-1}$ for each odonate species or both species combined; *I. verticalis* $n = 22$, *E. ebrium* $n = 19$; $^{*}P < 0.05$, $^{**}P < 0.01$).

Density units	*I. verticalis*	*E. ebrium*
Single species		
No $\cdot$ m^{-2}	−0.49*	−0.67**
No. $\cdot$ g^{-1}	−0.43	−0.64**
Species combined		
No $\cdot$ m^{-2}	−0.52*	−0.50*
No. $\cdot$ g^{-1}	−0.49*	−0.67**

great range in pellet mass at any head width suggests that small changes in slope would have little effect. I excluded all stage 4 animals from analysis because feeding may be reduced due to impending emergence and thus obscure any pattern related to food limitation.

Results

Density and Food Limitation

I used partial correlation analysis to test for a correlation between odonate population density and gut fullness while controlling for any effects of prey abundance. There were obvious changes in prey abundance during the study and I was concerned that these changes would obscure any relation between odonate density and gut fullness. Prey were grouped into two types for analysis: chironomids and small crustacea (Cladocera, ostracods, and copepods). Mean gut fullness for any day × station combination was correlated with mean odonate density and mean densities of the two prey types measured on the following day. I excluded any data points from the analysis if five or fewer animals were used in calculating gut fullness. On average there were 22.5 animals of each species (range 6−47) used in the calculation of each mean. Densities of odonates and prey were transformed to common logarithms before analysis, as the variance of the original data was dependent on the mean. The arcsine transformation was applied to the estimate of gut fullness, as fullness was expressed as a percentage.

Gut fullness of *I. verticalis* was negatively correlated with population density expressed as number per square metre but not as number per gram of substrate (Table 1). Gut fullness of *E. ebrium* was negatively correlated with population density expressed either as number per square metre or number per gram of substrate.

I also calculated correlation coefficients for each species' gut fullness with the population density of both species combined. Laboratory experiments indicated that interactions between conspecifics were indistinguishable from interactions between the two species (R. L. Baker, unpubl. data), and I felt that the degree of food limitation may be more strongly related to the

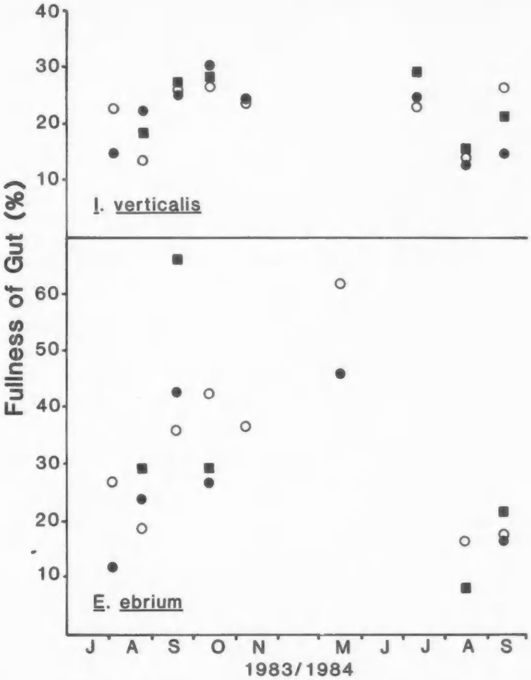

FIG. 3. Mean gut fullness of larval *I. verticalis* and *E. ebrium* at station 1 (●), station 2 (■), and station 3 (○).

density of both species combined. Very few larvae of any other zygopteran species were found in the pond; thus, the combined densities of *I. verticalis* and *E. ebrium* represent the density of Zygoptera. In general, correlations involving density of both species were similar to those using each species density alone. However, in the anlysis of the combined densities, gut fullness of *I. verticalis* was negatively correlated with density expressed as number per square metre.

The partial correlation coefficients between odonate density and gut fullness were not strongly affected by variation in prey density; the first-order correlations between odonate density and gut fullness were similar to those for the partial correlations. Also, there was no significant correlation between prey density and gut fullness nor between prey density and odonate density no matter how expressed.

Unfortunately, correlation analysis is not completely appropriate for the population data, as the individual points are not strictly independent; population density on any day will be partly dependent on the population density of the previous day. Therefore, the significance levels must be judged with caution. Another way of testing for effects of population density on food limitation is to study the correspondence between stations showing the lowest population densities and those showing the highest gut fullness. If exclusion from feeding areas is important in determining food limitation, one would predict that the station with the lowest population density would tend to have the highest gut fullness on any given day.

During summer and fall 1983, densities of both species at station 2 were an order of magnitude lower than those at stations 1 and 3; the ratio of prey to odonate larvae ranged from 3 to 7 times higher at station 2 compared with stations 1 and 3.

TABLE 2. Partial correlation coefficients for correlation analysis between the coefficient of variation of gut fullness and density with effects of gut fullness held constant (density expressed as in Table 1; *I. verticalis* $n = 22$, *E. ebrium* $n = 19$; no correlation was significant at the 0.05 level).

Density Units	*I. verticalis*	*E. ebrium*
Single species		
No. $\cdot$ m^{-2}	0.32	0.29
No. $\cdot$ g^{-1}	0.27	0.20
Species combined		
No. $\cdot$ m^{-2}	0.25	0.26
No. $\cdot$ g^{-1}	0.22	0.08

During late summer and fall 1984, densities of both species at station 2 were approximately one third to one half the densities at the other two stations; the ratio of prey to odonate larvae ranged from 10 to 200% higher at station 2 compared with stations 1 and 3. Therefore, if density was important in affecting gut fullness, one would expect larvae at station 2 to show the highest gut fullness. However, there was no indication that gut fullness of either *E. ebrium* or *I. verticalis* was consistently higher at station 2 (Fig. 3). I used Kruskal–Wallace tests to compare the gut fullness at the three stations for each day and species combination where larvae at station 2 showed the highest gut fullness; no test was significant at the 0.05 level.

Density and Variation in Food Limitation

Laboratory experiments (R. L. Baker, unpubl. data) indicated that the coefficient of variation in gut fullness was strongly dependent on gut fullness; larvae fed small amounts of food produced fecal pellets with low and highly variable weights, while larvae fed abundant food produced pellets with high but less variable weights. Therefore, I used partial correlation coefficients to test for effects of larval density on the coefficient of variation in gut fullness while controlling for effects of gut fullness. Neither species showed any significant correlations (Table 2).

Interpretation of these results suffers from the same problems as interpretation of correlations between gut fullness and population density. If density was positively related to the variation in food limitation, one would predict that, on any given day, the coefficient of variation of gut fullness would be lower at station 2 than at the other stations, as it had the lowest population density. However, for both species, the coefficient of variation of gut fullness at station 2 was similar to that at the other two stations.

Larval Size and Food Limitation

I used Mann–Whitney tests to determine if small larvae showed greater degrees of food limitation than large larvae. For every day × station combination, I compared the mean gut fullness of each developmental stage for which I had at least five larvae. For *I. verticalis*, I had sufficient data to compare stages 2 and 3 only; stages 1, 2, and 3 were available for *E. ebrium*.

Of the 12 tests involving stage 2 and stage 3 larvae of *I. verticalis*, only 1 indicated that smaller larvae had a lower gut fullness than the larger larvae. The test was barely significant at the 0.05 level and occurred at station 2 in September 1983 when the population density was low and the ratio of prey to odonate larvae was high. Only one out of four tests involving stage 2 and stage 3 larvae of *E. ebrium* was significant. Again, the difference was barely significant at the 0.05 level (only five stage 3 larvae were available for the test) and it occurred in October 1983 at station 3, when the population density was not particularly high and prey were common. None of the three tests involving stage 1 and stage 2 larvae of *E. ebrium* were significant. In all, only 2 of 19 tests were significant at the 0.05 level and neither occurred when population density was high nor when prey availability was low.

Discussion

Results provide little support for the hypothesis that some odonate larvae are excluded from profitable hunting sites in the field. Although the prediction that gut fullness should be inversely correlated with population density was supported by the results, there was no correspondence between population density and gut fullness measured at the different sites on any given day. It is possible that spacing behaviour acts to adjust the odonate population density to local prey availability, and thus, one should expect similar levels of gut fullness at all stations. However, this seems unlikely, as the prey availability, relative to odonate population density, was always, and usually much, higher at station 2 than at the other two stations. The low density of larvae at station 2 likely resulted from a low rate of oviposition at that site due to an absence of cover for adults; adults were far more common at stations 1 and 3 where the shore was thickly covered in willows and tall grass. Also, the inverse correlation between gut fullness and population density does not provide strong support for the exclusion hypothesis because the correlation could result from other forms of interference competition. For example, aggressive interactions between larval *I. verticalis* can distract larvae from feeding on *Daphnia* to such an extent that feeding rates are reduced by 75% (P. Crowley, University of Kentucky, pers. comm.). The prediction that variation in gut fullness should be positively correlated with density is more specific to the exclusion hypothesis, and thus, the lack of any significant correlation provides reason to reject the hypothesis.

That small larvae showed the same degree of food limitation as large larvae is the most damaging evidence against the exclusion hypothesis. Baker (1980) showed that larval size is important in determining which larvae will control a feeding area; large individuals of *Coenagrion resolutum* almost entirely excluded smaller individuals from using feeding sites. In addition, laboratory experiments with *I. verticalis* and *E. ebrium* indicated that larvae in each size class clearly dominated larvae in smaller size classes by forcing them to retreat (R. L. Baker, unpubl. data).

Lack of support for the exclusion hypothesis may reflect a lack of patchiness of prey under field conditions. Although laboratory experiments indicated that larvae of both *I. verticalis* and *E. ebrium* exhibit spacing behaviour in the laboratory (R. L. Baker, unpubl. data), food may not be clumped in the field. Although there are many reports of "patchiness" of larval prey such as Cladocera (Smyly 1957; Quade 1969; Goulden 1971) and chironomids (Minshall 1984), the patchiness is recognized only from the scale of the sampling methods. There is no evidence to suggest that prey in the field exist in discrete patches similar to those used in laboratory studies (Baker 1980, 1982; Ross 1971). Also, even if prey do exist in discrete patches, the patches may not be persistent enough for behavioural exclusion to have any effect on feeding of larvae. The high mobility of prey such as Cladocera and first instars of Chironomidae and the fact that the substrate (plants) is continually changing through growth and decay argue against the existence of discrete, persistent patches of prey.

Lack of support for the spacing hypothesis may also suggest that interactions are rare due to low population densities. Uttley (1980) suggested that densities of at least $1000 \cdot m^{-2}$ in a "usable" depth of only 8 cm would be needed for aggressive interactions of larval *I. elegans* to have any effect on feeding. In my study the combined densities of both species were usually much less than $1000 \cdot m^{-2}$. Also, by providing an abundance of substrate and cover, the thick vegetation in my study pond may have reduced the number of interactions. Ross (1971) reported that a lack of "environmental structure" increased the number of interactions between larvae of *A. junius* by increasing the degree of aggregation. Behavioural interactions between odonate larvae may only be important in habitats where a scarcity of substrate results in clumped distributions.

Acknowledgements

Many thanks to Nick Collins, Phil Crowley, and Dan Johnson for their helpful comments on an earlier draft of the paper. S. Dixon, M. Lydan, L. Soluk, and R. Tooley provided technical assistance. Research was supported by an NSERC Canada operating grant to R. L. Baker.

References

BAKER, R. L. 1980. Use of space in relation to feeding areas by zygopteran nymphs in captivity. Can. J. Zool. 58: 1060–1065.

1981. Behavioural interactions and use of feeding areas by nymphs of *Coenagrion resolutum* (Coenagrionidae: Odonata). Oecologia 49: 353–358.

1982. Effects of food abundance on growth, survival, and use of space by nymphs of *Coenagrion resolutum* (Zygoptera). Oikos 38: 47–51.

1983. Spacing behaviour by larval *Ischnura cervula* Selys: effects of hunger, previous interactions, and familiarity with an area (Zygoptera: Coenagrionidae). Odonatologica 12: 201–207.

1986a. Developmental stages and the analysis of zygopteran life histories. J. Freshwater Ecol. 3: 325–332.

1986b. Estimating food availability for larval dragonflies: a cautionary note. Can. J. Zool. 64. (In press)

BENKE, A. C. 1978. Interactions among coexisting predators — a field experiment with dragonfly larvae. J. Anim. Ecol. 47: 335–350.

BENKE, A. C., AND S. S. BENKE. 1975. Comparative dynamics and life histories of coexisting dragonfly populations. Ecology 56: 302–317.

FOLSOM, T. C., AND N. C. COLLINS. 1982. An index of food limitation in the field for the larval dragonfly *Anax junius* (Odonata: Aeshnidae). Freshwater Invertebr. Biol. 1: 25–32.

GOULDEN, C. E. 1971. Environmental control of the abundance and distribution of the chydorid Cladocera. Limnol. Oceanogr. 16: 820–831.

HILDREW, A. G., AND C. R. TOWNSEND. 1980. Aggregation, interference and foraging by larvae of *Plectrocnemia conspersa* (Trichoptera: Polycentropidae). Anim. Behav. 28: 553–560.

JOHNSON, D. M., R. E. BOHANAN, C. N. WATSON, AND T. H. MARTIN. 1984. Coexistence of *Enallagma divagans* and *Enallagma traviatum* (Zygoptera: Coenagrionidae) in Bays Mountain Lake, Tennessee: an in situ enclosure experiment. Adv. Odonatol. 2: 57–70.

JOHNSON, D. M., P. H. CROWLEY, R. E. BOHANAN, C. N. WATSON, AND T. H. MARTIN. 1985. Competition among larval dragonflies: a field enclosure experiment with *Tetragoneuria cynosura* and *Celithemis elisa* (Odonata: Anisoptera), Ecology 66: 119–128.

MACAN, T. T. 1977. The influence of predation on the composition of freshwater animal communities. Biol. Rev. Cambridge Philos. Soc. 52: 45–70.

McAuliffe, J. R. 1984. Competition for space, disturbance, and the structure of a benthic stream community. Ecology 65: 894–908.

Minshall, G. W. 1984. Aquatic insect–substrate relationships, p. 358–400. *In* V. H. Resh and D. M. Rosenberg [ed.] The ecology of aquatic insects. Praeger, New York, NY.

Morin, P. J. 1984. The impact of fish exclusion on the abundance and species composition of larval odonates: results of short-term experiments in a North Carolina farm pond. Ecology 65: 53–60.

Pierce, C. L., P. H. Crowley, and D. M. Johnson. 1985. Behavior and ecological interactions of larval Odonata. Ecology 66: 1504–1512.

Quade, H. W. 1969. Cladoceran faunas associated with aquatic macrophytes in some lakes in northwestern Minnesota. Ecology 50: 170–179.

Ross, Q. E. 1971. The effect of intraspecific interactions on the growth and feeding behavior of *Anax junius* (Drury) naiads. Ph.D. thesis, Michigan State University, East Lansing, MI.

Smyly, W. J. D. 1957. Distribution and seasonal abundance of Entomostraca in moorland ponds near Windermere. Hydrobiol. 11: 59–72.

Thompson, D. J. 1982. Prey density and survival in damselfly larvae: field and laboratory studies. Adv. Odonatol. 1: 267–280.

Uttley, M. G. 1980. A laboratory study of mutual interference between freshwater invertebrate predators. Ph.D. thesis, University of York, York, England.

Wiley, M., and S. L. Kohler. 1984. Behavioral adaptations of aquatic insects, p. 101–133. *In* V. H. Resh and D. M. Rosenberg [ed.] The ecology of aquatic insects. Praeger, New York, NY.

Zinc and Cadmium Transport by the Vertically Migrating Opossum Shrimp, *Mysis relicta*

J. A. Van Duyn-Henderson and D. C. Lasenby

Watershed Ecosystems Programme, Trent University, Peterborough, Ont. K9J 7B8

Van Duyn-Henderson, J. A., and D. C. Lasenby. 1986. Zinc and cadmium transport by the vertically migrating opossum shrimp, *Mysis relicta*. Can. J. Fish. Aquat. Sci. 43: 1726–1732.

Mysis feeding on sediments ingested 2–4 times more zinc and 8 times more cadmium than mysids feeding on zooplankton. Mysids feeding on sediments egested 3–5 times more zinc and 5–7 times more cadmium than those feeding on zooplankton. Concentrations of zinc and cadmium were 5–24 times higher in the faecal pellets than in the food. There was little difference in the amount of zinc and cadmium transported upward or downward per mysid. However, 3–4 times more zinc and 4–7 times more cadmium were concentrated and recycled by *Mysis* at the sediments than in the water column. On a population basis, mysids transported 5 μg Zn and 0.008 $\mu g\ Cd \cdot m^{-3} \cdot night^{-1}$ into the water column and 9 μg Zn and 0.020 $\mu g\ Cd \cdot m^{-2} \cdot d^{-1}$ to the sediments. It was suggested that mysids and their particulate products (faecal pellets, exuviae) may play an important role in the transport and recycling of cadmium and zinc to other members of the food web.

Les *Mysis* se nourrissant à partir des sédiments ingéraient de 2 à 4 fois plus de zinc et 8 fois plus de cadmium que les mysidés se nourrissant du zooplancton. Les mysidés se nourrissant à partir des sédiments excrétaient de 3 à 5 fois plus de zinc et de 5 à 7 fois plus de cadmium que ceux se nourrissant du zooplancton. Les concentrations de zinc et de cadmium des pastilles fécales étaient de 5 à 24 fois plus élevées que celles notées dans la nourriture. Il y avait peu de différences entre les quantités de zinc et de cadmium transportées vers le haut ou vers le bas par les mysidés, mais de 3 à 4 fois plus de zinc et de 4 à 7 fois plus de cadmium étaient concentrés et recyclés par les *Mysis* des sédiments, comparativement à ceux de la colonne d'eau. Dans l'ensemble, les mysidés transportaient 5 $\mu g \cdot m^{-3}$ de Zn et 0,008 $\mu g \cdot m^{-3}$ de Cd dans la colonne d'eau par nuit et 9 $\mu g \cdot m^{-2}$ de Zn et 0,020 $\mu g \cdot m^{-2}$ de Cd dans les sédiments par jour. On a émis l'hypothèse que les mysidés, et leurs produits particulaires (pastilles fécales et exuvies), pouvaient jouer un rôle important dans le transport et le recyclage du cadmium et du zinc vers les autres membres du réseau alimentaire.

Received April 15, 1985
Accepted May 6, 1986
(J8184)

Reçu le 15 avril 1985
Accepté le 6 mai 1986

Industrial and cultural activities in North America have led to the widespread dispersal of trace metals, and substantial quantities of these materials are ultimately deposited in the sediments of lakes and rivers (Evans and Rigler 1980; Forstner and Wittmann 1981). In most lakes, chemical and physical remobilization is minimal; hence, it is normally assumed that this sedimentary pool of trace metals is immobile and thus will not be returned to the open water (Forstner and Wittmann 1981). However, many vertically migrating benthic organisms (e.g. *Mysis*, *Pontoporeia*, *Chaoborus*), which inhabit the relatively uncontaminated pelagic zone by night and the contaminated sediments by day, may accumulate metals from the sediments and return them to the pelagic zone during their diurnal vertical migration. Fish that feed on these organisms may be exposed to a significant source of metals.

In this study, we examine the possibility that *Mysis relicta* can transport trace metals from the sediment to the water column and vice versa during diurnal vertical migration, providing a pathway for normally immobile contaminants in the sediments to return to the overlying water. Previous studies have suggested that *Mysis* feeds on sediments during the day (Stalberg 1933; Tattersall and Tattersall 1951; Green 1965; Lasenby and Langford 1973) and on zooplankton at night (Lasenby and Langford 1973; Morgan et al. 1978; Cooper and Goldman 1980; and others). Therefore, because *Mysis* feeds in both the benthic and pelagic communities, *Mysis* has the potential to ingest or adsorb metals from the sediments during the day and transport them into the water column at night, both directly as metal body burden and indirectly through metals in molted exoskeletons and faecal pellets containing egested sediments (Fig. 1). Similarly, *Mysis* can ingest or adsorb metals from the water column at night and transport them to the sediments during the day, through body burden, molted exuviae, and faecal pellets containing egested zooplankton (Fig. 1).

Many aquatic organisms concentrate metals and other contaminants in their faecal pellets (Johannes and Satomi 1966; Boothe and Knauer 1972; Benayoun et al. 1974). Therefore, in this study we also examine the possibility of concentration and recycling of metals by *Mysis* through ingestion and egestion of sediments while on the lake bottom and the ingestion and egestion of zooplankton while in the water column (Fig. 1).

The metals zinc and cadmium were chosen, since previous work has shown that they are among the most toxic trace metals and are possibly the most disruptive to plankton communities (Wood 1974; Marshall et al. 1981; Attar and Maly 1982). Our study focuses on *M. relicta* because it is the principal prey item for many sport- and game-fish (Fürst 1972; Morgan et al. 1978; Janssen and Brandt 1980; Parker 1980); thus, the possibility of

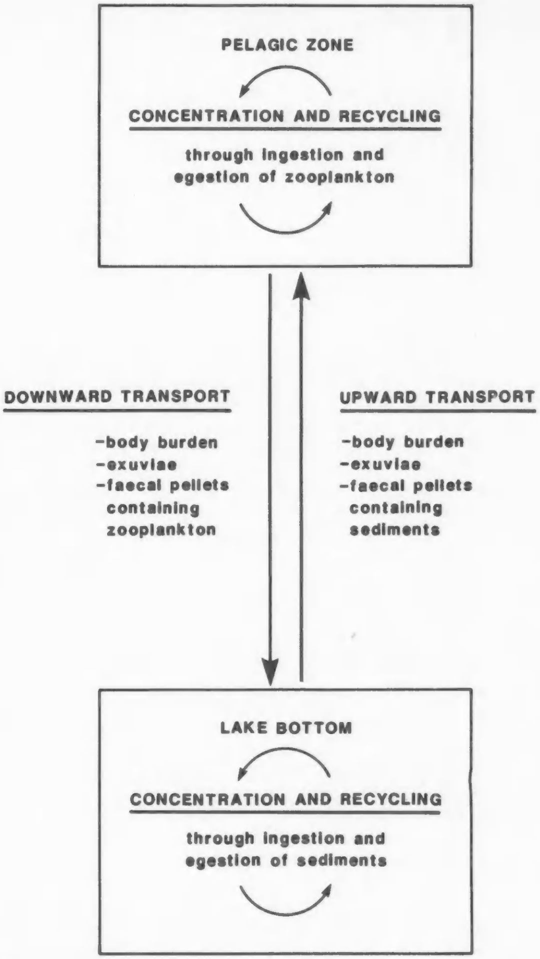
PELAGIC ZONE
CONCENTRATION AND RECYCLING
through ingestion and egestion of zooplankton
DOWNWARD TRANSPORT
-body burden
-exuviae
-faecal pellets containing zooplankton
UPWARD TRANSPORT
-body burden
-exuviae
-faecal pellets containing sediments
LAKE BOTTOM
CONCENTRATION AND RECYCLING
through ingestion and egestion of sediments

FIG. 1. Simplified schematic of vertical transport and recycling of metals by *M. relicta* during daily migratory cycle.

biological mobilization of trace metals into the food chain becomes particularly important. Also, mysids may play a significant role in the transport of toxic organics into the food chain in the Great Lakes (Delfino 1979; Evans et al. 1982).

Materials and Methods

Crystal Lake is a meso-eutrophic lake located on the southern edge of the Precambrian Shield in southern Ontario (78°19′W, 44°45′N; $Z_{max} = 37$ m, $A = 4.69$ km^2). Chemically, Crystal Lake water is characterized by Cd $< 0.01\ \mu g \cdot L^{-1}$, Zn $= 0.3\ \mu g \cdot L^{-1}$ (Van Duyn-Henderson, unpubl.), pH = 8.1, Ca $= 27.1\ mg \cdot L^{-1}$, and DOC $= 5.3\ mg \cdot L^{-1}$ (Ontario Ministry of the Environment, Central Region, Dorset, Ont., unpubl.). Crystal Lake was chosen as the study site because it has a resident population of mysids with a 2-yr life cycle (Sherman 1984). This ensured a wide size range of animals available during the study. In addition, Crystal Lake surficial sediments are enriched in both zinc and cadmium (approximately 360 μg Zn and 2 μg Cd$\cdot$g dry weight^{-1}, Van Duyn-Henderson 1985) relative to background concentrations, like other lakes in the Muskoka–Haliburton region (Smith 1983).

To determine if *Mysis* does have contact with the sediments and therefore has the potential to accumulate metals from this source, the diurnal vertical migration of *M. relicta* in Crystal Lake was studied on August 28, 1984. This was done by 5-m stage hauls using a Wisconsin plankton net (363-μm mesh) at approximately 4-h intervals over a 24-h period. To determine what mysids were feeding on, the gut contents of these mysids were examined according to the methods of Lasenby and Langford (1973).

To quantify transfer rates of metals to *Mysis* from their food sources, laboratory experiments using adult and immature mysids feeding on sediments or macrozooplankton were carried out to provide gravimetric estimates of ingestion and egestion rates. For each feeding experiment we used seven 1-L Nalgene beakers containing filtered (1-μm Nitex) Crystal Lake water and a measured amount of food. For sediment-feeding experiments the food consisted of 3.4 mg dry weight ± 0.3 SEM surficial (top 1 cm) lake sediment per beaker, added as wet sediment. Preliminary experiments showed that there was no increase in cadmium or zinc concentration in the water overlying the sediments over the duration of the experiment (J. A. Van Duyn-Henderson, unpubl.). For zooplankton-feeding experiments the food consisted of 4.3 mg dry weight ± 0.6 SEM macrozooplankton (greater than 363 μm, approximately 70% *Limnocalanus macrurus*, 25% *Daphnia galeata mendotae*, and 5% *Diaptomus oregonensis* by number) per beaker. Mysids were added to five of the beakers and allowed to feed for 12 h so that they ingested approximately half of the available food. Each experiment was run using either all adult mysids (5 replicates, 4 mysids per beaker) or all immature mysids (5 replicates, 10 mysids per beaker). The remaining two beakers were used as controls (food without mysids) for the determination of initial food dry weight and metal concentration and the possible presence of mysid faecal pellets. At the end of 12 h, mysids, uneaten food, and mysid faecal pellets were collected, dried on acid-washed polyethylene strips at 60°C to a constant weight, and stored in a desiccator for subsequent metal analysis. The ingestion rate for mysids feeding on sediments or zooplankton in milligrams of food per mysid per hour was calculated for each experimental container as the dry weight of food available at the start of the experiment minus the dry weight of food remaining at the end of the experiment divided by the number of mysids in each container and the duration of the experiment in hours. This ingestion rate was then multiplied by the metal concentration of the food in nanograms of metal per milligram of food to obtain the ingestion rate of metal for mysids feeding on sediments or zooplankton in nanograms of metal per mysid per hour. The egestion rate for mysids feeding on sediments or zooplankton in milligrams of faeces per mysid per hour was calculated for each experimental container as the dry weight of faeces in each beaker at the end of the experiment divided by the number of mysids per beaker and the duration of the experiment in hours. This egestion rate was then multiplied by the metal concentration of the faeces in nanograms of metal per milligram of faeces to obtain the egestion rate of metal in nanograms of metal per mysid per hour. Water, mysids, zooplankton, and sediments were collected from Crystal Lake not more than 24 h before each experiment. Experiments were carried out at 6°C in darkness and replicated once, except the experiments with immature mysids feeding on sediments which were replicated twice.

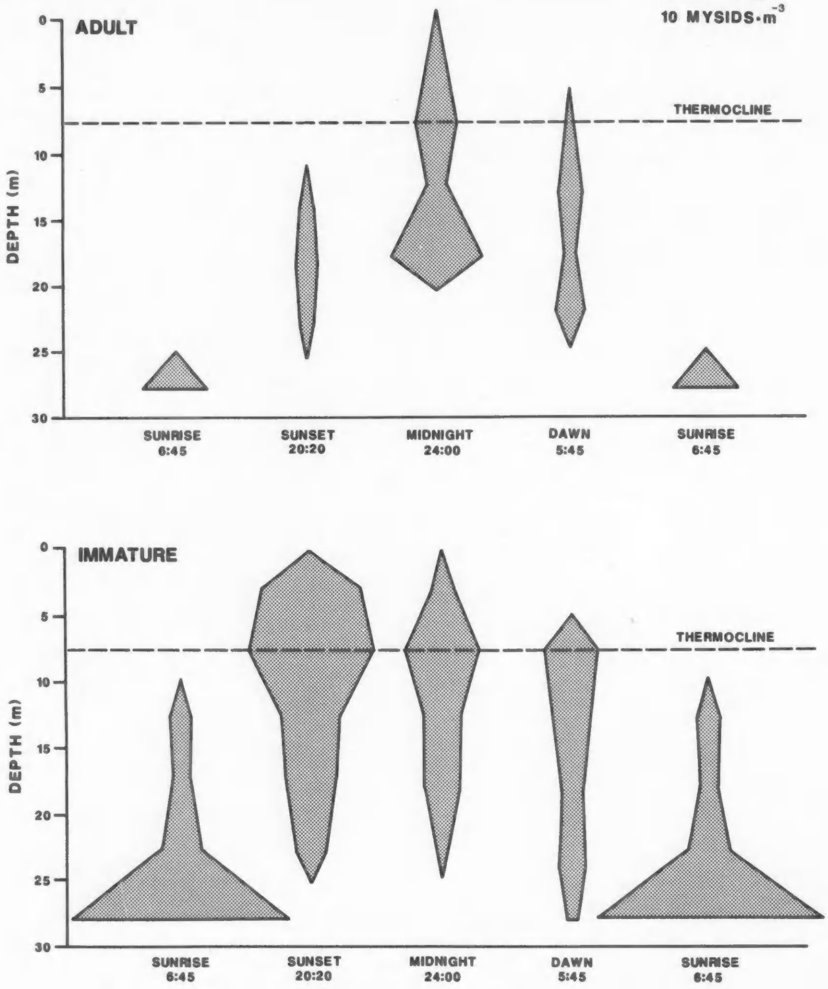

FIG. 2. Vertical distribution of *M. relicta* in Crystal Lake on August 28, 1984.

To estimate the contribution of mysid body burden to metal transport, mysids from feeding experiments which had been allowed to empty their guts were analyzed for cadmium and zinc concentration.

To obtain molted exoskeletons for metal analysis, 30 mysids were kept in individual 300-mL containers with Crystal Lake water, zooplankton, and sediment in an environmental chamber at 6°C and checked daily for the presence of exuviae. When a mysid had molted, both the mysid and the exuviae were collected, dried, and stored for subsequent metal analysis. The rate of metal loss via molting in nanograms of metal per mysid per hour was calculated as the amount of metal per exuvia in nanograms of metal per exuvia multiplied by the molting rate of 0.0026 $\text{molts}\cdot\text{mysid}^{-1}\cdot\text{h}^{-1}$ (or 1 molt every 16 d, from Berrill and Lasenby 1983).

All dried, weighed samples were digested in 30-mL Teflon FPE vials in 2 mL of concentrated (32%) hydrogen peroxide (Caledon reagent grade) at 180°C for 1–2 h. Samples were taken to dryness and then brought up to 1 mL with 0.1 *M* nitric acid (Baker Instra-Analyzed). Three anlytical blanks were digested concurrently to assess contamination and were always found to be less than 10% of sample metal concentrations. Accuracy and precision were checked against NBS standard reference No. 1755a (bovine liver) and were always within the range of the certified values (certified concentrations $X \pm \text{SM} = 123 \pm 8$ μg Zn and 0.44 ± 0.06 $\mu\text{g Cd}\cdot\text{g dry weight}^{-1}$; analytical concentrations $X \pm \text{SM}$ ($n = 17$) $= 124 \pm 20$ μg Zn and 0.38 ± 0.08 $\mu\text{g Cd}\cdot\text{g dry weight}^{-1}$). Samples were analyzed on a Scintrex Zeeman-modulated flameless AAS with a tungsten filament.

Results

In the field, both adult and immature mysids were concentrated at the sediments during the day. They were never captured in the water column during daylight hours. Mysids ascended at sunset to spend the night (approximately 12 h) in the water column, and returned to the sediments at sunrise (Fig. 2).

TABLE 1. Body burden, ingestion, egestion, and molting rates of zinc and cadmium for adult and immature *M. relicta* feeding on sediments and zooplankton (results of replicate experiments were pooled, as there was no significant difference between them, ANOVA $p < (0.05)$. Units are ng metal · mysid^{-1} · h^{-1}, SEM in parentheses; S = sediment, Z = zooplankton, A = adult, I = immature.

Metal	Food	Size	*n*	Body burden of metal	Ingestion rate of metal	Egestion rate of metal	Molting rate of metal
Zn	S	A	10	337 (45)	5.3 (0.5)	5.9 (0.9)	0.7 (0.5)
		I	14	75 (11)	2.6 (0.4)	3.6 (0.7)	0.06 (0.02)
	Z	A	10	370 (29)	3.3 (0.3)	1.9 (0.2)	0.7 (0.5)
		I	9	115 (15)	0.7 (0.1)	0.8 (0.1)	0.06 (0.02)
Cd	S	A	10	0.58 (0.07)	0.043 (0.004)	0.041 (0.010)	0.003 (0.001)
		I	14	0.25 (0.03)	0.018 ((0.002)	0.010 (0.002)	0.0006 (0.00006)
	Z	A	10	0.49(0.06)	0.0052 (0.0006)	0.0058 (0.0009)	0.003 (0.001)
		I	9	0.16(0.01)	0.0024 (0.0004)	0.0021 (0.0004)	0.0006 (0.00006)

TABLE 2. Amounts of zinc and cadmium transported and recycled by individual adult and immature *Mysis* and their particulate products while on the sediments and in the water column. Units are ng metal · mysid^{-1} · 12 h^{-1}.

			Transport			
Metal	Location	Mysid size	Body burden metal	Exuviae metal	Total metal	Recycling, faeces metal
Zn	Sediment	Adult	337	8	345	71
		Immature	75	0.7	76	43
	Water column	Adult	370	8	378	23
		Immature	115	0.7	116	10
Cd	Sediment	Adult	0.58	0.04	0.62	0.49
		Immature	0.25	0.007	0.26	0.12
	Water column	Adult	0.49	0.04	0.53	0.07
		Immature	0.16	0.007	0.17	0.03

The maximum density of mysids in the water column was 7 adult mysids · m^{-3} and 24 immature mysids · m^{-3} (Fig. 2). This represents a maximum density of mysids on the sediments of 17 adult mysids · m^{-2} and 37 immature mysids · m^{-2} (Fig. 2).

During the day, mysid guts contained mainly amorphous brownish flocculent material and sand grains, apparently of sedimentary origin. During the night, mysid guts contained mainly crustacean zooplankton remains.

Adult mysids had higher body burdens, molting, ingestion, and egestion rates of cadmium and zinc than immature mysids (Table 1). Mysids feeding on sediments ingested 2–4 times more zinc and 8 times more cadmium than mysids feeding on zooplankton (Table 1). Similarly, mysids feeding on sediments egested 3–5 times more zinc and 5–7 times more cadmium than mysids feeding on zooplankton (Table 1). Since there was no increase in cadmium or zinc concentration in the water, in the experimental beakers the higher ingestion and egestion rates of metal in sediment-feeding experiments were probably not due to increased accumulation from the water.

Each adult mysid transported 345 ng Zn and 0.62 ng Cd · d^{-1}, and each immature mysid transported 76 ng Zn and 0.26 ng Cd · d^{-1} to the sediments (Table 2). The metal transport was calculated by multiplying the rates of metal loss via molting (Table 1) by 12 h (the approximate length of time spent on the sediments per day, Fig. 2) and adding these rates to the metal body burdens for mysids feeding on sediments (Table 1). Mysid body burden contributed 96–99% of the total zinc and 94–96% of the total cadmium transported, while exuviae contributed 1–2% of the total zinc and 3–6% of the total cadmium transported to the sediments (Table 2). On a population basis, mysids transported 9 μg Zn and 0.020 μg Cd · m^{-2} · d^{-1} to the sediments, calculated by multiplying the amount of metal transported per mysid by their respective densities on the sediments (17 adult mysids · m^{-2}, 37 immature mysids · m^{-2}).

In addition, each adult mysid recycled 71 ng Zn and 0.49 ng Cd, and each immature mysid recycled 43 ng of Zn and 0.12 ng of Cd through the ingestion and egestion of sediments at the lake bottom each day (Table 2). This is equivalent to 3 μg Zn and 0.013 μg Cd · m^{-2} · d^{-1} recycled by the mysid population as faecal metal, calculated by multiplying the amount of metal recycled per mysid by the density of mysids on the sediment.

It was also estimated that mysids transported 378 ng Zn and 0.53 ng Cd · adult mysid^{-1} · night^{-1} and 116 ng Zn and 0.17 ng Cd · immature mysid^{-1} · night^{-1} into the water column (Table 2). The calculation of metal transport to the water column was identical to that of metal transport to the sediments, using 12 h in the water column (Fig. 2) and molting rates and body burdens of mysids feeding on zooplankton (Table 1). Of the total amount of zinc transported into the water column, 98–99% consisted of mysid body burden and 1–2% of exuviae. Of the total cadmium transported into the water col-

TABLE 3. Mean zinc and cadmium concentrations of faeces and food (SEM in parentheses) for adult and immature *M. relicta* feeding on zooplankton and sediments and calculated mean concentration factors of zinc and cadmium in the faecal pellets over the food.

Metal	Food	Size	*n*	Faeces metal concn. ($\mu g \cdot g^{-1}$)	Food metal concn. ($\mu g \cdot g^{-1}$)	Concentration factor
Zn	Sediment	Adult	10	2916 (706)	399 (63)	7.3
		Immature	14	5228 (1068)	355 (42)	14.7
	Zooplankton	Adult	10	2722 (528)	164 (30)	16.6
		Immature	9	2623 (762)	165 (41)	15.9
Cd	Sediment	Adult	10	15.3 (4.3)	3.0 (0.4)	5.1
		Immature	14	10.9 (2.9)	2.2 (0.3)	5.0
	Zooplankton	Adult	10	7.1 (1.5)	0.3 (0.02)	23.7
		Immature	9	4.8 (0.7)	0.5 (0.07)	9.6

umn, body burden contributed 92−94% and exuviae contributed 6−8% (Table 2). The amount of metal transported into the water coumn was estimated to be 5 μg Zn and 0.008 μg $Cd \cdot m^{-3} \cdot night^{-1}$, calculated using mysid densities of 7 adult $mysids \cdot m^{-3}$ and 24 immature $mysids \cdot m^{-3}$.

The amount of metal recycled in the water column through ingestion and egestion of zooplankton was estimated to be 23 ng Zn and 0.07 ng $Cd \cdot adult\ mysid^{-1} \cdot night^{-1}$ and 0.10 ng Zn and 0.03 ng $Cd \cdot immature\ mysid^{-1} \cdot night^{-1}$ (Table 2). On a population basis, this represents 0.4 μg Zn and 0.001 μg $Cd \cdot m^{-3} \cdot night^{-1}$ recycled as faecal metal.

Discussion

There seems to be little difference in the amount of zinc or cadmium transported upward or downward as body burden and molted exuviae by an individual mysid during diurnal vertical migration (Table 2). However, when first migrating upward, mysids would also transport a small amount of metal as sediments in the gut, to be egested as faecal pellets in the water column. Also, some additional downward transport of metal would occur in the form of zooplankton in the mysid guts and subsequently egested faecal pellets containing zooplankton.

As a result of mysid feeding on sediment of high metal concentration, more cadmium and zinc was recycled on the lake bottom than in the water column. The amount of cadmium recycled as faecal pellets at the sediments was 4−7 times greater than was recycled in the water column (Table 2). Similarly, mysids recycled 3−4 times more zinc as faecal pellets at the sediments than in the water column (Table 2).

Mysid faecal pellets sink at a rate of 80−170 $m \cdot d^{-1}$ (Evans et al. 1982; J. A. Van Duyn-Henderson, unpubl.); therefore, faeces produced in the water column can sink to the sediments in 3−7 h. Assuming that all faecal pellets produced in the water column reach the sediments, the amount of metal transported to the sediments per adult mysid would increase by another 23 ng of Zn and 0.07 ng of Cd, and the amount of metal transported to the sediment by each immature mysid would increase by another 10 ng of Zn and 0.03 ng of Cd (Table 2). Sinking faecal pellets of other zooplankton have been implicated in the vertical oceanic transport of cadmium (Benayoun et al. 1974), cesium (Fowler et al. 1973), zinc (Small and Fowler 1973), polonium (Cherry et al. 1975), and plutonium (Higgo et al. 1977), and our study indicates that faecal pellets may contribute to the downward transport of metals in freshwater lakes.

By migrating, the mysid population increases the amount of cadmium and zinc available in the water column at night by their metal body burden, and metal in molted exuviae. The amount of metal transported into the water column by the mysid population (5 μg Zn and 0.008 μg $Cd \cdot m^{-3} \cdot night^{-1}$) may seem insignificant when compared with the concentrations of zinc and cadmium in the lake water (0.3 μg Zn and <0.01 μg $Cd \cdot L^{-1}$, J. A. Van Duyn-Henderson, unpubl.). However, the metal body burden of *Mysis* may be a highly significant source of metal to the fish which selectively prey on *Mysis*. Food is the major source of cadmium to guppy (*Poecilia reticulata*) (Hatakeyama and Yasuno 1982), chromium, copper, manganese, iron, lead, and zinc to tropical fish (Patrick and Loutit 1978), mercury, zinc, manganese, cobalt, cesium, and iron to American plaice (*Hippoglossoides platesoides*) and two salmonids (Luoma 1983), and lead and mercury to young northern squawfish (*Ptychocheilus oregonensis*) (Bissonnette 1974). *Mysis* is the major prey item of fish such as alewife (*Alosa pseudoharengus*), kokanee salmon (*Oncorynchus nerka*), lake whitefish (*Coregonus clupeaformis*), lake trout (*Salvelinus namaycush*), smelt (*Osmerus mordax*), and others. For example, *Mysis* makes up 50−100% of the gut contents (by weight) of adult alewife, kokanee salmon, and Arctic char (*Salvelinus alpinus*), with the rest consisting largely of macrozooplankton (Fürst 1972; Morgan et al. 1978; Janssen and Brandt 1980; Parker 1980). Assuming cadmium and zinc concentrations of mysids and macrozooplankton to be roughly equivalent (as found in this study), this means that *Mysis* can make up 50−100% of the metal burden in the fish gut at any given time.

The amount of metal transported to the sediments by mysids as body burden and exuviae (Table 2) is probably underestimated because we calculated mysid density on the sediment by totalling the number of mysids in the water column above 1 m^2 of sediment (Fig. 2). This underestimates mysid density on the sediment because at night, mysids tend to migrate horizontally and vertically away from areas of daytime maximum densities (Nero and Davies 1982). Sherman (1984), using a bottom closing net, found mysid densities in Crystal Lake at the same time of year to be approximately 20 times higher than those in this study. These higher mysid densities would increase the estimated amount of zinc and cadmium added to the sediments by the mysid population to 180 μg Zn and 0.40 μg $Cd \cdot m^{-2}$. Seasonal variations in mysid density have been shown to range between 20- and 200-fold (Reynolds and

DeGraeve 1972; Grossnickle and Morgan 1979), which would of course influence our estimates of cadmium and zinc transport and recycling considerably.

Faecal pellets of mysids feeding on sediments and zooplankton were extremely concentrated in cadmium and zinc when compared with the food, with concentration factors ranging from 5 to 24 (Table 3). Faecal pellet concentration factors of this magnitude have been found for a variety of metals and aquatic invertebrates (Boothe and Knauer 1972; Benayoun et al. 1974; Elwood et al. 1976; Fowler 1977). *Mysis*' faecal pellets may be a highly significant source of metals to coprophagous organisms. Many aquatic organisms, including zooplankton, euphausiids, benthic invertebrates, and fish, ingest faecal pellets (Newell 1965; Johannes and Satomi 1966; Frankenberg and Smith 1967; Fenchel 1970; Turner and Ferrante 1979). When mysids concentrate and recycle metal from ingested zooplankton and sediments into faecal pellets, these faecal pellets may represent an addition of metal to the coprophagous community, even though there is no increase in the total amount of metal available in the water column or on the sediments. Thus, in view of the high concentration of metals in faecal pellets and the prevalence of coprophagy, mysid and other faecal pellets may provide a major mechanism for the transport of contaminants to other members of the food web.

In summary, it seems that *Mysis* can transport cadmium and zinc, and probably other metals, from the sediments into the water column and vice versa during their migratory cycle. Mysids can transport metals in two ways: (1) as body burden, providing a direct route for the transfer of metals to higher trophic levels such as fish, and (2) by concentrating metals in their exuviae and faecal pellets, which can provide a concentrated source of metals to other organisms which ingest them. In addition, mysids concentrate and recycle metals in the pelagic zone and at the lake bottom as a result of ingestion and egestion of zooplankton and sediments. Eventually, net transport of metals by *Mysis* is probably downward to the sediments as a result of metals in sinking exuviae, faecal pellets, and mysid carcasses which may accumulate on the lake bottom. In this way, mysids and other benthic invertebrates may play an important role in determining the concentration of metals in lake sediments.

Acknowledgements

This research was supported by a Natural Sciences and Engineering Research Council of Canada (NSERC) grant. We thank Mr. Daniel Pike, Ms. Joanne Young, Mr. Premek Hamr, and Ms. Brenda Lauay for technical assistance.

References

Attar, E. N., and E. J. Maly. 1982. Acute toxicity of cadmium, zinc and cadmium-zinc mixtures to *Daphnia magna*. Arch. Environ. Contam. Toxicol. 11: 291–296.

Benayoun, G., S. W. Fowler, and B. Oregioni. 1974. Flux of cadmium through euphausiids. Mar. Biol. 27: 205–212.

Berrill, M., and D. C. Lasenby. 1983. Lifecycles of the freshwater mysid shrimp *Mysis relicta* reared at two temperatures. Trans. Am. Fish. Soc. 112: 551–553.

Bissonnette, P. 1974. Extent of mercury and lead uptake from lake sediments by Chironomids, p. 609–621. *In* R. E. Wildung and H. Drucker [ed.] Biological implications of metals in the environment. Conf. 750929, NTIS, Springfield, VA.

Boothe, P. N., and G. A. Knauer. 1972. The possible importance of faecal material in the biological amplification of trace and heavy metals. Limnol. Oceanogr. 17: 270–274.

Cherry, R. D., S. W. Fowler, T. M. Beasley, and M. Heyraud. 1975. Polonium-210: its vertical oceanic transport by zooplankton metabolic activity. Mar. Chem 3: 105–110.

Cooper, S. D., and C. R. Goldman. 1980. Opossum shrimp (*Mysis relicta*) predation on zooplankton. Can. J. Fish. Aquat. Sci. 37: 909–919.

Delfino, J. J. 1979. Toxic substances in the Great Lakes. Environ. Sci. Technol. 13: 1462–1468.

Elwood, J. W., S. G. Hildebrand, and J. J. Beauchamp. 1976. Contribution of gut contents to the concentration and body burden of elements in *Tipula* spp. from a spring-fed stream. J. Fish. Res. Board Can. 33: 1930–1938.

Evans, M. S., R. W. Bathelt, and C. P. Rice. 1982. PCBs and other toxicants in *Mysis relicta*. Hydrobiol. 93: 205–215.

Evans, R. D., and F. H. Rigler. 1980. Calculation of the total anthropogenic lead in the sediments of a rural Ontario lake. Environ. Sci. Technol. 14: 216–218.

Fenchel, T. 1970. Studies on the decomposition of organic detritus derived from the turtle grass *Thalassia testudinum*. Limnol. Oceanogr. 15: 14–20.

Forstner, U., and G. T. W. Wittmann. 1981. Metal pollution in the aquatic environment. Springer-Verlag, New York, NY. 486 p.

Fowler, S. W. 1977. Trace elements in zooplankton particulate products. Nature (Lond.) 269: 51–53.

Fowler, S. W., M. Heyraud, L. F. Small, and G. Benayoun. 1973. Flux of 141-Ce through a euphausiid crustacean. Mar. Biol. 21: 317–325.

Frankenberg, D., and K. L. Smith, Jr. 1967. Coprophagy in marine animals. Limnol. Oceanogr. 12: 443–450.

Fürst, M. 1972. Experiments on the transplantation of new fishfood organisms into Swedish impounded lakes: the feeding habits of brown trout and char in Lake Blåsjön. Verh. Int. Ver. Limnol. 18: 1114–1121.

Green, R. H. 1965. The population ecology of the glacial relict shrimp *Pontoporeia affinis* Lindstrom in Cayuga Lake, N.Y. Ph.D. thesis, Cornell University, Ithica, NY.

Grossnickle, N. E., and M. D. Morgan. 1979. Density estimates of *Mysis relicta* in Lake Michigan. J. Fish. Res. Board. Can. 36: 694–698.

Hatakeyama, S., and M. Yasuno. 1982. Accumulation and effects of cadmium on guppy (*Poecilia reticulata*) fed cadmium-dosed Cladocera (*Moina macrocopa*). Bull. Environ. Contam. Toxicol. 29: 159–166.

Higgo, J. J. W., R. D. Cherry, M. Heyraud, and S. W. Fowler. 1977. Rapid removal of plutonium from the oceanic surface layer by zooplankton faecal pellets. Nature (Lond.) 266: 623–624.

Janssen, J., and S. B. Brandt. 1980. Feeding ecology and vertical migration of adult alewives (*Alosa pseudoharengus*) in Lake Michigan. Can. J. Fish. Aquat. Sci. 37: 177–184.

Johannes, R. E., and M. Satomi. 1966. Composition and nutritive value of faecal pellets of a marine crustacean. Limnol. Oceanog. 11: 191–197.

Lasenby, D. C., and R. R. Langford. 1973. Feeding and assimilation of *Mysis relicta*. Limnol. Oceanogr. 18: 280–285.

Luoma, S. N. 1983. Bioavailability of trace metals to aquatic organisms — a review. Sci. Total Environ. 28: 1–22.

Marshall, J. S., D. L. Mellinger, and J. I. Parker. 1981. Combined effects of cadmium and zinc on a Lake Michigan zooplankton community. J. Great Lakes Res. 7: 215–223.

Morgan, M. D., S. T. Threlkeld, and C. R. Goldman. 1978. Impact of the introduction of kokanee (*Oncorynchus nerka*) and opossum shrimp (*Mysis relicta*) on a subalpine lake. J. Fish. Res. Board Can. 35: 1572–1579.

Nero, R. W., and I. J. Davies. 1982. Comparison of two sampling methods for estimating the abundance and distribution of *Mysis relicta*. Can. J. Fish. Aquat. Sci. 39: 349–355.

Newell, R. 1965. The role of detritus in the nutrition of two marine deposit feeders, the prosobranch *Hydrobia ulvae* and the bivalve *Macoma balthica*. Proc. Zool. Soc. Lond. 144: 25–45.

Parker, J. I. 1980. Predation by *Mysis relicta* on *Pontoporeia hoyi*: a food-chain link of potential importance in the Great Lakes (a note). J. Great Lakes Res. 6: 164–166.

Patrick, F. M., and M. W. Loutit. 1978. Passage of metals to freshwater fish from their food. Water Res. 12: 395–398.

Reynolds, J. B., and G. M. DeGraeve. 1972. Seasonal population characteristics of the opossum shrimp *Mysis relicta* in Southeastern Lake Michigan: 1970–1971. Proc. Conf. Great Lakes Res. (Int. Assoc. Great Lakes Res.) 15: 117–131.

Sherman, R. K. 1984. Influence of oxygen concentration on the distribution, abundance, and life history of *Mysis relicta* (Lovén) in a temperate lake. M.S. thesis, Trent University, Peterborough, Ont. 182 p.

Small, L. F., and S. W. Fowler. 1973. Turnover and vertical transport of Zn by the euphausiid *Meganictyphanes norvegica* in the Ligurian Sea. Mar. Biol. 18: 284–290.

SMITH, P. J. 1983. Sediment chemistry in lakes in the Muskoka–Haliburton study area. Data Rep. 83/7, Ontario Ministry of the Environment, Dorset, Ont.

STALBERG, G. 1933. Beitrag zur Kenntnis der Biologie von *Mysis relicta* des Vattern. Ark. Zool. 26A: 1–29.

TATTERSALL, W. M., AND O. S. TATTERSALL. 1951. The British Mysidacea. Ray Society, London. 460 p.

TURNER, J. T., AND J. G. FERRANTE. 1979. Zooplankton faecal pellets in aquatic ecosystems. Bioscience 29: 670–677.

VAN DUYN-HENDERSON, J. A. 1985. Vertical transport of zinc and cadmium by *Mysis relicta*. M.S. thesis, Trent University, Peterborough, Ont. 143 p.

WOOD, J. M. 1974. Biological cycles for toxic elements in the environment. Science (Wash., DC) 183: 1049–1052.

Dynamics of Unexploited and Lightly Exploited Populations of Rainbow Trout (*Salmo gairdneri*) from Coastal, Montane, and Subalpine Lakes in Western Canada

D. B. Donald and D. J. Alger[1]

Inland Waters Directorate, 1st Floor Motherwell Building, 1901 Victoria Avenue, Regina, Sask. S4P 3R4

Donald, D. B., and D. J. Alger. 1986. Dynamics of unexploited and lightly exploited populations of rainbow trout (*Salmo gairdneri*) from coastal, montane, and subalpine lakes in western Canada. Can. J. Fish. Aquat. Sci. 43: 1733–1741.

Populations of rainbow trout (*Salmo gairdneri*) in one coastal and two montane lakes were characterized by a relatively stable age structure, approximately 50% annual mortality, maximum longevity of 7 yr, and close to linear growth beginning at age 1 or age 2. In contrast, populations in subalpine lakes were characterized by an unstable age structure, large annual variation in recruitment, maximum longevity of 13 yr or more, and growth patterns that were either asymptotic, complex, or linear. Age structure and thus year-class strength was directly related to cumulative summer temperature in one subalpine lake ($r = 0.71$, $N = 11$), and in others, strong year-classes were often associated with warm summers. These analyses indicate that the magnitude of recruitment in subalpine lakes was either primarily or at least partly due to annual differences in summer temperature. Longevity was inversely related to midsummer water temperature.

Des populations de truites arc-en-ciel (*Salmo gairdneri*) d'un lac côtier et de deux lacs de montagnes se caractérisaient par une structure des âges relativement stable, une mortalité annuelle d'environ 50 %, une longévité maximale de 7 années et une croissance presque linéaire aux âges 1 ou 2. Au contraire, des populations de lacs sub-alpins se caractérisaient par une structure des âges instable, une importante variation annuelle du recrutement, une longévité maximale de 13 ans ou plus et une croissance présentant une allure asymptotique, complexe ou linéaire. La structure des âges, donc l'importance des classes annuelles, était directement reliée à la température cumulative d'été dans un des lacs sub-alpins ($r = 0,71$, $N = 11$), tandis que dans d'autres lacs, les fortes classes annuelles étaient souvent associées aux étés chauds. Ces analyses montrent que l'importance du recrutement dans les lacs sub-alpins dépendait surtout, ou du moins en partie, des différences annuelles entre les températures d'été. La longévité présentait une relation inverse avec la température de l'eau à mi-été.

Received January 16, 1986
Accepted May 6, 1986
(J8610)

Reçu le 16 janvier 1986
Accepté le 6 mai 1986

Although there is a substantial literature on the population dynamics of rainbow trout (*Salmo gairdneri*), the majority of research has been directed toward populations exploited by recreational or commercial fisheries (Carlander 1969; Scott and Crossman 1973). Unexploited populations of fish in general and rainbow trout in particular have received less attention (Pauly 1980). Our objective was to study longevity, recruitment, growth, and age structure of rainbow trout populations from subalpine lakes and to compare these with populations in coastal and montane lakes. Eleven populations were studied, and all were either unexploited or were exploited at a very low level.

Characteristics of unexploited salmonid populations in the arctic and northern boreal region of Canada have been described by Johnson (1972, 1976, 1983). Johnson suggested that these characteristics should occur in the dominant species in other undisturbed ecosystems. Because subalpine lakes have several features in common with arctic lakes, including single fish species communities, short open-water period, and low productivity, our catch data from this type of lake provide an independent test (different area and species) of Johnson's theoretical predictions on the dynamics of the dominant species in unexploited populations.

Materials and Methods

Study Area

Eight of the 11 lakes surveyed are located in Jasper National Park in Alberta, two are located in Mount Revelstoke National Park in British Columbia, and one (Marion Lake) is in the University of British Columbia Research Forest near Vancouver. Data for Marion Lake were obtained from Calef (1973), Efford (1967), and Hall and Hyatt (1974). All of the lakes, perhaps with the exception of Marion Lake, acquired their rainbow trout populations through introductions of hatchery-reared fish during this century (Table 1). Two lakes, Cabin and Marion, are closed to fishing. Harvey Lake is inac-

---

[1] Present address: Department of Fisheries and Oceans, Room 207, 417 2nd Avenue W., Prince Rupert, B.C. V8J 1G8.

TABLE 1. Physical and biological features of coastal, montane, and subalpine lakes in western Canada. These lakes support unexploited or lightly exploited populations of rainbow trout.

Lake	Latitude	Longitude	Year stocked (first–last)	Elevation (m)	Area (ha)	Maximum depth (m)	Temperature (midsummer) (°C at 4 m)[a]	Number of vertebrate species
Coastal and montane lakes								
Marion	49°18′	122°32′	Early 1900s?[b]	300	13.3	5	18.0[c]	6[d,e,f]
Cabin	52°53′	118°08′	1929	1217	32.2	21	18.1	2
Iris	52°53′	118°13′	1940–72	1302	5.1	13	17.3	3
Subalpine lakes								
Harvey	53°09′	118°27′	1962–1967	1617	58.0	21	9.2	1
Topaz	53°23′	118°51′	1938	1773	128.5	28	11.5	1
Brazeau	52°25′	117°04′	1936–41	1808	214.2	13	10.3	1
Moat	52°43′	118°19′	?	1945	35.0	10	—	1
Twintree	53°23′	119°06′	Late 1930s	1558	320.1	51	11.6	1
Caribou (Upper)	53°25′	118°57′	Colonized–1940s	1788	43.2	29	9.4	1
Jade (Upper)	51°04′	118°04′	1941–55	1814	8.7	14	5.6	1
Jade (Lower)	51°04′	118°04′	1941–55	1762	4.8	23	5.7	1

[a] Measurements taken from August 2 to 21.
[b] Hall and Hyatt (1974).
[c] Efford (1967).
[d] Efford (1969).
[e] Calef (1973).
[f] Nilsson and Northcote (1981).

cessible and is not fished. The other eight lakes have a 4-mo fishing season that opens on July 1 and closes on October 30. The daily limit is five fish and the possession limit is 10. However, the total annual catch from each of these eight lakes was judged to be small because of access limitations. There are no roads to the lakes, and it is illegal for the public to land aircraft in the parks. Except for Iris, the lakes are remote and are a 1- to 3-d walk from the nearest road. At these remote lakes, anglers usually keep one or two fish for immediate consumption, and rarely retain the possession limit. Iris Lake is 1.5 km from a road, but because of better fishing opportunities nearby and the absence of an access trail, it is not visited regularly by fishermen.

The annual catch from the eight lakes that were fished was estimated at not more than 100 fish per lake, and it was probably much less at some lakes. For example, the total annual catch from Twintree, Upper Caribou, and Topaz lakes was probably not more than 50 fish per lake. This estimate takes into consideration the number of people who visit this area of the park (annual mean of 661, mandatory registration), the number of days spent there (average of 5.6), the total number of streams and lakes that are fished (12), and the number of visitors that purchase a fishing license (not more than 35%).

Fish

Rainbow trout were caught with mixed mesh monofilament gill nets. Equal lengths of 25-, 38-, 51-, 76-, 102-, and 127-mm (diagonal stretch measure) net were used at each lake. The age of each fish was determined from their otoliths by D. B. Donald, and the age–weight relationship for several lakes was plotted for those ages represented by three or more fish. The Fiddle River in Jasper National Park was sampled with an electrofisher to assess growth of age 0+ and age 1+ trout in this region and to confirm the pattern of annulus formation for young trout. The approximate error in age determination for older fish was within ±1 yr of the correct age for 22% of the otoliths or fish and within ±2 yr for 33% of the fish. The correct age was determined 45% of the time. These estimates were obtained from eighteen 5- to 11-yr-old trout of known age. These fish were reared in a hatchery for less than 12 mo and were then stocked into montane, subalpine, or alpine lakes. None of these lakes were the same lakes as those described here. Biogeographic regions referred to are those described and defined by Rowe (1972). Methods and procedures used to determine lake morphometry and water temperature, and to measure and age fish, are outlined in Donald et al. (1980).

Results

Coastal and montane lakes were characterized by a vertebrate community of from two to six species, maximum summer water temperatures in the order of 18°C (Table 1), and an open-water period of 6 mo (Cabin and Iris) or more (Marion). Gillnet catches indicated that rainbow trout were numerically dominant over lake chub (*Couesius plumbeus*) in Cabin Lake, but they were not the dominant species in Iris and Marion lakes. Iris Lake also supported longnose sucker (*Catostomus catostomus*) and lake chub, and Marion Lake supported kokanee (*Oncorhynchus nerka*), threespine stickleback (*Gasterosteus aculeatus*), and three amphibian species.

The age structure of rainbow trout populations in coastal and montane lakes was similar (Fig. 1), although the coastal population (Marion) does appear to have a more stable age structure than the montane populations. In all catches, 1- to 3-yr-old fish were dominant. The predominance of young fish in the catches indicates that substantial recruitment into the limnetic environment occurs during most years. Annual mortality was estimated from age frequency data (Fig. 1), and was in the order of 50%/yr. Maximum longevity was 7 yr. Growth was close to

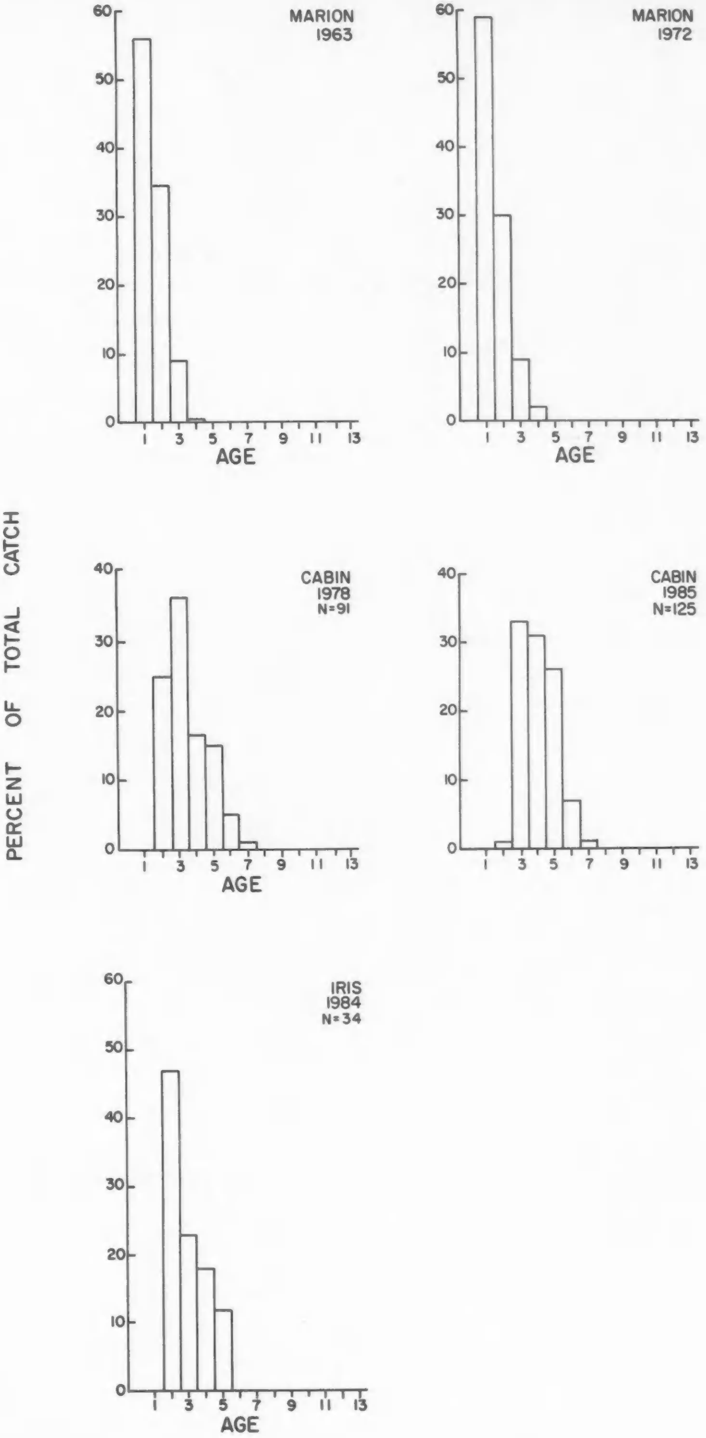

FIG. 1. Age frequency distribution of unexploited rainbow trout populations from coastal and montane lakes.

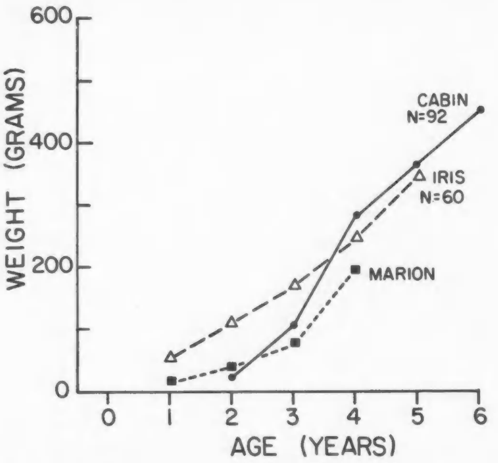

FIG. 2. Relationship between age and weight for rainbow trout populations from coastal and montane lakes. For most lakes, age–weight data collected over several years were combined.

linear from age 1 or age 2, and did not decline before all individuals in any given year-class had perished (Fig. 2).

Subalpine lakes were characterized by a single species fish community, maximum summer water temperatures that ranged from about 5 to 12°C (Table 1), and an open-water period of 2–4 mo.

Age structure of rainbow trout populations in subalpine lakes was not consistent (Fig. 3). Age structure was often different from one lake to another, and changed over a period of a few years in most lakes. Age structure was unimodal in some lakes (Moat, Upper Jade), bimodal (Lower Jade), or less distinct. Dominant and weak year-classes were present in all subalpine lakes, and these year-classes were often the same in lakes widely separate in distance. For example, the 1970 year-class was dominant in four lakes (Harvey, Topaz, Upper Jade, Lower Jade), and the 1979 year-class in three (Topaz, Moat, Lower Jade). The linear distance between Topaz and the Jade lakes is 253 km.

For Lower Jade Lake (1762 m asl), and probably Upper Jade Lake, year-class strength was positively correlated with the total number of degree-days above 0°C for June, July, and August (Fig. 3, $r = 0.71, N = 11, p < 0.05$). Temperature was measured nearby on Mt. Fidelity at 1875 m asl. In 1981 the catch from both of the Jade lakes consisted primarily of older fish. The upper lake was not fished again, but a younger cohort was caught in the lower lake during the following 2 yr (Fig. 3).

The total number of degree-days for June to August was not correlated with year-class strength for other subalpine lakes. However, dominant or abundant year-classes were often associated with years when summer temperatures were higher than usual. The three warmest summers (June, July, August) in Jasper and at Mt. Fidelity for the period 1968–82 were 1970, 1971, and 1979. These year-classes were often dominant or subdominant in subalpine lakes, although Brazeau Lake was a notable exception. The summer of 1976 was unusually cool in Jasper and at Mt. Fidelity (Fig. 3). The 1976 year-class was poorly represented in all subalpine lakes. Because of elevation differences, temperature measured at Jasper would not be the same as weather conditions at subalpine lakes in this area, although weather patterns or trends would be similar.

Precipition showed no obvious relationship with year-class strength and age structure.

Rainbow trout from subalpine lakes often lived for 13 yr (Fig. 3), and four individuals from a catch totaling 799 fish had otoliths indicating that maximum longevity in this environment could be from 14 to 19 yr. Longevity was inversely related to midsummer water temperature (Table 1; Fig. 1 and 3: $r = -0.81, N = 10, p < 0.05$) and to mean annual air temperature (Table 2). Longevity was directly related to maximum weight ($r = 0.63, N = 11, p < 0.05$).

In the subalpine environment, rainbow trout spawn from early June to mid-August depending on regional aspect and elevation. On September 27, age 0+ fish caught from the Fiddle River with an electrofisher weighed only 0.9 g ($N = 5$), and age 1+ fish with one distinct annulus weighed 9.7 g ($N = 6$). This latter weight was similar to weights obtained for age 1 trout caught with gill nets. Mean weight of 1-yr-old trout caught with nets in Topaz and Brazeau lakes was 14.1 g ($N = 2$) and 16.0 g ($N = 37$), respectively. In subalpine lakes, a sharp change in the rate of weight gain occurred during age 1 or age 2 (Fig. 4). In these lakes, growth rate was approximately linear from age 2 to age 6 or 8, and thereafter it declined once more in some lakes. The growth pattern was not consistent among lakes. The pattern was distinctly sigmoid in three lakes (Harvey, Twintree, Topaz), close to linear in one and probably two lakes (the Jade lakes), and complex in one lake (Brazeau). Growth was not plotted here for other subalpine lakes because of the small number of old fish in the catches.

Discussion

Age structure, longevity, recruitment, growth pattern, and growth rates of rainbow trout populations from lightly exploited and unexploited coastal and montane lakes (Fig. 1 and 2) were similar to rainbow trout populations from exploited lakes (for example, Larkin et al. 1957; Nilsson and Northcote 1981; Rawson and Elsey 1948). Therefore, a detailed discussion of the dynamics of these populations need not be presented here. The important features of these three unexploited populations were (1) they were similar to exploited populations, (2) they differed in several characteristics from populations inhabiting lakes in the subalpine environment, and (3) age structure was similar among lakes and between years.

Rainbow trout populations from subalpine lakes differed from those inhabiting coastal and montane lakes in their age structure, longevity, and growth pattern. With the exception of the Jade lakes, growth rates in subalpine lakes were similar to growth rates in coastal and montane lakes.

Age structure in subalpine lakes did not show a consistent pattern and was not stable. The correlation between summer temperature and age structure in the Jade lakes and the synchrony of dominant year-classes in several lakes suggest that summer temperature was an important factor determining the magnitude of recruitment. Warm summers probably enhance the survival of the egg and larval stage of rainbow trout. Other factors also influenced recruitment and thus determine age structure in subalpine lakes because strong year-classes in a few lakes were not associated with warm summers. The number of fish in the parent stock and density-dependent mortality due to cohort dominance might also contribute to unstable age structure.

Precipitation showed no obvious relationship with year-class strength or age structure, and is probably not important.

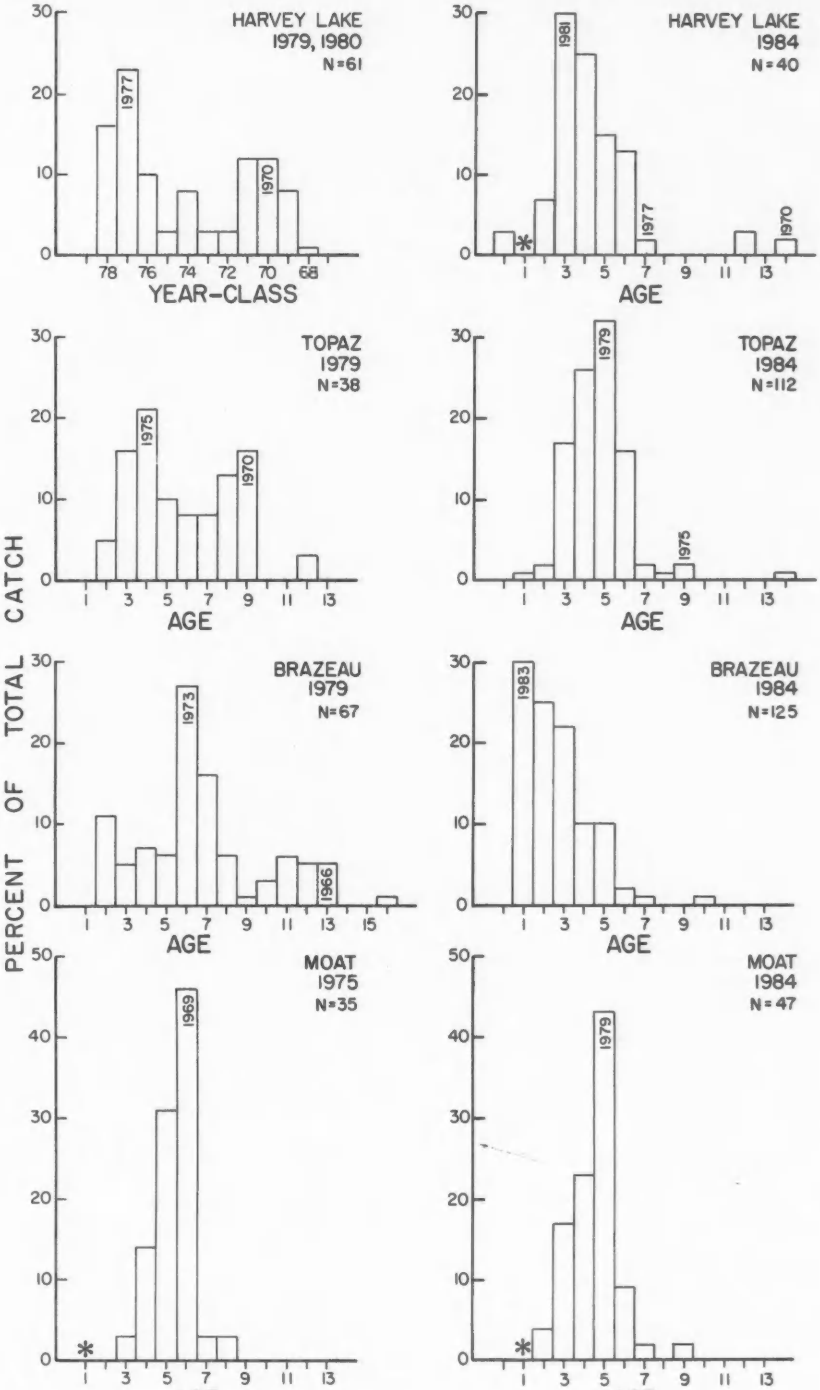

FIG. 3. Age or year-class frequency distribution for unexploited populations of rainbow trout from eight subalpine lakes. The year of the catch is located below the lake name. Samples collected in September when 1-yr-old fish should be vulnerable to gill nets are marked with an asterisk. The maximum age recorded from a small catch of fish taken from Twintree Lake in 1979 is marked with a triangle.

(*Fig. 3 concluded next page*)

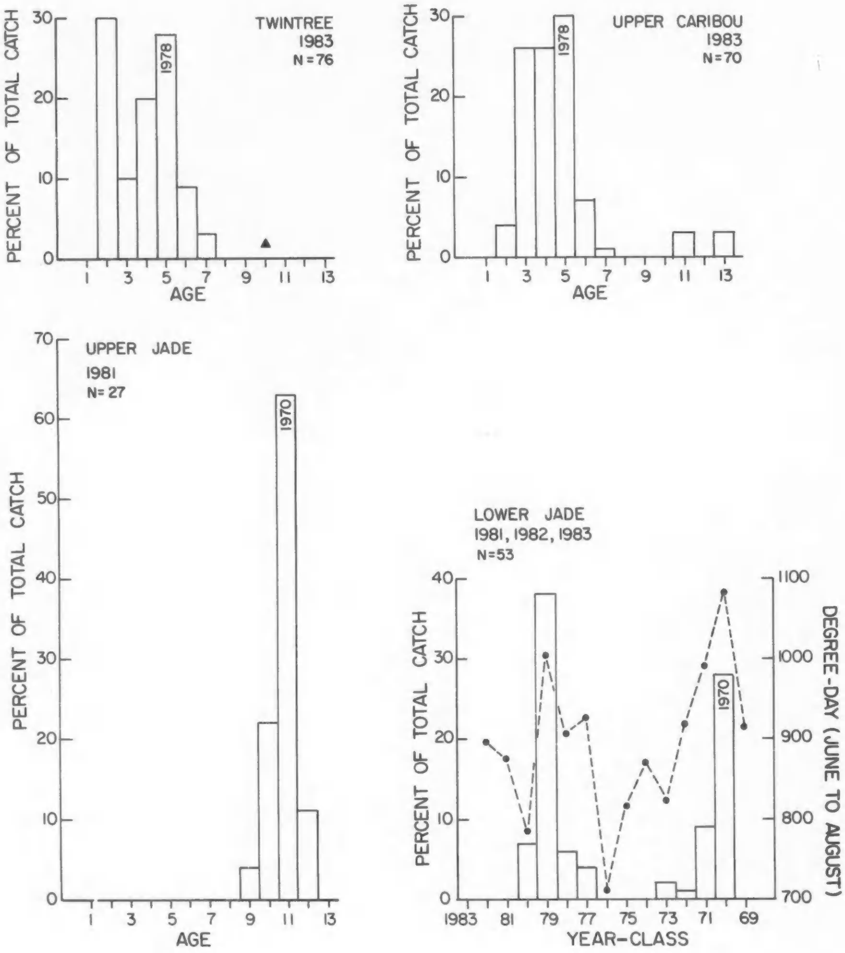

FIG. 3. (*Concluded*)

TABLE 2. Relationship between mean annual air temperature, maximum longevity, and mean maximum weight for four rainbow trout populations. Data are presented for those lakes located near a weather station.

Lake	Annual mean temperature (°C)[a]	Longevity (yr)	Weight at maximum age (g)
Marion	8.3	4	196
Iris	2.8	5	352
Cabin	2.8	7	736
Jade (Upper)	0.2	12	241

[a]Anonymous (1982).

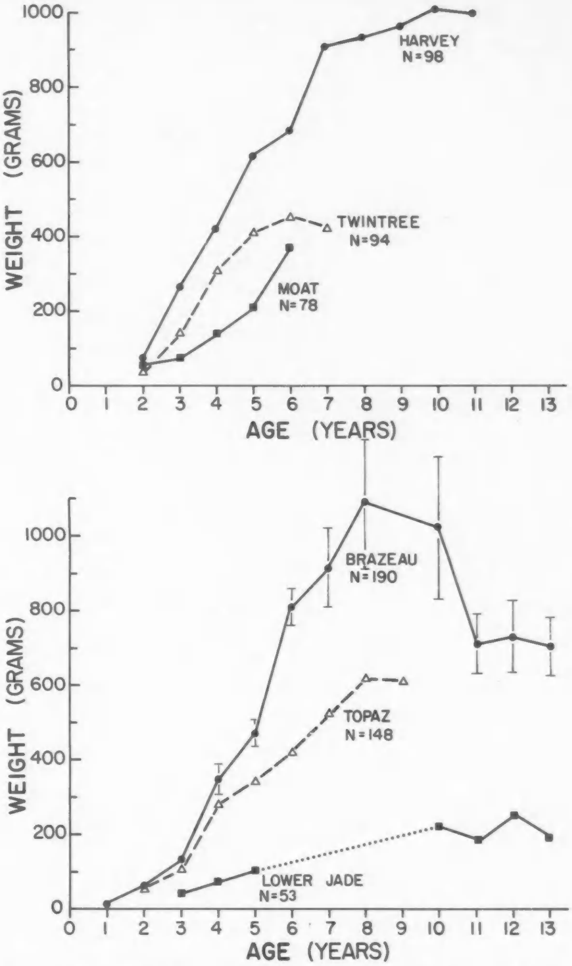

FIG. 4. Relationship between age and weight for rainbow trout from subalpine lakes. For most lakes, age—weight data collected over several years were combined. For Brazeau Lake, the standard error of the mean is also shown.

Throughout the summer, the winter snowpack melts at progressively higher elevation and maintains flow in spawning streams even in dry summers. Therefore, it is unlikely that reduced summer precipitation would affect the quantity and quality of spawning habitat, and subsequently recruitment of young fish.

Maximum longevity in subalpine lakes was greater than maximum longevity in coastal and montane lakes by 2—3 times from age 4 (Marion) or 7 (Cabin) to about age 13 in several subalpine lakes. Moat Lake was an obvious exception. Other publications on rainbow trout suggest that the maximum longevity for this species is about 8 yr (Larkin et al. 1957; Rawson 1953; Scott and Crossman 1973). Our results extend the known longevity of this species to at least 13 yr and possibly to 19 yr.

The growth pattern and weight gain (Fig. 2) for rainbow trout from coastal and montane lakes were typical of this species in western Canadian lakes (Larkin et al. 1957; Rawson and Elsey 1948), although growth in Marion Lake was perhaps somewhat less than usual (Efford 1969). In contrast with coastal and montane lakes, an asymptote was reached in the growth pattern in some subalpine lakes. The asymptote occurred at ages 6—8. It was evident in four of eight subalpine lakes (Fig. 4), and was suggested from small samples of older fish in one other lake (Upper Caribou). The change in growth rate near the middle of the life span in the subalpine environment was at least partly due to senescence. Some old and emaciated fish were caught in these lakes. Extended longevity and reduced exploitation in the subalpine environment were associated with the asymptotic growth pattern.

The complex growth pattern shown for Brazeau Lake could be the result of two independent events: (1) long-term changes in fish density and (2) senescence. In western Canada, growth rate of rainbow trout in lakes is inversely related to density of young fish (Donald and Anderson 1982). Substantial variation in annual recruitment could result in markedly different population densities. The relatively small size of old fish in Brazeau Lake (ages 11—13, Fig. 4) might be due to reduced growth caused by a more abundant and dense population, plus some weight loss due to senescence.

Growth in the two Jade lakes was similar, and was exceptionally slow. In these lakes, growth may be close to the minimum that is genetically possible for this species. A short open-water period, low summer temperatures, and the absence of other preferred food organisms such as Odonata and Amphipoda (Donald and Anderson 1982) probably contribute to a marginal environment and slow growth for rainbow trout. Stunted populations of brown trout (*Salmo trutta*)), brook trout (*Salvelinus fontinalis*), Arctic charr[2] (*Salvelinus alpinus*), and lake trout (*Salvelinus namaycush*) have been described for other mountain lakes (Donald and Alger 1986; Donald et al. 1980; Langeland 1978, 1982; Pechlaner 1984; Pechlaner and Zaderer 1985; Reimers 1958, 1979). The cause of the stunted or dwarf condition in these habitats is usually attributed to poor quality and quantity of food, as well as high densities of fish.

For rainbow trout, the Jade lakes are most certainly a harsh environment. Upper Jade Lake is situated on the north aspect of an unnamed mountain. Avalanches cover some of the lake each year with several metres of snow, and in summer the lake remains in shadow for much of the day. On August 10, 1981,

---

[2] The spelling differs from that (char) used in *A List of Common and Scientific Names of Fishes from the United States and Canada* (Am. Fish. Soc, Spec. Publ. No. 12, 4th ed., 1980) and is preferred by the authors.

Upper Jade Lake was only 50% ice free, and female rainbow trout had not completed spawning. This lake was all but frozen over on October 10, giving an ice-free period of about 50 d. Maximum summer temperature at 4 m was less than 6°C. The ice-free period for Lower Jade Lake is longer and was estimated to be about 90 d. Catch data from the Jade lakes indicate that recruitment fails or is severely reduced during many years. Age structure and thus recruitment was correlated directly with summer temperature. Optimum temperature for egg development in rainbow trout is about 17.5°C, and at this temperature, egg development from fertilization to hatching takes 18 d (Garside 1966). A 5°C, hatching takes 64 d, and at 2.5°C it takes 106 d. At the Jade lakes, eggs deposited in mid-August would not hatch before winter and would probably die before the following spring. Warm summers result in an early breakup followed by spawning, and thereafter a shorter period for egg development and hatching. Warm summers may favor substantial recruitment in other subalpine lakes for the same reason, although other factors are certainly involved as well.

Weather may also determine year-class strength for certain populations of lake whitefish (*Coregonus clupeaformis*) and American shad (*Alosa sapidissima*). Miller (1952) noted that strong year-classes were synchronized in several western lakes, and suggested that calm weather in fall was favorable for egg development. As well, Lawler (1965) noted that strong year-classes of lake whitefish in Lake Erie were associated with stable temperatures from fall to spring. These conditions were apparently optimum for embryonic development. Recruitment or year-class strength for American shad was related to total precipitation in May and June (Crecco et al. 1986). Substantial precipitation was associated with delayed spawning that favored survival of shad larvae.

Natural mortality in fish is correlated with growth parameters, although a temperature−mortality correlation is also evident to a lesser extent (Craig 1985; Pauly 1980). High temperatures and rapid growth result in a short life span, suggesting that physiological processes determine longevity. Temperature, respiration, and growth are, of course, interactive in poikilotherms, and their relative importance is difficult to separate. Our analyses of these relationships suggest that longevity in rainbow trout is primarily related to temperature and not to growth parameters (Table 2). However, environmental stress from competitors (Table 1), pathogens, and parasites also contributes to mortality and may have reduced longevity in those rainbow trout populations located at low elevation.

Johnson (1972, 1976, 1983) concluded that salmonids in arctic and northern boreal lakes have length and age frequency distributions that are characteristic of the dominant tree species in a climax forest. Because of the similarities in these two distinct ecosystems, he concluded that structure and the mechanisms responsible for this structure should be generally consistent for the dominant species in other ecosystems where unexploited populations occur. Northern single species populations of fish and dominant species in more complex environments maintain an age and length frequency distribution that remains relatively stable, and is characterized by high biomass accumulation, a high degree of uniformity in size irrespective of age, great mean age, and constant density. In subalpine environments, rainbow trout populations were characterized by extended longevity and, in most lakes, the absence of an age−weight relationship at old age. Both of these characteristics were predicted by Johnson. However, age structure in subalpine populations differed from those in arctic populations. In subalpine lakes, age structure changed over a period of several years and was not stable. Population densities might also fluctuate because of annual variation in recruitment.

Differences between characteristics of rainbow trout and arctic salmonid populations (Arctic charr and lake trout) are probably due to genetically determined attributes of each species as well as environmental restraint. Arctic charr and lake trout have probably evolved as the dominant species in northern freshwater habitats. Rainbow trout have evolved in and are adapted to complex marine and low-elevation freshwater environments in western North America (MacCrimmon 1971). Here, they frequently are not the dominant species, and biotic factors and warm temperatures influence population characteristics. Patterns observed in subalpine lakes may only be the expression of genetically determined characteristics in a unique and new environment. In the subalpine environment, ecological release from biotic interactions that cause mortality, plus positive (longevity) and negative (hatching success) effect of low temperature on specific physiological processes, determine population characteristics there.

Acknowledgments

This project was supported by Parks Canada and the Canadian Wildlife Service. We are grateful to R. S. Anderson, G. A. Antoniuk, G. Ranger, J. Kilistoff, and D. E. Patriquin for their contribution to this project.

References

ANONYMOUS. 1982. Canadian climate normals, 1951−1980, temperature and precipitation. Environment Canada Atmospheric Environment Service, Ottawa, Ont.

CALEF, G. W. 1973. Natural mortality of tadpoles in a population of *Rana aurora*. Ecology 54: 741−758.

CARLANDER, K. D. 1969. Handbook of freshwater fishery biology. Vol. 1. Life history data on freshwater fishes of the United States and Canada, exclusive of the Perciformes. Iowa State University Press, Ames, IA. 752 p.

CRAIG, J. F. 1985. Aging in fish. Can. J. Zool. 63: 1−8.

CRECCO, V., T. S. SAVOY, AND W. WHITWORTH. 1986. Effects of density-dependent and climatic factors on American shad, *Alosa sapidissima*, recruitment: a predictive approach. Can. J. Fish. Aquat. Sci. 43: 457−463.

DONALD, D. B., AND D. J. ALGER. 1986. Stunted lake trout (*Salvelinus namaycush*) from the Rocky Mountains. Can. J. Fish. Aquat. Sci. 43: 608−612.

DONALD, D. B., AND R. S. ANDERSON. 1982. Importance of environment and stocking density for growth of rainbow trout in mountain lakes. Trans. Am. Fish. Soc. 111: 675−680.

DONALD, D. B., R. S. ANDERSON, AND D. W. MAYHOOD. 1980. Correlations between brook trout growth and environmental variables for mountain lakes in Alberta. Trans. Am. Fish. Soc. 109: 603−610.

EFFORD, I. E. 1967. Temporal and spatial differences in phytoplankton productivity in Marion Lake, British Columbia. J. Fish. Res. Board Can. 24: 2283−2307.

1969. Energy transfer in Marion Lake, British Columbia, with particular reference to fish feeding. Int. Ver. Theor. Angew. Limnol. Verh. 17: 104−108.

GARSIDE, E. T. 1966. Effects of oxygen in relation to temperature on the development of embryos of brook trout and rainbow trout. J. Fish. Res. Board Can. 23: 1121−1134.

HALL, K. J., AND K. D. HYATT. 1974. Marion Lake (IBP) — from bacteria to fish. J. Fish. Res. Board Can. 31: 893−911.

JOHNSON, L. 1972. Keller Lake: characteristics of a culturally unstressed salmonid community. J. Fish. Res. Board Can. 29: 731−740.

1976. Ecology of arctic populations of the lake trout, *Salvelinus namaycush*, lake whitefish, *Coregonus clupeaformis*, Arctic char, *S. alpinus*, and associated species in unexploited lakes of the Canadian Northwest Territories. J. Fish. Res. Board Can. 33: 2459−2488.

1983. Homeostatic characteristics of single species fish stocks in

Arctic lakes. Can. J. Fish. Aquat. Sci. 40: 987–1024.

LANGELAND, A. 1978. Effect of fish (*Salvelinus alpinus*, arctic char) predation on the zooplankton in ten Norwegian lakes. Verh. Int. Ver. Limnol. 20: 2065–2069.

1982. Interactions between zooplankton and fish in a fertilized lake. Holarct. Ecol. 5: 273–310.

LARKIN, P. A., J. G. TERPENNING, AND R. R. PARKER. 1957. Size as a determinant of growth rate in rainbow trout *Salmo gairdneri*. Trans. Am. Fish. Soc. 86: 84–96.

LAWLER, G. H. 1965. Fluctuations in the success of year-classes of whitefish populations with special reference to Lake Erie. J. Fish. Res. Board Can. 22: 1197–1227.

MACCRIMMON, H. R. 1971. World distribution of rainbow trout (*Salmo gairdneri*). J. Fish. Res. Board Can. 28: 663–704.

MILLER, R. B. 1952. The relative strengths of whitefish year classes as affected by egg plantings and weather. J. Wildl. Manage. 15: 39–50.

NILSSON, N. A., AND T. G. NORTHCOTE. 1981. Rainbow trout (*Salmo gairdneri*) and cutthroat trout (*S. clarki*) interactions in coastal British Columbia lakes. Can. J. Fish. Aquat. Sci. 38: 1228–1246.

PAULY, D. 1980. On the interrelationships between natural mortality, growth parameters, and mean environmental temperature in 175 fish stocks. J. Cons. Int. Explor. Mer 39: 175–192.

PECHLANER, R. 1984. Dwarf populations of Arctic charr in high-mountain lakes of the Alps resulting from under-exploitation, p. 319–327. *In* L. Johnson and B. L. Burns [ed.] Biology of the Arctic charr, Proceedings of the International Symposium on Arctic Charr, Winnipeg, Manitoba, University of Manitoba Press, Winnipeg, Man.

PECHLANER, R., AND P. ZADERER. 1985. Interrelations between brown trout and chironomids in an alpine lake Gossenkollesee (Tyrol). Verh. Int. Ver. Limnol. 22: 2620–2627.

RAWSON, D. S. 1953. The limnology of Amethyst Lake, a high alpine type near Jasper, Alberta. Can. J. Zool. 31: 193–210.

RAWSON, D. S., AND C. A. ELSEY. 1948. Reduction in the longnose sucker population of Pyramid Lake, Alberta, in an attempt to improve angling. Trans. Am. Fish. Soc. 78: 13–31.

REIMERS, N. 1958. Conditions of existance, growth, and longevity of brook trout in a small high-altitude lake of the eastern Sierra Nevada. Calif. Fish Game 44: 319–334.

1979. A history of a stunted brook trout population in an alpine lake: a lifespan of 24 years. Calif. Fish Game 65: 196–215.

ROWE, J. S. 1972. Forest regions of Canada. Dep. Environ. Can. For. Serv. Publ. No. 1300: 1–172.

SCOTT, W. B., AND E. J. CROSSMAN. 1973. Freshwater fishes of Canada. Bull. Fish. Res. Board Can. 184: 966 p.

Functional Regression and Correlation Analysis

A. L. Jensen

School of Natural Resources, University of Michigan, Ann Arbor, MI 48109, USA

Jensen, A.L. 1986. Functional regression and correlation analysis. Can. J. Fish. Aquat. Sci. 43: 1742–1745.

In fisheries, many applications of regression analysis are based on functional relations, but application of predictive regression results in two regression equations. Ricker proposed application of a method developed by Teissier to estimate the geometric mean functional relation when the parameters of a functional relation are of biological significance. Functional regression results in a single equation relating variables as opposed to the two equations that result when predictive regression is applied. The geometric mean functional relation also is given by bivariate normal correlation analysis when the correlation coefficient is 1. Bivariate normal correlation analysis provides a model for functional regression. An equation for variation of observed values about the functional regression line is obtained, and functional regression is compared with predictive regression. If the model assumptions are met, the one equation of functional regression is less precise for prediction than the two equations of predictive regression. However, the confidence intervals for the estimates of the slopes for functional and predictive regression are nearly the same.

Bon nombre des applications de l'analyse de régression au domaine des pêches sont basées sur des relations fonctionnelles, mais l'application de la régression de prévision donne deux équations de régression. Ricker a proposé d'appliquer une méthode élaborée par Teissier afin d'estimer la relation fonctionnelle de moyennes géométriques lorsque les paramètres de la relation présentent une importance biologique. Les résultats de la régression fonctionnelle se présentent sous la forme d'une seule équation mettant en relation les variables plutôt que sous la forme des deux équations qui résultent de l'application de la régression de prévision. La relation fonctionnelle de moyennes géométriques est aussi obtenue par analyse de corrélation normale à deux variables lorsque le coefficient de corrélation est égal à 1. L'analyse de corrélation normale à deux variables constitue un modèle de régression fonctionnelle. L'auteur présente une équation de la variation des valeurs observées par rapport à la droite de régression fonctionnelle et compare cette dernière à la régression de prévision. Lorsque les hypothèses du modèle sont respectées, l'équation unique de régression fonctionnelle s'avère moins exacte pour la prévision que les deux équations de la régression de prévision. Les intervalles de confiance des estimations des pentes des régressions fonctionnelle ou de prévision sont cependant presque identiques.

Received July 23, 1985
Accepted May 7, 1986
(J8337)

Reçu le 23 juillet 1985
Accepté le 7 mai 1986

In applications of regression analysis to problems in fisheries, both variables often are random, and there are two regression lines that Ricker (1973) has called predictive regression lines. Such a situation is not satisfactory to the scientist who expects a single functional relation (Ricker 1973). For example, if the weight and length of a fish are measured over time, there is a functional relation between length and weight, and the parameters of this equation are of biological importance (Ricker 1973; Calder 1984). But growth occurs in spurts, and although the equation

$$(1) \quad W = aL^b,$$

where W = weight, L = length, and a and b are parameters, will fit the data well, it will not fit exactly, so there are two predictive regression lines. The situation is less clear when the relation between length and weight is determined by measurements on a group of individuals, but still the equation fits the data closely and the objective may be estimation of a single functional relation.

As a second example, consider the relation between metabolic rate and weight. The relation between low routine metabolic rate and weight is described nearly exactly by the parabolic equation

$$(2) \quad Q_{lr} = \alpha W^{\gamma}$$

where Q_{lr} = low routine metabolic rate, W = weight, and α and γ are parameters. The more carefully an experiment is controlled, the better the data fit this model. But many factors affect this relationship and some cannot be controlled without great expense, so there is always some variation and the model does not fit exactly. Hence, there are two predictive regression lines.

Although the functional relations cannot be observed in either of the above examples, the parameters of the functional relations are of biological significance and it is reasonable to estimate functional relations that cannot be observed just as it is reasonable to estimate population means and variances that cannot be observed. Ricker (1973) has proposed that functional relations be estimated using an approach first suggested by Teissier (1948) that Ricker (1973) called geometric mean functional regression.

I examine the relation between geometric mean functional regression and bivariate normal correlation analysis. The slope obtained by Teissier (1948), by minimization of the sum of the products of the vertical and horizontal distances from the observations to the line, is the same as the slope obtained with normal correlation analysis under the assumption that the correlation coefficient is 1. This is by definition the functional relation. Application of the correlation model for functional regression establishes a model for this approach and clarifies hypothesis testing related to functional regression. An equation is obtained for variation about the functional regression line.

Simple Linear Regression

Neter et al. (1985) discussed simple linear regression in detail. The simple linear regression model is

$$(3) \quad y_i = \alpha + \beta x_i + \xi_i$$

where y_i = observed random variable, ξ_i = normal, independently distributed random variables with mean 0 and variance $\sigma^2_{y \cdot x}$, x_i = a set of constants ($i = 1, 2, \ldots, n$), n = number of observations, and β and α are parameters. The variance of y adjusted for x, $\sigma^2_{y \cdot x}$, is the variation of y about the predictive regression line of y on x. Application of least squares gives the estimators of β and α and application of maximum likelihood gives the estimators of β, α, and $\sigma^2_{y \cdot x}$. The estimators are

$$(4) \quad \hat{\beta} = \frac{\sum_{i=1}^{n} (x_i - \bar{x})(y_i - \bar{y})}{\sum_{i=1}^{n} (x_i - \bar{x})^2} = \mathrm{SP}/\mathrm{SS}_x$$

$$(5) \quad \hat{\alpha} = \bar{y} - \hat{\beta}\bar{x}$$

$$(6) \quad \hat{\sigma}^2_{y \cdot x} = \frac{\sum_{i=1}^{n} (y_i - \bar{y}_i)^2}{n-2} = \frac{\mathrm{SS}_y(1 - r^2)}{n-2}$$

where SP is the sum of products of x and y, SS_x is the sum of squares of x, SS_y is the sum of squares of y, and r is the sample estimate of the correlation coefficient. The estimator of the variance of the estimate of the slope is

$$(7) \quad \hat{V}(\hat{\beta}) = \hat{\sigma}^2_{y \cdot x}/\mathrm{SS}_x.$$

Bivariate Normal Correlation Analysis

Neter et al. (1985) also gave a detailed description of bivariate normal correlation analysis. In bivariate normal correlation analysis the probability density of a pair (x, y) is given by the bivariate normal probability density function. In regression analysis the mean of one variable given the second variable is of interest, and for the bivariate normal density function of these relations are given by the equations

$$(8) \quad E(y|x) = \mu_y + \rho\frac{\sigma_y}{\sigma_x}(x - \mu_x) = \alpha_1 + \beta_1$$

$$(9) \quad E(x|y) = \mu_x + \rho\frac{\sigma_x}{\sigma_y}(y - \mu_y) = \alpha_2 + \beta_2$$

where σ_y = standard deviation of y, σ_x = standard deviation of x, μ_x = mean of x, μ_y = mean of y, x and y = jointly distributed random variables, ρ = correlation coefficient, $-1 < \rho < 1$, β_1 = slope of the predictive regression of y on x, β_2 = slope of the predictive regression of x on y, α_1 = intercept of the predictive regression of y on x, and α_2 = intercept of the predictive regression of x on y. If two variables follow the bivariate normal distribution, the mean of one variable given the second variable is linearly related to the value of the second variable, and there are two regression lines. If the correlation is 0, the two lines are perpendicular. If the correlation is 1, the two lines are colinear.

When both variables are random, as in most fishery analyses, bivariate normal correlation analysis is more appropriate than simple linear regression, but bivariate normal correlation analysis is seldom applied. The simple linear regression model is simpler, and few textbooks introduce correlation analysis because parameter estimates and the results of hypotheses tests for significance of regression are the same for simple linear regression and correlation analysis.

Functional Regression

Teissier (1948) obtained the slope of the geometric mean functional regression line by minimization of the sum of the products of the horizontal and vertical distances from the observations to the fitted regression line (Ricker 1973, 1975); this is not a simple optimization problem (Ricker 1975; Jolicoeur 1975). The same result is obtained with correlation analysis; setting $|\rho| = 1$, the two predictive regression lines (equations (8) and (9)) become colinear and are given by the equation

$$(10) \quad y_i = \mu_y + \mathrm{sign}(\rho)\frac{\sigma_y}{\sigma_x}(x_i - \mu_x) = \alpha_f + \mathrm{sign}(\rho)\,\beta_f x_i.$$

The term "sign(ρ)" indicates that the sign of the slope of the functional regression line is determined by the sign of the correlation coefficient (Halfon 1985). The functional relation between two variables is described by one regression equation. The functional equation is the same as the deterministic equation that would result if one variable predicted the other exactly, but as a component of the bivariate normal correlation model, it is better to term the relation functional. The functional regression line is the deterministic relation embedded in the statistical model. The bivariate normal correlation model provides a description of variation about the functional regression line and confidence intervals for the parameter estimates.

The estimators of the parameters of the functional relation are

$$(11) \quad \hat{\beta}_f = \mathrm{sign}(r)\ \mathrm{SS}_y/\mathrm{SS}_x = \mathrm{sign}(r)\ \hat{\sigma}_y/\hat{\sigma}_x$$

$$(12) \quad \hat{\alpha}_f = \bar{y} - \hat{\beta}_f\bar{x}.$$

The slopes of the predictive and functional regression lines are related by the equation (Ricker 1973)

$$\hat{\beta}_f = \hat{\beta}_1/r,$$

and when r is near 1 the estimates for predictive and functional regression are similar.

Based on the t-statistic for σ_y/σ_x, developed by Pitman (1939), which is

$$(13) \quad t = \frac{(\hat{\sigma}^2_y/\hat{\sigma}^2_x - \sigma^2_y/\sigma^2_x)\sqrt{n-2}}{\sqrt{4(1 - r^2)\hat{\sigma}^2_y\sigma^2_y/\hat{\sigma}^2_x\sigma^2_x}},$$

Joliçoeur and Mosimann (1968) derived the confidence interval for $\hat{\beta}_f$ which can be written as

$$(14) \quad \hat{\beta}_f\left(t_{\alpha/2}\sqrt{\frac{1 - r^2}{n-2}} \pm t_{\alpha/2}\sqrt{\frac{1 - r^2}{n-2} + 1}\right).$$

This gives the confidence interval of the slope exactly. The variance of $\hat{\beta}_f$ is (Ricker 1973)

$$(15)\quad V(\hat{\beta}_f) = \frac{\hat{\sigma}_y^2}{\hat{\sigma}_x^2}\left(\frac{1 - r^2}{n - 2}\right)$$

which is the same as the variance of $\hat{\beta}_1$ for predictive regression. An approximate confidence interval for $\hat{\beta}_f$ is

$$(16)\quad \hat{\beta}_f \pm \hat{\beta}_f\, t_{\alpha/2} \sqrt{\frac{1 - r^2}{n - 2}}.$$

In practice, the exact confidence interval should be applied because it is easily calculated, but in situations where functional regression is appropriate the correlation is high and the approximation is very close, which indicates that the confidence intervals of the slopes for functional regression and predictive regression are nearly identical.

Examples and Discussion

In bioenergetic analyses, low routine metabolic rate is related to weight using equation (2) (e.g. Norstrom et al. 1976; Jensen et al. 1982). In experiments to estimate α and γ the observations deviate slightly from equation (2) either because the model does not fit exactly or because we are unable to completely control the experimental conditions. Measurement error is small. The best regression method depends on our objective. Predictive regression gives the mean metabolic rate for a given weight or the mean weight for a given metabolic rate under conditions similar to those for which the parameters were estimated. There are two regression equations, and in each case the residual sum of squares is minimized.

Functional regression gives the functional value of weight for metabolic rate and the functional value of metabolic rate for weight. There is one equation and the residual sum of squares between observed and predicted values is not minimized. The residual sum of squares for functional regression will be larger than that for predictive regression. Variation of the observed values about the functional regression line is given by the equation

$$(17)\quad \frac{2SS_y(1 - |r|)}{n - 2}$$

and variation of the observed values about the predictive regression line is given by equation (6). The ratios of the variation about the functional regression line to the variation about the predictive regression line for some values of r are given below:

r	1	0.95	0.90	0.75	0.50	0.25	0
Ratio	0	1.03	1.05	1.14	1.33	1.60	2

If $r = 1$, variation about both lines is zero; if r is near 1, variation about the lines is nearly equal, and as r approaches zero, variation of the observed values about the functional regression line approaches twice the variation about the predictive regression line.

Functional regression is less precise than predictive regression. Functional regression assumes that all of the variation is one variable is explained by the other. But in fact, if ρ is not one, some of the variation in y is variation about the regression line, and this variation in y is not a result of variation in x. The square of the correlation coefficient gives simultaneously the proportion of the variation in x associated with y and the proportion of the variation in y associated with x. In predictive regression the functional slope is multiplied by the correlation coefficient to adjust the functional slope for variation in y not associated with variation in x; this gives $\hat{\beta}_1 = \sqrt{\rho^2 \sigma_y^2/\sigma_x^2}$.

TABLE 1. Total length (mm) and weight (g) for gizzard shad (*Dorsoma cepedianum*) in the western basin of Lake Erie. All individuals were females.

Length	Weight	Length	Weight
399	784	455	1112
402	665	448	962
406	694	451	1035
403	754	467	1159
397	647	470	1165
436	964	460	1235
450	1010	466	1065
440	913	472	1177
473	1333	451	1156
466	1224	462	1229
440	1039	475	1110
453	1217	489	1239
455	1112	473	1330
488	962		

Although in general, predictive regression is more precise than functional regression, Ricker (1973) has demonstrated that nonrandom sampling and violation of model assumptions can result in situations where functional regression is more precise than predictive regression. A general guide for situations that do not fit the model assumptions is not possible, and identification of the more precise method in such situations requires simulations such as those of Ricker (1973).

If the assumptions of the model are reasonably well met, sampling is random, and the objective is prediction of metabolic rate from weight, then predictive regression should be applied. If the correlation is high and the objective is to obtain the best single relation between metabolic rate and weight for the purpose of establishing a theoretical functional relation, then functional regression should be applied.

As a second example, functional and predictive regression were applied to fit the length–weight relation

$$(18)\quad \ln W = a + b \ln L$$

to observed data for gizzard shad (*Dorosoma cepedianum*) in the western basin of Lake Erie (Table 1). Both length and weight are random variables and measurement error is small. Applying predictive regression gives $\hat{\beta} = 3.29$, $\hat{\alpha} = -5.71$, $r = 0.94$, and $\hat{\sigma}_{y \cdot x}^2 = 5.91 \times 10^{-3}$. The confidence interval for β is 3.29 ± 0.53. To test for significance of the regression, we can test either $\beta = 0$ as in simple linear regression or $\rho = 0$ as in correlation analysis. Testing for $\rho = 0$, the test statistic is

$$(19)\quad t = \frac{(r - 1)\sqrt{n - 2}}{\sqrt{(1 - r^2)}} = 12.899$$

with $n - 2 = 23$ degrees of freedom, and the null hypothesis is rejected.

The estimate of the slope for functional regression is $\hat{\beta}_f = 3.51$ and the exact confidence interval is (3.02, 4.08). The average distance of the exact confidence bounds from the estimate of $\hat{\beta}_f$ is 0.53, which is identical to the bound for predictive regression. Applying the approximate confidence interval for β_f gives 3.51 ± 0.53. The precision of the estimates of the slopes for functional and predictive regression is the same.

The functional regression line cannot be applied to test for significance of a regression (Ricker 1973). If functional regression is viewed as a component of correlation analysis, then it is clear that the functional regression line cannot be applied to test for significance because to calculate the functional regression line, it has been assumed that the correlation is 1. But the functional regression line is a component of the bivariate normal correlation model, and the test for $\rho = 0$, given above, is appropriate to test for a significant association.

If the objective is to predict weight from length, and if the assumptions of the model are met reasonably well, then predictive regression should be applied. If it is necessary to obtain one functional relation between length and weight, then functional regression should be applied.

In some applications of regression, one relation is desired, whereas in other applications the best predictions are desired and two equations are acceptable. Functional regression gives the one regression equation that is necessary to establish theoretical relations, but if the assumptions of the bivariate normal correlation model are met, this one regression line does not predict as precisely as the two predictive regression lines. If the correlation coefficient is near 1, as it should be in situations where functional regression is applied, the difference in precision of prediction is small. The slope of the one functional regression line is estimated with the same precision as the slopes of the two predictive regression lines.

Acknowledgements

I thank Prof. Gary Fowler for many interesting discussions on regression analysis. The length–weight data were given to me by Dr. William Kovelac.

References

CALDER, W. A. III. 1984. Size, function, and life history. Harvard University Press, Cambridge, MA.

HALFON, E. 1985. Regression method in ecotoxicology: a better formulation using the geometric mean functional regression. Environ. Sci. Toxicol. 19: 747–749.

JENSEN, A. L., S. A. SPIGARELLI, AND M. M. THOMMES. 1982. PCB uptake by five species of fish in Lake Michigan, Green Bay of Lake Michigan, and Cayuga Lake, New York. Can. J. Fish. Aquat. Sci. 39: 700–709.

JOLICOEUR, P. 1975. Linear regressions in fishery research: some comments. J. Fish. Res. Board Can. 32: 1491–1494.

JOLICOEUR, P., AND J. E. MOSIMANN. 1968. Intervalles de confiance pour la pente de l'axe majeur d'une distribution normale bidimensionnelle. Biométrie-Praximétrie 9: 121–140.

NETER, J., W. WASSERMAN, AND M. H. KUTNER. 1985. Applied linear statistical models. Richard D. Irwin, Inc., Homewood, IL.

NORSTROM, R. J., A. E. MCKINNON, AND A. S. W. DEFREITAS. 1976. A bioenergetics-based model for pollutant accumulation by fish. Simulation of PCB and methylmercury residue levels in Ottawa River yellow perch (*Perca flavescens*). J. Fish. Res. Board Can. 33: 248–267.

PITMAN, E. J. G. 1939. A note on normal correlation. Biometrika 31: 9–12.

RICKER, W. E. 1973. Linear regression in fishery research. J. Fish. Res. Board Can. 30: 409–434.

1975. A note concerning Professor Jolicoeur's comments. J. Fish. Res. Board Can. 32: 1494–1498.

TEISSIER, G. 1948. La relation d'allométrie: sa significance statistique et biologique. Biometrics 4: 14–48.

Dependence of Exploitation Rates for Maximum Yield and Stock Collapse on Age and Sex Structure of Chinook Salmon (*Oncorhynchus tshawytscha*) Stocks

David G. Hankin[1]

Department of Fisheries, Humboldt State University, Arcata, CA 95521, USA

and M. C. Healey

Department of Fisheries and Oceans, Pacific Biological Station, Nanaimo, B.C. V9R 5K6

Hankin, D. G., and M. C. Healey. 1986. Dependence of exploitation rates for maximum yield and stock collapse on age and sex structure of chinook salmon (*Oncorhynchus tshawytscha*) stocks. Can. J. Fish. Aquat. Sci. 43: 1746–1759.

In this paper we investigate the equilibrium behavior of an age- and sex-structured version of the Ricker stock–recruitment model specifically tailored to the complex nature of chinook salmon (*Oncorhynchus tshawytscha*) biology and fisheries. Conclusions from our analysis include the following. (1) Exploitation rates for maximum yield (u_{msy}) and stock collapse (u_{max}) depend strongly on a stock's maturity schedule, being lowest for a late-maturing stock and greatest for an early maturing stock. (2) Values of exploitation rates for u_{max} overlap considerably with those for u_{msy}, emphasizing the probability of stock collapse in fully exploited mixed stock fisheries. (3) Values of u_{msy} and u_{max} are independent of the value of the Ricker β parameter but depend directly on the Ricker α parameter, indicating that management research should focus on obtaining better estimates of α, contrary to recent suggestions in the literature. (4) Because they mature at older ages, female chinook suffer greater cumulative fishery removal rates than males and decline in abundance more rapidly as exploitation increases. Consequently, the use of sex-independent maturity schedules can give misleading estimates for u_{msy} and u_{max}. (5) Maximum changes in mean age of stocks that can be attributed to fishing up effects ranged from 0.32 to 0.81 yr. Many stocks appear already to have declined in mean age by this amount, further emphasizing the probability of impending collapse of some stocks.

Les auteurs traitent du comportement à l'équilibre d'une version structurée par âges et sexes du modèle stock–recrutement de Ricker spécifiquement adaptée à la nature complexe de la biologie et des pêches du saumon quinnat (*Oncorhynchus tshawytscha*). Leur analyse a permis de tirer les conclusions suivantes : 1) les taux d'exploitation correspondant au rendement maximum (u_{rms}) et à l'effondrement du stock (u_{max}) sont fortement fonction du régime de maturité du stock, ces valeurs étant les plus faibles chez les stocks à maturation retardée et les plus élevées chez les stocks à maturation hâtive; 2) les taux d'exploitation correspondant à u_{max} recoupent de façon importante ceux correspondant à u_{rms}, ce qui souligne la probabilité de l'effondrement des stocks faisant l'objet d'une pêche mixte à exploitation maximale; 3) les valeurs de u_{rms} et de u_{max} sont indépendantes de la valeur du paramètre β de Ricker mais directement fonction du paramètre α de Ricker, indiquant que les recherches en gestion devraient donc être axées sur l'obtention de meilleures estimations de α contrairement à ce qui est mentionnée dans les publications récentes; 4) étant donné qu'elles atteignent la maturité à un âge plus avancé, les femelles du saumon quinnat subissent des taux cumulatifs d'élimination par la pêche plus élevés que les mâles et leur abondance décline plus rapidement à mesure que l'exploitation s'accroît. L'utilisation de régimes de maturité indépendants du sexe peut donc fausser les estimations de u_{rms} et de u_{max}; 5) les variations maximales de l'âge moyen des stocks qui peuvent être attribuées aux effets de la pêche varient de 0,32 à 0,81 année. Il semble que l'âge moyen de bon nombre de stocks ait déjà décliné de cette valeur, ce qui souligne la possibilité de l'effondrement imminent de certains de ces stocks.

Received October 9, 1985
Accepted May 7, 1986
(J8478)

Reçu le 9 octobre 1985
Accepté le 7 mai 1986

Among the Pacific salmon species (*Oncorhynchus* spp.), the chinook salmon (*O. tshawytscha*) is the only species that is harvested in North American coastal waters at several ages both as maturing and as immature fish. Since chinook may migrate to sea aged 1–3 yr, and may spend as little as one summer or as long as 5 yr at sea (Healey 1986a, 1986b), the ocean population consists of eight age classes, of which six are vulnerable to harvest. Both immature and maturing chinook aged 3–8 are harvested by hook and line (troll) fisheries which operate within about 20 km of the coast throughout the Pacific Northwest. Maturing chinook of the same age classes that are not intercepted by offshore troll fisheries are also harvested during their spawning migration near the coast and in major river estuaries by gillnet and purse-seine fisheries (Cleaver 1969; Healey 1982).

---

[1] Present address: Department of Fisheries and Wildlife, Oregon State University, Corvallis, OR 97330, USA.

The complexities of chinook life history patterns and the sequential intercepting nature of fisheries on chinook make analysis of their population dynamics more complex than for other species of Pacific salmon, and have raised unique management concerns. In particular, the wisdom of harvesting immature fish in troll fisheries has been questioned (Ricker 1976, 1980; Larkin 1981). Also, the demonstrated heritability of age of maturation (Donaldson and Menasveta 1961), together with long-term declines in the average size and age of chinook, has aroused concern that chinook fisheries have caused a genetic shift toward earlier age of maturation (Ricker 1980, 1981; Hankin and McKelvey 1985; Healey and Heard 1985; Healey 1986b). These concerns have developed in the absence of an analytic framework that adequately captures both the complexity of chinook salmon life history and the distinctions between fishery types. Absence of such an analytic framework has led, among other things, to the use of catch/catch plus escapement as an indicator of exploitation rate in analyses of chinook stock dynamics (Walters et al. 1982), and to assertions that chinook stocks are quite resilient to harvest and can withstand high exploitation rates (Healey and Heard 1985).

In this paper we present and investigate the equilibrium behavior of an age-structured version of the Ricker stock–recruitment model specifically tailored to the complex nature of chinook life histories and fisheries. Our model differs from previously published (static) "cohort analysis" models of chinook stocks (e.g. Argue et al. 1983; Johnson 1974) by its incorporation of a (dynamic) stock–recruitment relation, and our model analysis differs in our exploration of the effects of variation in life history parameters on model behavior. Model parameters represent fundamental sex-specific life history traits that characterize and distinguish chinook stocks. Age-structured (and sex-specific) versions of the Ricker model have been previously used in fisheries research (Reed 1980; McKelvey et al. 1980; Allen and Basasibwaki 1974), but they have not been applied to chinook salmon. (Charles and Reed (1985) presented a bioeconomic analysis appropriate for stocks of fish having sequential intercepting fisheries, including chinook salmon, but their principal concerns were economic and they did not attempt a detailed accounting of chinook life history.) By means of our model we demonstrate the importance of the Ricker α parameter and sex-specific maturity schedules in determining exploitation rates for maximum sustained yield (MSY) and stock collapse. We also illustrate that catch/catch plus escapement is a poor indicator of exploitation rate for chinook. Our analysis is relevant to the recent discussions about effects of size- and age-selective fisheries (Ricker 1980, 1981) and we compare model predictions of changes in age structure attributable to fishing with documented changes in chinook stocks over the past few decades.

Model Formulation

We first define stock- and sex-specific life history parameters that we assume are unaffected by fishing (but see Discussion): σ_{if} = probability that a female alive at age i will mature at age i; σ_{im} = probability that a male alive at age i will mature at age i; p_i = probability that an age i male or female will survive to age $i + 1$ if (a) it is not captured at age i and (b) it does not mature at age i. The σ_{if} and σ_{im} are age- and sex-specific maturation probabilities, and the p_i are conditional age-specific survival rates which we assume are independent of sex. In many instances, it will be impossible to obtain estimates for sex-specific maturation probabilities and it will be expedient to define σ_i as sex-independent but age-specific maturation probabilities. (However, this definition invokes an assumption that age-specific maturation probabilities are independent of sex, clearly in error for chinook.) For completeness in representation of most chinook stock types, ages i will range from age 2 to age 7, but a distinction will be made between the escapement (all ages) and spawning stock (which will exclude the numbers of precocious male *jacks*).

Fishing seasons for chinook stocks in coastal waters of North America generally occur in the spring and summer and often consist of a 2- to 5-mo troll fishery followed by a shorter terminal fishery in the summer. We approximate the sequential intercepting nature of these fisheries by assuming that all fisheries and escapement take place at time t, but that the offshore fishery takes place in the instant before the terminal fishery that takes place in the instant before escapement. This approximation effectively assumes that natural mortality of chinook is negligible during the fisheries; hence, the use of conditional ocean survival rates (the p_i). Because natural mortality of chinook at or older than age 2 is believed to be very low ($0.18 < \hat{M} < 0.32$ on an annual basis; Healey and Heard 1984), this approximation should have little substantive impact on either qualitative or quantitative model predictions. Age-specific exploitation rates in offshore and terminal fisheries are assumed independent of sex and are defined and denoted as follows: u_i = probability that an age i chinook, available to the offshore fishery at age i, will be captured at age i; v_i = probability that an age i chinook, available to the terminal fishery at age i, will be captured at age i.

Figure 1 illustrates how the above life history and fishery parameters determine the survivorship of a cohort of chinook salmon from the time that they are first exposed to potential offshore capture at age 2, until all fish have either matured, died from other causes, or been captured in offshore or terminal fisheries. (This figure assumes that $\sigma_{im} = \sigma_{if} = \sigma_i$, but analogous figures could be constructed separately for each sex if age-specific maturation probabilities were also sex specific.) Note that the effects of offshore harvest on early ages must be carried through to later ages because the offshore fishery may harvest age i fish that are not destined to mature at age i.

We begin formulation of our model for the case where $\sigma_{if} = \sigma_{im} = \sigma_i$, and we define $R(t)$ as the number of age 2 chinook that belong to a single stock and are available offshore at time t. (No further conceptual complexity is introduced by letting age-specific maturation probabilities be sex specific, but notational complexity makes initial model development less obvious.) We then use Fig. 1 to guide the mathematical representation for the number of age i fish (of both sexes) belonging to this stock that would be expected to be available offshore at time t. Denote these expected numbers available offshore at age i by $A_i(t)$. Then,

$$\begin{aligned}
A_2(t) &= R(t)\\
A_3(t) &= R(t-1)\,(1-u_2(t-1))\,(1-\sigma_2)p_2\\
A_4(t) &= R(t-2)\,(1-u_2(t-2))\,(1-u_3(t-1))\\
&\quad\times (1-\sigma_2)\,(1-\sigma_3)p_2p_3\\
A_5(t) &= R(t-3)\,(1-u_2(t-3))\,(1-u_3(t-2))\\
&\quad\times (1-u_4(t-1))\,(1-\sigma_2)\,(1-\sigma_3)\\
&\quad\times (1-\sigma_4)p_2p_3p_4
\end{aligned}$$

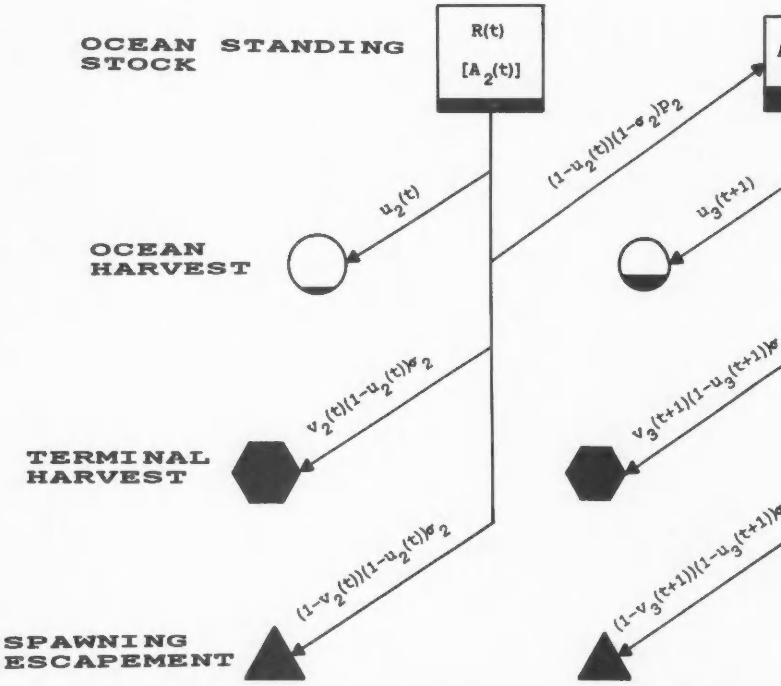
OCEAN STANDING STOCK
R(t)
[A_2(t)]
u_2(t)
(1-u_2(t))(1-σ_2)P_2
u_3(t+1)
OCEAN HARVEST
v_2(t)(1-u_2(t))σ_2
v_3(t+1)(1-u_3(t+1))σ
TERMINAL HARVEST
(1-v_2(t))(1-u_2(t))σ_2
(1-v_3(t+1))(1-u_3(t+1))σ
SPAWNING ESCAPEMENT

FIG. 1. Diagrammatic representation of life history and fisheries for a cohort of chinook salmon.
Shaded portions of the symbols represent the mature fraction. Ocean standing stock is reduced thr
freshwater are either captured in the terminal fishery or escape to spawn. Coefficients at each st
definitions of parameters). Size of symbols is intended only to indicate that progressively fewer

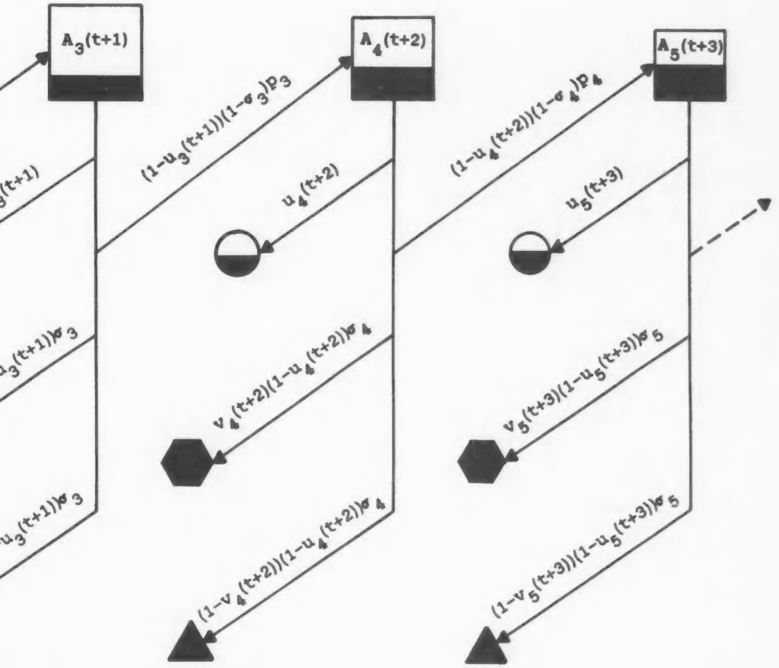
A3(t+1)
A4(t+2)
A5(t+3)
(1-u3(t+1))(1-σ3)P3
(1-u4(t+2))(1-σ4)P4
3(t+1)
u4(t+2)
u5(t+3)
u3(t+1))σ3
v4(t+2)(1-u4(t+2))σ4
v5(t+3)(1-u5(t+3))σ5
u3(t+1))σ3
(1-v4(t+2))(1-u4(t+2))σ4
(1-v5(t+3))(1-u5(t+3))σ5

almon. $R(t)$ = recruitment of the cohort at age 2; A_i = ocean standing stock at successive ages.
luced through ocean harvest (mature and immature fish) and maturation. Mature fish returning to
t each step in the diagram indicate transition probabilities from one step to the next (see text for
y fewer fish are available as time progresses from t through $t + 3$.

$$A_6(t) = R(t-4)(1-u_2(t-4))(1-u_3(t-3))$$
$$\times (1-u_4(t-2))(1-u_5(t-1))$$
$$\times (1-\sigma_2)(1-\sigma_3)(1-\sigma_4)(1-\sigma_5)p_2p_3p_4p_5$$
$$A_7(t) = R(t-5)(1-u_2(t-5))(1-u_3(t-4))$$
$$\times (1-u_4(t-3))(1-u_5(t-2))$$
$$\times (1-u_6(t-1))(1-\sigma_2)(1-\sigma_3)(1-\sigma_4)$$
$$\times (1-\sigma_5)(1-\sigma_6)p_2p_3p_4p_5p_6.$$

For example, the number of age 3 chinook available offshore at $t\,[A_3(t)]$ would be the number that (1) were recruited at age 2 one year previous $[R(t-1)]$, (2) were not captured offshore at age 2 $[1-u_2(t-1)]$, (3) did not mature at age 2 $(1-\sigma_2)$, and (4) survived from age 2 to age 3 (p_2). Note that because the p_i have been defined as conditional survival rates, they simply serve as multipliers. Similar expressions for numbers of males or females at age can be obtained by simply replacing the σ_i by σ_{im} or σ_{if} and multiplying by 0.5 (reflecting an assumed 1:1 sex ratio at age 2). For example,

$$A_{4f}(t) = 0.5R(t-2)(1-u_2(t-2))$$
$$\times (1-u_3(t-1))(1-\sigma_{2f})(1-\sigma_{3f})p_2p_3$$

so that $A_i(t) = A_{if}(t) + A_{im}(t)$ for the sex-specific case.

The above expressions for $A_i(t)$ may be simplified by introducing coefficients that combine those time-invariant parameters that reflect stock-specific life histories. These coefficients, denoted in the sex-specific case by a_{if} and a_{im}, capture and characterize the distinctive life history pattern of a particular chinook stock. For females, the a_{if} are

$$a_{2f} = 0.5$$
$$a_{3f} = 0.5(1-\sigma_{2f})p_2$$
$$a_{4f} = 0.5(1-\sigma_{2f})(1-\sigma_{3f})p_2p_3$$
$$a_{5f} = 0.5(1-\sigma_{2f})(1-\sigma_{3f})(1-\sigma_{4f})p_2p_3p_4$$
$$a_{6f} = 0.5(1-\sigma_{2f})(1-\sigma_{3f})(1-\sigma_{4f})$$
$$\times (1-\sigma_{5f})p_2p_3p_4p_5$$
$$a_{7f} = 0.5(1-\sigma_{2f})(1-\sigma_{3f})(1-\sigma_{4f})$$
$$\times (1-\sigma_{5f})(1-\sigma_{6f})p_2p_3p_4p_5p_6.$$

For males, the a_{im} have the identical form of the a_{if} except that σ_{im} replace the σ_{if}. The $A_i(t)$ may now be written as

$$A_2(t) = R(t) = A_{2f}(t) + A_{2m}(t)$$
$$A_3(t) = R(t-1)(1-u_2(t-1))\,[a_{3f} + a_{3m}]$$
$$A_4(t) = R(t-2)(1-u_2(t-2))(1-u_3(t-1))$$
$$\times [a_{4f} + a_{4m}]$$
$$A_5(t) = R(t-3)(1-u_2(t-3))(1-u_3(t-2))$$
$$\times (1-u_4(t-1))\,[a_{5f} + a_{5m}]$$
$$A_6(t) = R(t-4)(1-u_2(t-4))(1-u_3(t-3))$$
$$\times (1-u_4(t-2))(1-u_5(t-1))\,[a_{6f} + a_{6m}]$$
$$A_7(t) = R(t-5)(1-u_2(t-5))(1-u_3(t-4))$$
$$\times (1-u_4(t-3))(1-u_5(t-2))$$
$$\times (1-u_6(t-1))\,[a_{7f} + a_{7m}].$$

When sex is ignored ($\sigma_i = \sigma_{if} = \sigma_{im}$), coefficients a_i ($= a_{if} + a_{im}$) replace the quantities in square brackets.

Offshore yield (measured as number of fish) from a stock at time t would be

$$Y(t) = \sum_{i=2}^{7} u_i(t)\,A_i(t) = \sum_{i=2}^{7} u_i(t)\,[A_{if}(t) + A_{im}(t)].$$

Terminal fishery harvest (H), total escapement (E), and spawning stock (S) at time t consist only of mature fish and have the following forms:

$$H(t) = \sum_{i=2}^{7} v_i(t)(1-u_i(t))\,[\sigma_{if}A_{if}(t) + \sigma_{im}A_{im}(t)]$$
$$E(t) = \sum_{i=2}^{7} (1-v_i(t))(1-u_1(t))\,[\sigma_{if}A_{if}(t)$$
$$+ \sigma_{im}A_{im}(t)]$$
$$S(t) = \sum_{i=j+1}^{7} (1-v_i(t))(1-u_i(t))\,[\sigma_{if}A_{if}(t)$$
$$+ \sigma_{im}A_{im}(t)]$$

where j denotes the age of jacks (which is most often age 2). Spawning stock can be measured in terms of adult females alone by eliminating the terms $\sigma_{im}A_{im}(t)$ in $S(t)$. If sex of fish is ignored, then $\sigma_iA_i(t)$ replace the quantities in square brackets in expressions for $H(t)$, $E(t)$, and $S(t)$. Note that Y, H, E, and S could all be measured in units of biomass if each $A_{if}(t)$ and $A_{im}(t)$ were multiplied by age- and sex-specific weights w_{if} and w_{im} (see Discussion).

Thus far we have developed static "cohort analysis" representations for yields and escapement that give no real insight into the dynamics of an exploited chinook stock. Evaluation of the dynamic response of a chinook stock to fishing requires that one assume some underlying stock productivity model. For this purpose we adopt the Ricker stock–recruitment model (Ricker 1954). Its age-structured version becomes a nonlinear renewal equation (see McKelvey et al. 1980) of the form

$$R(t+2) = \alpha S(t)e^{-\beta S(t)}$$

where $S(t) = F[R(t-5), R(t-4), R(t-3), R(t-2), R(t-1)]$ (for $j = 2$).

Model Behavior at Equilibrium

Investigation of the dynamic behavior of the above model requires examination of its time-invariant equilibrium solutions, and hence assumptions regarding the time-dependent parameters $u_i(t)$ and $v_i(t)$. There are many possible sets of assumptions that one could make regarding the u_i and v_i, but we shall examine only one. We assume that age 2 chinook are not vulnerable to offshore capture, but that ages 3–7 are all fully vulnerable and are exploited at the same rate. We further assume that all ages in the escapement are equally vulnerable to terminal harvest. (This set of assumptions would give a reasonable representation for many chinook stocks in the southern end of the chinook's range, although noncatch fishing (*shaker*) mortality is ignored (see Ricker 1976).) Given these assumptions, we define

$$u_2(t) \equiv 0 \text{ for all } t$$
$$u^* = u_i(t) \text{ for all } t \text{ and for } i = 3, 4, \ldots, 7$$
$$v^* = v_i(t) \text{ for all } t \text{ and for } i = 2, 3, \ldots, 7.$$

At equilibrium, $R^* = R(t)$ for all t, and equilibrium expressions for offshore numbers of available fish (A^*), offshore yield (Y^*), terminal harvest (H^*), escapement (E^*), and spawning stock (S^*) are (for $j = 2$)

$$A^* = R^*\left[(a_{2f} + a_{2m}) + \sum_{i=3}^{7} (a_{if} + a_{im})(1 - u^*)^{i-3}\right]$$

$$Y^* = u^* R^*\left[\sum_{i=3}^{7} (a_{if} + a_{im})(1 - u^*)^{i-3}\right]$$

$$H^* = v^* R^*\left[\sum_{i=2}^{7} (\sigma_{if} a_{if} + \sigma_{im} a_{im})(1 - u^*)^{i-2}\right]$$

$$E^* = (1 - v^*)R^*\left[\sum_{i=2}^{7} (\sigma_{if} a_{if} + \sigma_{im} a_{im})(1 - u^*)^{i-2}\right]$$

$$S^* = (1 - v^*)R^*\left[\sum_{i=3}^{7} (\sigma_{if} a_{if} + \sigma_{im} a_{im})(1 - u^*)^{i-2}\right].$$

Equilibrium recruitment must satisfy $R^* = \alpha S^* e^{-\beta S^*}$, so that

$$R^* = \frac{\ln\left[\alpha(1 - v^*)\sum_{i=3}^{7} (\sigma_{if} a_{if} + \sigma_{im} a_{im})(1 - u^*)^{i-2}\right]}{\beta(1 - v^*)\sum_{i=3}^{7} (\sigma_{if} a_{if} + \sigma_{im} a_{im})(1 - u^*)^{i-2}}.$$

If spawning stock is measured in terms of females only, then the terms $\sigma_{im} a_{im}$ are eliminated in expressions for both S^* and R^*. Note that if (a) the stock were unexploited ($v^* = u^* = 0$), (b) all fish matured only at age 3 (so that $\Sigma(\sigma_{if} a_{if} + \sigma_{im} a_{im}) = p_2$), and (c) all fish survived from age 2 to age 3 ($p_2 = 1$), then the solution for R^* reduces to $R^* = (\ln \alpha)/\beta$ — the unexploited equilibrium recruitment for a single age spawning stock.

The above equilibrium solutions allow one to examine the dynamics of a chinook stock subject to sequential intercepting fisheries and, among other things, to investigate alternative joint management policies for both offshore and terminal fishery types. As Charles and Reed (1985) pointed out, economically efficient management will depend on the average costs and on the average prices per fish harvested in the two fishery types, as well on underlying stock−recruitment parameters. For many chinook stocks, however, it may be reasonable to assume that terminal fishery harvests are negligible, and we make this assumption (i.e. $v^* = 0$) so as to simplify the model analysis that follows.

Catch/Catch plus Escapement as an Indicator of Exploitation Rate

Analyses of the dynamics of exploited chinook stocks have routinely used (catch)/(catch + escapement) as an indicator of exploitation rate (e.g. Walters et al. 1982). "Escapement" for this calculation usually excludes jacks that are not subject to fishery removal (i.e. escapement is measured by the model's S rather than E). At equilibrium, this calculation gives

$$\frac{\text{catch}}{\text{catch + escapement}} = \frac{Y^*}{Y^* + S^*}$$

$$= \frac{u^* \sum_{i=3}^{7} a_i(1 - u^*)^{i-3}}{u^* \sum_{i=3}^{7} a_i(1 - u^*)^{i-3} + (1 - u^*)\sum_{i=3}^{7} b_i(1 - u^*)^{i-3}}$$

where $a_i = a_{if} + a_{im}$ and $b_i = \sigma_{if} a_{if} + \sigma_{im} a_{im}$. The solution is independent of R^* (and therefore α and β) and depends only on u^*, p^*, and the σ_{if} and σ_{im} (or σ_i). Only under one restrictive condition will this calculation be equal to the true exploitation rate u^*; namely, when male and female fish all mature at age 3. This simply points out that when those fish that are available for offshore capture are all destined to mature, then (catch)/(catch + escapement) provides an unambiguous measure of exploitation rate. The simple fixed life history pattern of coho salmon (*O. kisutch*), for which all adults mature at age 3 (in most stocks, ignoring jacks), provides an example of this situation. However, catch/catch plus escapement for chinook is more akin to the biostatistical rate of exploitation as defined by Ricker (1975, p. 184) and suffers from all of the shortcomings that he listed. This will be illustrated further by empirical examples in the following section.

Exploitation Rates for MSY and Stock Collapse

Exploitation rates that would cause stock collapse can be easily calculated from the equilibrium solution for R^* by noting that the numerator of the solution must always be positive for R^* to exceed zero. R^* will become negative when that quantity that is in square brackets is less than 1. Hence, exploitation rate at the point of stock collapse, $u^*_{\max}$ (for $v^* = 0$), is given implicitly by

$$\sum_{i=3}^{7} (\sigma_{if} a_{if} + \sigma_{im} a_{im})(1 - u^*)^{i-2} = 1/\alpha,$$

which may be solved by iteration for $u^*_{\max}$. The solution depends on a stock's underlying life history parameters (the σ_{if}, σ_{im}, and p^*) and on the α parameter of the stock−recruitment model.

Exploitation rates that would achieve MSY (in terms of number of fish caught) could be determined by substituting the equilibrium expression for R^* in the expression for Y^*, differentiating the derived expression with respect to u^*, and then setting the result equal to zero and solving for u^*. It is simpler to calculate Y^* for various values of u^* and thus to find u^*_{msy} numerically rather than analytically, however, and we have adopted this approach in the following section. (Although the Ricker β parameter will influence the *magnitude* of MSY, it will not influence the exploitation rate for MSY; u^*_{msy} also depends only on the Ricker α parameter and on p^*, σ_{if}, and σ_{im}. The choice of u^* that would maximize Y^* is the same as that choice that would maximize $Y^*\beta$.) Both u^*_{msy} and $u^*_{\max}$ were calculated to within 0.005 of their exact values.

Age Composition in the Escapement

For an unexploited chinook stock, the equilibrium escapement is given by

$$E^* = R^* \sum_{i=2}^{7} [\sigma_{if} a_{if} + \sigma_{im} a_{im}] = R^* Z.$$

The terms in square brackets represent the separate contributions of age i males and females to the escapement so that the proportions of age i females and males and the proportions of both sexes combined would be (in that order) $\sigma_{if} a_{if}/Z$, $\sigma_{im} a_{im}/Z$, and $(\sigma_{if} a_{if} + \sigma_{im} a_{im})/Z$. The average age of spawners in an unexploited stock could be calculated as

$$\gamma_{\text{un}} = \sum_{i=2}^{7} i[\sigma_{if} a_{if} + \sigma_{im} a_{im}]/Z,$$

the sum of the proportions at age times the respective ages i.

The maximum possible change in the average age in the escapement that could be directly attributed to fishing would be the difference between γ_{un} and the average age in the escapement when $u^* = u^*_{\max}$. The equilibrium escapement at the point of stock collapse would be

$$E^* = R^* \sum_{i=2}^{7} (\sigma_{if} a_{if} + \sigma_{im} a_{im}) (1 - u^*_{\max})^{i-2}$$
$$= R^* Q.$$

Age-specific proportions of females, males, and of both sexes would be (in that order) $\sigma_{if} a_{if} (1 - u^*_{\max})^{i-2}/Q$, $\sigma_{im} a_{im} (1 - u^*_{\max})^{i-2}/Q$, and $(\sigma_{if} a_{if} + \sigma_{im} a_{im}) (1 - u^*_{\max})^{i-2}/Q$. And the average age in the escapement at the point of stock collapse would be

$$\gamma_{\min} = \sum_{i=2}^{7} i(\sigma_{if} a_{if} + \sigma_{im} a_{im}) (1 - u^*_{\max})^{i-2}/Q.$$

If spawning stock is measured as total number of adults, then $\gamma_{\min}$ is determined solely by the Ricker α parameter and by the σ_{if} and σ_{im} (or σ_i). To illustrate this fact algebraically, let $c_i = (\sigma_{if} a_{if} + \sigma_{im} a_{im})/p^{*\,i-2}$, so that the p's in the denominator cancel those in the $(a_{if} + a_{im})$ numerator and c_i is a function of only σ_{if} and σ_{im}. Then, at stock collapse,

$$1/\alpha = \sum_{i=3}^{7} c_i [p^* (1 - u^*_{\max})]^{i-2}$$
$$\gamma_{\min} = \sum_{i=2}^{7} i c_i [p^* (1 - u^*_{\max})]^{i-2}/Q.$$

Thus, for a given α, the value of $u^*_{\max}$ will automatically adjust to the value of p^* so that the product $p^* (1 - u^*_{\max})$ is a constant for all p^*. (This result does not hold when spawning stock is measured by females only.)

Realistic Empirically Based Parameters

Stock−Recruitment Parameters

Healey (1982), Wong (1982), and van Hyning (1973) have estimated parameters of Ricker stock−recruitment models for chinook. In all instances, however, they analyzed a mixture of spawning stocks, and the data on which parameter estimates were based were subject to unknown (but probably large) degrees of error and bias. Their analyses may be regarded as, at best, defining a range of plausible parameter values for chinook stocks. We decided to investigate model performance using a range of stock−recruitment parameter values that reflected optimistic to pessimistic levels of stock productivity (as determined by the Ricker α value), but were within the range of parameters presented in these published analyses. We adjusted the Ricker β parameter values so that the unexploited equilibrium recruitment (R^*) for all parameter sets was 1000 fish for the case $p^* = 0.8$ and $\sigma_i = \sigma_{if} = \sigma_{im}$. (This adjustment of β was unimportant because those aspects of model behavior with which we were concerned were independent of the value of β.)

TABLE 1. Stock recruitment parameters (α, β) used for model analysis. The β parameter was adjusted in each case so that $R^* = 1000$ when the conditional ocean survival rate was 80% and age-specific maturation probabilities were sex independent (i.e. $p^* = 0.8$ and $\sigma_i = \sigma_{im} = \sigma_{if}$).

Stock type	Parameter range	α	β
Early maturing			
(Applegate R.)	Pessimistic	5	0.00183
	Reasonable (?)	10	0.00292
	Optimistic	15	0.00357
Mid-maturing			
(Skeena R.)	Pessimistic	5	0.00183
	Reasonable (?)	10	0.00306
	Optimistic	15	0.00378
Late maturing			
(Yukon drainage)	Very Pessimistic	5	0.00181
	Pessimistic (?)	10	0.00332
	Reasonable (?)	15	0.00420
	Optimistic	20	0.00482
"Generalized" coho			
stock	(From Wong 1982)	9.4	0.00265

To provide a basis for comparison with other species, we have also analyzed coho salmon dynamics. This species is harvested in fisheries similar to those for chinook, but almost entirely as maturing fish in their final (third) year of life. Stock−recruitment parameters (from Wong 1982, adjusted to give $R^* = 1000$) for coho were $\alpha = 9.375$ and $\beta = 0.00265$ (Table 1).

Maturity Schedules

Several authors have estimated age-specific maturity schedules for chinook (Cleaver 1969; Wright and Bernhardt 1982; Branski 1979; Borque and Pitre 1972; Parker and Kirkness 1956; Rich 1925). These estimates suffer from a variety of shortcomings from the point of view of application in our analysis. Several are not sex specific, and those that are appear to give too high a rate of maturity to fish aged 2 and 3 (Healey 1986a). Estimates based on cohort analyses of hatchery tag recoveries are limited to stocks that have early ages of maturation, and estimated maturation probabilities are strongly influenced by hatchery rearing and release practices (D. G. Hankin, unpubl.).

We therefore estimated sex-specific maturity schedules for three (exploited) chinook stocks exemplifying early-, mid-, and late-maturing stocks based on age and sex composition of spawning escapement. The three stocks were as follows: (1) the Applegate River stock in the Rogue River drainage of southern Oregon in which males currently mature at an average of 3 yr and females at 3.6 yr; almost all fish are mature by age 5 (B. McPherson and P. Frasier, Oregon Department of Fish and Wildlife, Corvallis, OR, unpublished carcass survey data for 1981, 1982, and 1983); (2) the Skeena River ocean-type stock in northern British Columbia in which males matured at an average of 3.9 yr and females at 5 yr; all were mature by age 6 (Godfrey 1968); and (3) stocks from the Andreafsky and

TABLE 2. Average age and sex composition of (exploited) spawning runs for early-maturing (Applegate River, unpublished carcass survey data for 1981, 1982, and 1983), mid-maturing (Skeena River, ocean-type chinook captured during research gillnetting at the river mouth 1964–66, Godfrey 1968), and late-maturing (Yukon tributaries, McBride et al. 1983; McBride and Wilcock 1983) stocks of chinook. Ages shown are year of life. Yukon fish are all yearling smolts; others are underyearling smolts. Actual figures used for estimation of maturation probabilities (Table 3) were carried to six decimal places.

Stock	Sex	Age (yr)						Total
		2	3	4	5	6	7	
Early	M	0.154	0.187	0.116	0.031	0.001	0.000	0.489
	F	0.001	0.250	0.234	0.024	0.002	0.000	0.511
	M + F	0.155	0.437	0.350	0.055	0.003	0.000	1.000
Mid	M	0.006	0.186	0.442	0.095	0.006	0.000	0.735
	F	0.000	0.000	0.028	0.200	0.037	0.000	0.265
	M + F	0.006	0.186	0.470	0.295	0.043	0.000	1.000
Late	M	0.000	0.004	0.221	0.327	0.077	0.011	0.640
	F	0.000	0.000	0.006	0.087	0.239	0.028	0.360
	M + F	0.000	0.004	0.227	0.414	0.316	0.039	1.000

TABLE 3. Estimated age-specific (σ_i for combined sexes) and age- and sex-specific (σ_{if}, for females and σ_{im}, for males) maturation probabilities for early-, mid-, and late-maturing chinook stocks based on data presented in Table 2. Actual figures used for model predictions were carried to five decimal places.

Stock type	Sex	Age (yr)					
		2	3	4	5	6	7
Early	M	0.099	0.303	0.608	0.945	1.000	1.000
	F	0.000	0.268	0.777	0.817	1.000	1.000
	M + F	0.042	0.282	0.712	0.884	1.000	1.000
Mid	M	0.002	0.130	0.683	0.885	1.000	1.000
	F	0.000	0.000	0.051	0.735	1.000	1.000
	M + F	0.001	0.075	0.392	0.778	1.000	1.000
Late	M	0.000	0.002	0.199	0.656	0.800	1.000
	F	0.000	0.000	0.005	0.145	0.825	1.000
	M + F	0.000	0.001	0.103	0.376	0.819	1.000

Salcha rivers in the Yukon River drainage in which males currently mature at an average age of 4.9 yr and females at 6 yr; all are mature by age 7 (McBride et al. 1983; McBride and Wilcock 1983) (Table 2).

Estimates of age- and sex-specific maturation probabilities for each stock were based on manipulation of the equilibrium solutions for age and sex composition of exploited chinook stocks. Let f_{if} and f_{im} denote the equilibrium proportions of age i females and males in the escapement, so that

$$\sum_{i=2}^{7}(f_{if}+f_{im})=1.$$

Some simple algebra can show that

$$\frac{f_{if}}{f_{(i+1)f}}=\frac{\sigma_{if}}{\sigma_{(i+1)f}(1-\sigma_{if})p^*(1-u^*)}\qquad \text{for } 2\leqslant i\leqslant 6$$

for females, and gives analogous expressions for males and for the case where sex is ignored (i.e. σ_i replace the σ_{if} or σ_{im} and f_i replace the f_{if} or f_{im}). For each case, the ratio of proportions at age depends only on the age- (and sex-) specific maturation probabilities at those two ages and on equilibrium survival and exploitation rates (p^* and u^*). If u^* and p^* are assumed known (and equilibrium proportions can be estimated from empirical data), then

$$\frac{f_{if}p^*(1-u^*)}{f_{(i+1)f}}=\frac{\sigma_{if}}{\sigma_{(i+1)f}(1-\sigma_{if})}.$$

Let λ be the maximum observed age in the escapement and assume that $\sigma_{\lambda f}=1$. Then, for $i=\lambda-1$:

$$\frac{f_{if}p^*(1-u^*)}{f_{(i+1)f}}=\frac{\sigma_{if}}{(1-\sigma_{if})},$$

which can be solved by iteration to give an estimate for $\sigma_{(\lambda-1)f}$. This estimate for $\sigma_{(\lambda-1)f}$ can then be used to generate an estimate for $\sigma_{(\lambda-2)f}$, and so on (for $2\leqslant i<\lambda-1$), using

$$\frac{f_{if}p^*(1-u^*)\hat{\sigma}_{(i+1)f}}{f_{(i+1)f}}=\frac{\sigma_{if}}{(1-\sigma_{if})}.$$

Application of these estimators required an assumption of equilibrium and knowledge of p^* and u^*. For the Applegate stock, we calculated the age-specific proportions of males and females in each of three (apparently "typical") years (1981, 1982, and 1983) and then averaged these proportions by age and sex to approximate the equilibrium f_{if} and f_{im}. For the Skeena stock, we averaged age- and sex-specific proportions for the years 1964, 1965, and 1966. For the Yukon drainage stocks, we combined carcass survey data for the two tributaries for 1980 and 1982 and then averaged figures across the two years (and assumed that these two years were "typical").

Since the sex and age compositions in Table 2 were obtained from stocks already under moderate to intensive fishing pressure, we assumed reasonably high rates of u^*: 0.3 for the Yukon stock, 0.35 for the Skeena River stock, and 0.45 for the Applegate stock. These choices were based on estimates of offshore fishery exploitation rates for coded-wire tagged hatchery chinook (D. G. Hankin, unpubl.) released from the Klamath River in northern California (assumed similar to the Applegate stock) and the Elk River in southern Oregon (Elk River chinook are principally caught off British Columbia).

We wish to emphasize that estimates of age- and sex-specific maturation probabilities, calculated using the above methods, were not intended to represent the best possible estimates of these quantities for the three specific stocks. Rather, they were

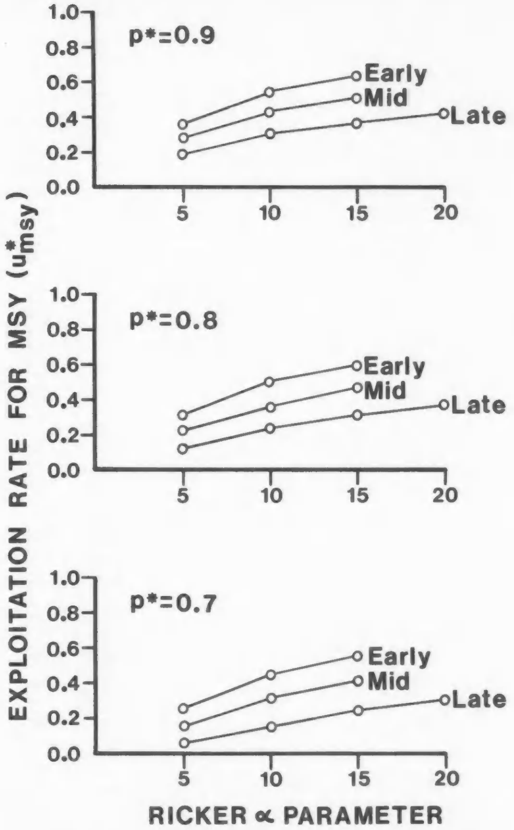

FIG. 2. Model predictions of exploitation rates for MSY for early-, mid-, and late-maturing chinook stocks plotted against values of the Ricker α parameter for three values of the conditional ocean survival rate ($p^* = 0.7, 0.8, 0.9$).

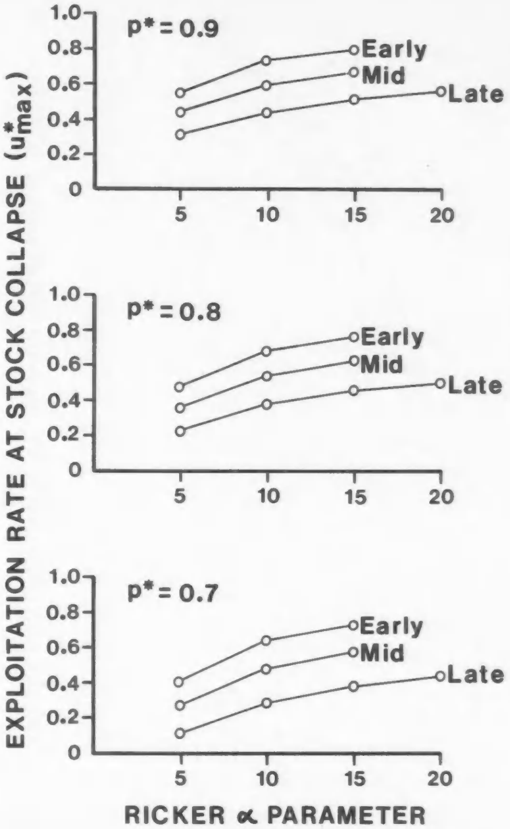

FIG. 3. Model predictions of exploitation rates at the point of stock collapse for early-, mid-, and late-maturing chinook stocks plotted against values of the Ricker α parameter for three values of the conditional ocean survival rate ($p^* = 0.7, 0.8, 0.9$).

intended to be representative of parameters for early-, mid-, and late-maturing stocks in general, of which the specific populations are examples. Among other things, the calculated estimates were sensitive to our choices for u^* which, although based on empirical data, were not stock specific. However, the method of estimation was consistent with our model, calculated estimates had an empirical basis, and, most importantly, estimates clearly distinguished among the three stocks. Also, we are aware of no alternative method for estimating maturation schedules for wild chinook stocks in the absence of tag recovery data. We feel that the estimates were entirely adequate for our purposes of contrasting model predictions, as they depended on stock type.

Mortality Schedules

Parker and Kirkness (1956) and Cleaver (1969) estimated natural mortality rates for chinook salmon from recaptures of tagged fish. In both instances, mortality and maturation were confounded so that no unique estimate of mortality existed. However, both authors estimated the natural mortality rate to be about 35% per year. Ricker (1976) considered this rate to be too high, particularly in comparison with estimated rates for other Pacific salmon species. A more suitable average mortality rate for fish in maturing age classes might be 20%, and this is the value (i.e. $p^* = 0.80$) we used in estimating maturity rates (Table 3). Because of the uncertainty in this parameter, however, we again investigated model predictions using a range of values from 10 to 30% ($p^* = 0.70, 0.80, 0.90$). For the comparison with coho, we used only $p^* = 0.80$.

Model Predictions

Exploitation Rates for MSY and Stock Collapse

Model-based calculations of exploitation rates for maximum sustained yield (u^*_{msy}) and stock collapse (u^*_{max}) for early-, mid-, and late-maturing chinook stocks are plotted as functions of the conditional ocean survival rate (p^*) and the Ricker α parameter in Fig. 2 and 3. When spawning stock was measured by the total number of adults (males and females), sustainable exploitation rates were virtually identical for both sex-independent ($\sigma_i = \sigma_{if} = \sigma_{im}$) and sex-specific ($\sigma_{if} \neq \sigma_{im}$) maturity parameters; minor discrepancies were attributable to very slight differences in age composition that resulted from using the two different maturity parameter sets. Exploitation rates for MSY and stock collapse increased with increasing ocean survival rate (for fixed α) and with increasing α (for

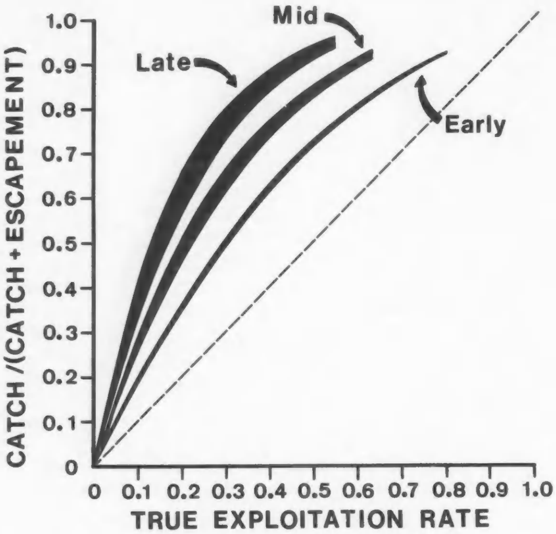

FIG. 4. Calculated values of equilibrium catch/catch plus escapement plotted against true exploitation rate for early-, mid-, and late-maturing chinook stocks. Upper boundaries show calculated values for $p^* = 0.7$; lower boundaries of the shaded regions show calculated values for $p^* = 0.9$. A slope of 1 is indicated by the broken line.

fixed p^*). Calculated exploitation rates were lowest for the late-maturing stock ($0.060 \leq u^*_{\text{msy}} \leq 0.420$ and $0.11 \leq u^*_{\text{max}} \leq 0.555$), intermediate for the mid-maturing stock ($0.155 \leq u^*_{\text{msy}} \leq 0.495$ and $0.265 \leq u^*_{\text{max}} \leq 0.665$), and highest for the early-maturing stock ($0.260 \leq u^*_{\text{msy}} \leq 0.635$ and $0.420 \leq u^*_{\text{max}} \leq 0.795$).

Figure 4 illustrates the fact that catch/catch plus escapement does not directly reflect true exploitation rate for chinook salmon and is strongly influenced by stock-specific maturation schedule. For example, for $p^* = 0.8$ and a true exploitation rate of 0.30, calculated values of catch/catch plus escapement were about 0.50, 0.64, and 0.77 for early-, mid-, and late-maturing stocks. The influence of p^* was substantial only for the mid- and late-maturing stocks, but even for these stocks the range in calculated values of catch/catch plus escapement (as p^* ranged from 0.7 to 0.9) was small compared with differences due to maturation schedules.

For the "typical" coho salmon stock used for comparison with these chinook stocks, we set $p^* = 0.8$ and assumed that $\sigma_{2f} = 0$, $\sigma_{2m} = 0.2$, and $\sigma_{3f} = \sigma_{3m} = 1$ (for the sex-specific case) or $\sigma_2 = 0.1$ and $\sigma_3 = 1$ (for the sex-independent case). As for the chinook stocks, both sex-independent and sex-specific maturity parameters resulted in the same values for u^*_{msy} and u^*_{max}: $u^*_{\text{msy}} = 0.70$ and $u^*_{\text{max}} = 0.850$. These figures were higher than those for any of the chinook stocks, regardless of the optimism with which p^* and α were set. For the coho stock, catch/catch plus escapement would directly reflect (and be equal to) the true exploitation rate for all exploitation rates and any survival rate.

Fishery-Induced Changes in Mean Age

Mean ages in the escapement (γ_{un}) for unexploited chinook stocks ranged from about 3.6 to 3.8 yr, 4.4 to 4.6 yr, and 5.3 to 5.5 yr for the early-, mid-, and late-maturing stocks (Table 4). The upper and lower figures in each case reflected the upper ($p^* = 0.9$) and lower ($p^* = 0.7$) limits of the conditional ocean survival rates used for calculations. For the coho stock, mean age in the escapement for an unexploited stock was about 2.9 yr for $p^* = 0.8$.

TABLE 4. Mean ages in the escapement in unexploited stocks (γ_{un}) and at the point of stock collapse (γ_{min}) for early-, mid-, and late-maturing chinook stocks as they depend on conditional ocean survival rate (p^*) and the Ricker α parameter. γ_{un} are independent of α (for fixed p^*) and γ_{min} are independent of p^* (for fixed α). The first of two figures for γ_{un} and γ_{min} gives mean age for the sex-specific ($\sigma_{if} \neq \sigma_{im}$) maturity parameters, and the second figure gives mean age for the sex-independent ($\sigma_i = \sigma_{if} = \sigma_{im}$) maturity parameters.

Stock	p^*	α	γ_{un}	γ_{min}
Early	0.7	5	3.60, 3.62	3.22, 3.26
	0.8	10	3.70, 3.71	2.91, 2.96
	0.9	15	3.78, 3.79	2.73, 2.79
Mid	0.7	5	4.45, 4.38	4.26, 4.19
	0.8	10	4.54, 4.47	4.05, 3.96
	0.9	15	4.62, 4.55	3.92, 3.83
Late	0.7	5	5.33, 5.31	5.25, 5.23
	0.8	10	5.42, 5.40	5.10, 5.08
	0.9	15	5.50, 5.48	5.01, 4.99
		20		4.94, 4.93

Mean ages in the escapement at the point of stock collapse (γ_{min}) were independent of p^* for each stock (as previously proven algebraically), but decreased with increasing value of the Ricker α parameter (because u^*_{max} increased with α). At α values of 5, 10, and 15, mean ages at stock collapse were about 3.2, 2.9, and 2.7 yr for the early-maturing stock, 4.2, 4.0, and 3.9 yr for the mid-maturing stock, and 5.3, 5.1, and 5.0 yr for the late-maturing stock. At $\alpha = 20$, mean age at the point of stock collapse was about 4.9 yr for the late-maturing stock, and this figure was about 2.5 yr for the coho stock (Table 4).

The difference between γ_{un} and γ_{min} can be viewed as the maximum possible change in the average age in the escapement of a chinook stock that could be attributed strictly to the effects of an offshore fishery (i.e. assuming that the maturity parameters remained fixed under exploitation). Since γ_{min} was independent of p^* (for fixed α) and γ_{un} was independent of α (for fixed p^*) for each stock type, minimum predicted changes in mean age were achieved at the lowest ocean survival rates ($p^* = 0.7$) and the smallest Ricker α values ($\alpha = 5$), and maximum changes were achieved at the highest ocean survival rates ($p^* = 0.9$) and the largest Ricker α values ($\alpha = 15$ for the early- and mid-maturing stocks and $\alpha = 20$ for the late-maturing stock). Maximum changes in mean age ranged from about 0.4 to 1.0 yr for the early-maturing stock, 0.2 to 0.7 yr for the mid-maturing stock, and 0.1 to 0.55 yr for the late-maturing stock. These changes exceeded one full year only for the most optimistic parameter values for the early-maturing stock ($p^* = 0.9$ and $\alpha = 15$) (Fig. 5).

Fishery Effects on Sex Composition

Contrasts of the age and sex composition in the spawning escapement for unexploited and maximally exploited ($u^* = u^*_{\text{max}}$) stocks seemed to give more informative descriptions of potential fishery-induced changes, particularly as they related to shifts in sex composition. Figure 6 shows the proportions of males and females at age in the three chinook stocks, at unexploited equilibrium and at stock collapse, for $p^* = 0.8$ and for

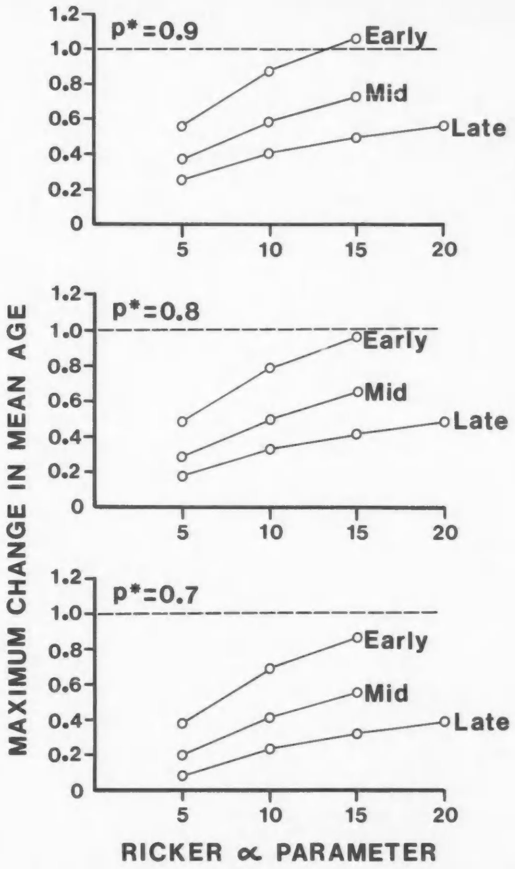

FIG. 5. Model predictions of the maximum possible changes in mean age in the escapement ($\gamma_{un} - \gamma_{min}$) that could be directly attributed to the effects of fishing for early-, mid-, and late-maturing chinook stocks plotted against the Ricker α parameter for three values of the conditional ocean survival rate ($p^* = 0.7, 0.8, 0.9$). Broken lines indicate a change of exactly 1 yr.

Ricker α parameters that we regarded as "most plausible" ($\alpha = 10$ for the early- and mid-maturing stocks and $\alpha = 15$ for the late-maturing stock). The most pronounced feature of changes in stock composition was a shift to dominance by males. For example, for the early-maturing stock, only about 7% of the unexploited escapement was accounted for by age 2 (male) jacks, whereas this figure rose to more than 32% at the point of stock collapse. Overall shifts in sex composition were also considerable: proportions of males at unexploited equilibrium were 0.51, 0.56, and 0.56 for early-, mid-, and late-maturing stocks, but had increased to 0.65, 0.75, and 0.69 at stock collapse.

Up to this point, our summary of model predictions has been based on results obtained when both male and female adults were given equal weight as spawners, and for this variant of our model, predictions based on sex-independent maturity parameters were essentially equivalent to those based on sex-specific maturity parameters. However, the dramatic shifts in sex composition of the escapement (and spawning stock) that the model predicted as a result of exploitation caused us to consider the possible differences in model prediction that might result if spawning stock were measured solely in terms of adult females age 3 and older. For the sample model predictions that follow, we again selected the "most plausible" sets of Ricker parameters (α and β) for each stock, and then doubled these values (reflecting an approximate 50:50 sex ratio at unexploited equilibrium) because only females were included in the spawning stock. (For the sex-independent maturity parameters, this procedure generated exactly the same model predictions as for the original Ricker parameters when both males and females contributed to spawning stock.) We set $p^* = 0.8$.

TABLE 5. Exploitation rates for MSY (u^*_{msy}) and at stock collapse (u^*_{max}), and mean ages in unexploited escapement (γ_{un}) and in escapement at stock collapse (γ_{min}) for sex-independent ($\sigma_{if} = \sigma_{im} = \sigma_i$) and sex-specific ($\sigma_{if} \neq \sigma_{im}$) maturity parameters for a typical coho stock and for early-, mid-, and late-maturing chinook stocks. Calculations were based on measuring spawning stock in terms of numbers of adult (age > 2) females only and assumed a conditional ocean survival rate of 80% ($p^* = 0.8$).

Stock type	α	β	u^*_{msy}	u^*_{max}	γ_{un}	γ_{min}
Coho						
$\sigma_{if} = \sigma_{im}$	18.75	0.0053	0.700	0.850	2.88	2.52
$\sigma_{if} \neq \sigma_{im}$	18.75	0.0053	0.725	0.865	2.88	2.49
Early-maturing chinook						
$\sigma_{if} = \sigma_{im}$	20	0.0059	0.500	0.685	3.71	2.96
$\sigma_{if} \neq \sigma_{im}$	20	0.0059	0.515	0.695	3.70	2.89
Mid-maturing chinook						
$\sigma_{if} = \sigma_{im}$	20	0.0061	0.375	0.540	4.47	3.96
$\sigma_{if} \neq \sigma_{im}$	20	0.0061	0.275	0.400	4.54	4.20
Late-maturing chinook						
$\sigma_{if} = \sigma_{im}$	30	0.0084	0.315	0.450	5.40	4.99
$\sigma_{if} \neq \sigma_{im}$	30	0.0084	0.260	0.375	5.42	5.10

The differences between model predictions based on sex-independent versus sex-specific maturity parameters were inconsistent when spawning stock was measures solely in terms of adult females (Table 5). For the mid- and late-maturing stocks, the use of sex-independent maturity parameters resulted in serious "overestimation" of exploitation rates for MSY and stock collapse when compared with those figures generated using sex-specific maturity parameters. For example, for the mid-maturing stock, use of sex-independent maturity parameters gave $u^*_{msy} = 0.375$ and $u^*_{max} = 0.54$, whereas the sex-specific maturity parameters gave $u^*_{msy} = 0.275$ and $u^*_{max} = 0.40$. In contrast, for the early-maturing chinook stock and for the coho salmon stock, the reverse took place: calculated values for u^*_{msy} and u^*_{max} were slightly higher for the sex-specific maturity parameters than for the sex-independent maturity parameters.

The apparent inconsistency of these trends can be resolved by contrasting the specific ways in which the sex-specific maturity parameters altered the number of adult females that returned at age 3 and older. For the simple coho salmon stock, $\sigma_{2f} = 0$, but $\sigma_2 = 0.1$. This meant that the sex-independent maturity parameters resulted in more females returning at age 2 (when they would not be counted as adult spawners) and fewer females returning at age 3 (when they would be counted) than was the case for the sex-specific maturity parameters (for

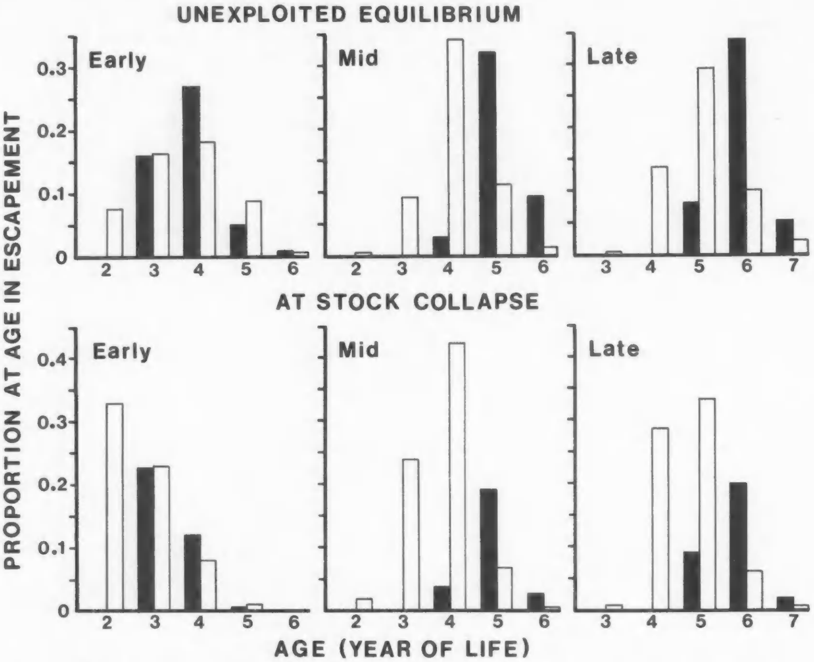

FIG. 6. Model predictions of equilibrium age and sex compositions (females shaded, males open) in escapement for unexploited early-, mid-, and late-maturing chinook stocks plotted above model predictions of age and sex composition at the point of stock collapse for these same stocks. Model predictions assumed that $p^* = 0.8$ and used the "most plausible" values for Ricker α parameters ($\alpha = 10$ for early- and mid-maturing stocks, $\alpha = 15$ for late-maturing stock).

which all females returned at age 3). Thus, for coho salmon (and the early-maturing chinook stock), predicted exploitation rates for MSY were greater for sex-specific maturity parameters than for sex-independent parameters. In contrast, for the mid- and late-maturing stocks, the use of sex-independent maturity parameters allocated "too many" adult females to those younger (but mature) age groups that would remain abundant under exploitation (e.g. $\sigma_4 = 0.103$, but $\sigma_{4f} = 0.005$ for the late-maturing stock). In general, measurement of the adult stock by adult females only, and use of sex-independent maturity parameters, would result in "overestimation" of sustainable harvest rates (when compared with the more realistic sex-specific maturity parameters) for all stocks except those for which the sex-independent maturity parameters would result in a substantial female return at age 2 (prior to model maturity).

Discussion

Model predictions presented in this paper suggest that most chinook stocks, particularly those that might be characterized as mid- or late-maturing, must be substantially less resilient to high exploitation rates than are "typical" coho salmon stocks. Plausible exploitation rates for MSY (in terms of number of fish caught) ranged from 0.06 to 0.635 for late-maturing to early-maturing chinook stocks; even the most optimistic scenarios for the early-maturing stock ($p^* = 0.9$, $\alpha = 15$) failed to produce exploitation rates for MSY that were as high as those calculated for coho salmon (for which $u^*_{\text{msy}} = 0.70-0.72$). Exploitation rates that would produce MSY for early-maturing chinook stocks seem likely to be about 0.50, and if our "most plausible" choices of Ricker α parameters are realistic, then probable exploitation rates for MSY for most mid-maturing stocks may be about 0.40, and for most late-maturing stocks may be as low as 0.25. If MSY were measured in terms of pounds of fish landed, these exploitation rates would be lower still (see Ricker 1976). The wide range in exploitation rates for MSY and their overlap with exploitation rates that would produce stock collapse have obvious and disturbing implications for persistence of late-maturing chinook in contemporary mixed stock troll fisheries (see Paulik et al. 1967).

Model predictions of exploitation rates for MSY and stock collapse for mid- and late-maturing chinook stocks may be regarded by many salmon biologists as unreasonably low. Quite low exploitation rates can result in very substantial reductions in year class strength, however, because chinook may be available to troll fisheries for several successive seasons as immature fish. As a simple illustration, consider the number of females that might reach age 5 for a late-maturing chinook stock. Assume, for simplicity, that there is no ocean natural mortality, that the annual troll fishery exploitation rate is 0.30 from age 3 on, and that all females mature at age 5. If the number of females alive at age 3 = 1000, then only $1000 \times (1 - 0.30)^3 = 343$ females would return to spawn at age 5. Though unsophisticated, this calculation captures the way in which a "moderate" annual exploitation rate (0.30) can remove a very substantial (0.66) proportion of a year class in a late-maturing chinook stock.

The simple calculation above also provides an explanation for why catch/catch plus escapement provides a poor indicator of exploitation rate for chinook salmon (Fig. 4). Because late-maturing chinook are available to troll fisheries as immature fish for more years than early-maturing chinook, calculated values of catch/catch plus escapement will be much greater for late-maturing stocks than for early-maturing stocks given the same underlying exploitation rate in the same fishery. Thus, although calculations of catch/catch plus escapement have merit as measures of *cumulative* removal rates, one cannot directly infer exploitation rates from calculated values of catch/catch plus escapement. In this sense, catch/catch plus escapement does not provide a useful measure of real fishing intensity.

Most of the model predictions presented in this paper were based on an assumption that the total number of adult males and females is a meaningful measurement of spawning stock. The principal justifications for this assumption were pragmatic rather than theoretical: published estimates of stock−recruitment parameters have measured spawning stock by the total number of adults, and age and sex composition data in chinook catch and spawning escapement are rarely available. However, when spawning stock was measured in terms of adult females only, and sex-specific maturity parameters were used, mid- and late-maturing chinook stocks were predicted to be even less resilient to harvest than when spawning stock was measured by males and females. Measuring spawning stock by adult females alone makes good biological sense. Females first mature at least 1 yr later than males in virtually all chinook stocks, and exploitation may strongly shift the sex composition of spawning escapement toward males (Fig. 6). As the number of fish in the spawning escapement is reduced by exploitation, the proportion of females also decreases. This must result in a reduction in reproductive potential of the spawning stock that exceeds that reflected by declines in the total number of adults.

There are also good biological reasons to suppose that the number of adult females is itself an inadequate measure of spawning stock reproductive potential. The reproductive value of a female chinook probably increases with size and age; indeed, this notion is an accepted "fact" in fisheries science. (Beverton and Holt (1957) originally formulated their stock−recruitment model measuring adult stock by the number of eggs deposited, not the number of females.) Larger and older female chinook carry more eggs (Healey and Heard 1984), and their eggs are of a larger size (Hankin and McKelvey 1985; D. G. Hankin, unpubl. data). Larger females may dig deeper nests in coarser gravel wherein survival to emergence may be improved (see van den Berghe and Gross (1984) re coho salmon nest depths, Ricker (1980) re gravel size, and Shelton (1955) re improved emergence success in larger gravel). The best single measure of female reproductive potential may be female weight rather than fecundity (see Hankin and McKelvey (1985) re the correlation between ovary weight and length and Hankin (1980)).

If the most appropriate measure of chinook spawning stock is adult female biomass, then model predictions presented in this paper, including those based on adult female stock rather than total escapement, will have overestimated sustainable exploitation rates that chinook stocks can withstand. Reduction in female stock biomass at any particular exploitation rate would be much greater than reduction in female numbers (see Ricker 1963).

The focus of most recent work on fitting stock−recruitment curves to Pacific salmon (e.g. Walters and Ludwig 1981; Ludwig and Walters 1981) has been on errors of estimation of catch and escapement, rather than on whether or not the measurements of escapement have any biological validity or meaning (irrespective of errors of estimation). While errors of estimation are undeniably important, they are probably no more important than are errors of measurement that arise due to misspecification of the quantity to be estimated (i.e. misspecification of spawning stock as the total number of adult spawners). Also, more attention seems to have been placed on estimation of the Ricker β parameter than on estimation of the Ricker α parameter (e.g. Walters and Hilborn 1976). This focus may be misplaced.

Exploitation rates for MSY and stock collapse depend only on the Ricker α parameter, stock-specific maturity parameters, and ocean survival rates. As shown in this paper, sex and age composition data in spawning escapement may allow rough, but useful, estimates of maturity parameters. Estimation of the α parameter ought not to require collection of spawning stock data at densities that would allow detection of overcompensation (i.e. estimation of β). The α parameter may be regarded as the recruitment per "spawner" at extremely low stock size (Ricker 1975, p. 348), and quite simplistic fitting methods could establish a plausible range of α for a given stock. Existing data could thus be used to calculate a range for desirable exploitation rate, and fisheries could be managed for exploitation rate rather than escapement. Existing troll fishery exploitation rates can, in theory, be estimated from the sequences of recoveries of tagged groups of chinook that have been released from hatcheries throughout the Pacific Northwest over the past decade (D. G. Hankin, unpubl.).

This alternative management strategy would require collection of both sex and age (or size) composition data during spawning surveys. The costs of such surveys would necessarily be greater than for current surveys. Unless the model predictions presented in this paper are seriously in error, however, we feel that compelling arguments can be made for the routine collection of these data for chinook salmon. Walters and Ludwig (1981) previously pointed out that existing estimates of escapement for Pacific salmon are of little value without attached measures of precision. To this we add that, for chinook salmon at least, they may also be of little value if they fail to adequately represent the true nature of spawning stock reproductive potential, irrespective of errors of estimation.

Finally, we wish to compare model predictions of shifts in age and sex composition of chinook spawning stocks with those changes that have been empirically observed. One of the principal motivations for the research described in this paper was a desire to determine analytically what might be the maximum possible changes in the mean ages of chinook spawning populations that could be directly attributable to offshore exploitation. Model predictions suggest that maximum changes in mean age attributable to fishing up effects (Ricker 1975) range from 0.41 to 0.75 yr if sex-independent maturity schedules are used and 0.32 to 0.81 yr if sex-specific maturity schedules are used (Table 5).

Ricker (1980) and Healey (1982) reported declines in the mean age of chinook in troll and other fisheries since the early 1900's. The declines ranged from very modest off the Columbia River (0.18 yr between 1919−20 and 1964−65) to substantial off the west coast of the Queen Charlotte Islands (2.30 yr between 1929 and 1965) (Ricker 1980). For the British Columbia coast as a whole, mean age of chinook in the troll fisheries apparently declined about 1 yr between 1920 and 1950 but changed little after 1950 (Healey 1982). These observed changes in mean age took place during the period of major expansion of ocean troll fisheries for chinook in British Columbia; these fisheries have contributed greatly to the overexploitation of chinook in recent years (Healey 1982; Walters et al. 1982). Because the ocean troll fishery harvests a mixture of stocks, and because fishing patterns and ocean conditions have changed over the years, changes in age composition in the ocean fisheries are difficult to interpret in terms of individual spawning population dynamics. It seems certain that the observed changes in age composition (and presumably also in the size of chinook landed) represent more than just fishing up effects, but whether or not genetic selection for small size and early age of maturation has occurred remains controversial (Ricker 1980, 1981; Healey 1986b).

The observed declines in mean age of chinook in ocean fisheries are, however, as great or greater than the changes that our model suggests would signal approaching stock collapse. A recent analysis of southern British Columbia spawning populations of chinook (Walters and Cahoon 1985) indicates that, since 1950, progressively fewer populations have made up the majority of the spawning escapement. This change has not, as yet, been accompanied by the complete disappearance of many spawning populations. Walters and Cahoon's (1985) analysis does demonstrate, however, that, as fishing has intensified, more and more chinook populations have come to persist only as remnants that contribute little to the commercial catch. If the recent trends in ocean exploitation rates continue, we would predict that stock declines of this sort will increase dramatically in frequency and will soon involve the more productive wild stocks.

Acknowledgements

We thank the *Journal* for encouraging the kind of exchange (Hankin and McKelvey 1985; Healey and Heard 1985) that led us to collaborate on this paper. Most of the senior author's research was accomplished while on sabbatic leave at Oregon State University, and the senior author thanks the Department of Fisheries and Wildlife, OSU, and the Oregon Sea Grant College Program for their support of his sabbatic. We also thank the Oregon Department of Fish and Wildlife for providing us with unpublished carcass survey data for the early-maturing Applegate chinook stock, and M. Henderson and R. Reisenbichler for commenting on a draft of the manuscript. Funding for publication was provided by NOAA Office of Sea Grant, Department of Commerce, under grant No. NA81AA-D-00086.

References

Allen, R. L., and P. Basasibwaki. 1974. Properties of age structure models for fish populations. J. Fish. Res. Board Can. 31: 1119–1125.

Argue, A. W., R. Hilborn, R. M. Peterman, M. J. Staley, and C. J. Walters. 1983. Strait of Georgia chinook and coho fishery. Can. Bull. Fish. Aquat. Sci. 211: 91 p.

Beverton, R. J., and S. J. Holt. 1975. On the dynamics of exploited fish populations. Fish. Invest. Ser. II, XIX: 533 p.

Borque, S. C., and K. Pitre. 1972. Size and maturity of troll-caught chinook salmon (*Oncorhynchus tshawytscha*) caught off the west coast of Vancouver Island in 1969 and 1970. Can. Dep. Environ. Fish. Mar. Serv. Tech. Rep. 1972–7: 1–47.

Branski, C. 1979. Maturity rates for Puget Sound chinook stocks. Wash. Dep. Fish. Tech. Rep. 43: 1–13.

Charles, A. T., and W. J. Reed. 1985. A bioeconomic analysis of sequential fisheries: competition, coexistence and optimal harvest allocation between inshore and offshore fleets. Can. J. Fish. Aquat. Sci. 42: 952–962.

Cleaver, F. C. 1969. Effects of ocean fishing on the 1961-brood fall chinook salmon from Columbia River hatcheries. Fish. Comm. Or. Res. Rep. 1: 1–75.

Donaldson, L. R., and D. Menasveta. 1961. Selective breeding of chinook salmon. Trans. Am. Fish. Soc. 90: 160–164.

Godfrey, H. 1968. Ages and physical characteristics of maturing chinook salmon on the Nass, Skeena and Fraser rivers in 1964, 1965 and 1966. Fish. Res. Board Can. MS Rep. 967: 1–38.

Hankin, D. G. 1980. A multistage recruitment process in laboratory fish populations: implications for models of fish population dynamics. Fish. Bull. 78: 555–578.

Hankin, D. G., and R. McKelvey. 1985. Comment on fecundity of chinook salmon and its relevance to life history theory. Can. J. Fish. Aquat. Sci. 42: 393–394.

Healey, M. C. 1982. Catch, escapement and stock–recruitment for British Columbia chinook salmon since 1951. Can. Tech. Rep. Fish. Aquat. Sci. 1107: 77 p.

1986a. The life history of chinook salmon (*Oncorhynchus tshawytscha*), p. 000–000. *In* M. C. Healey and R. R. Wallace [ed.] Canadian aquatic resources. Can. Bull. Fish. Aquat. Sci. 215.

1986b. Optimum size and age at maturity in Pacific salmon and effects of size-selective fisheries, p. 39–52. *In* D. J. Meerburg [ed.] Salmonid age at maturity. Can. Spec. Publ. Fish. Aquat. Sci. 89.

Healey, M. C., and W. R. Heard. 1984. Inter- and intra-population variation in the fecundity of chinook salmon (*Oncorhynchus tshawytscha*) and its relevance to life history theory. Can. J. Fish. Aquat. Sci. 41: 476–483.

1985. Reply to comment on fecundity of chinook salmon and its relevance to life history theory. Can. J. Fish. Aquat. Sci. 42: 394–395.

Johnson, F. C. 1974. First interim report on salmon fishery modelling. Natl. Bur. Stand. Rep. 74522. Washington, DC.

Larkin, P. A. 1981. A perspective on population genetics and salmon management. Can. J. Fish. Aquat. Sci. 38: 1469–1475.

Ludwig, D., and C. J. Walters. 1981. Measurement errors and uncertainty in parameter estimates for stock and recuitment. Can. J. Fish. Aquat. Sci. 38: 711–720.

McBride, D. N., H. H. Hamner, and L. S. Buklis. 1983. Age, sex, and size of Yukon River salmon catch and escapement, 1982. Alaska Dep. Fish Game Data Rep. 90: 1–141.

McBride, D. N., and J. A. Wilcock. 1983. Alaska chinook salmon (*Oncorhynchus tshawytscha* Walbaum) catch and escapement, 1961–1980, with age, size and sex composition estimates. Alaska Fish Game Inf. Leafl. 212.

McKelvey, R., D. G. Hankin, K. Yanosko, and C. Snygg. 1980. Stable cycles in multistage recruitment models: an application to the northern California Dungeness crab (*Cancer magister*) fishery. Can. J. Fish. Aquat. Sci. 37: 2323–2345.

Parker, R. R., and W. Kirkness. 1956. King salmon in the ocean troll fishery of southeastern Alaska. Alaska Dep. Fish. Res. Rep. 1: 1–64.

Paulik, G. J., A. S. Hourston, and P. A. Larkin. 1967. Exploitation of multiple stocks by a common fishery. J. Fish. Res. Board Can. 24: 2527–2537.

Reed, W. J. 1980. Optimum age-specific harvesting in a nonlinear population model. Biometrics 36: 579–593.

Rich, W. H. 1925. Growth and degree of maturity of chinook salmon in the ocean. Bull. U.S. Bur. Fish. 41: 14–91.

Ricker, W. E. 1954. Stock and recruitment. J. Fish. Res. Board Can. 11: 559–623.

1963. Big effects from small causes: two examples from fish population dynamics. J. Fish. Res. Board Can. 20: 257–264.

1975. Computation and interpretation of biological statistics of fish populations. Bull. Fish. Res. Board Can. 191: 382 p.

1976. Review of the rate of growth and mortality of Pacific salmon and non-catch mortality caused by fishing. J. Fish. Res. Board Can. 33: 1483–1524.

1980. Causes of the decrease in age and size of chinook salmon (*Oncorhynchus tshawytscha*). Can. Tech. Rep. Fish. Aquat. Sci. 944: 25 p.

1981. Changes in the average size and age of Pacific salmon. Can. J. Fish. Aquat. Sci. 38: 1636–1656.

Shelton, J. M. 1955. The hatching of chinook salmon eggs under simulated natural conditions. Prog. Fish-Cult. 17: 20–35.

van den Berghe, E. P., and M. R. Gross. 1984. Female size and nest depth in coho salmon (*Oncorhynchus kisutch*). Can. J. Fish. Aquat. Sci. 41: 204–206.

van Hyning, J. M. 1973. Stock–recruitment relationships for Columbia River chinook salmon, p. 89–97. *In* B. B. Parrish [ed.] Fish stocks and recruitment. Rapp. Verbaux Cons. Int. Explor. Mer. 164.

WALTERS, C. J., AND P. CAHOON. 1985. Evidence of decreasing spatial diversity in British Columbia salmon stocks. Can. J. Fish. Aquat. Sci. 42: 1033–1037.

WALTERS, C. J., AND R. HILBORN. 1976. Adaptive control of fishing systems. J. Fish. Res. Board Can. 33: 145–159.

WALTERS, C. J., R. HILBORN, M. STALY, AND F. WONG. 1982. An assessment of major commercial fish and invertebrate stocks on the west coast of Canada. Report to the Pearse Commission on Pacific fisheries policy. (Available from Environmental and Social Systems Analysts, Ltd., 678 W. Broadway, Vancouver, B.C. V5Z 1G6).

WALTERS, C. J., AND D. LUDWIG. 1981. Effects of measurement errors on assessement of stock–recruitment relationships. Can. J. Fish. Aquat. Sci. 38: 704–710.

WONG, F. Y. C. 1982. Analysis of stock–recruitment dynamics of British Columbia salmon. M.Sc. thesis, University of British Columbia, Vancouver, B.C. 221 p.

WRIGHT, S., AND J. BERNHARDT. 1982. Maturity rates of ocean-caught chinook salmon. Bull. Pac. Mar. Fish. Comm. 8: 49–59.

Apex Predation by Yellowfin Tuna (*Thunnus albacares*): Independent Estimates from Gastric Evacuation and Stomach Contents, Bioenergetics, and Cesium Concentrations

Robert J. Olson

Inter-American Tropical Tuna Commission, c/o Scripps Institution of Oceanography, La Jolla, CA 92093, USA

and Christofer H. Boggs[1]

Center for Limnology, University of Wisconsin, Madison, WI, 53706, USA

Olson, R. J., and C. H. Boggs. 1986. Apex predation by yellowfin tuna (*Thunnus albacares*): independent estimates from gastric evacuation and stomach contents, bioenergetics, and cesium concentrations. Can. J. Fish. Aquat. Sci. 43: 1760–1775.

Three approaches for estimating predation by yellowfin tuna (*Thunnus albacares*) were compared: (1) stomach analysis adjusted for gastric evacuation; (2) food energy required as a function of swimming speed in yellowfin tracked at sea; and (3) food intake needed to maintain observed cesium concentrations. Gastric evacuation data from captive yellowfin were best fit by linear functions of time for four foods. Fish with high lipid content (mackerel, *Scomber japonicus*) were evacuated at a slower rate (proportion per hour) than smaller fish (smelt, *Hypomesus pretiosus*), squid (*Loligo opalescens*), and small fragile fish (nehu, *Stolephorus purpureus*), all of which had lower lipid contents. Tuna captured in the eastern Pacific had daily rations averaging 3.9% of body mass based on stomach contents and gastric evacuation rates, 5.2% based on bioenergetics estimates, and 6.7% based on the cesium estimate. Swimming costs accounted for one-third to one-half of the energy budget. Annual predation by the eastern Pacific yellowfin population averaged 4.3–6.4 million metric tons during 1970–72, depending on the method used for estimating ration; 34% was frigate tunas (*Auxis* spp.). High growth and turnover rates (*P/B* ratios) of tropical tunas in contrast with low conversion and trophic transfer efficiencies suggest a trophic structure that differs from more productive ecosystems.

Les auteurs comparent trois méthodes pour l'estimation de la prédation par l'albacore à nageoires jaunes (*Thunnus albacares*) : 1) l'analyse du contenu stomacal corrigé en fonction de l'évacuation gastrique; 2) l'énergie alimentaire nécessaire présentée comme une fonction de la vitesse de nage d'albacores dont les déplacements ont été relevés en mer; et 3) l'ingestion alimentaire nécessaire au maintien des concentrations de césium observées. Les données sur l'évacuation gastrique d'albacores gardés en captivité étaient le mieux représentées par des fonctions linéaires temporelles, ceci pour quatre aliments. Les poissons à forte teneur en lipides (maquereaux, *Scomber japonicus*) étaient évacués plus lentement (proportion par heure) que des poissons plus petits (éperlans, *Hypomesus pretiosus*), des calmars, *Loligo opalescens* et un petit poisson fragile (néhu, *Stolephorus purpureus*), tous à teneur en lipides moins élevée. La ration quotidienne des albacores capturés dans l'est du Pacifique s'élevait en moyenne à 3,9 % de la masse corporelle, sur la base du contenu stomacal et des taux d'évacuation gastrique, de 5,2 %, sur la base des estimations bioénergétiques, et de 6,7 %, sur la base des concentrations de césium. L'énergie consacrée à la nage représentait du tiers à la demie du bilan énergétique. La prédation annuelle de la population d'albacores de l'est du Pacifique s'est élevée en moyenne à 4,3–6,4 millions de tonnes métriques au cours de la période 1970–1972, tout dépendant de la méthode utilisée pour l'estimation de la ration; 34 % de celle-ci était composée de thazards (*Auxis* spp.). La croissance rapide et les taux de renouvellement élevés des thons tropicaux comparativement aux faibles efficacités de conversion et de transfert trophique, portent à croire à l'existence d'une structure trophique différente de celle des écosystèmes plus productifs.

Received August 6, 1985
Accepted May 9, 1986
(J8372)

Reçu le 6 août 1985
Accepté le 9 mai 1986

Yellowfin tuna (*Thunnus albacares*) are abundant and ubiquitous in tropical regions of the world's oceans. Tunas are opportunistic, generalist predators (Alverson 1963; Blackburn 1968; Magnuson and Heitz 1971). Metabolic rates of tunas greatly exceed those of cold-bodied fishes (Stevens and Dizon 1982) due to their obligate continuous activity (Magnuson 1978) and high "standard" metabolic rates (Brill 1979; Gooding et al. 1981). Estimates of food consumption and an understanding of energy partitioning are needed to explain the ecological strategy of this high-cost mode of living (Stevens and Neill 1978; Kitchell 1983). The large energy requirements of yellowfin, their abundance, and their broad diet make this species useful for estimating pelagic productivity at the intermediate trophic levels occupied by their prey.

Several methods for estimating daily rates of food consumption in fishes have been employed. Direct methods entail quantifying the amount of food in the stomachs of wild-caught fish and adjusting for the gastric evacuation rate determined by laboratory experiments (Elliott and Persson 1978; Jobling 1981a). Indirect methods include constructing energy and nutrient budgets (Davis and Warren 1971; Mann 1978). Both approaches have drawbacks. Direct methods are laborious and provide infrequent point estimates of in situ feeding rate. Bioenergetics modeling of food consumption can be biased by errors in parameter estimation (Bartell et al. 1986) but are useful for evaluating the effect of temperature, body size, and activity of a predator on its food resource (Kitchell 1983). Comparing estimates of food consumption from direct and indirect methods can provide valuable independent validation of laboratory-measured bioenergetics parameters (Rice and Cochran 1984).

---

[1] Present address: NOAA, National Marine Fisheries Service, SWFC Honolulu Laboratory, 2570 Dole Street, Honolulu, HI 96822-2396, USA.

In our study, three independent approaches were taken to estimate the flux of energy through a tuna population. In the first, stomach analysis on thousands of field-caught yellowfin tuna was combined with laboratory determinations of gastric evacuation rates for mixed meals of different food items to estimate the daily ration of yellowfin at sea and to estimate predation rates on various prey organisms. The second approach was to employ a model derived from energy expenditures in yellowfin as a function of size and swimming speed in the laboratory (Boggs 1984). This model was applied to swimming speeds measured by acoustic telemetry of yellowfin at sea (Carey and Olson 1982) to estimate typical energy and food requirements. In the third approach, previous determinations of trophic level and cesium concentration in yellowfin and their prey (Mearns et al. 1981) and residence time of cesium in tuna tissue (Folsom et al. 1967) were used to estimate the amounts of prey consumed by yellowfin.

This diversified investigation of food consumption by yellowfin allows for comparison and corroboration of methods, and thus overcomes some of the inadequacies of each approach. The objective was to determine if food consumption by yellowfin in nature was consistent with laboratory results showing a very high energy demand. Validation of laboratory results was sought to increase the credibility of "top-down" trophic models that use bioenergetics parameters such as predation rate (Laevastu and Larkins 1981; Polovina 1984), gross conversion efficiency (Longhurst 1983), or trophic transfer efficiency (Adams et al. 1983) of major predators to describe the trophic system at lower levels. We estimated these parameters for yellowfin tuna, a dominant apex predator in the eastern tropical Pacific Ocean, and used them to estimate the minimum production rate of a variety of prey types.

Materials and Methods

Gastric Evacuation Experiments

Experimental yellowfin were caught by pole-and-line boats using live bait. They were delivered to the Kewalo Research Facility (Nakamura 1972) of the National Marine Fisheries Service in Honolulu, Hawaii, within 2–6 h and placed in 40- or 700-m^3 outdoor tanks. Ambient temperature ranged from 23.5 to 25.5°C. All experiments were conducted within 45 d of capture. Yellowfin exhibit the least degenerative physiological change of any tuna species in captivity. Individuals have been maintained for several years and have gained mass up to 50 kg (C. H. Boggs, pers. obs.).

Sixty-nine yellowfin averaging 36.2 cm in fork length (range = 23.6–45.1 cm) and 973 g (range = 220–1756 g, excluding stomach contents) were individually tagged (with color codes) for easy recognition and were trained to accept mixed meals of dead mackerel (*Scomber japonicus*), squid (*Loligo opalescens*), smelt (*Hypomesus pretiosus*), and nehu (*Stolephorus purpureus*). The foods were selected based on their taxonomic and/or gross morphological similarity to important yellowfin prey in the eastern Pacific (Alverson 1963; Anonymous 1984). Red crabs (*Pleuroncodes planipes*), an important prey, were offered but not eaten by the captive yellowfin.

All food species were acquired frozen, thawed in air, blotted, and weighed to the nearest 0.01 g. Some of the larger mackerel and squid were cut in half to allow ingestion by the yellowfin. Samples of each food type were dried at 60°C to a constant mass to determine water content. Replicate subsamples of dried specimens were analyzed for lipid content using a Soxhlet apparatus (Joslyn 1950) and chloroform–methanol, 2:1 by volume.

The yellowfin were not fed for 24 h prior to experimental feedings, allowing enough time to clear their guts. Although Noble (1973) found that fish may process food more slowly after a moderate period of food deprivation than when feeding continuously, a fairly high frequency of empty stomachs suggests that intervals without food are typical for tunas (Alverson 1963). Mixed meals of the four food organisms were offered, one food particle at a time. The time that each preweighed food particle was eaten by each individually recognized (tagged) fish was recorded to the nearest minute. Feeding continued until the tuna were satiated. The elapsed time from ingestion of each food particle to the time the fish were killed was recorded. Freshly killed fish were weighed to the nearest gram, and fork length was measured to the nearest millimetre. Hemostats were used to ligate the alimentary canal at the esophagus and pyloric sphincter. The stomach was removed from the yellowfin, slit, and the food remains removed, sorted by species, blotted, and weighed to the nearest 0.01 g. The elapsed time from handling the fish to weighing the stomach contents was about 5 min. Stomach contents were oven dried at 60°C to a constant mass at 0.01 g accuracy.

The evacuation data were analyzed separately by food species. Evacuation functions[2] were fitted using wet-mass data, since wet mass was the quantity measured during stomach analysis, and we wished to calculate daily ration on a wet-mass basis. Some data were eliminated prior to curve fitting to correct for a significant bias in this type of data (Olson and Mullen 1986). The problem becomes important when the duration of gastric evacuation experiments is long enough that at least some test individuals empty their stomachs. Empty stomachs must be omitted during data analysis because the exact time they became empty cannot be determined. Prior to the time when the fastest digestors in a sample begin to empty their stomachs, the data include the full range of intraspecific variability expected. But subsequent to that time, an ever-increasing proportion of the sample representing the faster digestors is eliminated from the distribution. Thus, as postprandial time increases, the distribution becomes constricted by the time axis. Olson and Mullen (1986) showed conclu-

---

[2] Functions actually represent gastric retention, but we follow convention in calling them gastric evacuation functions.

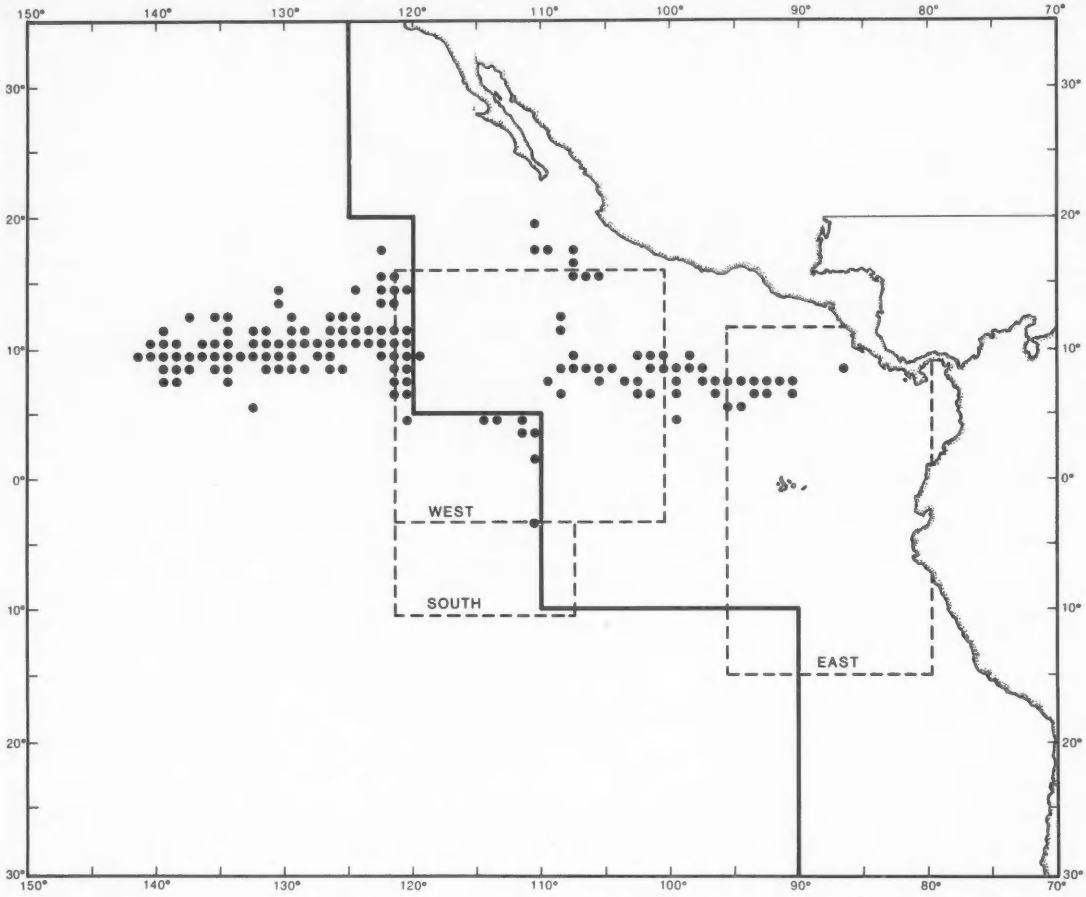

FIG. 1. Sampling locations in the eastern tropical Pacific from which stomachs of yellowfin tuna were collected during 1970−72. The western boundary of the regulated fishing area (bold line) encloses 1.696×10^{13} m^2 (Sharp and Francis 1976). The broken lines enclose three sampling areas of the EASTROPAC oceanographic expedition (Blackburn et al. 1970).

sively that "constricted" data distributions can cause serious bias in evacuation rate estimates and a false indication or exaggeration of curvature. Therefore, the data were truncated prior to curve fitting to eliminate those points associated with postprandial times when empty stomachs appear. A simple procedure for choosing points of truncation was explained by Olson and Mullen (1986).

The gastric evacuation data were fitted to linear, square root, and exponential models and the fits evaluated using residual mean squares and statistical procedures of residual analysis, including tests for normality (Filliben 1975), homoscedasticity, and autocorrelation (Wesolowski 1976). The Y_i values (proportion of initial amount recovered from the stomach) were transformed as $\ln(Y_i + 1.0)$ and $\sqrt{Y_i + 0.5}$ for the exponential and square root models, respectively (Zar 1974). An arcsine transformation was attempted, but did not improve the approximation of this proportion data to normality. The data were analyzed for the effect of food type, meal size, yellowfin size, mixed meals, partial food particles, and food composition on evacuation rates using analysis of covariance (Dixon and Massey 1957).

Stomach Samples

Yellowfin stomach samples from fish captured by the eastern tropical Pacific purse-seine fishery during 1970−72 (Fig. 1) were collected by scientific technicians at tuna canneries in San Diego and San Pedro, California. These yellowfin were captured during daylight hours, and most often in schools associated with dolphins (*Stenella attenuata* and *S. longirostris*). Fork length of sampled fish was measured to the nearest millimetre and the stomachs were preserved by freezing.

Stomach contents were identified to the lowest possible taxa, counted, and weighed to the nearest 0.1 g. After removing the food, the stomachs were weighed to the nearest 1.0 g. This was used to adjust for the often missing anteriormost portion of the stomachs due to the canneries' method of eviscerating tuna. A relationship between complete empty stomach mass and yellowfin fork length was determined from an independent sample of 95 yellowfin which we eviscerated. In partially filled complete stomachs the contents were distributed fairly evenly throughout the stomach. Thus, it seemed reasonable that the proportion of each prey category in the stomach contents (if any) missing from each sample was proportional to the weight of the stomach missing.

A second adjustment was made to account for reduced stomach contents due to gear retention and disturbance, since feeding presumably ceases when dolphins and associated yellowfin are chased and while enclosed in a purse seine, but digestion continues at least until death or freezing. The average duration of pursuit and enclosure was determined for fishing operations in the early 1970's and used in conjunction with evacuation rates to adjust upward the weight of stomach contents at time of gut removal.

Stomach contents data were stratified into arbitrary age-classes based on yellowfin fork length. Age-class subdivisions were selected to approximate the sizes of yellowfin upon completing their first, second, and third years based on yellowfin otolith increment counts (A. Wild, Inter-American Tropical Tuna Commission, c/o Scripps Institution of Oceanography, La Jolla, CA, pers. comm.).

In representing the relative biomass of prey types consumed, the contribution of each prey to the daily meal was determined by accounting for differences in evacuation rate of each prey. The components of the diet were expressed as proportions of the daily meal.

Ration Estimates

Since preliminary analysis indicated that the evacuation data were poorly fitted by an exponential function, even before data were omitted as described above, an alternative to those methods for calculating daily ration which require an a priori assumption of exponential gastric evacuation (e.g. Elliott and Persson 1978) was needed. A method (Robson 1970) that is appropriate for a variety of evacuation functions was described in detail by Olson and Mullen (1986). The model predicts feeding rate ($\hat{r}$, grams per hour) by dividing the mean stomach contents per predator ($\bar{W}$, grams) by the integral (A, proportion × hours = hours) of the function that best fits experimental gastric evacuation data. A represents the average amount of time required to evacuate the average proportion of all meals present in the stomach at any instant in time. For a predator that consumes a variety of prey organisms which are evacuated at different rates:

$$(1)\quad \hat{r} = \sum_{i=0}^{I} \frac{\bar{W}_i}{A_i}$$

where subscripts i refer to each of the I prey types. Daily meal is calculated by multiplying $\hat{r}$ by 24 h, and daily ration is daily meal expressed as a percent of body mass.

Bioenergetics Model

Energy requirement calculations were based on a separate study by Boggs (1984) wherein mass and energy content of starved yellowfin were compared with controls to estimate metabolic rates following the approach described by Brett (1973). The method of estimating metabolic rates from starved fish can be used to estimate rates in the field by adjusting for mass, length, and speed and by including the increase due to SDA. Brett (1973) and Boggs (1984) did not find that starvation per se reduced metabolic rate in the highly active fishes studied. The lack of postprandial metabolic increment (SDA), reduced activity, and mass loss during starvation does reduce metabolic rate (Beamish 1964; Glass 1968; Jobling 1980a). However, nonfeeding, mass-specific, speed-specific metabolic rates are not reduced by starvation (Jobling 1980a). In Boggs's (1984) experiments the volitional speeds maintained by tuna differed between individuals, and other individuals were forced to swim fast by altering buoyancy and lift (Magnuson 1970, 1973, 1978). The effects of mass, speed, and length on the metabolic rates of 21 yellowfin were used by Boggs (1984) to fit a model for standard metabolism ($\dot{E}_0$, joules per gram per day) plus swimming work ($\dot{E}_V$, joules per gram per day) where

$$(2)\quad \dot{E}_0 = aM^{\beta}$$

$$(3)\quad \dot{E}_V = fV^{\gamma} L^{\delta}$$

where M is wet mass (grams), V is speed (centimetres per second), L is fork length (centimetres), and a, β, f, γ, and δ are empirically determined constants.

Horizontal and vertical movements of four yellowfin were tracked by Carey and Olson (1982) using acoustic telemetry. The vertical vector of the movements was ignored, since calculations indicated that horizontal movements accounted for almost 100% of distance covered. Swimming speeds were grouped in increments of 0.5 body lengths$\cdot$s^{-1}, and the average speed (centimetres per second) and total tracking duration (hours) in each increment were calculated. Then, equation 3 was used to calculate the cost of locomotion ($\dot{E}_V$) for the mean speed in each increment for the four tracked yellowfin.

The sum of locomotory costs at each speed increment was added to standard metabolism ($\dot{E}_0$). Growth rates (grams per day) for eastern Pacific yellowfin of the sizes tracked by Carey and Olson (1982) were calculated based on a size–time relationship determined from recent yellowfin otolith increment counts (A. Wild, pers. comm.) and a previous tetracycline increment validation study (Wild and Foreman 1980). Growth (grams per day) was transformed into joules per day ($\dot{E}_G$) assuming a caloric density of $6.03 \times 10^3\ \mathrm{J \cdot g^{-1}}$ for wild yellowfin (Boggs 1984). Energy losses due to excretion, egestion, and food assimilation were assumed to account for 35% of the energy consumed in food (Kitchell et al. 1978). Thus, total energy requirements (joules per gram per day) were estimated at

$$(4)\quad \frac{\dot{E}_0 + \dot{E}_V + \dot{E}_G}{1 - 0.35}.$$

Cesium Budget

The rate of cesium intake was assumed to balance the rate of cesium loss and to maintain the measured cesium concentration in yellowfin (Mearns et al. 1981) during growth. The rate of loss in yellowfin was assumed to be comparable with the biological half-life of cesium in albacore, *Thunnus alalunga* (Folsom et al. 1967; Young 1970), which is similar to that in other marine fishes (Baptist and Price 1962). A 50% decrease in concentration over 53 d (Folsom et al. 1967) is equivalent to an exponential decline ($\mathrm{Cs_{out}}$) in total cesium content of about 1.3%$\cdot$d^{-1}. Growth (G) was estimated at 0.63% wet mass$\cdot$d^{-1} (=percent cesium content per day) for the average-sized yellowfin measured by Mearns et al. (1981). A reasonable value (0.8) (Isaacs 1972) was assumed for cesium assimilation efficiency. Yellowfin cesium concentration ($\mathrm{Cs_Y}$, micrograms per kilogram wet mass) was several times greater than prey cesium concentration ($\mathrm{Cs_P}$) (Mearns et al. 1981). Thus, food intake (F, percent body mass per day) was calculated as

$$(5)\quad F = \frac{(\mathrm{Cs_{out}} + G)\,\mathrm{Cs_Y}}{(0.8)\mathrm{Cs_P}}.$$

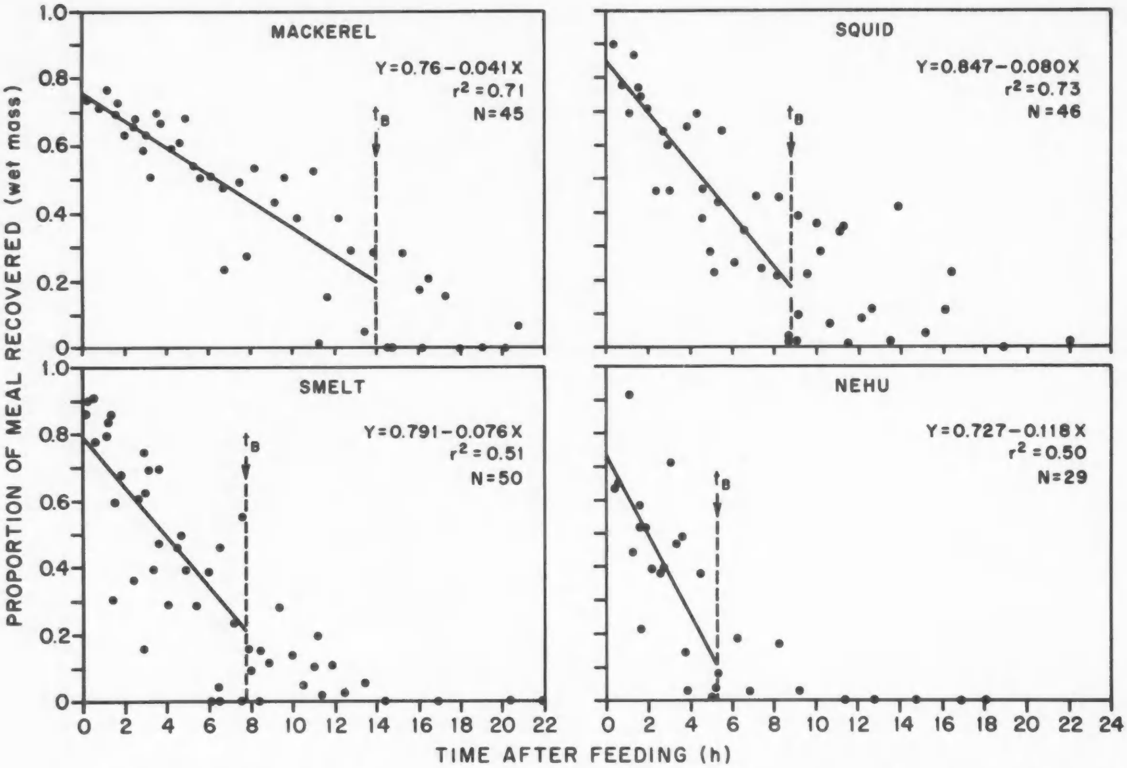

FIG. 2. Proportion of initial wet mass of four experimental foods recovered from the stomachs of captive yellowfin versus time after feeding. T_B is the point beyond which data were omitted prior to curve fitting (see text).

The total cesium concentration in the diet was determined from the values given by Mearns et al. (1981) using the proportions of different prey in the diet of age-class 1 and 2 yellowfin in this study. The cesium concentration of squid was used for cephalopods and other invertebrates and that for frigate tuna (*Auxis thazard*) was used for scombrids. The cesium concentration of flyingfish was used for all other fishes. This latter value was assumed, since these other fishes were generally smaller and thus were probably at a trophic level closer to that of flyingfish than that of frigate tuna.

Results and Discussion

Gastric Evacuation

The experimental yellowfin became satiated after about 30 min of feeding. Mean sizes of the four food organisms and the various combinations in which they were consumed are presented in Tables 1 and 2, respectively. Wet mass of the experimental meals averaged 77.1 g ($N = 69$, $\sigma = 36.4$ g, range = 15.8−164.8 g) and was positively correlated ($r = 0.424$, $P < 0.001$) with predator wet body mass (less food mass in the stomach). Relative meal size averaged 8.53% of wet body mass ($\sigma = 3.88\%$, range = 1.31−18.31%) and was negatively correlated ($r = -0.438$, $P < 0.001$) with wet body mass. Subtracting mean water content per food type (Table 1) resulted in a mean experimental meal of approximately 18.9 g ($\sigma = 8.9$ g, range = 3.8−40.2 g) dry mass.

TABLE 1. Mean size, water content, and lipid content of four experimental foods used in the gastric evacuation experiments (standard deviation in parentheses).

Food species	Mean mass (g)	Mean length (mm)[a]	% water	% lipid Dry mass	% lipid Wet mass	N
Mackerel	62.9	188	73.7	30.7(2.2)	8.1(0.6)	7
Squid	53.2	160[b]	76.8	19.1(1.0)	4.4(0.2)	4
Smelt	17.8	126	76.5	23.6(1.1)	5.5(0.3)	5
Nehu	0.4	40	76.2	18.0(1.2)	4.3(0.3)	4

[a] Fork length.
[b] Length excludes tentacles.

Amounts of the four food types (proportion of initial wet mass) recovered from the yellowfin stomachs as a function of time after feeding are presented in Fig. 2. Prior to curve fitting, the data were truncated at postprandial times marked t_B (Fig. 2) to avoid a serious bias resulting from distributions constricted by the X-axis ($Y = 0$) (Olson and Mullen 1986). For data with variance comparable with that of Fig. 2, Olson and Mullen (1986) found, using Monte Carlo simulations, that data constriction causes the slope to be biased by about 18% ± 9% (mean ± 1 SD). This can cause the illusion of a tail (reduced slope) at later stages of digestion, which may partly explain why curvilinear functions are commonly used with this type of

TABLE 2. Mixed meal combinations of mackerel (M), squid (Sq), smelt (Sm), and nehu (N) ingested by the experimental yellowfin. Individual food particles were numbered, weighed, and fed in order to individually color-code tagged yellowfin.

Combination No.	Food species	Number that ate meal combination
—	M	2
—	Sq	2
—	Sm	2
—	N	1
1	M, Sq	10
2	M, Sm	3
3	M, N	4
4	Sq, Sm	10
5	Sq, N	1
6	Sm, N	2
7	M, Sq, Sm	11
8	Sq, Sm, N	6
9	M, Sm, N	9
10	M, Sq, Sm, N	6

data. The only option to circumvent this problem was to omit some data.

Several different mathematical models have been utilized to describe the time course of stomach emptying in fishes, including a linear model (e.g. Swenson and Smith 1973; Jones 1974), an exponential model (e.g. Elliott and Persson 1978), and a square root model (e.g. Jobling 1981a). The four data sets (Fig. 2, $X_i < t_B$) were fitted to these three models. For all four food types, residual mean squares (untransformed) of the three fits were homogeneous (F_{max}-test, $P > 0.05$, Sokal and Rohlf 1969). Therefore, residual analysis was used to evaluate the fits. For all four food species, residual analyses indicated that the linear model gave a superior fit, and these regressions (Fig. 2) were accepted to represent gastric evacuation rates in yellowfin.[3] The data for dry mass recovered from the stomachs also appeared to be linear. For comparison purposes, Olson and Mullen (1986) fitted the complete unedited data sets (less empty stomachs) to the same three functions. Again, residual mean squares failed to indicate a superior fit to any of the functions (F_{max}-test, $P > 0.05$, Sokal and Rohlf 1969). Residual analysis showed that the linear model gave the best fit for three of the four foods. The squid data were best described by the square root function. Although the exponential model is conceptually more satisfying than the linear model, concensus shows that linear gastric evacuation is plausible for piscivorous fishes that eat large prey (Simenstad and Cailliet 1986). Previous work substantiates this (Swenson and Smith 1973; Diana 1979; Adams et al. 1982).

It is noteworthy that the intercepts of the regression lines fall considerably below 100% (Fig. 2). Wet mass of the food in the stomachs a few minutes after feeding was considerably less than the wet mass of food prior to feeding. Magnuson (1969) found the same phenomenon when feeding smelt to skipjack tuna (*Katsuwonus pelamis*). In Magnuson's experiments, an average of 17.3% of the wet mass of smelt was lost from the food within a few minutes after ingestion. In our experiments, 20.9% of the wet mass of smelt was quickly lost. Magnuson theorized that this loss was equal to the mass of water absorbed by the food during the process of thawing in fresh water. In the present experiments, all food items were air-thawed. Nevertheless, the most plausible explanation for this sudden decrease in food mass is water loss, as there were no visible signs of digestive action on the food particles removed from fish killed within a few minutes after eating. Tuna stomachs may rapidly express water from the food, resulting in a rapid initial loss of mass (Fig. 2). Subsequently, food appears to gradually rehydrate with digestive fluids to facilitate mechanical breakdown. Significant positive correlations between percent water in food removed from stomachs and time after feeding were obtained for squid ($P < 0.001$) and nehu ($0.05 > P > 0.02$); correlations were positive but not significant for mackerel and smelt ($0.20 > P > 0.10$).

Factors Affecting Evacuation Rates

The type of prey organism ingested affects significantly the rate at which food is passed from the stomachs of fishes (Windell 1978; Fänge and Grove 1979). In yellowfin, significant differences in evacuation rate occurred among the four food types (ANCOVA, $P < 0.0005$). Mackerel were evacuated at a significantly slower rate than squid, smelt, and nehu (*t*-tests for slopes, $P < 0.01$, Zar 1974), which were evacuated at about equal rates (ANCOVA, $P > 0.25$). However, intercepts of the regression lines for squid, smelt, and nehu were significantly different ($P < 0.0005$), and thus a common regression line was not adequate to describe these three data sets.

The evidence for an effect of meal size on gastric evacuation rate of fishes is equivocal. Large meals may take longer to be totally eliminated from the stomach than small meals (Barrington 1957; Steigenberger and Larkin 1974; Jones 1974). However, the amount of food digested during a given time (grams per hour) may increase in proportion to meal size (Hunt 1960; Kitchell and Windell 1968; see review by Windell 1978). In the latter case, the percentage of the meal evacuated per unit time remains constant, and thus the time required to evacuate a meal remains approximately the same regardless of food volume (Magnuson 1969; Tyler 1970; Elliott 1972; Bagge 1977).

The yellowfin gastric evacuation data for each food type were subdivided into three groups according to relative meal size (below 8.0%, between 8.1 and 11.5%, and above 11.6% of body mass). The results of analyses of covariance performed on the subgroups indicated that relative meal size had a significant effect on the evacuation rate of mackerel ($P < 0.0005$), but not on those of squid, smelt, and nehu. Small meals of mackerel were evacuated significantly faster than medium and large meals of mackerel (*t*-tests for slopes, $P < 0.002$). Therefore, the gastric evacuation rate for mackerel in yellowfin appears to be consistent with the hypothesis of more rapid digestion of small meals, while those for squid, smelt, and nehu seem to follow the alternative hypothesis of a constant percentage per unit time.

Mackerel are larger and appear to be considerably more digestion resistant than the other three food types. The musculature of mackerel is compact, while that of smelt and nehu tends to fall apart in the stomach, providing increased surface area for digestive activity to take place. Squid also have dense musculature; however, the body cavity is more accessible and

---

[3] For calculating daily ration, another equation representing the evacuation rate for mackerel in small meals was used (equation 7). See discussion of the effect of meal size and daily ration based on stomach analysis.

TABLE 3. Observed and adjusted stomach contents (% of body mass) and size characteristics of four age-classes of yellowfin tuna from which stomach samples were taken in the eastern Pacific Ocean. Adjustments for partial stomachs and gear disturbance are described in the text.

Age-class	Fork length (mm)	Body mass (g)			Observed stomach contents			Adjusted stomach contents		
		Min.	Max.	Mean	Min.	Max.	Mean	Min.	Max.	Mean
1	≤550	968	3 255	2 629	0	4.98	0.31	0	5.97	0.39
2	551−865	3 310	13 140	8 603	0	3.31	0.48	0	5.55	0.62
3	866−1220	13 187	37 914	22 655	0	4.64	0.38	0	5.50	0.52
4+	>1220	38 010	95 415	53 411	0	2.99	0.39	0	5.46	0.57

the body wall is thinner than in mackerel. These results suggest that two or more models of gastric evacuation may be applicable in a single predator, depending on prey type.

Body size is recognized as one of the principal factors which can influence gastric motility in fishes (Windell 1978; Fänge and Grove 1979). However, within the size range of yellowfin in this study, analysis of covariance showed that evacuation rates were not significantly influenced by yellowfin size ($P > 0.05$).

Whether foods that are evacuated at distinctly different rates retain their distinct evacuation rates when fed in mixed meals is unknown. Windell (1967) and Elliott (1972) reported that mixed meals of organisms that have similar evacuation rates in bluegill sunfish (*Lepomis macrochirus*) and brown trout (*Salmo trutta*) were evacuated at the same rate as the organisms separately. In the present study, no indication was found to suspect that measuring evacuation rates of food organisms in mixed meals influenced the rate determinations for each food type. For example, evacuation rates (slopes) for mackerel by yellowfin which ate meal combinations 1, 2, 3, 7, 9, and 10 (Table 2) were not significantly different (ANCOVA, $P > 0.05$).

To analyze the effect of cutting some food items into pieces, analysis of covariance was conducted on the data for each food type grouped by whole food specimens, anterior halves, posterior halves, and mixed anterior and posterior halves. Low F-ratios resulted ($P > 0.25$), indicating that the practice of cutting food items did not significantly affect the evacuation rates in these experiments.

Previous workers using prepared foods have demonstrated that low-energy foods are emptied from the stomach more rapidly than foods of high caloric content (Grove et al. 1978; Flowerdew and Grove 1979; Jobling 1981b). Elevated energy levels in natural organisms are commonly related to increased quantities of lipids in the tissues, and the presence of lipids, particularly when in excess of 15% of dry mass (Windell 1978), appears to have a retarding effect on gastric evacuation (Quigley and Meschan 1941; Windell 1967; Fänge and Grove 1979). This is generally attributed to a feedback mechanism, possibly triggered by a hormone similar to enterogastrone in mammals (Hunt and Knox 1968) produced in response to the presence of lipids or the digestive products of lipids in the duodenum (Windell 1967; Hunt 1975; Jobling 1980b).

In yellowfin, gastric evacuation rates (regression coefficients, Fig. 2) were correlated with total lipid content (Table 1) (lipid as percent wet mass: $r = 0.885$, $N = 20$, $P < 0.001$; lipid as percent dry mass: $r = 0.888$, $N = 20$, $P < 0.001$) and calories per gram of wet mass ($r = 0.983$, $N = 20$, $P < 0.001$) of the food. It appears, then, that the relationships between caloric content, total lipid content, and evacuation rate found for prepared foods hold true for the natural food organisms tested here. Thus, the high lipid content of mackerel could explain its slow evacuation rate in yellowfin.

Rapid Evacuation Rates in Tunas

This study provides evidence that yellowfin evacuate food from the stomach faster than most other fishes studied, and at about the same rate as skipjack tuna. Magnuson (1969) found that only 1 of 12 species of carnivorous fishes he reviewed had a higher rate of emptying than skipjack. Yellowfin and skipjack emptied their stomachs of smelt in an average of 10.4 and 12 h (Magnuson 1969), respectively. Other piscivores of similar body length reviewed by Magnuson required four to five times longer than skipjack to evacuate a meal. Experiments by Steigenberger and Larkin (1974) on northern squawfish (*Ptychocheilus oregonensis*) were conducted on fish similar in size to our yellowfin, at the same water temperature, and using fish as experimental food. The squawfish required almost 2 h more to empty their stomachs of 3- to 6-cm juvenile rainbow trout (*Salmo gairdneri*) than it took the yellowfin to evacuate nehu, a comparably sized food.

Tunas are a highly specialized group of fishes that must swim continuously to maintain hydrostatic equilibrium and to ventilate their gills (Magnuson 1973; Roberts 1978). Energy expenditures for both "standard" metabolism (Brill 1979) and the metabolic work required for swimming (Gooding et al. 1981; Graham and Laurs 1982; Boggs 1984) are substantially higher than those typical of most other fishes (e.g. Brett 1972). Yet, yellowfin and skipjack are abundant in tropical seas where primary production is purported to be low (but see Kerr 1983) and the food distributions are known to be patchy (Blackburn 1968). It is advantageous for the tropical tunas to have the ability to process large amounts of food in a short time when food is available. The more rapidly food is digested and evacuated from the stomach, the more food a tuna can acquire from what may be very short-lived aggregations of prey. Any excess energy that is left after meeting metabolic demands is used for growth or stored as body lipids for reproduction and migration (Sharp and Dotson 1977).

Consumption Estimates

Stomach contents and gastric evacuation

Total adjustments of prey mass for partial stomachs and gear disturbance by age-class in the 1970−72 stomach samples amounted to increases of 26−46% of the mean observed stomach contents (Table 3). A relationship between complete empty stomach mass (Y, grams) and yellowfin fork length (X, millimetres) was used to adjust for partial stomachs:

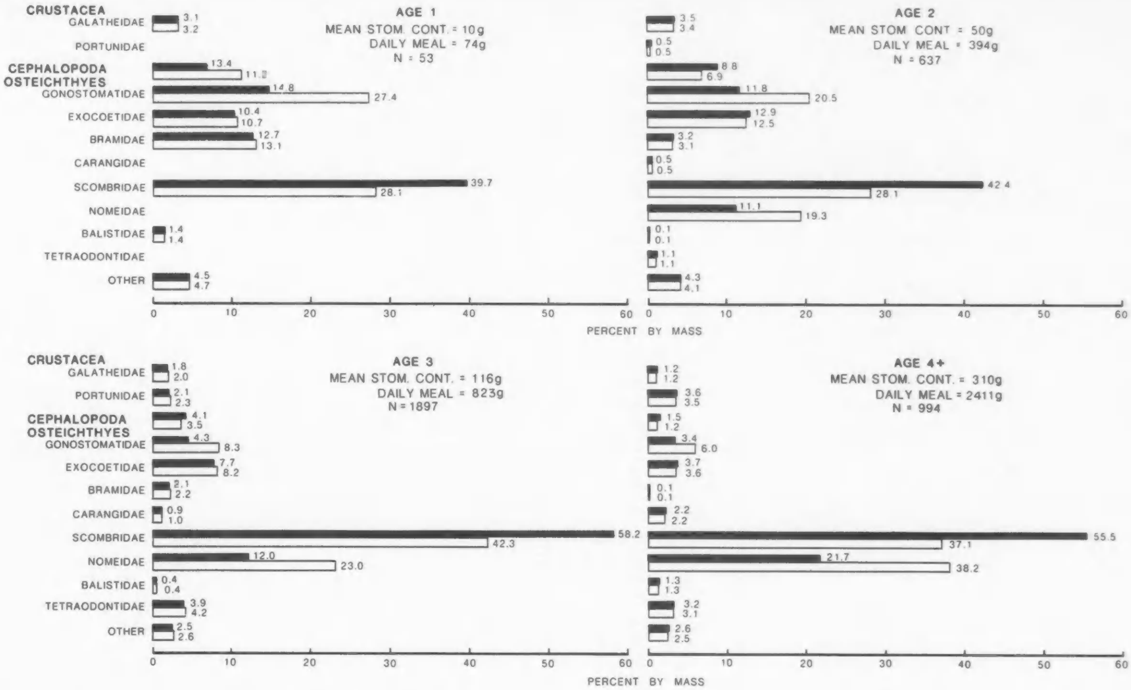

FIG. 3. Percent by mass of adjusted stomach contents (black bars) and of daily meal (white bars) for prey found in yellowfin stomachs sampled during 1970–72.

(6) $\ln Y = -12.61 + 2.59 \ln X \; (r^2 = 0.968).$

The average duration of pursuit and gear enclosure by purse seiners in the early 1970's (2.25 h) and the gastric evacuation functions (Fig. 2) were used to calculate adjustments for reduced stomach contents due to fishing gear disturbance. The effect of this adjustment was to increase ration by about 25%.

Mean adjusted stomach contents pooled ranged between 0.39 and 0.62% and maximum adjusted amounts between 5.46 and 5.97% of wet body mass (Table 3). Yellowfin prey were matched with the most similar food organisms tested in the gastric evacuation experiments (Table 4). We assume that the evacuation functions for mackerel, squid, and nehu in small captive yellowfin approximate those of frigate tunas, cephalopods, and gonostomatids/nomeids, respectively, in wild yellowfin. The mean gastric evacuation rate and intercept for the four experimental food organisms (Table 4) were assumed to approximate those of all other prey in yellowfin stomachs. The error created by application of the mean rate to organisms with chitinous exoskeletons is probably not too important to the total ration estimate because crustaceans represented only 3.1–4.8% by mass of the stomach contents (Fig. 3). Since the stomach contents indicated that small meals are common, and meal size had an effect on the evacuation rate of mackerel, the regression equation (from ANCOVA above) for mackerel in small meals was used to calculate A_i for the Scombridae:

(7) $Y = 0.856 - 0.0693X \; (r^2 = 0.925).$

Estimates of average hourly feeding rate, $\hat{r}$, for eastern Pacific yellowfin were calculated from equation 1 using values for $\overline{W}_i$ and of A_i from data in Fig. 3 and Table 4, respectively. Empty stomachs were included for calculating $\overline{W}_i$, since they, as well as full stomachs, reflect the natural feeding condition of the population. Yellowfin are known to feed in the daytime as well as at night (Watanabe 1958; Kume and Morita 1966). Lacking quantitative evidence for diel differences in feeding rate, we have assumed a daily feeding period of 24 h (steady state), recognizing that under some circumstances, nighttime feeding may decline or not occur, which would reduce ration estimates by as much as 50%. Daily meal, then, is assumed to be $24\hat{r}$. Daily rations are the daily meals expressed as a percent of mean mass of yellowfin sampled in each age-class (Table 3).

TABLE 4. Yellowfin prey categories, corresponding gastric evacuation rates (b_1) and intercepts (b_0) from linear regressions fit to evacuation data for mackerel in small meals[a] (M), squid (Sq), and nehu (N) (Fig. 2), mean b_1 and b_0 of M, Sq, N, and smelt (Sm) regressions, and A's used in the food consumption model (equation 1). A's were calculated as the area (integral) under the evacuation function: $A = |b_0^2/2b_1|$ (hours).

Prey	Experimental food species	Regression values		A
		b_1	b_0	
Scombridae	M	−0.0693[a]	0.856[a]	5.29
Gonostomatidae	N	−0.1182	0.727	2.24
Nomeidae	N	−0.1182	0.727	2.24
Cephalopoda	Sq	−0.0800	0.847	4.48
Others	Mean of M, Sq, Sm, N	−0.0859	0.805	3.77

[a] From equation 7.

The initial reduction of wet mass immediately following ingestion in yellowfin is not accounted for in calculating $\hat{r}$ from equation 1. This phenomenon probably occurs with prey in nature as well as in the laboratory. Thus, in calculating daily rations for yellowfin in the eastern Pacific, $\hat{r}$ values were increased by the difference between 100% and the intercept for each food type (Table 4).

Mean daily rations were 2.8, 4.6, 3.6, and 4.5% of body mass per day for age-classes 1, 2, 3, and 4+, respectively. The expected decrease in daily ration with increased size (Kitchell et al. 1978) was not observed. Perhaps the ration of the smallest age-class was poorly represented through some selectivity in the catch. Although the estimated rations are similar to daily rations calculated for small fishes using field data (Seaburg and Moyle 1964; MacKinnon 1973a, 1973b; Swenson and Smith 1973; Lane 1975; Thorpe 1977; Diana 1979; Lane et al. 1979), they are larger than expected for fish of this size.

The tendency to overestimate ration by the assumption of a 24-h feeding period may be offset due to negatively biased stomach samples. Sampling difficulties and an unknown rate of regurgitation during capture would reduce the apparent food mass in stomach samples. Also, gastric motility presumably ceases at death, but digestion is a chemical process that may continue at a reduced rate until the stomach is frozen (Eggers 1977) and after thawing.

Average daily food consumption by eastern Pacific yellowfin appears to be a small fraction of the maximum possible rate, as evidenced in the laboratory and in the field. Assuming that fish with full stomachs could have continued feeding on the same prey at a rate sufficient to maintain that quantity in the stomachs for 24 h, maximum daily rations would average about 40% of body mass. This is higher, but not double, the maximum rations determined for 1.4-kg skipjack fed small food particles ad libitum for a 12-h daylight period (28−35% of body mass) (Kitchell et al. 1978).

Estimates from bioenergetics

The mass-specific rate of "standard" metabolism in skipjack tuna was found to decrease significantly with increasing mass in spinalectomized skipjack by Brill (1979). This decrease ($\beta = -0.44$, equation 2) was greater than in other fishes. By extrapolating from swimming metabolism to zero speed, Gooding et al. (1981) found that standard metabolism increased significantly with mass ($\beta = 0.19$). No significant effect of mass on standard metabolism (determined by extrapolation) was found by Boggs (1984). These contradictory results may be related to a small range in mass in the latter two studies. The mean value for standard metabolism ($\dot{E}_0$) determined by Boggs (1984) for yellowfin was $38.4\ \mathrm{J \cdot g^{-1} \cdot d^{-1}}$ ($a = 38.4$, $\beta = 0$, equation 2).

Boggs (1984) found that mass-specific swimming metabolism ($\dot{E}_V$) of yellowfin had a length exponent (δ) of -1.28, a speed exponent (γ) of 1.64, and a coefficient (f) of 13.7. The speed exponent (γ) was lower than the 2.5−2.8 predicted by hydrodynamic theory (Wu and Yates 1978) but similar to the exponent (1.9) resulting from reanalysis of data on salmon (Wu and Yates 1978; Boggs 1984). In general, the effect of speed on metabolic rate in fishes (Beamish 1978) is less than that predicted by hydrodynamic theory.

Daily swimming costs (Table 5) calculated using equation 3 accounted for one-third to one-half of the energy budget (Table 6) of the four yellowfin tracked by Carey and Olson (1982). The mean swimming cost (weighted by the duration of each track) amounted to $100\ \mathrm{J \cdot g^{-1} \cdot d^{-1}}$. The most frequently recorded speeds of the four tracked yellowfin were less than $100\ \mathrm{cm \cdot s^{-1}}$ (less than one body length per second for these fish, Table 5), but faster speeds were common, and speeds as high as $300-400\ \mathrm{cm \cdot s^{-1}}$ were maintained for over half an hour. These short times spent at high speeds contributed substantially to the total estimated cost of swimming (Table 5). Daily swimming costs varied by a factor of 4 among the four tracked yellowfin. There was a trend for speeds and locomotory costs to be low in the two fish that were tracked for a full day or longer (Table 5).

Estimates of total energy consumption ranged from 175 to $441\ \mathrm{J \cdot g^{-1} \cdot d^{-1}}$ (Table 6). When total energy requirements were converted into a daily ration using a caloric equivalent of $4.60\ \mathrm{kJ \cdot g}$ wet mass^{-1} for food (Kitchell et al. 1978), the mean ration for 87- to 98-cm yellowfin was equivalent to about 5.2% of wet body mass per day. This was about 1.1−1.4 times the estimates from stomach contents and gastric evacuation rates for similarly sized yellowfin (age-classes 2 and 3). This suggests that the energy requirements we estimated were reasonable and that extrapolation of the empirical model for swimming costs (equation 3) did not result in values that were unrealistically low.

Sharp and Francis (1976) estimated a mean energy requirement of $319\ \mathrm{J \cdot g^{-1} \cdot d^{-1}}$ for 12.6-kg yellowfin based on a hydrodynamic model for power output and assuming that yellowfin swim at $300\ \mathrm{cm \cdot s^{-1}}$ for 1.2 h per day and at near minimum speeds (Magnuson 1973) the rest of the day. Sharp (1984) used the same hydrodynamic model to estimate an average energy requirement of $232\ \mathrm{J \cdot g^{-1} \cdot d^{-1}}$ for two yellowfin tracked by Carey and Olson (1982). Both of these estimates (Sharp and Francis 1976; Sharp 1984) are within the range of total energy expended estimated using equation 4 (Table 6). Sharp and Francis's (1976) model includes the effects of transition between laminar and turbulent boundary layer conditions. If the velocity exponent does increase radically at Reynold's numbers above about 10^6 (Sharp and Francis 1976), then the values given in Tables 5 and 6 could be underestimates.

Energy can be supplied from stored reserves of fat as well as from food consumption. Thus, bioenergetics estimates of required energy may exceed actual consumption over a short term. Of course, fat reserves are ultimately derived from surplus energy intake, but the feeding conditions that permit such fat storage are probably not represented by the average stomach contents observed in the field. It is clear from our laboratory studies that yellowfin can eat much more than the overall average rates indicate, and it is clear from field studies that fat content in tunas is highly variable and can increase dramatically in certain areas (Dotson 1978; Vlieg et al. 1983). Tuna bioenergetics may be pictured as "speculative" (Stevens and Neill 1978) in the sense that tuna may exhaust their energy reserves in migrating hundreds of kilometres (Sharp and Dotson 1977) to reach good foraging habitats. This gamble must succeed frequently enough to permit rapid rates of growth among survivors, but the gamble must sometimes fail, resulting in energy depletion, disease, and vulnerability to predation. This would help explain the high natural mortality rates of tuna (Murphy and Sakagawa 1977). Depletion of fat reserves during reproduction would increase the potential for severe energy depletion and might explain reports that sex ratios are skewed strongly towards males in very large yellowfin (Cole 1980; Anonymous 1983). Further investigation of fat dynamics could suggest patterns in foraging behavior,

TABLE 5. Speeds and swimming costs of four yellowfin tuna tracked by Carey and Olson (1982). Observed speeds were grouped by 0.5 body lengths (bl)$\cdot$s^{-1} increments. The average speed and the total time spent in each increment were used to calculate swimming costs.

Fish ID No. (fork length)	Speed interval ($\mathrm{bl \cdot s^{-1}}$)	Mean speed ($\mathrm{cm \cdot s^{-1}}$)	Power output ($\mathrm{J \cdot g^{-1} \cdot h^{-1}}$)	Duration (h)	Swimming cost ($\mathrm{J \cdot g^{-1}}$)	Daily swimming cost ($\mathrm{J \cdot g^{-1} \cdot d^{-1}}$)
2	0–0.5	40	0.8	0.4	0.3	
(87 cm)	0.5–1.0	77	2.4	2.1	5.1	
	1.0–1.5	118	4.9	2.0	9.7	
	1.5–2.0	152	7.4	1.5	11.4	
	2.0–2.5	189	10.6	1.4	14.5	
	2.5–3.0	236	15.3	0.7	11.4	
	3.0–3.5			0	0	
	3.5–4.0	274	19.6	0.3	5.9	
	4.0–4.5	377	33.1	0.4	14.3	
	4.5–5.0	396	36.8	0.4	15.5	
			Total	9.3	88.2	228
3	0–0.5	38	0.7	4.9	3.9	
(89 cm)	0.5–1.0	67	1.9	19.4	36.1	
	1.0–1.5	115	4.6	11.1	50.6	
	1.5–2.0	150	7.1	9.8	69.6	
	2.0–2.5	186	10.1	0.7	7.0	
	2.5–3.5			0	0	
	3.5–4.0	316	24.0	0.2	4.0	
			Total	46.1	170.9	89
4	0–0.5	34	0.6	2.1	1.1	
(98 cm)	0.5–1.0	70	1.8	5.9	10.5	
	1.0–1.5	120	4.3	4.9	21.1	
	1.5–2.0			0	0	
	2.0–2.5	219	11.6	1.4	16.8	
	2.5–3.0	294	18.8	0.5	10.0	
	3.0–3.5	295	19.0	0.2	3.5	
	3.5–4.0	370	27.5	0.5	14.2	
			Total	15.5	77.3	120
5	0–0.5	31	0.5	11.2	5.4	
(96 cm)	0.5–1.0	66	1.6	7.2	11.8	
	1.0–1.5	117	4.3	3.6	15.4	
	1.5–2.0	177	8.4	0.7	6.2	
	2.0–2.5	214	11.5	0.3	3.5	
	2.5–3.5			0	0	
	3.5–4.0	354	26.3	0.6	14.5	
			Total	23.6	56.7	58
			Grand total	94.5	393	

energy utilization, and movements of tunas.

An estimate from cesium concentrations

The proportions of food in the diet (stomach contents adjusted for differential rates of gastric evacuation) of age-class 1 and 2 yellowfin (white bars, Fig. 3) were used to represent those of a typical yellowfin in the size range used by Mearns et al. (1981) in their measurements of cesium concentrations. Thus, approximately 28% of the diet (by wet mass) was frigate tunas and other scombrids, 12% was squid and other invertebrates, 12% was flyingfish, and 48% was other fishes (34% gonostomatids and nomeids). Assigning these proportions (Materials and Methods) to the cesium concentrations of prey given by Mearns et al. (1981) resulted in an estimate of total dietary cesium concentration (Cs_P) of about 21.8 μg$\cdot$wet kg food^{-1}. Yellowfin cesium concentration (Cs_Y) was given as 60.5 μg$\cdot$wet kg^{-1}. Thus, from equation 5 the estimated daily ration is 6.7% of body mass per day. This is 2.4 and 1.5 times higher than the estimates from gastric evacuation rates and stomach contents for yellowfin of similar size (age-classes 1 and 2, respectively). The greatest difference is due to the anomalous low ration estimate from stomach contents of age-class 1. The cesium budget estimate is 29% higher than the ration estimate from energy requirements (mean ration, Table 6). The cesium estimate was made for smaller fish than the bioenergetics model estimate, and a larger ration is expected in smaller yellowfin (Kitchell et al. 1978).

The data on cesium concentrations were limited, and the assumptions required to translate these into a ration are crude. This approach may be the least accurate of the three. However, the consistency of results from the cesium approach and the bioenergetics approach implies that stomach analysis under-

TABLE 6. Daily ration estimates (% body mass $\cdot$ d^{-1}) for four yellowfin tuna tracked by Carey and Olson (1982) based on energy expenditures for swimming, standard metabolism, growth, excretion, egestion, and food assimilation.

			Energy expended ($J \cdot g^{-1} \cdot d^{-1}$)					
Fish ID No.	Fork length (cm)	Mass (kg)	Swimming cost (Table 5)	Standard metabolism ($\dot{E}_0$)	Growth ($\dot{E}_G$)	Excretion, egestion, and assimilation	Total consumed	Ration ($\% \cdot d^{-1}$)
2	87	13.4	228	38	21	155	441	9.6
3	89	14.3	89	38	20	79	226	4.9
4	98	19.3	120	38	18	95	270	5.9
5	96	18.1	58	38	18	62	175	3.8
Mean			100[a]	38	19		241[b]	5.2[c]

[a] Weighted mean from grand total in Table 5.

[b] From equation 4 using weighted mean swimming costs of 100 $J \cdot g^{-1} \cdot d^{-1}$.

[c] Based on total of 241 $J \cdot g^{-1} \cdot d^{-1}$.

estimates the true amount of food in stomachs of yellowfin at sea, especially in smaller fish. For comparable age-classes, the bioenergetics estimate (5.2%) averaged 1.3 times higher (ages 2 and 3) and the cesium estimate (6.7%) averaged 1.8 times higher (ages 1 and 2) than the direct estimates from stomach contents and gastric evacuation rates. Together, the indirect estimates averaged 1.5 times the results from the direct method.

Apex Predation and Trophic Relations

It is difficult to estimate biomass or production at intermediate trophic levels in pelagic marine ecosystems by direct sampling. As an alternative, bioenergetics models combined with estimates of apex predator biomass from fisheries statistics, tag and recapture studies, or surveys can be used to estimate the rate of prey production required to balance consumption by predators (Laevastu and Larkins 1981; Polovina 1984). This trophic approach can be extended down through the food web to estimate production and biomass at lower levels. The trophic model inputs are predation rates determined from studies like this one, and turnover rates determined from studies of age structure (Allen 1971) and natural mortality (Pauly 1980) or from other estimates of annual production to annual mean biomass (P/B) ratio (Banse and Mosher 1980; Adams et al. 1983; Longhurst 1983; Polovina 1984).

Total predation by yellowfin in the eastern tropical Pacific depends on the number of yellowfin in that region. Cohort analysis has been used to estimate the size of the exploited yellowfin population (Anonymous 1983) in the regulated area shown in Fig. 1. The average of estimates for 1970–72 is 4×10^7 individuals (3×10^8 kg). This population was subdivided among the four age-classes used to stratify the stomach contents data (Table 3) according to average size composition of the catch (Anonymous 1983, p. 87). Dividing the numbers and biomass of yellowfin in each age-class by the area of the regulated fishery (Sharp and Francis 1976) (Fig. 1) results in estimates of yellowfin density (Fig. 4).

Predation rates on each prey type can be estimated from their proportion in the diet. Proportions of prey in the stomach contents (black bars, Fig. 3) do not adequately represent relative biomass of prey types consumed due to differential rates of digestion and gastric evacuation (Hess and Rainwater 1939; Macdonald et al. 1982). Although Persson (1984) recommended otherwise, stomach contents were adjusted for differential rates of gastric evacuation (white bars, Fig. 3). This adjustment substantially reduced the proportion of Scombridae in the diet compared with the proportion found in stomach samples. Nevertheless, in the offshore areas (Fig. 1), scombrids (almost entirely frigate tunas, *Auxis* spp.) were the most important prey by mass in all age-classes except 4+. Small epipelagic and mesopelagic fishes, Nomeidae (mostly *Cubiceps pauciradiatus*), and Gonostomatidae (mostly *Vinciguerria lucetia*), respectively, were either first, second, or third most important prey by mass in the diet of each age-class. Exocoetidae (flyingfish) and cephalopods (mostly squids) were also important by mass. The food habits of yellowfin inhabiting inshore and island areas differ from this pattern (King and Ikehara 1956; Alverson 1963).

Total annual predation by the yellowfin population was divided into predation on each major prey type using the adjusted proportions in the diet (Fig. 4). Assuming that a long-term equilibrium exists, the energy passed from prey trophic levels to the predators represents production rather than a decline in standing stock of prey. Under this assumption, predation rates of yellowfin tuna represent minimum rates of production, and in many cases, the only estimates of production for these pelagic animals. Actual predation rates may be about 1–1.5 times higher than these estimates, since the consumption estimates based on energy requirements and cesium concentrations were about 1.5 times the consumption estimates based on stomach contents. This range (1–1.5 times) is incorporated in the following estimates.

The annual production of frigate tunas in the regulated fishing area (Fig. 1) during 1970–72 must have amounted to at least 1.4–2.1 million metric tons (t). This amount was calculated by multiplying the predation rate on Scombridae (Fig. 4) by the area of the regulated fishing region (Fig. 1) and the range in the ration estimates (1–1.5 times). This production is more than the average annual world catch of all tunas during those years (1.2 million t, FAO 1974). It amounts to about 11–17 times the average biomass of yellowfin caught in this area annually during those years (Anonymous 1983). Frigate tunas are important prey of other apex predators that inhabit the region (Uchida 1981), so these figures underestimate total production of frigate tunas. Possible interaction between frigate tunas and young stages of other tunas could have important implications on the tuna stocks. If frigate tunas prey on larval or postlarval yellowfin, then increasing the commercial harvest of yellowfin, resulting in larger standing stocks

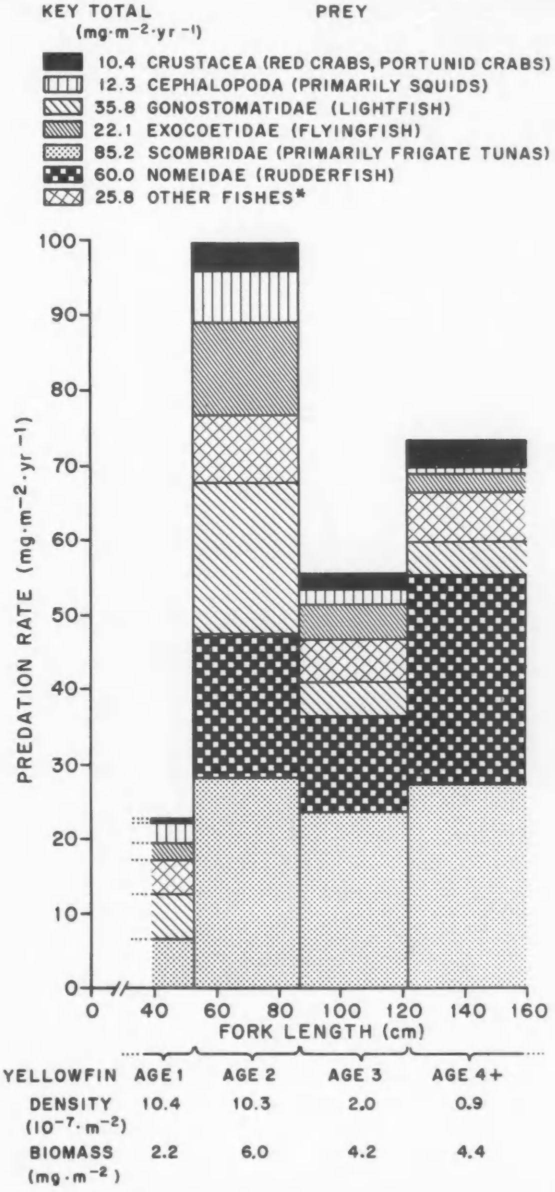

FIG. 4. Total prey biomass ($mg \cdot m^{-2}$) consumed per year by the yellowfin population in the eastern tropical Pacific Ocean in 1970–72 based on stomach contents and gastric evacuation rates. Yellowfin density and biomass are given at the bottom for each age-class. *The "other fishes" category was composed primarily of Bramidae, Carangidae, Balistidae, and Tetraodontidae.

of yellowfin prey, might have a deleterious effect on yellowfin recruitment. Previous to this study there were no estimates of standing stock or production for the frigate tunas. These species are largely unexploited in the eastern tropical Pacific.

Turnover rates for frigate tunas can be approximated using an equation relating the P/B ratio to body mass (Banse and Mosher 1980) and from the natural mortality rate ($P/B = M$, Allen 1971). Average mass at maturity (400 g) and von Bertalanffy growth parameters ($L_\infty = 53$ cm, $K = 0.4$) were estimated from the sparse data summarized by Uchida (1981). The body mass relationship implies an annual P/B ratio of 0.5, but Banse and Mosher's (1980) equation was derived from data on small, temperate fishes. Empirical relationships between P/B ratios and body mass should be interpreted cautiously (McLaren and Corkett 1984). Longhurst (1983) discussed the reasons for larger P/B ratios for marine fishes in the tropics. Pauly's (1980) formula for natural mortality (M) as a function of L_∞, K, and mean environmental temperature (25°C) suggests a P/B ratio of 0.8 for frigate tunas. Fishing mortality (F) in the eastern tropical Pacific is negligable (Anonymous 1983). Based on our production estimate, this would indicate a standing stock of at least 1.7–2.6 million t of frigate tunas in the regulated fishing area (Fig. 1).

The turnover rate for the yellowfin tuna population can be approximated as the total mortality rate ($P/B = Z = M + F$). Fishing mortality averaged 0.44 during 1970–72, and natural mortality was estimated at 0.8 (Anonymous 1983). Thus, P/B was about $1.2 \cdot yr^{-1}$. In contrast, Banse and Mosher's (1980) equation gives an estimate of only 0.2 for an average mass at maturity of 30 kg (Cole 1980). Some estimates for tropical marine fishes range as high as 3.4–4.5 (Longhurst 1983). The P/B for skipjack tuna in the Pacific Ocean is about 5.3 at MSY (R. F. Francis, National Marine Fisheries Service, Northwest and Alaska Fisheries Center, 2725 Montlake Blvd East, Seattle,WA 98112, pers. comm.).

High P/B ratios could result from an abundant food supply, a high trophic transfer efficiency, or both. Using our estimate of food consumption by yellowfin tuna, we can proceed to make a direct estimate of gross conversion efficiency and trophic transfer efficiency. The average food consumption for an individual yellowfin tuna estimated from bioenergetics was $241\ J \cdot g^{-1} \cdot d^{-1}$ whereas growth was estimated at only $19\ J \cdot g^{-1} \cdot d^{-1}$ (Table 6), indicating a gross conversion efficiency of only 8%. Annual yellowfin production was about 1.2 times the standing stock of yellowfin whereas annual consumption by yellowfin was estimated at 15–22 times the standing stock of yellowfin (Fig. 4), indicating a trophic transfer efficiency of only 8–5%. These efficiencies seem low compared with those in more productive ecosystems (Kozlovsky 1968; Adams et al. 1983; Longhurst 1983; Polovina 1984).

The availability of food is difficult to address without a more complete trophic analysis. Primary production and standing stocks of phytoplankton, zooplankton, crustacean micronekton, and fish–cephalopod micronekton in the eastern tropical Pacific were measured by the EASTROPAC oceanographic expedition (Owen and Zeitzschel 1970; Blackburn et al. 1970). These studies examined areal and seasonal variations over a year (1967–68) in a comprehensive survey of a magnitude that is unlikely to be repeated. They found that the average standing stock of fish–cephalopod micronekton in the western region (Fig. 1) was about $3\ mL \cdot m^{-2}$ or about $3\ g \cdot m^{-2}$ for a 200-m water column (Blackburn et al. 1970). This is only twice as much as would be consumed annually by the estimated standing stock of frigate tunas if they ate 4% of their body mass per day.

Only 2.8% or $0.08\ g \cdot m^{-2}$ of the fish–cephalopod standing stock measured by Blackburn et al. (1970) consisted of epipelagic fishes whereas 90% ($0.23–0.35\ g \cdot m^{-2} \cdot yr^{-1}$) of predation by yellowfin in the offshore regions (Fig. 1) was on epipelagic fishes, predominantly frigate tunas, nomeids, and exocoetids (Fig. 4). These estimates are not strictly comparable, since some of the prey consumed by yellowfin were larger than micronekton (1 − 10 cm), but they suggest some degree of scarcity and/or a high annual turnover rate for the epipelagic forage fishes.

Sharp and Francis (1976) estimated that daily consumption by the yellowfin population was small compared with the standing stocks measured by Blackburn et al. (1970). They considered the relative effective productivity at different size-related trophic levels as well as the underestimation of the standing stocks of the more mobile tuna forage species, and argued that yellowfin with fork length greater than 40 cm were not food limited. Of course, the forage available to yellowfin should be based on the productivity of their forage rather than standing stock, but Sharp and Francis were not confident that the available information from the EASTROPAC files was adequate regarding the standing stock figures beyond an absolute minimum estimation (G. D. Sharp, P.O. Box 12294, Gainesville, FL 32607, pers. comm.). One should consider that a proportion of the yellowfin forage comprises organisms larger than micronekton, and these prey would be less abundant and less productive than the micronekton. Also, the importance of foraging by other apex predators must be considered.

The population of four dolphin species (*Stenella* spp. and *Delphinus delphis*) is estimated at 7−8 million individuals (R. S. Holt, National Marine Fisheries Service, Southwest Fisheries Center, P.O. Box 271, La Jolla, CA 92038, pers. comm.), and the food consumption of the spotted dolphin (*S. attenuata*) population (3.1−3.5 million individuals) is estimated to be roughly equivalent to that of the yellowfin population (E. F. Vetter, National Marine Fisheries Service, Southwest Fisheries Center, P.O. Box 271, La Jolla, CA 92038, pers. comm.). Thus, food consumption by all four dolphin species could amount to 2 times that of the yellowfin population. Dolphins consume many of the same types of prey as yellowfin (Perrin et al. 1973). We estimate prey consumption by yellowfin to represent less than 33% $(100\% \times (1/(1 + 2)))$ of the apex predation in this community. The predation rates of other tuna species, billfishes (Istiophoridae and Xiphiidae), dolphinfish (Coryphaenidae), sharks, and seabirds require further investigation before concluding that the food supply is more than adequate.

Conclusions and Implications

The estimates of daily ration for yellowfin tuna derived from the bioenergetics model and tracking study were median among the three independent estimates, lending validity to the use of such models in trophic analyses. The differences between our direct and indirect estimates imply that ration estimates derived from gastric evacuation rates and stomach contents data were too low or that the bioenergetics and cesium budget estimates were too high. The possibility that the bioenergetics model overestimates tuna energy requirements deserves consideration. Metabolic rates of tunas are reported to be 2−3 times higher than in other active fishes swimming at similar speeds (Gooding et al. 1981; Stevens and Dizon 1982; Boggs 1984). Perhaps these findings are due to some bias in the measurement of tuna metabolic rates (due to capture stress, confinement, handling, poor nutrition, starvation, etc.). The independent estimate of energy requirements from stomach contents and gastric evacuation rates indicates that the bioenergetics model could be positively biased by about 30%. This is not enough to account for the major difference between tunas and equally active, cold-bodied fishes. In contrast, the other independent estimate (from cesium concentrations) suggests that the bioenergetics model is not positively biased.

Ration estimates for dominant apex predators and estimates of trophic transfer efficiency are the raw materials required for "top-down" trophic models that can provide estimates of production and biomass for animals at lower trophic levels. Our independent estimates of ration varied above and below the bioenergetics estimate by less than 30%. Direct sampling of forage biomass at sea may be much less precise than estimates based on the "top-down" approach. Direct standing stock estimates such as those of Blackburn et al. (1970) are hampered by gear inadequacies, time limitations, and increasing costs of ship time. Increased understanding of patchy distributions (Fasham 1978; Wormuth and Roper 1983), gear avoidance, and gear selectivity (Kashkin and Parin 1983; Pearcy 1983) suggests that the estimates of Blackburn et al. (1970) may be least accurate for the highly mobile types of prey consumed by yellowfin. Direct sampling must be repetitive to provide more than point estimates whereas trophic models can be dynamic and descriptive of changes at lower levels as a function of the bioenergetics and food habits of the apex predators (Laevastu and Larkins 1981; Stewart et al. 1981). Major apex predators are much more effective than research vessels as samplers of production at intermediate trophic levels.

The "top-down" trophic approach in our study reveals a huge unexploited resource in the form of the frigate tunas in the eastern tropical Pacific. The relationship between frigate tuna production and yellowfin tuna production requires further examination. A more complete trophic analysis could indicate the presence or absence of a food surplus for yellowfin tuna. Such a model will require inputs for the other predators. If adequate estimates for the prey are also found, the analysis can be extended down to the level of primary production and compared with independent estimates, which was done by Adams et al. (1983), Longhurst (1983), and Polovina (1984). At present, there is no compelling evidence for or against food limitation of yellowfin tuna.

The low trophic transfer efficiency between ingestion and production by yellowfin in contrast with their high growth rate, mortality rate, and production to biomass ratio suggests a trophic structure that differs from that of more productive ecosystems. A high production to biomass ratio could be maintained without a high transfer efficiency as long as the ratio between the production of forage and the standing stock of predators is large. In this situation the predator population puts a higher proportion of energy into turnover and maintains a smaller standing stock. This may be characteristic of many tropical pelagic predators that grow rapidly in spite of high metabolic rates in an oligotrophic habitat.

Acknowledgments

Numerous people deserve credit for the success of these investigations. James Joseph, Inter-American Tropical Tuna Commission, and James Kitchell, University of Wisconsin, made this work possible. We sincerely thank the National Marine Fisheries Service, Izadore Barrett, and Richard Shomura for providing us the unique opportunity of working with live tunas at the Kewalo Research Facility (KRF), Honolulu, Hawaii. Valuable expertise was provided by Andrew Dizon, Richard Brill, Randy Chang, Martina Queenth, and Tom Kazama of the KRF. For assistance and advice, we are indebted to Marshall Adams, Roger Carpenter, Lo-chai Chen, David Farris, Sharon Hendrix, John Hunter, Stuart Innes, Witold Klawe, John Magnuson, Ashley Mullen, Jacinta Olson, Jim Rice, Kurt Schaefer, Michael Scott, Gary Sharp, Paul Smith, Patrick Tomlinson, Michael Walker, and George Yates. Support was provided by the Inter-American Tropical Tuna Commission and the National Science Foundation via grant No. PCM-8013473.

References

ADAMS, S. M., B. L. KIMMEL, AND G. R. PLOSKEY. 1983. Sources of organic matter for reservoir fish production: a trophic–dynamic analysis. Can. J. Fish. Aquat. Sci. 40: 1480–1495.

ADAMS, S. M., R. B. MCLEAN, AND M. M. HUFFMAN. 1982. Structuring of a predator population through temperature-mediated effects on prey availability. Can. J. Fish. Aquat. Sci. 39: 1175–1184.

ALLEN, K. R. 1971. Relation between production and biomass. J. Fish. Res. Board Can. 28: 1573–1581.

ALVERSON, F. G. 1963. The food of yellowfin and skipjack tunas in the eastern tropical Pacific Ocean. Bull. Inter-Am. Trop. Tuna Comm. 7: 293–396. (In English and Spanish)

ANONYMOUS. 1983. Annual report of the Inter-American Tropical Tuna Commission, 1982. Inter-American Tropical Tuna Commission, La Jolla, CA. 294 p. (In English and Spanish)

1984. Annual report of the Inter-American Tropical Tuna Commission, 1983. Inter-American Tropical Tuna Commission, La Jolla, CA. 272 p. (In English and Spanish)

BAGGE, O. 1977. Meal size and digestion in cod (*Gadus morhua* L.) and sea scorpion (*Myoxocephalus scorpius* L.). Medd. Dan. Fisk. Havunders. N.S. 7: 437–446.

BANSE, K., AND S. MOSHER. 1980. Adult body mass and annual production/biomass relationships of field populations. Ecol. Monogr. 50: 355–379.

BAPTIST, J. P., AND T. J. PRICE. 1962. Accumulation and retention of cesium^{137} by marine fishes. Fish. Bull. U.S. 62: 177–187.

BARRINGTON, E. J. W. 1957. The alimentary canal and digestion, p. 109–161. *In* M. E. Brown [ed.] The physiology of fishes. Vol. I. Metabolism. Academic Press, New York, NY.

BARTELL, S. M., J. E. BRECK, R. H. GARDNER, AND A. L. BRENKERT. 1986. Individual parameter perturbation and error analysis of fish bioenergetics models. Can. J. Fish. Aquat. Sci. 43: 160–168.

BEAMISH, F. W. H. 1964. Influence of starvation on standard and routine oxygen consumption. Trans. Am. Fish. Soc. 9: 103–107.

1978. Swimming capacity, p. 101–187. *In* W. S. Hoar and D. J. Randall [ed.] Fish physiology. Vol. VII. Locomotion. Academic Press, New York, NY.

BLACKBURN, M. 1968. Micronekton of the eastern tropical Pacific Ocean: family composition, distribution, abundance, and relations to tuna. Fish. Bull. U.S. 67: 71–115.

BLACKBURN, M., R. M. LAURS, R. W. OWEN, AND B. ZEITZSCHEL. 1970. Seasonal and areal changes in standing stocks of phytoplankton, zooplankton, and micronekton in the eastern tropical Pacific. Mar. Biol. 7: 14–31.

BOGGS, C. H. 1984. Tuna bioenergetics and hydrodynamics. Ph.D. thesis, University of Wisconsin, Madison, WI. 198 p.

BRETT, J. R. 1972. The metabolic demand for oxygen in fish, particularly salmonids, and a comparison with other vertebrates. Resp. Physiol. 14: 151–170.

1973. Energy expenditure of sockeye salmon, *Oncorhynchus nerka*, during sustained performance. J. Fish. Res. Board Can. 30: 1799–1809.

BRILL, R. W. 1979. The effect of body size on the standard metabolic rate of skipjack tuna, *Katsuwonus pelamis*. Fish. Bull. U.S. 77: 494–498.

CAREY, F. G., AND R. J. OLSON. 1982. Sonic tracking experiments with tunas. Int. Comm. Cons. Atl. Tunas, Collect. Vol. Sci. Pap. 17(2): 444–457.

COLE, J. S. 1980. Synopsis of biological data on the yellowfin tuna, *Thunnus albacares* (Bonnaterre, 1788), in the Pacific Ocean, p. 71–150. *In* W. H. Bayliff [ed.] Synopses of biological data on eight species of scombrids. Inter-Am. Trop. Tuna Comm. Spec. Rep. No. 2.

DAVIS, G. E., AND C. E. WARREN. 1971. Estimation of food consumption rates, p. 227–248. *In* W. E. Ricker [ed.] Methods for assessment of fish production in fresh waters. 2nd ed. I.B.P. Handb. No. 3.

DIANA, J. S. 1979. The feeding pattern and daily ration of a top carnivore, the northern pike (*Esox lucius*). Can. J. Zool. 57: 2121–2127.

DIXON, W. J., AND F. J. MASSEY, JR. 1957. Introduction to statistical analysis. McGraw-Hill, New York, NY. 488 p.

DOTSON, R. C. 1978. Fat deposition and utilization in albacore, p. 341–355. *In* G. D. Sharp and A. E. Dizon [ed.] The physiological ecology of tunas. Academic Press, New York, NY.

EGGERS, D. M. 1977. Factors in interpreting data obtained by diel sampling of fish stomachs. J. Fish. Res. Board Can. 34: 290–294.

ELLIOTT, J. M. 1972. Rates of gastric evacuation in brown trout, *Salmo trutta* L. Freshwater Biol. 2: 1–18.

ELLIOTT, J. M., AND L. PERSSON. 1978. The estimation of daily rates of food consumption for fish. J. Anim. Ecol. 47: 977–991.

FÄNGE, R., AND D. GROVE. 1979. Digestion, p. 161–260. *In* W. S. Hoar, D. J. Randall, and J. R. Brett [ed.] Fish physiology, Vol. VIII. Bioenergetics and growth. Academic Press, New York, NY.

FAO. 1974. Yearbook of fishery statistics. Food Agric. Org. U.N. Catches and landings, 1963. Vol. 36: 590 p.

FASHAM, M. J. R. 1978. The statistical and mathematical analysis of plankton patchiness. Annu. Rev. Oceanogr. Mar. Biol. 16: 43–79.

FILLIBEN, J. J. 1975. The probability plot correlation coefficient test for normality. Technometrics 17: 111–117.

FLOWERDEW, M. W., AND D. J. GROVE. 1979. Some observations of the effects of body weight, temperature, meal size and quality on gastric emptying time in the turbot, *Scophthalmus maximus* (L.) using radiography. J. Fish Biol. 14: 229–238.

FOLSOM, T. R., D. R. YOUNG, AND C. SREEKUMARAN. 1967. An estimate of the response rate of albacore to cesium, p. 337–345. *In* D. J. Nelson and F. C. Evans [ed.] Symposium on radioecology. Proc. Second Natl. Symp., Ann Arbor, MI.

GLASS, N. R. 1968. The effect of time of food deprivation on the routine oxygen consumption of largemouth black bass (*Micropterus salmoides*). Ecology 49: 340–343.

GOODING, R. M., W. H. NEILL, AND A. E. DIZON. 1981. Respiration rates and low-oxygen tolerance limits in skipjack tuna, *Katsuwonus pelamis*. Fish. Bull. U.S. 79: 31–48.

GRAHAM, J. B., AND R. M. LAURS. 1982. Metabolic rate of the albacore tuna *Thunnus alalunga*. Mar. Biol. 72: 1–6.

GROVE, D. J., L. G. LOIZIDES, AND J. NOTT. 1978. Satiation amount, frequency of feeding and gastric emptying rate in *Salmo gairdneri*. J. Fish Biol. 12: 507–516.

HESS, A. D., AND J. H. RAINWATER. 1939. A method for measuring the food preference of trout. Copeia 3: 154–157.

HUNT, B. P. 1960. Digestion rate and food consumption of Florida gar, warmouth, and largemouth bass. Trans. Am. Fish. Soc. 89: 206–211.

HUNT, J. N. 1975. Interactions of the duodenal receptors which control gastric emptying. Scand. J. Gastroenterol. 10(Suppl. 35): 9–21.

HUNT, J. N., AND M. T. KNOX. 1968. Regulation of gastric emptying, p. 1917–1935. *In* C. F. Code [ed.] Handbook of physiology. Sect. 6, Vol. 4. American Physiological Society, Washington, DC.

ISAACS, J. D. 1972. Unstructured marine food webs and "pollutant analogues." Fish. Bull. U.S. 70: 1053–1059.

JOBLING, M. 1980a. Effects of starvation on proximate chemical composition and energy utilization of plaice, *Pleuronectes platessa* L. J. Fish Biol. 17: 325–334.

1980b. Gastric evacuation in plaice, *Pleuronectes platessa* L.: effects of dietary energy level and food composition. J. Fish Biol. 17: 187–196.

1981a. Mathematical models of gastric emptying and the estimation of daily rates of food consumption of fish. J. Fish Biol. 19: 245–257.

1981b. Dietary digestibility and the influence of food components on gastric evacuation in plaice, *Pleuronectes platessa* L. J. Fish Biol. 19: 29–36.

JONES, R. 1974. The rate of elimination of food from the stomachs of haddock *Melanogrammus aeglefinus*, cod *Gadus morhua* and whiting *Merlangius merlangus*. J. Cons. Int. Explor. Mer 35: 225–243.

JOSLYN, M. A. 1950. Methods in food analysis applied to plant products. Academic Press, New York, NY. 525 p.

KASHKIN, N. I., AND N. V. PARIN. 1983. Quantitative assessment of micronektonic fishes by nonclosing gear (a review). Biol. Oceanogr. 2: 263–287.

KERR, R. A. 1983. Are the ocean's deserts blooming? Science (Wash., DC) 220: 397–398.

KING, J. E., AND I. I. IKEHARA. 1956. Comparative study of food of bigeye and yellowfin tuna in the central Pacific. Fish. Bull. U.S. 57: 61–85.

KITCHELL, J. F. 1983. Energetics, p. 312–379. *In* P. Webb and D. Weihs [ed.] Fish biomechanics. Praeger Publications, New York, NY.

KITCHELL, J. F., W. H. NEILL, A. E. DIZON, AND J. J. MAGNUSON. 1978. Bioenergetic spectra of skipjack and yellowfin tunas, p. 357–368. *In* G. D. Sharp and A. E. Dizon [ed.] The physiological ecology of tunas. Academic Press, New York, NY.

Kitchell, J. F., and J. T. Windell. 1968. Rate of gastric digestion in pumpkinseed sunfish, *Lepomis gibbosus*. Trans. Am. Fish. Soc. 97: 489–492.

Kozlovsky, D. G. 1968. A critical evaluation of the trophic level concept. I. Ecological efficiencies. Ecology 49: 48–60.

Kume, S., and Y. Morita. 1966. Ecological studies of bigeye tuna: III. On bigeye tuna, *Thunnus obesus*, caught by "nighttime longline" in the north Pacific Ocean. Rep. Nankai Reg.Fish. Res. Lab. 24: 21–30. (In Japanese; English summary)

Laevastu, T., and H. A. Larkins. 1981. Marine fisheries ecosystem: its quantitative evaluation and management. Fishing News Books, Farnham, Surrey, England. 162 p.

Lane, E. D. 1975. Quantitative aspects of the life history of the diamond turbot, *Hypsopsetta gluttulata* (Girard), in Anaheim Bay, p. 153–173. *In* E. D. Lane and C. W. Hill [ed.] The marine resources of Anaheim Bay. Calif. Dep. Fish Game Fish Bull. 165: 153–173.

Lane, E. D., M. C. S. Kingsley, and D. E. Thornton. 1979. Daily feeding and food conversion efficiency of the diamond turbot: an analysis based on field data. Trans. Am. Fish. Soc. 108: 530–535.

Longhurst, A. 1983. Benthic–pelagic coupling and export of organic carbon from a tropical Atlantic continental shelf — Sierra Leone. Estuarine Coastal Shelf Sci. 17: 261–285.

Macdonald, J. S., K. G. Waiwood, and R. H. Green. 1982. Rates of digestion of different prey in Atlantic cod (*Gadus morhua*), ocean pout (*Macrozoarces americanus*), winter flounder (*Pseudopleuronectes americanus*), and American plaice (*Hippoglossoides platessoides*). Can. J. Fish. Aquat. Sci. 39: 651–659.

MacKinnon, J. C. 1973a. Analysis of energy flow and production in an unexploited marine flatfish population. J. Fish. Res. Board Can. 30: 1717–1728.

1973b. Metabolism and its relationship with growth rate of American plaice, *Hippoglossoides platessoides* Fabr. J. Exp. Mar. Biol. Ecol. 11: 297–310.

Magnuson, J. J. 1969. Digestion and food consumption by skipjack tuna (*Katsuwonus pelamis*). Trans. Am. Fish. Soc. 98: 379–392.

1970. Hydrostatic equilibrium of *Euthynnus affinis*, a pelagic teleost without a gas bladder. Copeia 1970: 56–85.

1973. Comparative study of adaptations for continuous swimming and hydrostatic equilibrium of scombroid and xiphoid fishes. Fish. Bull. U.S. 71: 337–356.

1978. Locomotion by scombrid fishes: hydromechanics, morphology, and behavior, p. 239–313. *In* W. S. Hoar and D. J. Randall [ed.] Fish physiology. Vol. VII. Locomotion. Academic Press, New York, NY.

Magnuson, J. J., and J. G. Heitz. 1971. Gill raker apparatus and food selectivity among mackerels, tunas, and dolphins. Fish. Bull. U.S. 69: 361–370.

Mann, K. H. 1978. Estimating the food consumption of fish in nature, p. 250–273. *In* S. D. Gerking [ed.] Ecology of freshwater fish production. John Wiley & Sons, New York, NY.

McLaren, I. A., and C. J. Corkett. 1984. Singular, mass-specific P/B ratios cannot be used to estimate copepod production. Can. J. Fish. Aquat. Sci. 41: 828–830.

Mearns, A. J., D. R. Young, R. J. Olson, and H. A. Schafer. 1981. Trophic structure and the cesium–potassium ratio in pelagic food webs. Calif. Coop. Oceanic Fish. Invest. Rep. 22: 99–110.

Murphy, T. C., and G. T. Sakagawa. 1977. A review and evaluation of estimates of natural mortality rates of tunas. Int. Comm. Cons. Atl. Tunas, Collect. Vol. Sci. Pap. 6(1): 117–123.

Nakamura, E. L. 1972. Development and uses of facilities for studying tuna behavior. p. 245–277. *In* H. E. Winn and B. L. Olla [ed.] Behavior of marine animals: current perspectives in research. Vol. 2. Vertebrates. Plenum Press, New York, NY.

Noble, R. L. 1973. Evacuation rates of young yellow perch, *Perca flavescens* (Mitchill). Trans. Am. Fish. Soc. 4: 759–763.

Olson, R. J., and A. J. Mullen. 1986. Recent developments for making gastric evacuation and daily ration determinations. Environ. Biol. Fishes 16: 183–191.

Owen, R. W., and B. Zeitzschel. 1970. Phytoplankton production: seasonal change in the oceanic eastern tropical Pacific. Mar. Biol. 7: 32–36.

Pauly, D. 1980. On the interrelationships between natural mortality, growth parameters and mean environmental temperature in 175 fish stocks. J. Cons. Int. Explor. Mer 39: 195–212.

Pearcy, W. G. 1983. Quantitative assessment of the vertical distributions of micronektonic fishes with opening/closing midwater trawls. Biol. Oceanogr. 2: 289–310.

Perrin, W. F., R. R. Warner, C. H. Fiscus, and D. B. Holts. 1973. Stomach contents of porpoise, *Stenella* spp., and yellowfin tuna, *Thunnus albacares*, in mixed-species aggregations. Fish. Bull. U.S. 71: 1077–1092.

Persson, L. 1984. Food evacuation and models for multiple meals in fishes. Environ. Biol. Fishes 10: 305–309.

Polovina, J. J. 1984. Model of a coral reef ecosystem, Part I: ECOPATH and its application to French Frigate Shoals. Coral Reefs 3: 1–11.

Quigley, J. P., and I. Meschan. 1941. Inhibition of the pyrloric sphincter region by the digestion products of fat. Am. J. Physiol. 134: 803–807.

Rice, J. A., and P. A. Cochran. 1984. Independent evaluation of a bioenergetics model for largemouth bass. Ecology 65: 732–739.

Roberts, J. R. 1978. Ram gill ventilation in fish, p. 83–88. *In* G. D. Sharp and A. E. Dizon [ed.] The physiological ecology of tunas. Academic Press, New York, NY.

Robson, D. S. 1970. On the relation between feeding rate and stomach content in fishes. Biometrics Unit Mimeo. Ser. BU-328-M, Cornell University, Ithaca, NY.

Seaburg, K. G., and J. B. Moyle. 1964. Feeding habits, digestive rates, and growth of some Minnesota warmwater fishes. Trans. Am. Fish. Soc. 93: 269–285.

Sharp, G. D. 1984. Ecological efficiency and activity metabolism, p. 459–474. *In* M. J. R. Fasham [ed.] Flows of energy and materials in marine ecosystems: theory and practice. NATO Advanced Research Institute, May 13–19, 1982, Carcans, France. Plenum Press, New York, NY.

Sharp, G. D., and R. C. Dotson. 1977. Energy for migration in albacore, *Thunnus alalunga*. Fish. Bull. U.S. 75: 447–450.

Sharp, G. D., and R. C. Francis. 1976. An energetics model for the exploited yellowfin tuna, *Thunnus albacares*, population in the eastern Pacific Ocean. Fish. Bull. U.S. 74: 36–50.

Simenstad, C. A., and G. M. Cailliet. 1986. Contemporary studies of fish feeding: proceedings of GUTSHOP'84. Dev. Environ. Biol. Fishes 7. (In press)

Sokal, R. R., and F. J. Rohlf. 1969. Biometry: the principles and practice of statistics in biological research. W. H. Freeman, San Francisco, CA. 776 p.

Steigenberger, L. W., and P. A. Larkin. 1974. Feeding activity and rates of digestion of northern squawfish (*Ptychocheilus oregonensis*). J. Fish. Res. Board Can. 31: 411–420.

Stevens, E. D., and A. E. Dizon. 1982. Energetics of locomotion in warm-bodied fish. Annu. Rev. Physiol. 44: 121–131.

Stevens, E. D., and W. H. Neill. 1978. Body temperature relations of tunas, especially skipjack, p. 315–359. *In* W. S. Hoar and D. J. Randall [ed.] Fish physiology. Vol. VII. Locomotion. Academic Press, New York, NY.

Stewart, D. J., J. F. Kitchell, and L. B. Crowder. 1981. Forage fishes and their salmonid predators in Lake Michigan. Trans. Am. Fish. Soc. 110: 751–763.

Swenson, W. A., and L. L. Smith, Jr. 1973. Gastric digestion, food consumption, feeding periodicity, and food conversion efficiency in walleye (*Stizostedion vitreum vitreum*). J. Fish. Res. Board Can. 30: 1327–1336.

Thorpe, J. E. 1977. Daily ration of adult perch, *Perca fluviatilis* L. during summer in Loch Leven, Scotland. J. Fish Biol. 11: 55–68.

Tyler, A. V. 1970. Rates of gastric emptying in young cod. J. Fish. Res. Board Can. 27: 1177–1189.

Uchida, R. N. 1981. Synopsis of biological data on frigate tuna, *Auxis thazard*, and bullet tuna, *A. rochei*. U.S. Dep. Commer. NOAA Tech. Rep. NMFS Circ. 436: 63 p. (FAO Fish. Synop. 124)

Vlieg, P., G. Habib, and G. I. T. Clement. 1983. Proximate composition of skipjack tuna *Katsuwomus pelamis* from New Zealand and New Caledonian waters. N.Z. J. Sci. 26: 243–250.

Watanabe, H. 1958. On the difference of the stomach contents of the yellowfin and bigeye tunas from the western equatorial Pacific. Rep. Nankai Reg. Fish. Res. Lab. 7: 72–81. (In Japanese; English summary)

Wesolowski, G. O. 1976. Multiple regression and analysis of variance: an introduction for computer users in management and economics. John Wiley & Sons, New York, NY. 292 p.

Wild, A., and T. J. Foreman. 1980. The relationship between otolith increments and time for yellowfin and skipjack tuna marked with tetracycline. Bull. Inter-Am. Trop. Tuna Comm. 17: 509–560. (In English and Spanish)

Windell, J. T. 1967. Rates of digestion in fishes, p. 151–173. *In* S. D. Gerking [ed.] The biological basis of freshwater fish production. John Wiley & Sons, New York, NY.

1978. Digestion and the daily ration of fishes, p. 159–183. *In* S. D. Gerking [ed.] Ecology of freshwater fish production. John Wiley & Sons, New York, NY.

WORMUTH, J .H., AND C. F. E. ROPER. 1983. Quantitative sampling of oceanic cephalopods by nets: problems and recommendations. Biol. Oceanogr. 2: 357–377.

WU, T. Y., AND G. T. YATES. 1978. A comparative mechanophysiological study of fish locomotion with implications for tuna-like swimming mode, p. 313–337. *In* G. D. Sharp and A. E. Dizon [ed.] The physiological ecology of tunas. Academic Press, New York, NY.

YOUNG, D. R. 1970. The distribution of cesium, rubidium and potassium in the quasi-marine ecosystem for the Salton Sea. Ph.D. thesis, Scripps Institution of Oceanography, University of California, San Diego, CA. 213 p.

ZAR, J. H. 1974. Biostatistical analysis. Prentice-Hall, Englewood Cliffs, NJ. 620 p.

Application of Dual-Beam Acoustic Survey Techniques to Limnetic Populations of Juvenile Sockeye Salmon (*Oncorhynchus nerka*)

Janusz J. Burczynski

BioSonics, Inc., 4520 Union Bay Place NE, Seattle, WA 98105, USA

and Robert L. Johnson[1]

International Pacific Salmon Fisheries Commission, Cultus Lake, B.C. V0X 1H0

Burczynski, J. J., and R. L. Johnson. 1986. Application of dual-beam acoustic survey techniques to limnetic populations of juvenile sockeye salmon (*Oncorhynchus nerka*). Can. J. Fish. Aquat. Sci. 43: 1776–1788.

Two hydroacoustic surveys of Cultus Lake, British Columbia, were conducted in July 1983 and February 1984 to estimate the size and distribution of the juvenile sockeye salmon (*Oncorhynchus nerka*) population. The surveys demonstrated the application of a combined dual-beam/echo integration technique for obtaining accurate abundance estimates and other quantitative data. The dual-beam system measured in situ the target strengths (and backscattering cross section) of individual fish. For each survey the mean backscattering cross section of the sampled population was used to scale the integrator outputs to absolute fish density and abundance estimates. Based on previously derived empirical formulas, the mean target strengths compared well with the mean lengths of fish captured by trawl. For this monospecies population with a dominant single-size group of fish, the variance in integrator outputs was due almost entirely to the spatial distribution of fish and not to the variance in measured backscattering cross sections. The confidence intervals of biomass estimates depend on autocorrelation between consecutive acoustic samples, which is related to the spatial distribution of the surveyed population. Trawl catches indicated that about 95% of the fish in the lake were juvenile sockeye salmon. Population estimates made by hydroacoustics were consistent with other available biological data.

Deux relevés hydroacoustiques du lac Cultus (Colombie-Britannique) ont été réalisés en juillet 1983 et février 1984 afin d'y estimer la taille et la distribution de la population de saumons rouges (*Oncorhynchus nerka*) juvéniles. Les relevés ont permis de faire la démonstration d'une technique à double faisceau et à intégration des échos pour l'obtention d'estimations précises de l'abondance et d'autres données quantitatives. Le système à double faisceau a permis de mesurer *in situ* les index de réflexion (et l'écho) de poissons distincts. Au cours de chaque relevé, la moyenne de l'écho de la population a été utilisée pour ajuster la sortie de l'intégrateur aux estimations absolues de la densité et de l'abondance des poissons. Sur la base de formules empiriques obtenues antérieurement, les index de réflexion moyens se comparaient bien aux longueurs moyennes des poissons capturés au chalut. Dans le cas de cette population monospécifique à groupe dominant de même taille, la variance des sorties de l'intégrateur s'expliquait presque entièrement par la distribution spatiale des poissons et non par la variance des échos mesurés. Les intervalles de confiance des estimations de biomasse sont fonction de l'autocorrélation des échantillons acoustiques consécutifs qui est elle-même reliée à distribution spatiale de la population examinée. Selon les prises faites par chalutage, environ 95 % des poissons de ce lac étaient des saumons rouges juvéniles. Les estimations de population faites par techniques hydroacoustiques étaient cohérentes avec les autres données biologiques disponibles.

Received September 18, 1985
Accepted May 20, 1986
(J8418)

Reçu le 18 septembre 1985
Accepté le 20 mai 1986

The application of acoustic techniques has become increasingly important in fisheries research and management over the past decade. Echo integration of the output of a single-beam echo sounder has been the most common acoustic technique for assessing the size and distribution of fish populations. The major stumbling block for making absolute estimates by echo integration has been the problem of measuring the average backscattering cross section of fish, σ_{bs}, in situ, or its decibel equivalent, target strength. The dual-beam technique for measuring fish target strengths in situ was first proposed by Ehrenberg (1974) and subsequently by Traynor and Ehrenberg (1979) and Dickie et al. (1983).

Since 1971 the International Pacific Salmon Fisheries Commission has been using a single-beam integrator technique to determine fish abundance, distribution, and relative variability of lake-rearing juvenile sockeye salmon (*Oncorhynchus nerka*) stocks in the Fraser River watershed. The scope of the application of acoustic research has expanded since to include 15 major rearing lakes in the watershed ranging in surface area from 627 to 36 422 ha. This increased scope has motivated investigations into alternative data acquisition and processing methods that would speed data turnaround and provide increased accuracy and precision in the population estimates.

In this paper, we report the results of two surveys using a combined dual-beam/echo integration system to assess the size

---

[1] Present address: Canadian BioSonics, Ltd., P.O. Box 436, Sardis, B.C. V2R 1A7.

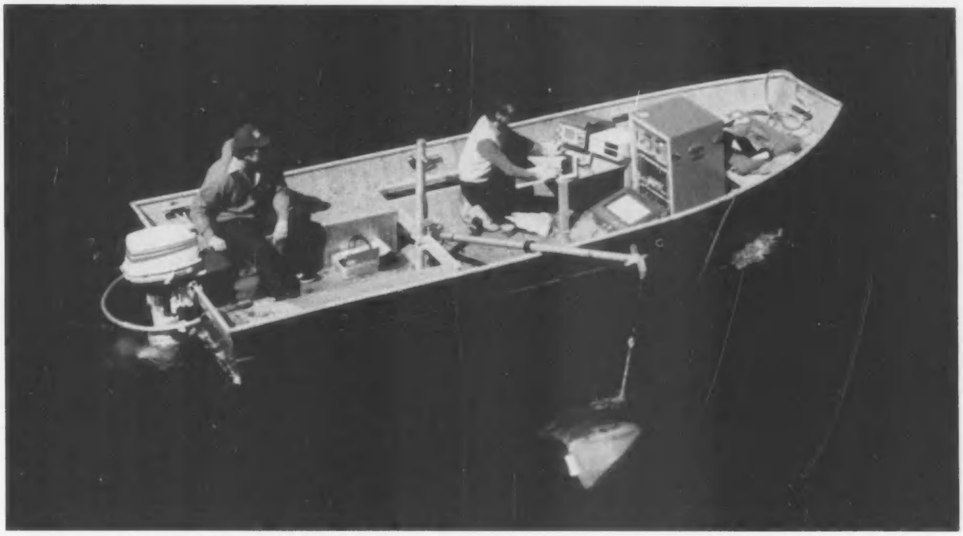

FIG. 1. Hydroacoustic system in a small boat similar to that used for surveys on Cultus Lake. (Photo by J. Stamets)

and distribution of the juvenile sockeye salmon population in Cultus Lake, British Columbia. The study addressed the following objectives: (1) estimation of the abundance of the 1982 brood of juvenile sockeye salmon in Cultus Lake in July 1983 and February 1984; (2) determination of the horizontal and vertical distributions of juvenile sockeye population in the lake; (3) comparison of the size distribution of juvenile sockeye caught by trawl with the distribution of acoustic target strengths determined by the dual-beam system; (4) analysis of the survey data for estimation of the variance and confidence intervals of the population estimates.

Site Description

Cultus Lake is located in the province of British Columbia, Canada, 90 km east of Vancouver and 3 km from the United States − Canada border. It is fed by numerous small streams in a steep drainage basin with the outlet through Sweltzer Creek which flows into the Vedder River and eventually to the Fraser River. Cultus Lake is a small lake of approximately 627 ha surface area and a maximum depth of 42 m. It has steep sides and a relatively flat bottom. Due to the ease of access and a natural run of sockeye salmon, the lake has been the center for numerous studies of the juvenile sockeye population. In recent years it has drawn the attention of various investigators for the purpose of acoustic studies. Nunnallee (1980) described the lake as an ideal site for the study of the application of acoustic assessment techniques to a fish population under natural conditions.

Methods

Survey Design

The first survey was scheduled for July 1983 to assure that the juvenile sockeye had left the littoral areas and moved into the limnetic zone of the lake where their summer feeding habits are well known. The second survey was scheduled for February 1984 when the brood had attained most of its freshwater growth and mortality and was nearing its time for migration to the Pacific Ocean.

It has been observed on echograms in the past that the sockeye generally feed during hours of darkness in midwater and are best distributed for acoustic detection at this time. During the day, the fish are grouped closer to the bottom and are harder to quantify acoustically (Johnson and Burczynski 1985). For this reason, all acoustic survey work was performed during hours of darkness on the nights of 6 and 7 July 1983 and 21 February 1984.

The acoustic system was installed on a small boat in a fashion similar to that illustrated in Fig. 1 for the July survey and in a larger boat for the February survey.

On 6 July 1983, echo integration data were collected on a standard acoustic survey composed of seven parallel transects (Fig. 2). These transects were well marked so that they could be accurately navigated using a compass and visual bearing. Boat speed was held constant throughout the night at about 2.7 m/s. Dual-beam data were collected on the night of 7 July 1983 on transect 6 and on a north−south transect (Fig. 2).

The same transects were repeated for the February 1984 survey. However, in 1984 the echo sounder was configured for simultaneous 20 log(R)/40 log(R) operation. This permitted the dual-beam data on transect 6 and the north−south transect to be collected simultaneously with echo integration data. Thus, the February hydroacoustic survey was completed on a single night.

Data Acquisition and Reduction

The BioSonics dual-beam/echo integration system was used for acoustic data acquisition and processing. It consisted of the following equipment: a 420-kHz, 6°/15° dual-beam transducer installed in a towed body, a model 101 echo sounder with dual receivers, a model 121 digital echo integrator, a model 181 dual-beam processor, a modified Ross 250 chart recorder, an Otrona Attache microcomputer, and a BioSonics/Sony cassette recording/playback system. The equipment was powered by a gasoline generator.

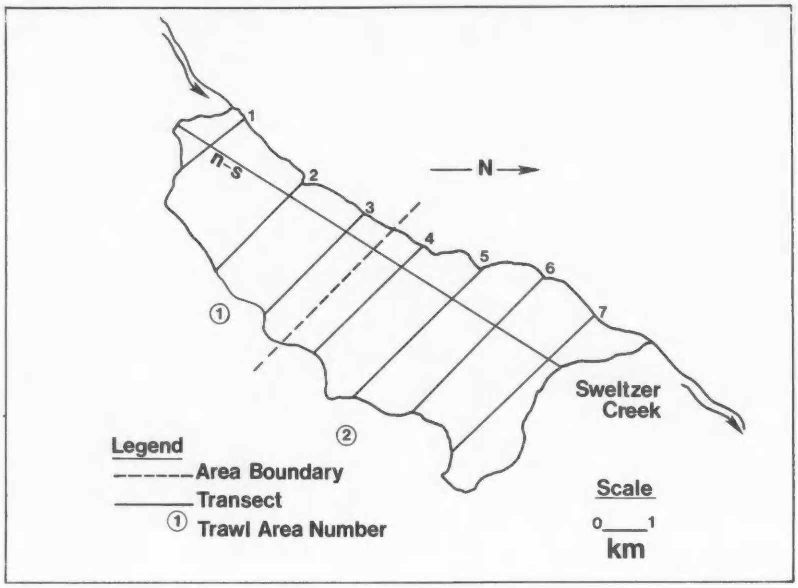
1
n–s
2
—N→
3
4
5
6
7
①
②
Sweltzer Creek
Legend
------Area Boundary
———Transect
① Trawl Area Number
Scale
0 1
km

FIG. 2. Location of hydroacoustic transects (1–7 and north–south (n–s)) and trawl sampling areas (1 and 2 circled) on Cultus Lake for July 1983 and February 1984 surveys.

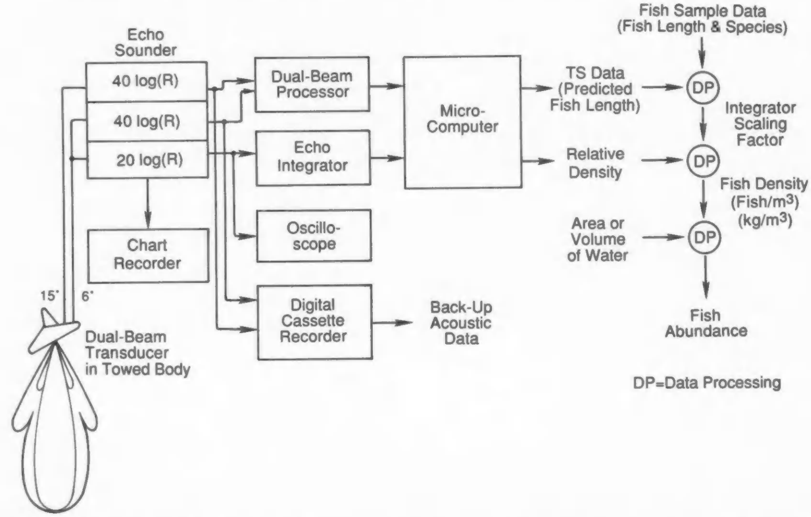
Echo Sounder
40 log(R)
40 log(R)
20 log(R)
Chart Recorder
15°
6°
Dual-Beam Transducer in Towed Body
Dual-Beam Processor
Echo Integrator
Oscillo-scope
Digital Cassette Recorder
Micro-Computer
Back-Up Acoustic Data
TS Data (Predicted Fish Length)
Relative Density
Area or Volume of Water
Fish Sample Data (Fish Length & Species)
DP
DP
DP
Integrator Scaling Factor
Fish Density (Fish/m³) (kg/m³)
Fish Abundance
DP=Data Processing

FIG. 3. Block diagram of combined dual-beam/echo integration system showing data acquisition and processing steps for Cultus Lake surveys.

A system block diagram and flow chart for data processing is shown in Fig. 3. The parameters of the acoustic system are given in Table 1 for the two surveys.

The transducer transmitted at four pulses per second while being towed at about 1 m below the surface of the lake. The detected output of the echo sounder was fed to the chart recorder, the echo integrator, and/or the dual-beam processor. The survey data were also recorded on cassette tape using the BioSonics recording/playback system.

The echo integrator data were collected using the narrow beam (6°) with the TVG set at 20 log(R). For both surveys, the water column was divided into 20 vertical 2-m intervals beginning 2 m from the transducer. The integrator averaged echo returns in 1-min intervals, which corresponded to 162-m segments of transect line at a boat speed of 2.7 m/s. The integrator outputs, which were proportional to fish densities, were transferred to microcomputer floppy disks in real time during the survey. The relative fish densities were later scaled to absolute fish densities based on system parameters obtained during equipment calibration and the mean backscattering cross section obtained from dual-beam processing.

The dual-beam processor and postprocessing software im-

TABLE 1. Characteristics of acoustic equipment.

Year	Source level, SL (dB || μPa at 1 m)	Overall system gain at 1 m, G_1 ($dB \|\| V \cdot \mu Pa^{-1}$)		Transducer's beam pattern factor, b^2_{av} (θ)	Pulse duration (ms)	Ping rate (Hz)
		20 log (*R*)	40 Log (*R*)			
1983	218.04	−156.66	−175.70	1.278×10^{-3}	0.5	4
1984	212.12	−144.44	−165.29	1.278×10^{-3}	0.5	4

TABLE 2. Trawl descriptions and environmental data for Cultus Lake trawl surveys in July 1983 and February 1984.

	Trawl description				Environmental data		
	Transect	Time (PST)	Duration (min)	Depth (m)	Sky	Light	Temperature (°C)
			11–12 July 1983				
Area 1	3	22:49	3.0	13	Overcast	Dark	16.0
	3	23:12	5.0	25	Overcast	Dark	16.0
Area 2	7	02:08	2.0	25	Overcast	Dark	18.0
			22 February 1984				
Area 1	2–3	19:45	3.0	31	Rain	Dark	4.0
	2–3	20:06	4.0	13	Rain	Dark	4.0
	2–3	20:30	3.0	19	Rain	Dark	4.0
Area 2	5	18:45	5.0	7	Rain	Dark	4.0
	5	19:00	5.0	25	Rain	Dark	4.0
	5	19:25	3.0	31	Rain	Dark	4.0

plemented the method of Ehrenberg (1974, 1984) for measuring fish target strengths from single-target echoes. The dual-beam data were collected at 40 log(*R*) TVG by transmitting pulses on the narrow (6°) transducer element and receiving echo returns on both the 6 and 15° elements.

The criteria of amplitude and duration of echo were applied for classification of single fish and other targets. If the amplitude of an echo was between minimum and maximum threshold, and its duration was more than 80% but not exceeding 110% of transmitted pulse length, it was classified as a single fish return. The maximum threshold was adjusted 6 dB below measured bottom echo, and the minimum threshold was set up 6 dB above the background noise. The beam pattern threshold was 3 dB, which was considered optimum by the method of Traynor and Ehrenberg (1979).

The data recorded by the dual-beam processor were transferred to microcomputer data files for further analysis. The postprocessing software computed target strengths and backscattering cross sections of single targets based on the peak signal amplitudes on the narrow and wide beams (as recorded by the dual-beam processor). Mean target strengths and backscattering cross sections were obtained, as well as the depth distributions of target strength values. Although parameters of multiple-target echoes were recorded, they were not included in the target strength analysis.

Trawl samples of the fish population were taken on the nights of 11 July and 22 February from a boat equipped with a hydraulic drum winch and boom for launching and retrieving a 3 × 6 m midwater trawl with 0.6-cm-square mesh at the cod end. The net was calibrated by depth/cable length such that it could be fished at any desired depth. Boat speed during trawling was about 0.6 m/s. Trawl samples of the fish population were taken in each of the two designated trawl areas during each survey (Fig. 2). The depths of the trawl samples (Table 2) were chosen based on fish distribution data obtained during the hydroacoustic surveys. The captured fish were immediately subjected to a mild concentration of 2-phenoxyethanol and subsequently preserved in a 10% formalin solution. Basic meristic information, including fork length and weight of each fish, was recorded about 1 mo later when the effects of the fixation had stabilized. Subsequent measurements were adjusted for shrinkage according to Rogers (1964). Length frequencies were tabulated for all species.

Survey Data Analysis

The survey data analysis was divided into the following sections: (a) comparison of target strength results obtained from the dual-beam data and fish samples by trawl; (b) estimation of fish densities, and horizontal and vertical distribution from integrator data scaled by dual-beam results; (c) fish population estimates; (d) statistical analysis of variance and confidence intervals of the population estimates.

Comparison of Dual-Beam Data and Fishing Data

A greal deal of experimental and theoretical research has been done on the target strength of fish. The experiments show that there exist distinguished relationships between the fish target strength and its size for a given species and wavelength (e.g. Love 1971, 1977; McCartney and Stubbs 1971; Nakken and Olsen 1977). This suggests that information on fish size can be obtained from target strength measurements of free-swimming fish.

A fish acoustic directivity pattern is not uniform; the amount of acoustic energy reflected back depends on fish orientation towards a transducer. The shape of a fish's directivity pattern depends on its size, anatomy (mainly the size and shape of a swimbladder), and acoustic wavelength. However, most of the energy is reflected from the dorsal and ventral aspect of the fish, and the target strength values are largest from these directions. Examples of measured fish directivity pattern can be found in the literature (e.g. Acker 1977; Haslett 1977).

Love (1971, 1977) introduced the equation that relates the scattering cross section of fish, its length, and wavelength:

$$(1)\quad \sigma/\lambda^2 = a(L/\lambda)^b$$

where σ = scattering cross section of fish, λ = wavelength, L = fish length, and a and b = empirically determined constants which depend on fish anatomy (species), size, and wavelength.

This formula can be transformed to log form as:

$$(2)\quad \mathrm{TS} = A \log(L) + B \log(f) + C$$

where TS = target strength of fish ($\mathrm{TS} = 10 \log(\sigma/4\pi)$), f = acoustic frequency, and A, B, and C = constants.

Love (1971, 1977) conducted a large number of measurements for different species and he also compiled available data published by other authors. His empirical formulas probably give us the best available averaging of the relationship between fish target strength and size for various species.

For target strength measurements made from the dorsal aspect, the following equation applies (Love 1971):

$$(3)\quad \mathrm{TS}_D = 19.1 \log(L) - 0.9 \log(f) - 62.0$$

where TS_D = target strength (dorsal aspect) (decibels), L = fish length (centimetres), and f = frequency (kilohertz).

However, it is unlikely that all fish are ensonified from their dorsal aspect during a survey. Although one can expect that most fish during a survey are horizontally aligned, it is likely that on the average they also divert slightly in orientation. Love (1977) developed empirical target strength formulas for fish ensonified at various angles ranging from 0 to 180° from the dorsal aspect. For ensonification from 0 to 45° with equal probability at each position, data from Love (1977) gives an average target strength for ±45° aspect of

$$(4)\quad \mathrm{TS}_{45} = 18.4 \log(L) - 1.6 \log(f) - 61.6.$$

Love (1977) stated that this relationship should be valid in the range $1 < L/\lambda < 100$. For a 420-kHz system ($\lambda = 0.344$ cm), equations (3) and (4) should be valid for fish lengths ranging between 0.34 and 34.4 cm.

The target strength distribution obtained from the dual-beam measurements and the estimated target strength from measures of fork length of fish sampled by trawl were compared using frequency plots. The lengths of trawl-caught fish were converted to estimated target strength using equations (3) and (4). Also, predicted fish length was calculated from acoustic data using the same formulas.

Fish Density and Population Estimation

Mean fish densities for each parallel transect and each depth stratum within those transects were estimated by averaging the appropriate integrator output values and multiplying them by the integrator scaling factor. The integrator scaling factor was derived from the mean backscattering cross section obtained with the dual-beam processor. The areal (horizontal) distribution of fish in the lake was derived from the mean densities (fish per cubic metre) per transect segment. Vertical distributions of fish were plotted from the mean densities per stratum for each transect and for all transects combined.

The total fish abundance in each stratum across the lake was derived by multiplying the mean densities (fish per cubic metre) by the total volume of that stratum (cubic metres). Strata volumes were calculated using a bathymetric map. Total fish abundance for the entire lake was then estimated by summing the fish abundances in all integrated strata.

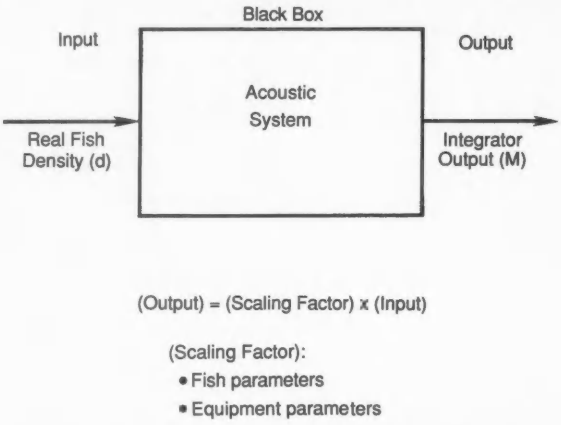

FIG. 4. Concept of scaling factor as an output/input relationship of the acoustic system.

Variance and Confidence Intervals of Estimates

One of the survey objectives was to acquire empirical statistical data in order to obtain quantitative information of practical significance relating to the variability of σ_{bs} and the integrator output for precision of population estimates.

For purposes of analysis, an acoustic system consisting of a transducer, an echo sounder with TVG, and an echo integrator can be considered as a "black box" where fish density is the input and the integrator data are the output (Fig. 4). Assuming a linear relationship between input and output, then

$$(5)\quad M = Cd$$

where M = integrator output (mean squared voltages), d = fish density, and C = scaling factor reflecting the input/output relationship of the acoustic system.

Estimated fish quantity can be obtained by extrapolating the mean density determined from integrator samples into the whole volume of water occupied by the surveyed fish population. This can be obtained simply by multiplying the mean density ($\bar{d}$) by the total volume of surveyed water:

$$(6)\quad \hat{Q} = \bar{d}V$$

where $\bar{d}$ = mean density of fish, $\hat{Q}$ = estimated quantity of fish, and V = total volume of water occupied by the population.

Many authors (Burczynski 1982; Shotton and Bazigos 1984; Johannesson and Mitson 1983) analyzing acoustic surveys considered the integrator output ($\bar{M}$) and fish density ($\bar{d}$) as random variables, while the scaling factor (C) was treated as a constant value. Fish are considered to be randomly distributed in the water column and integrator output values are acquired in the form of samples along the survey transect. Therefore, the mean density may be expressed as

$$(7) \quad \bar{d} = \bar{M}/C.$$

In such a case, the variance of density simply becomes

$$(8) \quad \mathrm{Var}(\bar{d}) = \mathrm{Var}\ (\bar{M})/C^2.$$

However, the scaling factor for the acoustic system can be split into two components, one depending on parameters of the equipment and the other on parameters of the surveyed fish (Burczynski 1982):

$$(9) \quad C = C_e\bar{\sigma}_{bs}$$

where C_e = equipment scaling factor and $\bar{\sigma}_{bs}$ = average backscattering cross section of surveyed fish. The equipment scaling factor can be measured, and its value is constant for a relatively long period of time. It may be expressed according to Ehrenberg and Kanemori (1978) as

$$(10) \quad C_e = \pi\tau c p_0^2\, g_x^2\, b_{av}^2\ (\theta)$$

where π = the constant pi, τ = pulse duration, c = sound velocity in water, p_0^2 = transmitted squared rms pressure at 1 m from the transducer, g_x^2 = squared fixed through system gain for the equipment, and $b_{av}^2\ (\theta)$ = mean square beam pattern factor of the transducer.

Because of the complex nature of acoustic scattering from fish and the fact that the size, species, orientation, and position of surveyed fish in the beam cannot be determined or controlled during the survey, the fish backscattering cross section becomes a statistical variable. Thus, equations (7) and (9) may be written as

$$(11) \quad \bar{d} = \bar{M}/C_e\bar{\sigma}_{bs}.$$

In this case, the density of fish is expressed as a quotient of two statistical components and a constant. The variance of the mean density ($\bar{d}$) must take into account the variance of two statistical components ($\bar{M}$ and $\bar{\sigma}_{bs}$). Ignoring higher order terms of the Taylor series expansion, the variance of the mean density ($\bar{d}$) can be expressed as follows (Bevington 1969):

$$(12) \quad \frac{\mathrm{Var}\ (\bar{d})}{\bar{d}^2} = \frac{\mathrm{Var}\ (\bar{M})}{\bar{M}^2} + \frac{\mathrm{Var}(\bar{\sigma}_{bs})}{\bar{\sigma}_{bs}} - \frac{2\ \mathrm{cov}\ (\bar{M}\bar{\sigma}_{bs})}{\bar{M}\bar{\sigma}_{bs}}.$$

If we assume, for simplicity, that the integrator output ($\bar{M}$) and the mean backscattering cross section of the fish ($\bar{\sigma}_{bs}$) are uncorrelated, the covariance term equals zero. Then, the equation reduces to

$$(13) \quad \mathrm{Var}\ (\bar{d}) = \bar{d}^2 \left[\frac{\mathrm{Var}\ (\bar{M})}{\bar{M}^2} + \frac{\mathrm{Var}\ (\bar{\sigma}_{bs})}{\bar{\sigma}_{bs}^2}\right]$$

The variance of the mean density reflects the confidence intervals of the density estimates. Assuming that the sequential integrator samples are independent and that the mean output is normally distributed, the confidence limit at the 95% level of significance is

$$(14) \quad \mathrm{CL} = \bar{d} \pm 1.96\sqrt{\mathrm{Var}\ (\bar{d})}$$

where Var ($\bar{d}$) is calculated from equation (13) and

$$(15) \quad \mathrm{Var}\ (\bar{M}) = \frac{1}{n}\ \mathrm{Var}\ (M)$$

$$(16) \quad \mathrm{Var}\ (\bar{\sigma}_{bs}) = \frac{1}{n_t}\ \mathrm{Var}\ (\sigma_{bs})$$

where Var (M) = integrator sample variance, n = number of integrator sequences, Var (σ_{bs}) = backscattering cross section sample variance, and n_t = number of dual-beam fish echoes used to calculate $\bar{\sigma}_{bs}$.

The same rules apply to confidence intervals of fish population estimates, which can be expressed as

$$(17) \quad \mathrm{CL} = \hat{Q} \pm 1.96\sqrt{\mathrm{Var}\ (\hat{Q})}.$$

In reality, the assumption of independent integrator output samples may not apply to $\bar{M}$. Since acoustic integrator data are collected in a sequential fashion along a transect, there is a high likelihood of trends developing in the sample units. For this reason, Shotton and Bazigos (1984) suggested that methods for estimating variance must consider the effects of dependence on sequential observations. Bayley and Hammersley (1948) used the following relationship to adjust for autocorrelation of such sequential observations:

$$(18) \quad \mathrm{Var}\ (\bar{M}) = \frac{\mathrm{Var}\ (M)}{n}\left[1 + 2\sum_{i=1}^{n-1}\left(1 - \frac{i}{n}\right)\rho_i\right]$$

where ρ_i = serial correlation with lag i, Var (M) = integrator sample variance, and n = number of echo integrator sequences.

When sample elements from an acoustic survey form discrete clusters, a single-stage cluster sampling method may be applied to account for the effects of autocorrelation. Williamson (1982) has used the following approximate expression for the variance for the mean integrator output M:

$$(19) \quad \mathrm{Var}\ (\bar{M}) \approx \frac{1}{N^2}\frac{t}{t-1}\left[\sum_{i=1}^{t} M_i^2 + \bar{M}^2\sum_{l=1}^{t} n_i^2 - 2\bar{M}\sum_{i=1}^{t} M_i n_i\right]$$

where t = total number of transects, n_i = number of observations within a transect i, N = total number of observations ($N = \sum_i n_i$), and M_i = sum of n_i integrator observations in transect i. The variance estimate is considered good when the coefficient of variation of n is less than 0.2 (Kish 1965):

$$(20) \quad \frac{\mathrm{Var}\ (\bar{n})^{0.5}}{\bar{n}} = \left\{\frac{\Sigma n_i^2 - [(\Sigma n_i)^2/t]}{t(t-1)}\right\}^{0.5}\left\{\frac{\Sigma n_i}{t}\right\}^{-1} < 0.2.$$

The adjusted variance of the mean integrator output may subsequently be applied to equation (15) to derive the variance of the mean density. The expression for confidence limits at the 95% level of significance will remain the same as in equations (14) and (17).

Results and Discussion

Fishing Results

The vast majority of the fish captured in the trawling operations were found to be juvenile sockeye in both July 1983 and February 1984 (95 and 96%, respectively). The July samples ranged in fork length from 2.7 to 21.3 cm with a mean of 4.54 cm. The February samples ranged in fork length from 2.8 to 18.0 cm with a mean of 7.17 cm. The pertinent environmental and catch data are summarized in Tables 2 and 3, respectively.

TABLE 3. Catch statistics, by species, for Cultus Lake trawl surveys in July 1983 and February 1984. Data are mean values for number of fish caught, fish lengths, and standard deviation of fish lengths for transects shown in Table 2.

	11–12 July 1983			22 February 1984		
	N	*L* (cm)	SD	*N*	*L* (cm)	SD
Sockeye (0+, 1+)	397	4.50	0.730	440	7.20	0.792
Sockeye (yearling)	2	20.65	0.650	2	15.50	2.500
Sculpin	14	3.32	0.423	1	3.70	0.000
Stickleback	0	0.00	0.000	12	4.31	0.703
Cyprinid	3	4.63	1.239	1	12.00	0.000
Overall	416	4.54	1.352	456	7.166	1.116

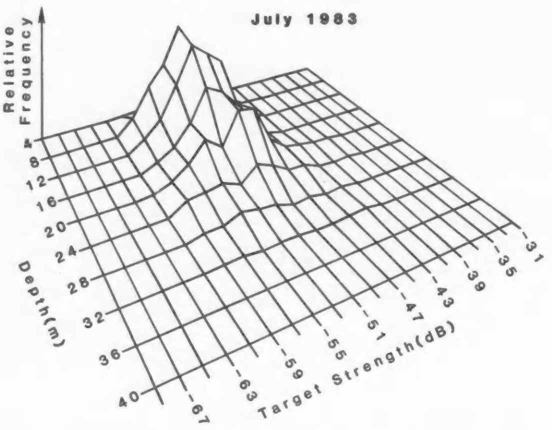

FIG. 5. Frequency distribution of fish target strengths vs. depth for July 1983 survey of Cultus Lake.

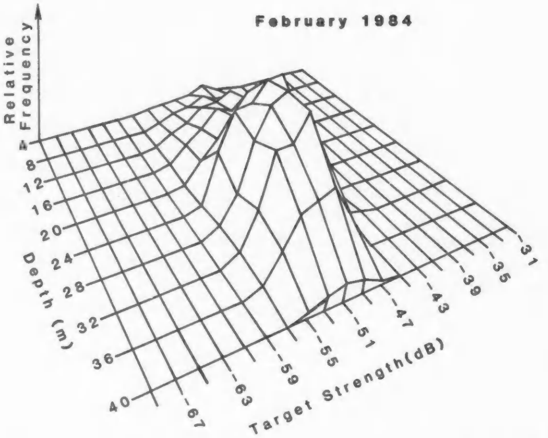

FIG. 6. Frequency distribution of fish target strengths vs. depth for February 1984 survey of Cultus Lake.

Due to the slow trawling speed and the size of the net, large fish would not be expected to be captured in these samples. However, based on past gillnet sampling in Cultus Lake, it is known that larger fish do reside in the lake. Kokanee, squawfish, and Dolly Varden (*Salvelinus malma*) ranging in fork length from 20 to 67 cm have been captured. Since proportionately small numbers of these species were in the lake during the two acoustic surveys, they were omitted from this analysis. Additionally, threespine stickleback (*Gasterosteus aculeatus*) and redside shiners (*Richardsonius balteatus*) are often found near the surface in relatively small numbers. Since the depth strata started at 2 m below the transducer, which was towed about 1 m below the surface, it was assumed that few of these fish could be detected; therefore, they were also omitted from the target strength analysis.

Dual-Beam Target Strength Results

The dual-beam target strength data are presented in three-dimensional plots in Fig. 5 and 6 for the two surveys. The target strengths of single fish detected during the July 1983 survey ranged from −61 to −39 dB with an average value of −52.3 dB and a standard deviation of 3.4 dB. The target strengths of single fish during the February 1984 survey were slightly larger, ranging from −59 to −40 dB with an average of −49.8 dB and a standard deviation of 3.0 dB.

The majority of the single fish detections recorded by the dual-beam system were distributed within a depth range of 6−26 m in July. The target strengths within this range were between −59 and −43 dB. In February, the single fish detections were distributed throughout the water column, with the majority of the detections between 2 and 30 m. The target strengths within this range were between −57 and −40 dB.

Comparison of Target Strength and Fish Length

Visual comparison of distributions of single fish target strengths recorded by the dual beam and calculated from measured length of trawl-caught fish using Love's (1971, 1977) formulas is shown in Fig. 7 and 8. Table 4 gives the comparison of mean values and standard deviation between acoustic and trawl data on single fish.

Both distributions of target strength and fish length match well when compared visually (Fig. 7 and 8). Love's equation (4), which averages fish target strength over 45° from its dorsal aspect, gives better visual matching between acoustic and fishing data than equation (3), which refers to the maximum value of target strength.

The mean values of fish sampled by trawl and calculated from dual-beam data are very close. However, the dorsal aspect equation (3) produced more accurate results for smaller fish (July 1983), while equation (4) averaging target strength over 45° fits better for larger fish (February 1984). The reason for this variation is unknown. Possibly it is due to the different orientation of the fish during the two surveys.

TABLE 4. Comparison of dual-beam results and fish length data from trawl.

Survey	Mean target strength, TS (dB)	SD	Number of echoes measured	Mean length of fish from trawl, L (cm)	SD	Number of fish measured	Mean length (cm) of fish calculated from TS according to Love	
							Equation (3) dorsal aspect	Equation (4) averaged aspect 45°
July 1983	−52.3	3.4	1326	4.5	1.3	416	4.3	5.4
February 1984	−49.8	3.0	5845	7.2	1.1	456	4.8	7.4

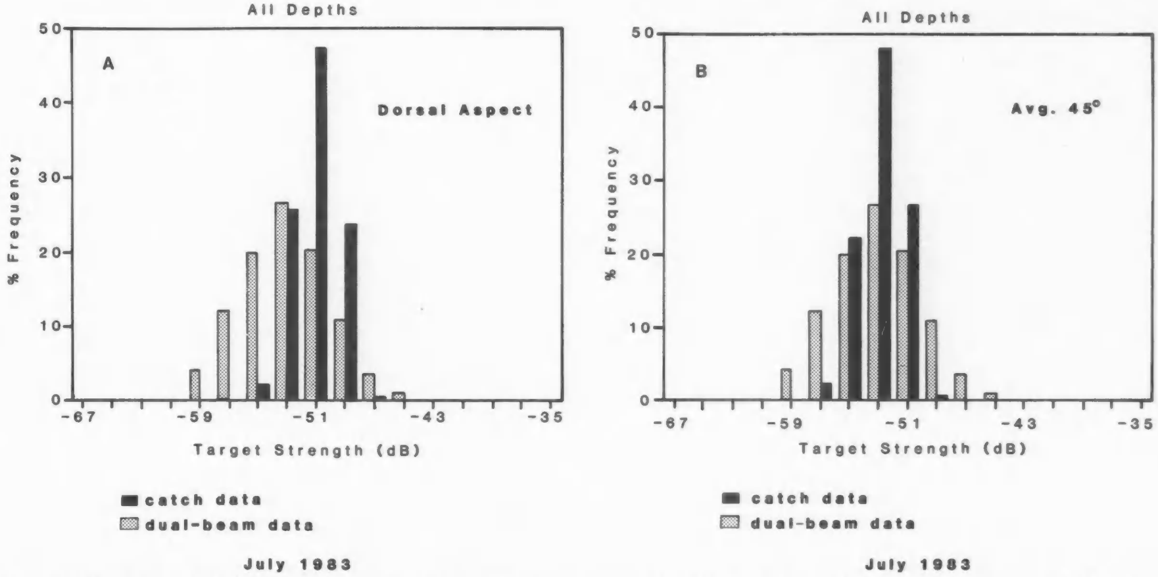

FIG. 7. Distribution of fish target strengths measured by the dual-beam system in July 1983 compared with distribution of measured fish lengths converted to target strengths based on empirical formulas of Love (1971, 1977) for (A) dorsal aspect measurements and (B) measurements averaged from 0 to 45° from dorsal aspect.

In any case, the spread of the acoustic data was approximately twice that of measured fish length data. A non-uniform fish backscattering directivity pattern is the major reason for the spread of acoustic data. The same fish can give different values of target strength, depending on the orientation of the fish in relation to the transducer. Additionally, the trawl gear tends to filter very small fish, and large fish avoid capture due to the slow velocity of the net.

Acoustic data on fish target strength and size of trawl-caught fish were in agreement and both show proportional growth of the surveyed fish. This agreement indicates that there is potential in the application of acoustic techniques for the sizing of free-swimming fish. However, at this stage the methods should be used with caution. For different species and size groups of fish, the empirical constants in formulas (2), (3), and (4) can be different. Fish behavior and, especially, change in the orientation angle when diving or changing feeding habits affects measured target strength and may introduce an error or ambiguity into the resulting data.

Distribution of Fish Density

During the nighttime, the fish were well dispersed in midwater and thus made good targets for purposes of echo integration and dual-beam processing. Most of the fish were distinguishable as individual targets, as illustrated by the representative chart recording shown in Fig. 9.

The overall vertical distributions of mean fish densities for the two surveys are shown in Fig. 10. In July the majority of fish were distributed at depths between 8 and 26 m. In February the fish were more widely distributed throughout the water column, presumably due to a change in the lake's thermal structure. For this reason, it was necessary to collect more trawl data at different depths to adequately sample the sockeye population (Table 2).

The horizontal distributions of fish density obtained from integrator data in July 1983 and February 1984 are shown in Fig. 11 and 12, respectively. In July the densities appeared to be highest at the northern extreme of the lake (transect 7) with moderately high densities shore-oriented between the north and south ends of the lake. The lowest densities were found in the central portion of transects 2 and 3 and toward the west shore of transect 5. Shore orientation might be expected at this time of year, as the juvenile sockeye have just begun to utilize the limnetic zone of the lake and may still be exhibiting preference toward the littoral region.

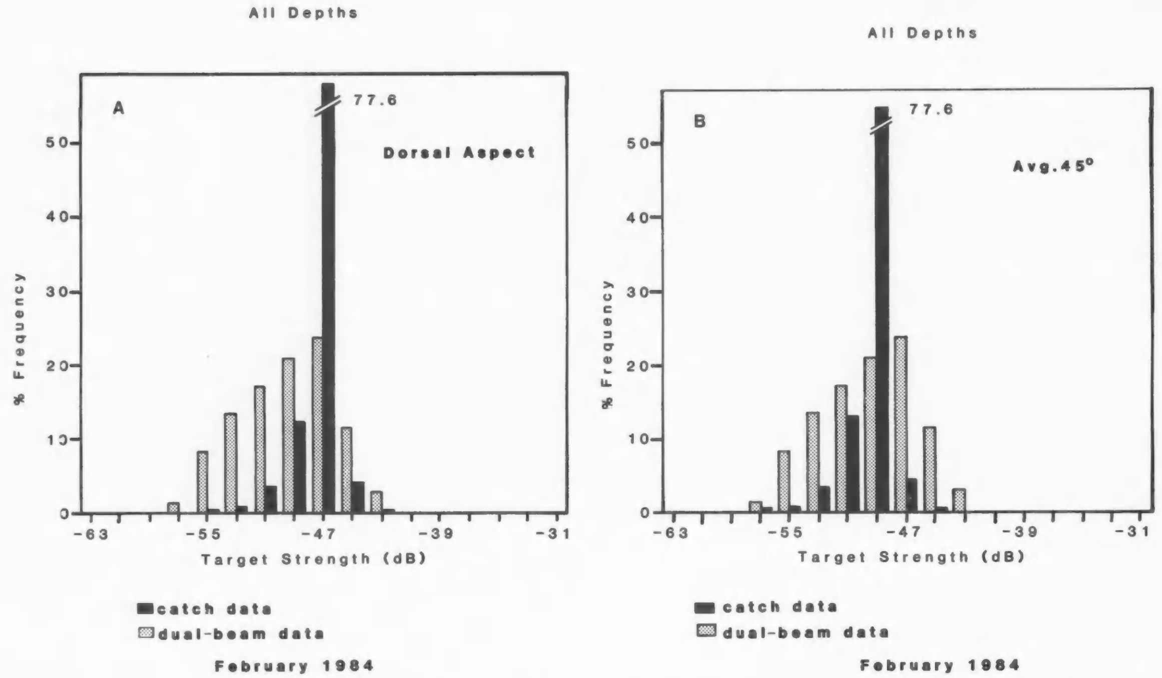

FIG. 8. Distribution of fish target strengths measured by the dual-beam system in February 1984 compared with distribution of measured fish lengths converted to target strengths based on empirical formulas of Love (1971, 1977) for (A) dorsal aspect measurements and (B) measurements averaged from 0 to 45° from dorsal aspect.

TABLE 5. Summary of sockeye quantity estimates for surveys in 1983 and 1984.

	1983		1984	
	Fish quantity, $\hat{Q}$ (millions)	Confidence interval (%)	Fish quantity, $\hat{Q}$ (millions)	Confidence interval (%)
Stratified independent samples	2.66	±7.6	2.30	±6.0
Adjusted for autocorrelation	2.66	±24.0	2.30	±5.8
Cluster sample analysis	2.88	±20.9	2.41	±10.6

In February the population was more evenly distributed throughout the lake, as most likely they had stabilized in their feeding habits as described by Levy and Hall (1985) for Babin Lake.

Population Estimate

The total fish population in Cultus Lake was estimated acoustically to be 2 880 000 on 6 July 1983 and 2 380 000 on 21 February 1984. These estimates were based on echo integration data obtained on the seven parallel transects. The integrator scaling factors were estimated from the dual-beam data collected on 7 July and 21 February, respectively.

The total sockeye population in Cultus Lake was estimated at 2 660 000 on 6 July 1983 and 2 300 000 on 21 February 1984 (Table 5). The difference between the population estimated in July 1983 and February 1984 can be explained by natural mortality. The July estimate was obtained by scaling the total estimated fish population by the proportion of sockeye in the trawl catches and then eliminating all fish outside the 6- to 26-m depth range. In February the estimate was simply scaled by the trawl catches, since the population did not exhibit a definite stratification in the lake. Although a few large resident fish may have intermingled with the smaller sockeye in the 2- to 30-m depth range, it is believed that they represented an insignificant proportion of the total biomass in the lake during both surveys.

A potential egg deposition of 39 951 000 would have been expected from the 1982 brood stock, based on an escapement of 10 249 females and a fecundity of 3898 eggs per female.

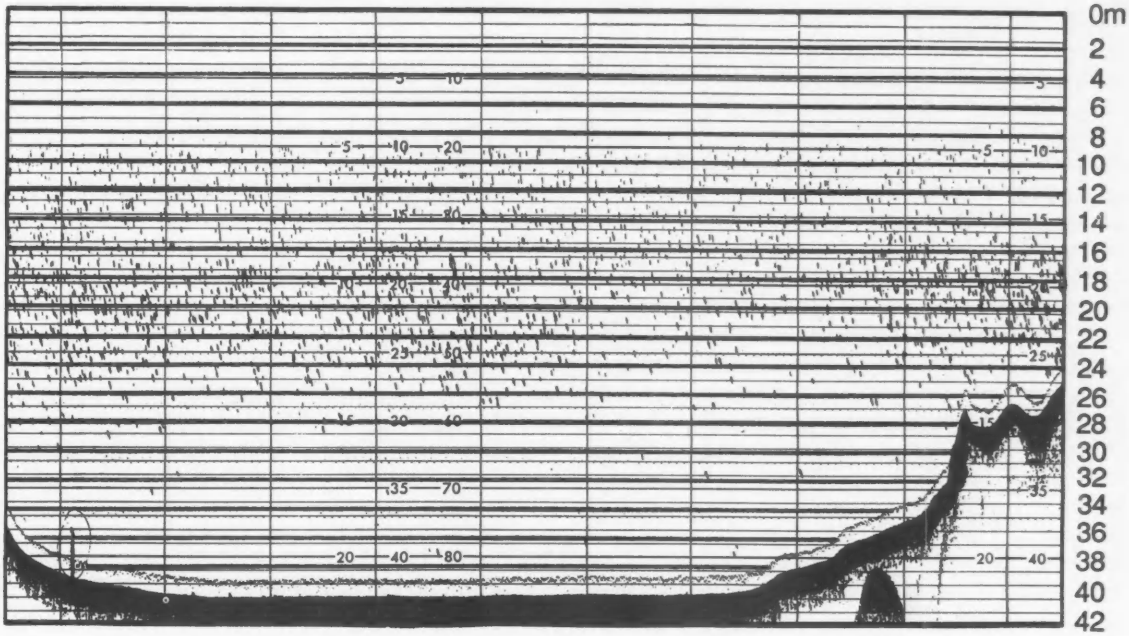

FIG. 9. Sample chart recording from transect 6 for July 1983. Data recorded at 20 log(R) TVG.

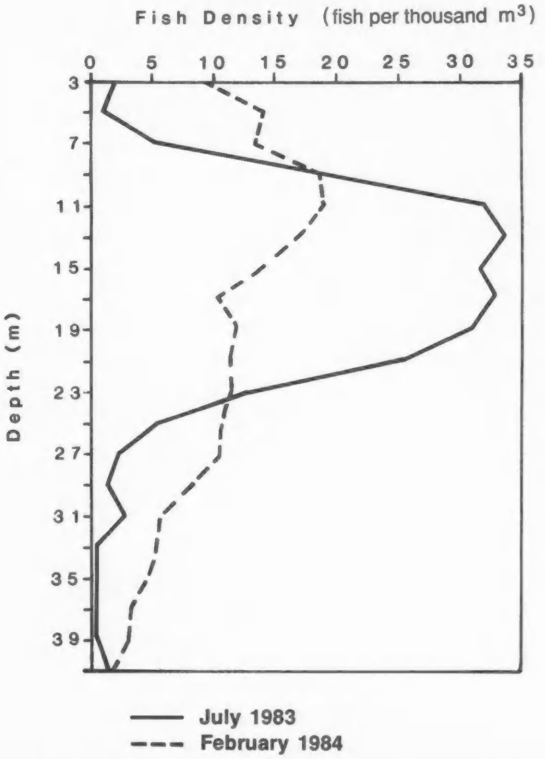

FIG. 10. Overall mean vertical density distributions of fish in Cultus Lake determined by echo integration, July 1983 and February 1984.

Thus, the population estimates represent a survival of about 6.7% of the potential egg deposition to July 1983 and 5.8% to February 1984 (data from unpublished files of the International Pacific Salmon Fisheries Commission, P.O. Box 30, New Westminster, B.C.).

A subsequent count of the outmigrant smolts was conducted at a counting fence located about 300 m downstream from the outlet at the north end of the lake on Sweltzer Creek. The counts were initiated on 1 April 1984 and concluded on 4 June 1984 using an experimental 5% sampling device. The final cumulative count through the fence was 1 630 000 sockeye smolts (R. Kent, International Pacific Salmon Fisheries Commission), pers. comm.). This figure is probably low due to the difficulty in calibrating the sampler under a high migration rate and because of fish spilling over the side of the device, as observed during the operation. If we also take into consideration the presence of residual sockeye (2-yr-old fish) or kokanee remaining in the lake and the vulnerability to predation at the outlet by the squawfish as documented by Steigenberger and Larkin (1974), we may assume a reasonable comparison with the acoustic results.

Variance and Confidence Intervals

Three approaches to the variance estimate were undertaken in this study. One assumed stratified independent samples, and two assumed autocorrelation in the sequential output units as described earlier. Table 5 lists the results of the three techniques in terms of the confidence limits computed according to equations (14) and (17).

Assuming stratified independent samples, the July 1983 confidence limits for the estimated sockeye population of ±7.6% were in agreement with the February 1984 confidence limits of ±6.0%.

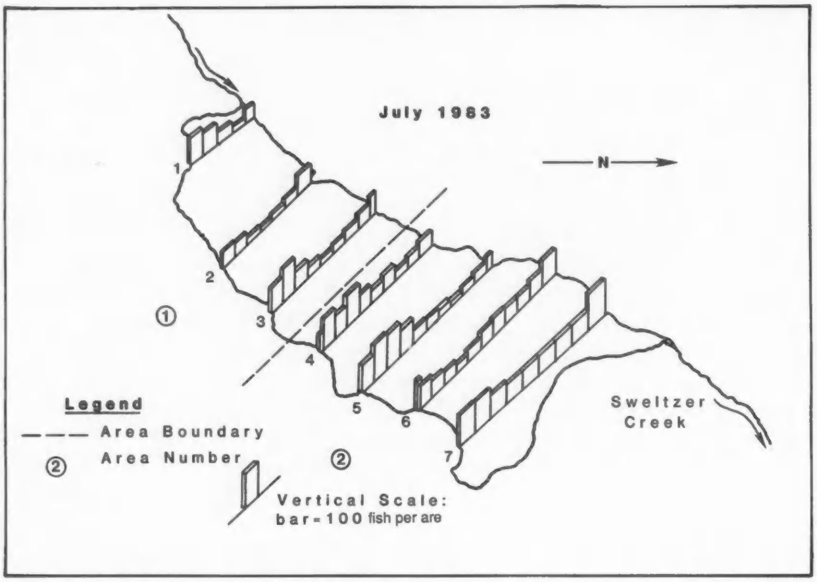
July 1983
N
1
2
3
4
5
6
7
①
②
Sweltzer Creek
Legend
Area Boundary
② Area Number
Vertical Scale: bar = 100 fish per are

FIG. 11. Horizontal distribution of mean fish densities in Cultus Lake determined by echo integration, July 1983.

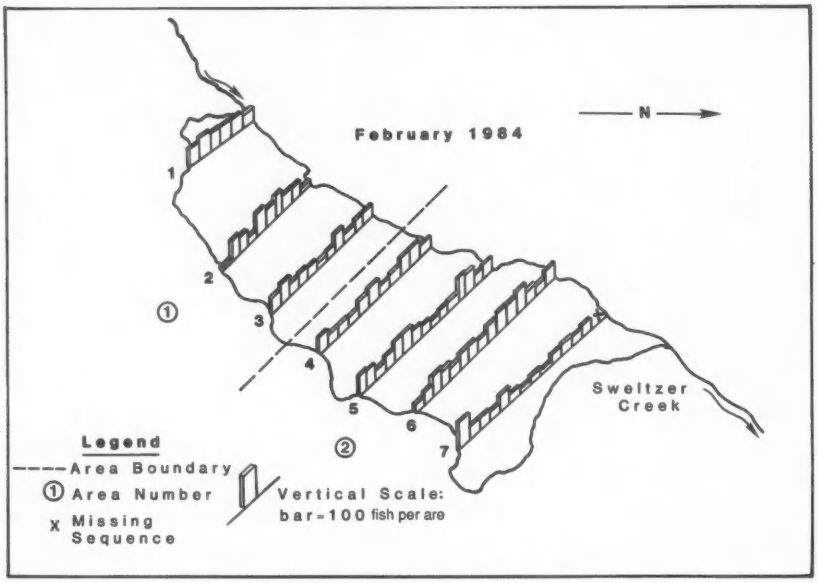
February 1984
N
1
2
3
4
5
6
7
①
②
Sweltzer Creek
Legend
Area Boundary
① Area Number
x Missing Sequence
Vertical Scale: bar = 100 fish per are

FIG. 12. Horizontal distribution of mean fish densities in Cultus Lake determined by echo integration, February 1984.

However, when the effects of autocorrelation were taken into account, the differences between the confidence intervals for the two surveys increased. In July there was a shore-oriented trend in the distribution (Fig. 11) and the integrator samples were strongly autocorrelated (Fig. 13). Adjusting for autocorrelation according to equation (18) (Bayley and Hammersley 1948) resulted in a threefold increase in the range of the confidence limits ±24%. Applying the cluster sample technique (equation (19)) to the same data (Williamson 1982) yielded similar results ±20.1% with a slightly higher estimate of the fish quantity ($\hat{Q}$). The higher estimate of $\hat{Q}$ was a result of a nonstratified volumetric extrapolation technique, whereas in the independent sample technique and the adjusted autocorrelation approach, the volumetric extrapolation was stratified over depth.

In February 1984, there was less trend in the distribution

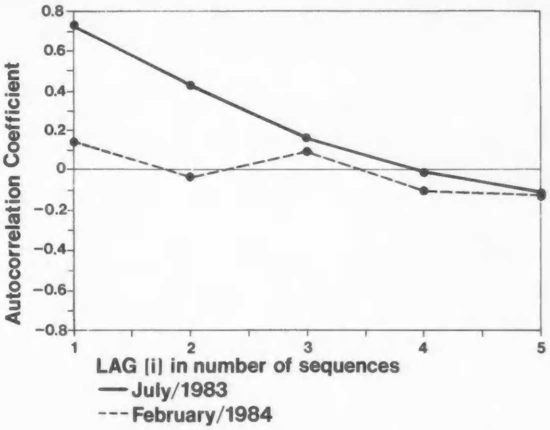

FIG. 13. Autocorrelation coefficients vs. lag (*i*) in number of echo integrator sequences for July 1983 and February 1984 surveys of Cultus Lake.

than in July 1983 (Fig. 12) and there was practically no autocorrelation between integrator samples (Fig. 13). Thus, the adjustment for autocorrelation had less of an effect, as noted in Table 5. When autocorrelation was taken into account, the confidence limits decreased slightly from ±6.0 to ±5.8%, while the culster sample approach increased the confidence limits slightly to ±10.6%.

The coefficient of variation for both surveys was equal to 0.1, and therefore the estimate of variance using the cluster technique can be considered good according to equation (20).

The autocorrelation between sequential integrator outputs depends on spatial distribution of surveyed fish and on size of the sequential sampling unit. The more autocorrelated the samples, the worse the confidence interval of the estimates (see Table 5). The sequential sampling unit can be adjusted to minimize autocorrelation between sequential integrator outputs.

Of the two components of variance for fish density (equation (13)), the integrator variance was significant, while the backscattering cross section variance was negligible. The normalized variance for the integrator values, i.e. Var $(\bar{M})/\bar{M}^2$, ranged from 5.2×10^{-3} to 1.0 in July 1983 and 0.0 to 6.7×10^{-2} in February 1984. Since the surveyed population consisted almost entirely of a single species of a single size group, and since a large number of dual-beam samples were processed, the variance of the backscattering cross section of the fish was very small, with a normalized mean variance Var $(\bar{\sigma}_{bs})/\bar{\sigma}_{bs}^2$ of 1.1×10^{-3} and 1.2×10^{-4}, respectively.

For both surveys, the variance of the population was small and confidence intervals were good. The variance of the backscattering cross section of fish was so small that it was insignificant compared with the variance of integrator output. If various fish species and size groups can be stratified horizontally and vertically, poststratification of survey data may improve the precision of the population estimates.

Bias of Estimate

Bias in the fish population estimate can be caused by systematic errors due to the spatial distribution of fish or errors in estimation of the integrator scaling factor.

The fish density estimates are based on assumptions that fish echo signals received by the acoustic equipment represent samples of the true proportion of the fish population in the whole surveyed volume of water. The coverage error appears when part of the surveyed population of fish is not sampled acoustically. It can be caused by various phenomena related to fish behavior patterns. For example, fish may avoid the moving vessel (this happens usually with fish schools), or some part of the fish echoes may be masked by the bottom echo or noise.

Depthwise distribution of fish echoes was measured when the boat was moving and also drifting. No differences were observed in either case. Fish were favorably distributed in midwater away from the bottom and no reaction of the fish to the moving boat was apparent. Fish echoes were well above the noise level (the average fish echo was about 12 dB above the minimum signal threshold).

An error in estimation of the integrator scaling factor can be caused by an error of hydroacoustic calibration, a change of equipment parameters, and/or the improper estimate of the fish's mean backscattering cross section. Calibration of the equipment in a tank with a standard transducer before and after each survey indicated that there was no change in the instrument parameters. The accuracy of measurement in a tank was ±0.5 dB. However, the bias in estimates of fish backscattering cross section can occur even with properly calibrated equipment. For example, if the surveyed fish population consists of several size groups and species, the samples available for dual-beam processing are not necessarily in proportion to the real composition of the various size groups and species due to their different behavior patterns. However, for the surveys reported here, practically all the fish were sockeye salmon of the same size group. The data showed close to normal distributions for both fish sizes and target strengths.

Our conclusion is that bias related to coverage error and to estimation of the integrator scaling factor was not significant and probably negligible.

Summary

These surveys demonstrated that the combined dual-beam/echo integration technique can produce consistent and accurate estimates of fish population. This information should be useful for fish stock managers and fisheries scientists. In particular, this technique can provide reliable information on fish density and quantity and the vertical and horizontal distributions of the surveyed fish. The most significant element of this technique is that the same fish population can be sampled simultaneously using both echo integration and dual-beam processing.

Estimates of the fish population in Cultus Lake appear to be reasonable and in agreement with other estimates. The sockeye population was estimated to be 2 660 000 in July 1983 and 2 300 000 in February 1984. These estimates represent a survival rate of about 6.7% to July 1983 and 5.8% to February 1984, respectively. The 1984 sockeye smolt outmigration was estimated at 1 633 000 based on counts made between 1 April and 4 June 1984.

Fish target strengths measured by the dual-beam system compared well with the lengths of trawl-caught fish, according to empirical formulas developed by Love (1971, 1977). This indicates that there is potential in the application of the dual-beam technique for acoustic estimation of size of surveyed fish. However, these results are preliminary and were obtained under favorable conditions (i.e. practically monospecies population with only one size group of fish). More experimental and theoretical work should be done in this field.

For estimating the variance and confidence intervals of population estimates, both the variance of the integrator output and the variance of the fish's backscattering cross section should be taken into account. Both of these statistical variables are important. The significance of each component for the final result depends on the distribution of sample data of M and σ_{bs}.

The other important factor for the estimation of confidence intervals is autocorrelation between consecutive integrator samples along a transect. The autocorrelation depends on spatial distribution of sampled fish. The more correlated the samples are, the wider the confidence interval is.

References

Acker, W. C. 1977. Acoustic assessment of north Pacific salmon stocks. Rapp. P.-V. Reun. Cons. Int. Explor. Mer 170: 189–195.

Bayley, G. V., and J. M. Hammersley. 1948. The effective number of independent observations in an autocorrelated time series. J. R. Stat. Soc. 8(1-B): 184–197.

Bevington, P. R. 1969. Data reduction and error analysis for the physical sciences. McGraw Hill, New York, NY. 363 p.

Burczynski, J. 1982. Introduction to the use of sonar systems for estimating fish biomass. FAO Fish. Tech. Pap. 191. Rev. 1: 89 p.

Dickie, L. M., R. G. Dowd, and P. R. Boudreau. 1983. An echo counting and logging system (ECOLOG) for demersal fish size distributions and densities. Can. J. Fish. Aquat. Sci. 40: 487–498.

Ehrenberg, J. E. 1974. Two applications for a dual-beam transducer in hydroacoustic fish assessment system. Proc. IEEE Conf. Eng. Ocean Environ. 1: 152–155.

1984. Principles of dual-beam processing for measuring fish target strengths. Technical Note No. 41. BioSonics, Inc., Seattle, WA. (Available from BioSonics, Inc., 4520 Union Bay Place NE, Seattle, WA 98105)

Ehrenberg, J. E., and R. Y. Kanemori. 1978. A microcomputer-based echo integration system for fish population assessment. Proc. IEEE Conf. Eng. Ocean Environ. 204–207.

Haslett, R. W. G. 1977. Automatic plotting of polar diagrams of fish in roll, pitch, and yaw. Rapp. P.-V. Reun. Cons. Int. Explor. Mer 170: 74–81.

Johannesson, K. A., and R. B. Mitson. 1983. A practical manual for aquatic biomass estimation. FAO Fish. Tech. Pap. 240: 249 p.

Johnson, R. L., and J. J. Burczynski. 1985. Application of dual-beam acoustic procedures to estimate limnetic juvenile sockeye salmon. International Pacific Salmon Fisheries Commission. Progress Report No. 41: 50 p. (Available from International Pacific Salmon Fisheries Commission, P.O. Box 30, New Westminster, B.C.)

Kish, L. 1965. Survey sampling. John Wiley & Sons, New York, NY. 643 p.

Levy, D. A., and K. J. Hall. 1985. A Review of the limnology and sockeye salmon ecology of Babine Lake. Tech. Rep. No. 27. Westwater Research Centre, University of British Columbia, Vancouver. 101 p. (Available from University of British Columbia, Vancouver, B.C.)

Love, R. H. 1971. Dorsal-aspect target strength of an individual fish. J. Acoust. Soc. Am. 49: 816–823.

1977. Target strength of an individual fish at any aspect. J. Acoust. Soc. Am. 62: 1397–1403.

McCartney, B. A., and A. R. Stubbs. 1971. Measurement of the acoustic target strength of fish in dorsal aspect including swim-bladder resonance. J. Sound Vib. 15(3): 397–420.

Nakken, O., and K. Olsen. 1977. Target strength measurement of fish. Rapp. P.-V. Reun. ICES 170: 52–69.

Nunnallee, E. P., Jr. 1980. Application of an empirically scaled digital echo integrator for assessment of juvenile sockeye salmon (*Oncorhynchus nerka* Walbaum) populations. Ph.D. dissertation, University of Washington, Seattle, WA. 120 p.

Rogers, D.E. 1964. Variability in measurement of length and weight of juvenile sockeye salmon and three-spine stickleback. Univ. Wash. Fish. Res. Inst. Circ. No. 224: 34 p.

Shotton, R., and G. P. Bazigos. 1984. Techniques and considerations in the design of acoustic surveys. Rapp. P.-V. Reun. Cons. Int. Explor. Mer 184: 34–57.

Steigenberger, L. W., and P. A. Larkin. 1974. Feeding activity and rates of digestion of northern squaw fish (*Ptychocheilus oregonensis*). J. Fish. Res. Board Can. 31: 411–420.

Traynor, J. J., and J. E. Ehrenberg. 1979. Evaluation of the dual-beam acoustic fish target strength method. J. Fish. Res. Board Can. 36: 1065–1071.

Williamson, N. J. 1982. Cluster sampling estimation of the variance of abundance estimates derived from quantitative echo sounder surveys. Can. J. Fish. Aquat. Sci. 39: 229–231.

Plankton Size Spectra in Relation to Ecosystem Productivity, Size, and Perturbation

W. Gary Sprules

Department of Zoology, University of Toronto, Erindale College, Mississauga, Ont. L5L 1C6

and M. Munawar

Department of Fisheries and Oceans, Great Lakes Fisheries Research Branch, Canada Centre for Inland Waters, Burlington, Ont. L7R 4A6

Sprules, W. G., and M. Munawar. 1986. Plankton size spectra in relation to ecosystem productivity, size, and perturbation. Can. J. Fish. Aquat. Sci. 43: 1789–1794.

Quantification and comparisons of the structure of open-water plankton communities from 25 inland lakes of Ontario, from the Laurentian Great Lakes Superior, Huron, St. Clair, Ontario, and Erie, and from the Central Gyre in the North Pacific Ocean were made on the basis of the normalized biomass size spectrum. Residual variation around the fitted straight lines (corresponding to a theoretical steady state) was least for the large, oligotrophic Lake Superior and the North Pacific Gyre and greatest for eutrophic Saginaw Bay and shallow Lake Erie, suggesting progressive departure from steady-state conditions with increasing system productivity. The slopes of the normalized spectra decrease with increasing eutrophy, indicating that nannoplankton abundances are similar in all communities studied, but that associated zooplankton abundances vary by 2.5 orders of magnitude. Our results suggest that parameterization of particle-size models for prediction of potential fish production must be adjusted according to the size and productivity of the ecosystem, and that routine monitoring of communities by the normalized biomass spectrum could provide early warning of nutrient or toxic stress in aquatic ecosystems.

Les auteurs ont quantifié et comparé, sur la base de la gamme des tailles de la biomasse normalisée, la structure de communautés planctoniques d'eau libre de 25 lacs intérieurs de l'Ontario, y compris les Grands Lacs Supérieur, Huron, Ontario et Érié et le lac Sainte-Claire, et les eaux du courant giratoire central du nord de l'océan Pacifique. La variation résiduelle aux droites ajustées (correspondant à un état d'équilibre théorique) était la moins importante dans le cas du lac Supérieur, important et oligotrophe, et du tourbillon du nord du Pacifique, et la plus importante dans celui de la baie Saginaw, eutrophe, et du lac Érié, peu profond; ce qui porte à croire à un écart progressif par rapport à l'état d'équilibre à mesure que la productivité du système s'accroît. Les pentes de la gamme normalisée diminuaient avec l'augmentation du caractère eutrophe, ce qui montre que l'abondance du nanoplancton était semblable dans toutes les communautés étudiées, mais que celle du zooplancton variait de 2,5 ordres de grandeur. Les résultats obtenus indiquent que la paramétrisation des modèles à « tailles de particules » pour la prévision de la production de poisson doit être ajustée à la taille et à la productivité de l'écosystème et que le contrôle de routine des communautés fondé sur la gamme de biomasse normalisée pourrait permettre de déceler à l'avance des contraintes par carence de matières nutritives ou effets toxiques dans les écosystèmes aquatiques.

Received November 4, 1985
Accepted May 22, 1986
(J8542)

Reçu le 4 novembre 1985
Accepté le 22 mai 1986

Sheldon et al. (1972) have shown that the biomass distribution of plankton organisms assumes a characteristic and predictable shape within latitudinal pelagic regions of the Atlantic and Pacific oceans. These empirical regularities are predictable from considerations of predator to prey size ratios, growth efficiencies, and ecological efficiencies that typify aquatic ecosystems (Kerr 1974; Sheldon et al. 1977; Platt and Denman 1978). Resultant "particle-size" models permit quite accurate predictions of fish stock and yield from inexpensively collected data on the biomass of smaller particles such as algae (Sheldon et al. 1977; Moloney and Field 1985). The existence of comparable regularities in the biomass distribution of freshwater plankton has been confirmed (Sprules et al. 1983), and the models have been refined to permit prediction of stock and yield of particles anywhere on the size spectrum, independently of their trophic position (Borgmann 1982).

This important theoretical development stems from sampling data broadly representative of the Atlantic and Pacific oceans, but restricted largely to particles in the 0- to 100-μm size range. Furthermore, subsequent applications of the particle-size models assume roughly similar amounts of particulate material in logarithmically equal size ranges, an assumption based only on "...an interpretative summary of the information..." presented (Sheldon et al. 1972, p. 336). This summary is a reasonable first approximation, but more quantitative analyses of the large variation in particle-size spectra among ocean sites (Sheldon et al. 1972) and among lakes (Sprules et al. 1983) are required to provide a general form of the particle-size models for prediction of aquatic stocks. In this paper, we will present a more quantifiable expression of the biomass size distribution, and we will use this to contrast the structure of plankton communities in aquatic ecosystems varying extensively in size and productivity.

TABLE 1. Details of sampling procedures for study sites.

	Phytoplankton		Zooplankton			
	Depth (m)	Sampler[a]	Depth (m)	Sampler[b]	Date	Reference
Lake Superior	0–20	A	0–50[c]	70 μm, 100 cm, 71%	Sept. 1983	Munawar and Munawar 1978
Lake Huron	0–20	A	0–50[c]	64 μm, 40 cm, 60%	July 1971	Munawar and Munawar 1979
Lake Ontario	0–20	A	0–6	64 μm, 50 cm, 71%	June 1984	—
Lake Erie	0–10	A	0–20	110 μm, 30 cm, 70%[d]	Aug. 1984	—
Lake St. Clair	0–bott[e]	B	0–bott[e]	110 μm, 30 cm, 70%[d]	June–July 1984	—
Inland lakes	0–4	C	0–bott[e]	110 μm, 30 cm, 70%	Summer 1979[f]	Sprules et al. 1983
Pacific Ocean[g]	0–200	B	0–200	183-μm bongo net	1973, 1974	Rodriguez and Mullin 1986

[a] A, integrating sampler (Schroeder 1969); B, pooled bottle samples; C, tygon tubing (9.5-mm I.D.).
[b] Mesh size, mouth diameter, and filtering efficiency of townet.
[c] Except at shallower stations where depth is from surface to 2 m above bottom.
[d] Isokinetic nets, lower hoop 50 cm in diameter.
[e] Approximately 1–2 m off bottom.
[f] Seven separate seasonal samples pooled together (Sprules et al. 1983).
[g] 434 samples from various stations (near 28°N, 155°W), cruises, and the two years averaged together to produce one spectrum.

TABLE 2. Normalized spectrum slopes, intercepts, and coefficients of determination (r^2) for study sites (n = number of stations or sites).

		Slope		Intercept		
	n	Median	Range	Median	Range	r^2
North Pacific Central Gyre[a]	1	−1.16	—	0.10	—	0.97
Lake Superior	11	−1.10	−1.00 to −1.15	0.61	0.41–0.73	0.94–0.98
Lake Huron[b]	8	−1.02	−0.90 to −1.18	0.90	0.64–1.65	0.59–0.94
Lake Ontario	4	−0.97	−0.90 to −1.04	1.82	1.35–2.16	0.82–0.90
Lake Erie	4	−0.99	−0.77 to −1.24	1.99	1.79–2.41	0.62–0.90
Lake St. Clair	14	−0.90	−0.76 to −1.05	1.46	1.11–1.83	0.68–0.89
Inland lakes	25	−0.98	−0.92 to −1.05	1.36	0.92–1.93	0.93–0.98

[a] Only one conglomerate sample (see Table 1).
[b] Including Saginaw Bay.

Methods

Data Collection

We present information on plankton size spectra from 25 inland Ontario lakes, from the Laurentian Great Lakes Superior, Huron, St. Clair, Erie, and Ontario, and from the Central Gyre in the North Pacific ocean. Although techniques of sample collection and processing are broadly comparable among sites, differences in detail make possible only a general description of methods (Table 1). Both phytoplankton and zooplankton are from samples integrated through the water column. Varying numbers of stations in each of the Great Lakes (Table 2) were selected from a larger inventory (e.g. Munawar and Munawar 1982) to give broad coverage, principally of offshore waters in all lakes, but also of some inshore areas of Lakes Superior, Huron, and St. Clair. The 25 inland lakes are from a larger study of Ontario lakes (Zimmerman et al. 1983). Each lake was sampled fortnightly during late May to early September 1979 at the deepest point. The resulting samples of phytoplankton and zooplankton were pooled to give a single sample of each representing a seasonal average (Sprules et al. 1983). The Pacific Ocean "station" actually represents "microplankton" (10^{-4} to 10^{-1} μg) and "macrozooplankton" (1 to 10^3 μg) samples from various cruises and depths in the North Pacific Central Gyre averaged to provide, effectively, a single plankton sample (Rodriguez and Mullin 1986).

Phytoplankton samples from all lakes were preserved in Lugol's solution and a settled aliquot (Utermöhl 1958) examined microscopically (Munawar and Munawar 1978; Sprules et al. 1983). The volume of each cell or colony was computed from simple geometric models, and the biomass of each was determined assuming a specific gravity of unity. Zooplankton samples were preserved in formalin and subsamples examined microscopically. The biomass of each individual encountered was computed utilizing a microcomputer-based measuring caliper routine (Sprules et al. 1981) incorporating length – wet weight regressions pooled from the literature (Sprules 1984). For the Pacific Ocean, phytoplankton (microplankton) was processed as described above except that organism size in 13 weight classes was expressed as micrograms carbon dry weight. Zooplankton were sieved into six size classes, the total dry weight of each class determined, and division by organism abundance used to compute average particle weights, expressed as micrograms carbon dry weight (Rodriguez and Mullin 1986).

Normalized Spectra

Sheldon et al.'s (1972) original data on the biomass size spectrum were generated by use of a Coulter counter. The horizontal axis of such a spectrum is one of organism volume (usually expressed as equivalent spherical diameter) measured on a logarithmic scale, each category of which is double the

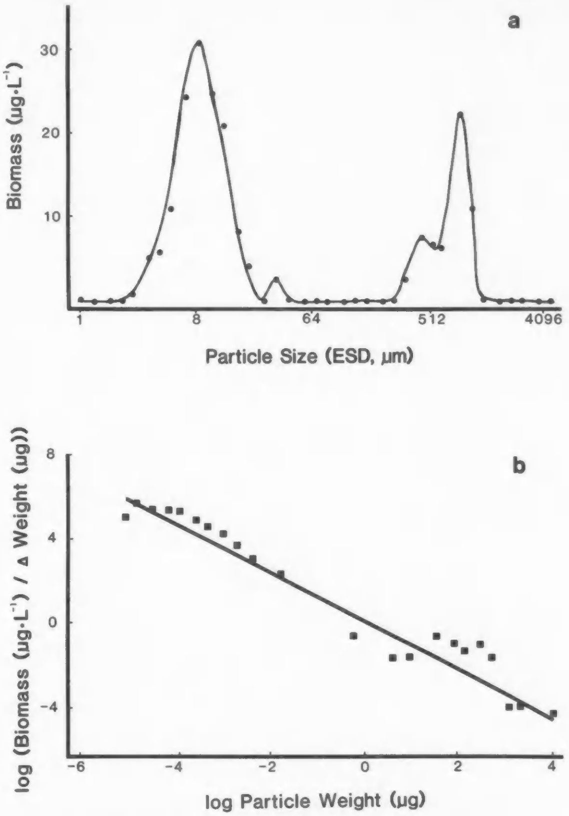

FIG. 1. Examples of (a) "Sheldon" and (b) normalized spectra. Data are for an offshore station in Lake Superior. Missing points on the normalized spectrum indicate no detectable biomass in those weight categories. ESD = equivalent spherical diameter.

volume of the preceding. Organism density for each volume category is plotted linearly on the vertical axis as ppb, which is the same as micrograms per litre if plankton organisms are assumed to have specific gravity of unity (Fig. 1a). The difficulty with such an expression of community size structure is that variation in shape and configuration cannot easily be quantified. We prefer instead the "normalized" biomass size spectrum (Fig. 1b) that has properties of integration suited to the theorist (Platt and Denman 1978) and that facilitates quantification of variation in system structure for the empiricist. Organisms are still grouped into adjacent categories of volume doubling, but size is expressed as fresh weight on a logarithmic scale (Fig. 1b). The vertical axis is the total fresh biomass (per litre) of organisms in a particular weight category divided by the change in weight across the category, all on a logarithmic scale. This is close, but not identical, to the numerical density of organisms in the weight class.

For a pelagic community conforming to the theoretical steady state, the normalized spectrum will be linear with a slope close to -1 (Kerr 1974; Sheldon et al. 1977; Platt and Denman 1978). The slope of such spectra, and the pattern of residual variation around the line, can thus serve both to characterize the size structure of the community and to indicate degree of departure from the theoretical steady state. The *Y*-intercept of these lines (at $X = 0$) is a general measure of organism abundance in the community.

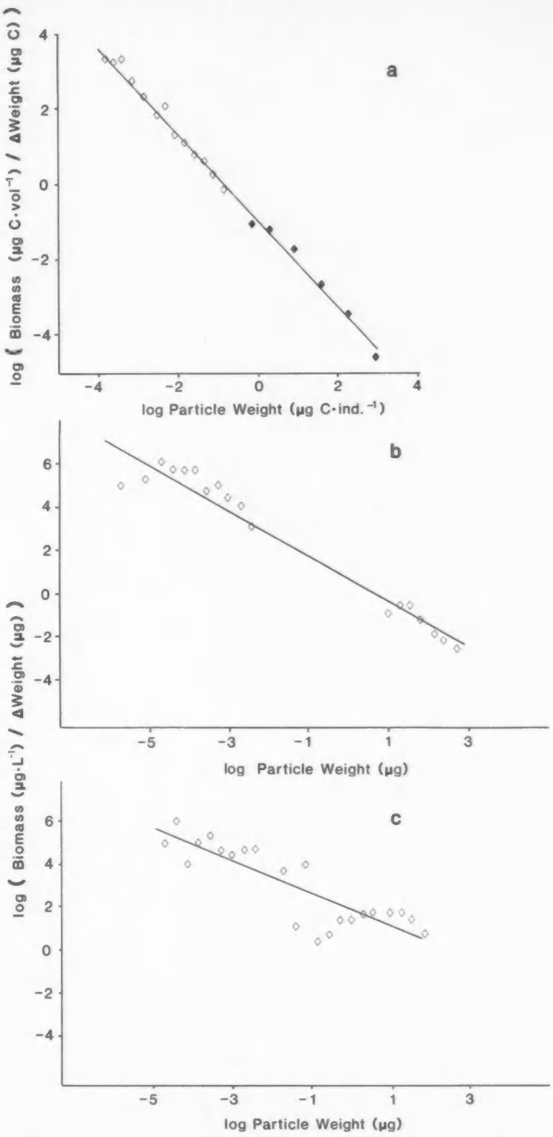

FIG. 2. Typical normalized spectra for (a) the North Pacific Central Gyre ($r^2 = 0.97$; open symbols are microplankton, closed symbols are macrozooplankton (adapted from Rodriguez and Mullin 1986)), (b) Lake Superior ($r^2 = 0.96$), and (c) Lake St. Clair ($r^2 = 0.73$). Note the different units for the Pacific Ocean data.

We have constructed normalized biomass spectra for each of the 66 lake stations (Table 2) in the following manner (that for the Pacific Ocean was provided by Rodriguez and Mullin (1986)). The weight of each phytoplankton and zooplankton individual from a subsample was determined as described above. All individuals were placed into their respective weight categories and the fresh biomass summed for each category. These totals were adjusted for gear efficiency and aliquot size to give biomass concentration (micrograms per litre) in each category. Division of these totals by the width of the corresponding weight interval, followed by logarithmic transformation, yields the normalized biomass spectrum for the particular station (Fig. 1b). The straight line is fitted by least squares linear regression.

Results and Discussion

It should be noted that the lines we have fitted by linear regression do not represent the curve of best fit to the normalized data (Fig. 1b), but rather serve as a reference point for assessing departure from the theoretical steady-state structure of the plankton communities. The gross configuration of the points and degree of variation around the reference lines are of primary interest.

Normalized spectra vary among habitats in both slope and degree of residual variation (Table 2; Fig. 2). The small variation of points around the line for the Pacific Ocean (Fig. 2a) suggests that this plankton community is close to steady state, and, in fact, such an open ocean community was taken as the model for establishment of basic particle-size theory. Such communities are assumed to be close to steady state, major predator–prey interactions are confined to the upper mixed layer with minimal influence of benthic or onshore processes, prey are reasonably constant fractions of their predators' size, and specific growth and ecological efficiencies of component organisms are weight dependent (Sheldon et al. 1972; Kerr 1974; Platt and Denman 1978).

Residual variation in the spectra for Lake Superior, a large, oligotrophic ecosystem of low productivity, is also low (Table 2), although there is more pattern to the residuals than for the ocean (Fig. 2b). Hence, this community also appears to be close to steady state in the sense we have defined. This is consistent with the comparative isolation of the offshore community due to the great depth and large surface area of the lake and with the evidence that the Lake Superior water mass is relatively uniform and unchanging (Munawar et al. 1978; Kwiatkowski 1980).

Residual variation for the individual inland lakes is also low (Table 2), probably because each spectrum is based on pooled samples that integrate seasonal variation in plankton abundances. For the remaining Great Lakes, variation around the linear trend is higher, particularly for Lake St. Clair (Table 2; Fig. 2c). This lake is very shallow and turbid, receives major nutrient discharges from large inflowing rivers, and theoretically flushes approximately every 7 d (Leach 1972). Its plankton community probably never reaches steady state. Although fewer data are available for Lakes Ontario and Erie, their plankton communities also show relatively high residual variation (Table 2). This is probably due to comparatively high levels of contaminants in both and, in the case of shallow Lake Erie, the influence of littoral and benthic processes on the open water. The Lake Huron plankton spectra show intermediate degrees of residual variation (Table 2). It is interesting that the highly eutrophic, and presumably seasonally variable, Saginaw Bay shows the poorest fit of all ($r^2 = 0.59$).

The slopes of the normalized spectra also vary in a consistent fashion among the communities studied (Fig. 3). Although there is high variability in slopes within ecosystems, there is nevertheless a tendency for them to become less negative from the Pacific Ocean to Lakes Erie and Ontario (Fig. 3). Part of this pattern is due to concomitant increases in intercepts of the lines that reflect increasing organism abundance, but the tendency for the lines to converge at the upper left (Fig. 3) indicates a reduction in slopes as well. Relatively uniform abundances of small algae among ecosystems (roughly 0.5 order of magnitude variation, upper left of Fig. 3) is thus associated with high variability in the abundance of large zooplankton (roughly 2.5 orders of magnitude, lower right of Fig. 3). A given abundance of small algae in Lakes Erie and Ontario leads to a considerably higher abundance of large zooplankton than does the same stock of algae in the Pacific Ocean and Lake Superior (Fig. 3).

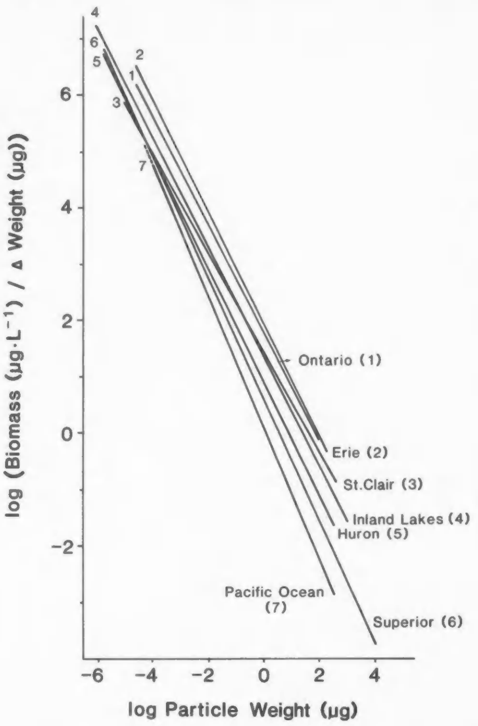

FIG. 3. Normalized biomass spectra for all study sites. Except for the Pacific Ocean, for which only one conglomerate spectrum was available (Table 1), each line has been determined by selecting the median slope and median intercept (Table 2) for the particular ecosystem. Numerals are to aid in location of both extremes of the lines. The different measurement units for the Pacific Ocean do not affect the slope of the line, but the line has been shifted to the right on the assumption that dry weight of carbon is 5% of fresh biomass (Finlay and Uhlig 1981; Latja and Salonen 1978). Broken-line portion of the Pacific Ocean line indicates the presence of organisms that were too small to process.

The variation in slopes of the normalized spectra, and to a lesser extent changes in residual variation around the spectrum, is related to overall productivity of the systems we have studied. When the lakes are ranked on a rough scale of increasing trophy, there is a pattern of decreasing slope of the normalized spectrum (Fig. 4). Again, variability is high, but oligotrophic systems such as the Pacific Ocean and Lakes Superior and Huron tend to have more negative slopes than do eutrophic Saginaw Bay and western Lake Erie. This is precisely the pattern predicted by models of plankton ecosystem dynamics (Walters et al. 1980). In eutrophic ecosystems, nutri-

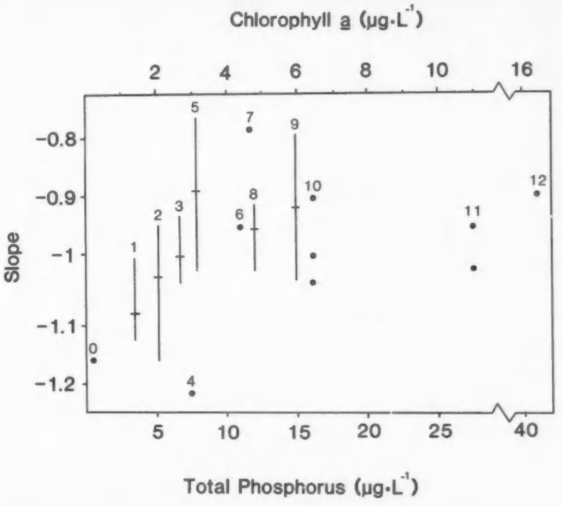

FIG. 4. Relation between normalized spectrum slope and rough measures of ecosystem productivity. Position of each site on the graph has been determined from seasonally averaged chlorophyll *a* and total phosphorus data, depending on which were available (Leach 1972; Vollenweider et al. 1974; Weiler 1981; Munawar and Munawar 1982). Only an approximate correspondence between the upper and lower *X*-axes is claimed, and therefore, positions are approximate, but rank order is probably correct. Medians (cross bars) and ranges (vertical lines) or individual values (points) of the slopes of the normalized spectra are presented. Sites: 0, North Pacific Gyre; 1, Lake Superior (n = 11 stations); 2, Lake Huron, excluding Saginaw Bay (n = 7); 3, oligotrophic inland lakes (n = 20); 4, Lake Erie east station; 5, Lake St. Clair central stations (n = 9); 6, Lake Ontario east station; 7, Lake Erie central station; 8, mesotrophic inland lakes (n = 5); 9, Lake St. Clair southeast stations (n = 5); 10, Lake Ontario central stations (note three points); 11, Lake Erie western basin (note two points); 12, Saginaw Bay, Lake Huron. The subdivisions within the Great Lakes are as typically presented (e.g. Vollenweider et al. 1974). Two water masses in Lake St. Clair have been identified (Leach 1980).

ents entering at a high rate are cycled quickly through fast-growing nannoplankton to produce relatively high abundances of zooplankton grazers (e.g. Lakes Ontario and Erie, Fig. 3). By contrast, in oligotrophic ecosystems, nutrients entering at a lower rate are cycled more slowly through nannoplankton to produce lower abundances of zooplankton grazers (e.g. Pacific Ocean, Fig. 3). The important point is that resultant nannoplankton abundances are *not* substantially different (hence, conversion of lines in Fig. 3). Roughly equivalent abundances of nannoplankton produce greater abundances of zooplankton in more productive lakes than in less productive ones (Fig. 3 and 4).

Conclusion

Our results indicate clear differences in the biomass structure of aquatic plankton communities that are related both to the size and productivity of the ecosystem. Recognition of these trends is possible because the slope, intercept, and residual variation of the normalized biomass size spectrum are quantitative indices of system structure. Although our data base is extensive, particularly in the physical size of ecosystems and the inclusion of both marine and freshwater habitats, it is limited to plankton communities and contains relatively little information on seasonal variability or benthic–pelagic coupling. Nevertheless, the trends we have noted are likely correct to a first approximation and are of sufficient general importance to warrant further investigation.

Perhaps of greatest significance is the fact that the slope of the normalized biomass size spectrum varies among ecosystems to the degree that the abundance of zooplankton grazers supported by a relatively constant stock of nannoplankton can vary by 2.5 orders of magnitude. If these varying stocks of zooplankton support correspondingly varying stocks of fish (and additional data are clearly required for confirmation), then obviously a single parameterization of particle-size models for general prediction of aquatic stocks is not realistic. Our results indicate that there may be homogeneous subsets of ecosystems within which structure is sufficiently uniform to justify application of particle-size models such as those proposed by Dickie et al. (1987) and Borgmann (1987). But for each homogeneous subset, a different parameterization of the model would be required according to the relevant ecosystem characteristics. This procedure thus allows more robust fine-tuning of this kind of model. In the Great Lakes fisheries context, this means that prediction of potential fish production or yield in, say, large, unproductive Lakes Superior and Huron would be made using a different version of a particle-size model than would be used, say, in smaller, more productive Lake Erie. Precision of estimates of potential fish production would thereby be increased.

The normalized biomass size spectrum can also be recommended for routine monitoring purposes in important ecosystems such as the Great Lakes. Collection and processing of required data is comparatively simple, yet the diagnostic potential of the spectrum appears high (Kerr and Dickie 1984). We have clearly shown that variations in ecosystem productivity are reflected in the normalized spectrum, and it is reasonable to expect that such variation through time within an ecosystem would be similarly manifested. More interesting is the possibility that increases in the amount of residual variation around the idealized linear normalized spectrum are indicative of perturbation from the steady state. Routine monitoring of the size spectrum could thus lead to early identification of toxic or nutrient stress through examination of temporal changes in residual variation. This and other features of the normalized spectrum that we have noted deserve additional investigation.

Acknowledgements

We are grateful for the help provided by Eddy Jin who enumerated all of the zooplankton and some of the phytoplankton, collated much of the data, and drafted the figures and by Warren Norwood who helped process the remaining phytoplankton data. Discussions at the ASPY Symposium with members of the Productivity Working Group and with Carl Walters, Jim Kitchell, Don McQueen, Uwe Borgmann, Stuart Pimm, and Jan Beyers contributed greatly to the ideas presented here. Milos Legner has provided thoughtful comment on many occasions. Comments by Steve Kerr helped improve the manuscript. Operating grants to WGS from the Natural Sciences and Engineering Research Council of Canada, the Canadian National Sportsmen's Fund, and the Ontario Ministry of Natural Resources are gratefully acknowledged.

References

BORGMANN, U. 1982. Particle-size conversion efficiency and total animal production in pelagic ecosystems. Can. J. Fish. Aquat. Sci. 39: 668–674.

1987. Models on the shape of, and biomass flow up, the biomass size spectrum. Can. J. Fish. Aquat. Sci. 44(Suppl.). (In press)

DICKIE, L. M., S. R. KERR, AND P. SCHWINGHAMER. 1987. An ecological approach to fisheries assessment. Can. J. Fish. Aquat. Sci. 44(Suppl.). (In press)

FINLAY, B. J., AND G. UHLIG. 1981. Calorific and carbon values of marine and freshwater Protozoa. Helgol. Wiss. Meeresunters. 34: 401−412.

KERR, S. R. 1974. Theory of size distribution in ecological communities. J. Fish. Res. Board Can. 31: 1859−1862.

KERR, S. R., AND L. M. DICKIE. 1984. Measuring the health of aquatic ecosystems. *In* V. W. Cairns, P. V. Hodson, and J. C. Nriagu [ed.] Contaminant effects on fisheries. John Wiley & Sons Inc., New York, NY.

KWIATKOWSKI, R. E. 1980. Regionalization of the upper Great Lakes with respect to surveillance eutrophication data. J. Great Lakes Res. 6: 38−46.

LATJA, R., AND K. SALONEN. 1978. Carbon analysis for the determination of individual biomasses of planktonic animals. Verh. Int. Ver. Limnol. 20: 2556−2560.

LEACH, J. H. 1972. Distribution of chlorophyll *a* and related variables in Ontario waters of Lake St. Clair. Proc. 15th Conf. Great Lakes Res. 1972: 80−86.

1980. Limnological sampling intensity in Lake St. Clair in relation to distribution of water masses. J. Great Lakes Res. 6: 141−145.

MOLONEY, C. L., AND J. G. FIELD. 1985. Use of particle-size data to predict potential pelagic-fish yield of some South African areas. S. Afr. J. Mar. Sci. 3: 119−128.

MUNAWAR, M., AND I. MUNAWAR. 1978. Phytoplankton of Lake Superior 1973. J. Great Lakes Res. 4: 415−442.

1979. A preliminary account of Lake Huron phytoplankton, April to December, 1971. Fish. Mar. Serv. Tech. Rep. 917: 1−15.

1982. Phycological studies in Lakes Ontario, Erie, Huron, and Superior. Can. J. Bot. 60: 1837−1858.

MUNAWAR, M., I. F. MUNAWAR, L. R. CULP, AND G. DUPUIS. 1978. Relative importance of nannoplankton in Lake Superior phytoplankton biomass and community metabolism. J. Great Lakes Res. 4: 462−480.

PLATT, T., AND K. DENMAN. 1978. The structure of pelagic marine ecosystems. Rapp. P.-V. Reun. Const. Int. Explor. Mer 173: 60−65.

RODRIGUEZ, J., AND M. M. MULLIN. 1986. Relation between biomass and body weight of plankton in a steady state oceanic ecosystem. Limnol. Oceanogr. 31: 361−370.

SCHROEDER, R. 1969. Ein summierender Wasserschopfer. Arch. Hydrobiol. 66: 241−243.

SHELDON, R. W., A. PRAKASH, AND W. H. SUTCLIFFE JR. 1972. The size distribution of particles in the ocean. Limnol. Oceanogr. 17: 327−340.

SHELDON, R. W., W. H. SUTCLIFFE JR., AND M. A. PARANJAPE. 1977. Structure of pelagic food chain and relationship between plankton and fish production. J. Fish. Res. Board Can. 34: 2344−2353.

SPRULES, W. G. 1984. Towards an optimal classification of zooplankton for lake ecosystem studies. Verh. Int. Ver. Limnol. 22: 320−325.

SPRULES, W. G., J. M. CASSELMAN, AND B. J. SHUTER. 1983. Size distribution of pelagic particles in lakes. Can. J. Fish. Aquat. Sci. 40: 1761−1769.

SPRULES, W. G., L. B. HOLTBY, AND G. GRIGGS. 1981. A microcomputer-based measuring device for biological research. Can. J. Zool. 59: 1611−1614.

UTERMÖHL, H. 1958. Zur Vervolkommung der Quantitativen Phytoplankton Method. Mitt. Int. Ver. Limnol. 9: 1−38.

VOLLENWEIDER, R. A., M. MUNAWAR, AND P. STADELMANN. 1974. A comparative review of phytoplankton and primary production in the Laurentian Great Lakes. J. Fish. Res. Board Can. 31: 739−762.

WALTERS, C. J., R. A. PARK, AND J. F. KOONCE. 1980. Dynamic models of lake ecosystems, p. 455−479. *In* E. D. Le Cren and R. H. Lowe-McConnell [ed.] The functioning of freshwater ecosystems. Cambridge University Press, Cambridge.

WEILER, R. R. 1981. Chemistry of the North American Great Lakes. Verh. Int. Ver. Limnol. 21: 1681−1694.

ZIMMERMAN, A. P., K. M. NOBLE, M. A. GATES, AND J. E. PALOHEIMO. 1983. Physicochemical topologies of south-central Ontario lakes. Can. J. Fish. Aquat. Sci. 40: 1788−1803.

Hypersaline Gradients in Two Canadian High Arctic Lakes

Kenton M. Stewart

Department of Biological Sciences, State University of New York, Buffalo, NY 14260, USA

and Robert F. Platford

National Water Research Institute, Box 5050, Burlington, Ont. L7R 4A6

Stewart, K. M., and R. F. Platford. 1986. Hypersaline gradients in two Canadian High Arctic lakes. Can. J. Fish. Aquat. Sci. 43: 1795–1803.

The meromictic Sophia and Garrow lakes are probably saline relicts of cutoff fjords on the uplifted Cornwallis and Little Cornwallis islands in the High Arctic of the Canadian Archipelago. Sophia and Garrow have brackish (S = 2–4) upper and hypersaline (S = 55–90) lower waters with ion ratios (especially the lower waters) similar to that of the sea. Substantial oxygen extends well below the chemocline in Sophia. The stability of these lakes is among the highest known. Because of their size, depth, and unusually warm lower waters, it seems likely that an unfrozen "thermal chimney" extends beneath the lakes through the surrounding permafrost. We feel that the hypersaline gradients evolved primarily by descent of "salt fingers" during freeze out from above, and not by solute rejection from the ground during uplift and permafrost growth, or through taliks connected to the sea, as proposed by Pagé et al. (1984. Limnol. Oceanogr. 29: 564–573).

Les lacs méromictiques Sophia et Garrow constituent probablement les restes salins de fjords coupés de la mer des îles Cornwallis et Little Cornwallis de l'archipel canadien du Haut Arctique qui ont été soulevées. Les eaux de ces lacs sont saumâtres (S = 2–4) dans leur partie supérieure et hypersalées (S = 55–90) dans leur partie inférieure; les rapports ioniques (particulièrement dans les eaux inférieures) sont semblables à ceux des eaux marines. Une teneur appréciable en oxygène est notée bien en deçà de la chémocline dans le lac Sophia. La stabilité de ces lacs compte parmi les plus élevées connues. Étant donné leur taille, leur profondeur et leurs eaux inférieures anormalement chaudes, il est probable qu'une « cheminée thermale » non gelée s'étende en dessous des lacs à travers le pergélisol environnant. Nous croyons que les gradients hypersalins sont apparus suite à la descente de « coins salins » au cours du gel et non suite au rejet de soluté à partir du sol lors du soulèvement et de la croissance du pergélisol ou par l'intermédiaire de taliks reliés à la mer, comme l'ont proposé Pagé et *al.* (1984. Limnol. Oceanogr. 29 : 564–573).

Received January 3, 1986
Accepted May 22, 1986
(J8628)

Reçu le 3 janvier 1986
Accepté le 22 mai 1986

Meromictic lakes, in which chemical gradients overwhelm temperature gradients in governing the stable density structure, are found from the tropics to the poles. This paper concerns two such unusual lakes in the High Arctic of the Canadian Archipelago. We examine here some comparative limnological data, mostly from a limited period in August 1982, and also consider the development of hypersaline gradients.

Study Site and Lakes

Sophia and Garrow lakes are located on Cornwallis and Little Cornwallis Islands in the Northwest Territories at a latitude of about 75°N (Fig. 1). This treeless tundra region is characterized by a cold desert-like climate with a mean annual temperature of −16.2°C and precipitation of 13.0 cm as recorded at Resolute (Vowinckel and Orvig 1970). The regional glacial history (Blake 1964; Thorsteinsson 1958) suggests that the lakes are likely relict fjord basins that were separated from the sea following glacial retreat and isostatic rebound. Table 1 provides some morphometric comparisons. Both lakes have an outflow which is active only in the summer. The lake-ice thickness may exceed 2 m. Sophia Lake is usually ice free for only about 1 mo. In 1980, 1981, and 1982, Garrow Lake never completely lost its ice. This difference is a bit puzzling because the maximum and mean depths of both lakes are quite similar. However, the length, orientation to wind (Sophia lies east and west, Garrow north and south), and internal thermal structure differ slightly and those features may influence the extent and duration of open water.

Methods

Water temperatures were measured on both lakes with a calibrated thermistor connected, via a coaxial cable, to a Keithley model 135 multimeter. Temperatures were easily resolved to ±0.1° but, owing to minor uncertainties unknown to us during the field measurements, are now believed to be accurate to only ±1.0°.

Irradiance measurements were made with a Lambda Instruments model 185A meter and model 192S underwater quantum sensor in the photosynthetically active range (PAR) of 400–700 nm.

The August 1982 sampling was done at a single station near the deep region of both lakes. Sophia Lake was ice free but approximately three fifths of Garrow Lake was covered with drifting and broken ice in its southerly end. Sampling in Garrow was from the north edge of the loose ice pack.

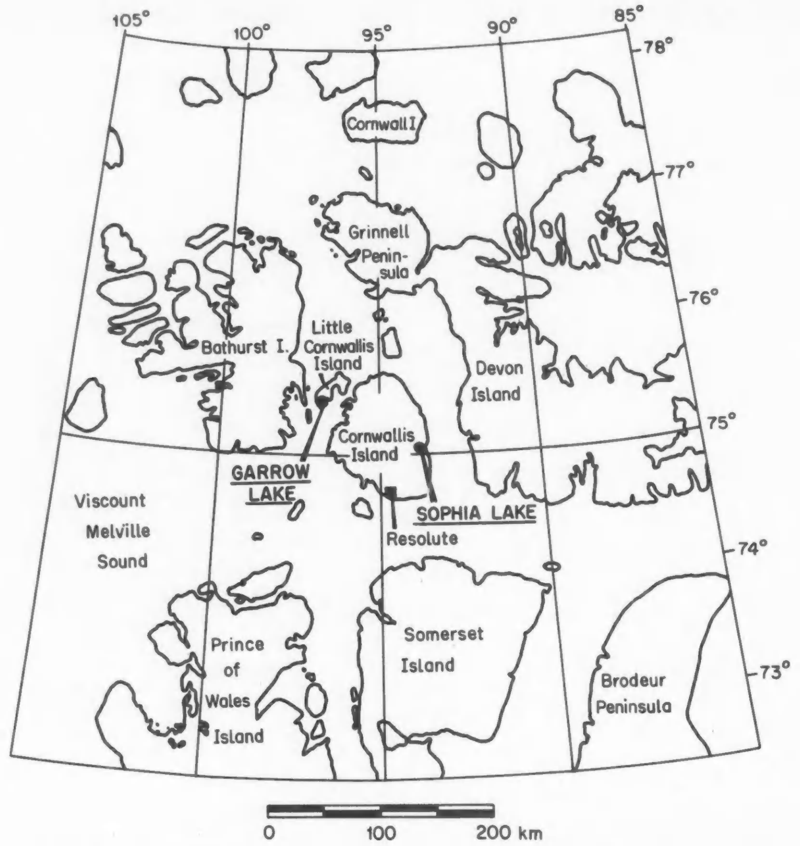

FIG. 1. Portion of the Canadian Archipelago showing the location of Sophia and Garrow lakes.

TABLE 1. Morphometric data of lakes. Note from elevation and depths that both lakes have cryptodepressions.

	Sophia Lake	Garrow Lake
Surface area (ha)	339	432
Area (catchment per lake)	20.1	2.5
Length (km)	4.8	3.2
Volume (10^6 m^3)	75.8	99.1
Maximum depth (m)	50	49
Mean depth (m)	22.4	22.9
Elevation (m)	? but < Garrow	6.7

Water samples from selected depths were collected with a 2.2-L Van Dorn sampler. Dissolved oxygen was determined by the Winkler azide method (American Public Health Association 1971). The major inorganic ions were determined as follows: sodium and potassium by flame photometry, magnesium and calcium by atomic absorption spectrometry, chloride by Mohr titration with silver nitrate, sulfate by MTB colorimetry, and alkalinity by infrared spectrometry of total carbon dioxide. The minor constituents were determined as follows: lead, zinc, and iron by atomic absorption spectrometry and selenium and arsenic by ion chromatography. The imprecision is 2–5 units in the last significant figure given in Table 2.

The ionic balance of the inorganic constituents agreed to within ±3%, leading us to assign the same uncertainty to the major ion concentrations. Chloride, sodium, magnesium, sulfate, calcium, potassium, and bicarbonate, in that order, accounted for 99.9% of the equivalents present. The uncertainty in the heavy metal concentrations was about 10 $\mu g \cdot kg^{-1}$ for the hypersaline lower waters. The more saline waters had to be diluted before analysis, thus accounting for the poorer precision. The arsenic and selenium values probably have detection limits of about 10 $\mu g \cdot kg^{-1}$. Some chemical and physical results for two strings of samples are given in Tables 2 and 3.

Salinities were determined both on the day of sampling by means of an AO Goldberg T/C model 10419 refractometer (0–160‰ range, ±1‰) and, later, from pycnometric measurements of densities (Table 2) and the relation of the latter to salinity (Millero et al. 1976). Densities were estimated for two conditions for application to stability calculations. First, the relationship of Ichiye (1966) was used which states that density increases with salinity approximately 8×10^{-4} $g \cdot cm^{-3}$ for each 1‰ increase. As an example, seawater with a salinity of 32 would have a density of 1.0256 $g \cdot cm^{-3}$. The indirect refractometer determinations of densities were corrected for temperature variations in situ. Second, densities were also determined from 10 to 20°C by means of a pycnometer having an estimated precision of ±0.0005 $g \cdot cm^{-3}$. This latter density

TABLE 2. Chemical and physical properties (ions and TDS in g·kg^{-1} of Sophia (S) and Garrow (G) lakes, August 1982.

Sample depth (m)	Na^+	Mg^{2+}	Ca^{2+}	K^+	Cl^-	SO_4^{2-}	HCO_3^-	TDS[a]	σ_t[b] (g·cm^{-3})	S[c]	θ[d]
S-0	0.32	0.042	0.037	0.009	0.725	0.07	<0.01	1.2	0.5	1.3	0.069
S-5	0.32	0.043	0.037	0.009	0.730	0.07	<0.01	1.2	0.5	1.3	0.069
S-10									0.5	1.3	0.069
S-12									35.0	45	2.533
S-15									35.5	45	2.560
S-20	16.5	2.0	0.74	0.52	28.8	4.3	(0.2)[e]	53.1	39.5	50	2.906
S-30	18.4	2.3	0.75	0.60	29.8	4.8	(0.2)	56.8	40.5	52	3.051
S-33	17.6	2.1	0.72	0.58	31.0	4.6	(0.2)	56.8	43.2	52	3.163
S-40	17.7	2.2	0.73	0.58	31.6	4.6	(0.2)	57.6	43.4	55	3.211
G-0	1.02	0.134	0.078	0.031	2.02	0.25	(0.01)	3.5	2.5	4	0.201
G-5	1.25	0.164	0.091	0.036	2.40	0.30	(0.01)	4.2	3.0	4	0.230
G-10									5.7	6	0.490
G-15									37.3	45	2.614
G-20	20.1	2.7	0.88	0.51	35.3	5.7	(0.2)	65.4	49.5		3.634
G-30	24.5	3.1	1.01	0.74	42.9	6.3	(0.3)	78.8	60.5		4.37
G-40	28.2	3.5	1.12	0.90	49.5	7.2	(0.3)	90.6	69.8		5.23
G-Creek	1.01	0.135	0.088	0.029	2.01	0.25	(0.01)	3.53	2.5		0.201
Seawater	10.0	1.22	0.40	0.32	17.8	2.8	(0.1)	32.6	25.5	32	1.740

[a] Total dissolved solids (sum of columns 2−8) agree within 3% on average with values calculated from 1.806 × (chloride concentration), the conventional method for calculating seawater salinities.

[b] The in situ water density is given by $e_t = 1 + \sigma_t (10^{-3})$. The change in density on going from 0 to 20°C is less than 0.5% for these waters.

[c] Salinity calculated from σ_t (Millero et al. 1976).

[d] Freezing point depression (kelvins) of the samples.

[e] Estimated from 0.06 × (chloride concentration) if below detection limit.

TABLE 3. Heavy metal concentrations (μg·L^{-1}) in 1982.

	Sophia Lake		Garrow Lake	
	Above chemocline	Below chemocline	Above chemocline	Below chemocline
Lead	<1	<100	4	<100
Zinc	4	<200	4	<100
Iron	3	<200	3	<200
Arsenic	<20	<100	<20	<200
Selenium	<10	<100	<10	<100

was converted to the in situ σ_t value by means of the expression $\sigma_t = 10^3 (e_t - 1)$; the in situ density was obtained by a short extrapolation of the laboratory density values to those at the water temperatures. The freezing points were determined with an Advanced Instruments, Inc. osmometer and are precise to 0.001 K.

Total inorganic carbon (TIC), dissolved organic carbon (DOC), and particulate organic carbon (POC) were determined on an Oceanography International Corporation 0524B total carbon system (Oceanography International Corporation 1978). Samples from the field were prepared on the day of sampling for later analysis as follows. For TIC, 40-mL vials (Supelco with teflon lined caps) were filled to overflowing (no air bubbles). Later, Hamilton syringes were used to extract subsamples through the teflon cap for direct injection into the carbon analyzer. For DOC, samples were filtered through precombusted (2 h at 400°C) Gelman glass fiber filters (which retain 99.9% of particles >0.3 μm in size) and acidified with 1.5 M H_3PO_4 to convert all inorganic matter to CO_2. For POC, the filters were placed in borosilicate glass ampules. After acidification of both DOC and POC samples, $K_2S_2O_8$ was added as an oxidant, and the ampules were purged, sealed, and autoclaved (4 h at 130°C) to convert all organic matter to CO_2.

Results and Discussion

Meromictic lakes are normally characterized by their lack of complete vertical mixing, a continuing absence of oxygen in the monimolimnion, and an increase in relative salinity and density with depth below the chemocline. In Sophia and Garrow lakes, the temperature and oxygen concentrations peak at intermediate depths (Fig. 2). In both lakes the maximum oxygen concentration (supersaturated to ~227% in Sophia and 135% in Garrow) lies above the depths of maximum temperature. The intermediate peaking of temperature, found in other saline Arctic lakes that have been cut off from the sea (Hattersley-Smith et al. 1970; Jeffries et al. 1984) and in some Antarctic lakes (Hoare et al. 1964; Yoshida et al. 1975), has been attributed to solar heating through clear waters to a salinity gradient (Shirtcliffe and Benseman 1964; Ragotzkie and Likens 1964). Interestingly, this warm "lens" region is a common feature of heliothermal lakes at wide ranging latitudes within 80° of the equator (Sonnenfeld and Hudec 1980; Kirkland et al. 1983).

The oxygen falls to zero at about the level of the chemocline in Garrow Lake but extends well below the chemocline in Sophia. Arctic regions are generally regarded as being organically depauperate (Remmert 1980). However, given the relatively large ratio of Sophia's catchment area to lake area (Table 1), and potential organic contributions to the highly saline zones with time, such extensive monimolimnetic quantities of oxygen in Sophia are puzzling and unusual for mero-

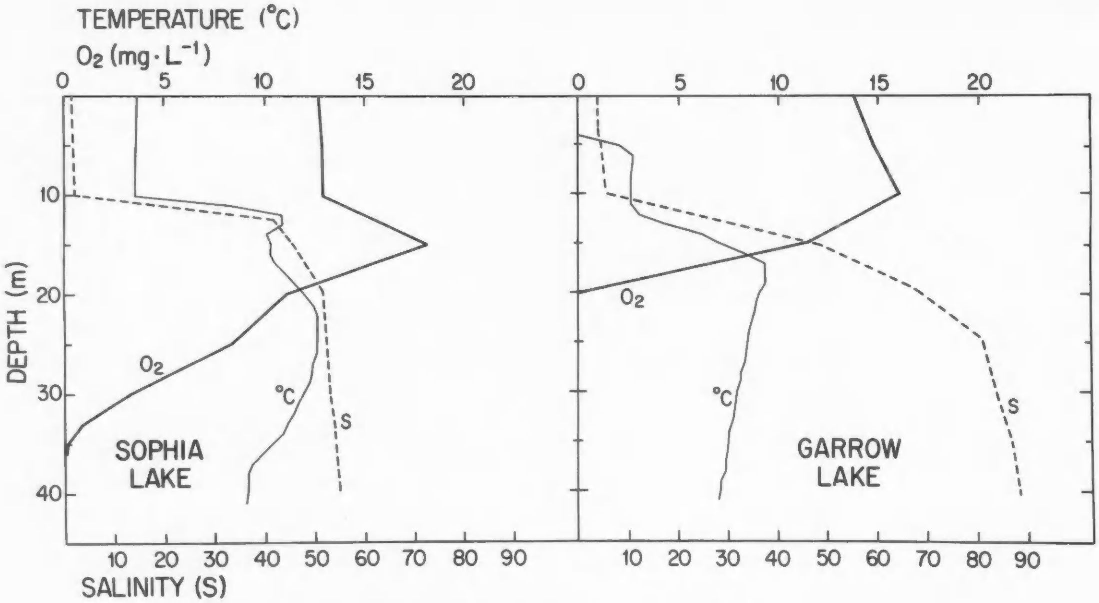

FIG. 2. Profiles of temperature, O_2, and salinity in Sophia (26 August 1982) and Garrow (28 August 1982) lakes.

mictic lakes generally. Oxygen contributions, particularly from descending saline plumes during freeze out, or generation in the lower transparent waters by photosynthetic pelagic and/or benthic flora, are possible mechanisms for enrichment. Subterranean contributions, as postulated for an Antarctic lake by Weand et al. (1975) and for Sophia Lake by Pagé et al. (1984), seem questionable because such additions from the sea would likely have less oxygen and also lower salinity than the hypersaline lower waters of those lakes contain. It is curious that Pagé et al. (1984, their table 1) recorded no oxygen below 11 m in Sophia Lake. In light of our measurements on 26 August 1982 (Fig. 2), rechecked at selected depths on 30 August 1982, and the absence of detectable H_2S at depths <35 m on either of those occasions, we now suspect that the lower water oxygen analyses of Pagé et al. (1984) for Sophia were in error. It is unlikely that annual variations alone would account for such differences between their and our results. We also note an internal inconsistency (poor ion balance) in some other chemical data of Pagé et al. (1984, their table 1).

The comparative semilog plots of light decay (Fig. 3) show a significant change in slope and decrease in light transmission around 20 m for Garrow Lake. The marked turbidity around this level was also noted by Fallis and Harbicht (1980) who attributed it to a bacterial plate. Sharp changes in light attenuation appear to be common features of lakes with bacterial layer and reductive zone associations (Takahashi and Ichimura 1968).

There is a marked increase of TIC from the mixolimnion to the monimolimnion in both lakes (Fig. 4) that generally parallels the corresponding salinity curves (Fig. 2). The particularly large rise in Garrow was also observed in 1980 by Dickman and Ouellet (1983). In comparison, the relative constancy of the DOC and POC pools, as well as their mean DOC:POC ratios of roughly 6:1 or higher, is striking. Such constancy is a feature common to some temperate lakes and has been attributed (Wetzel 1983) to the lack of disturbance by external

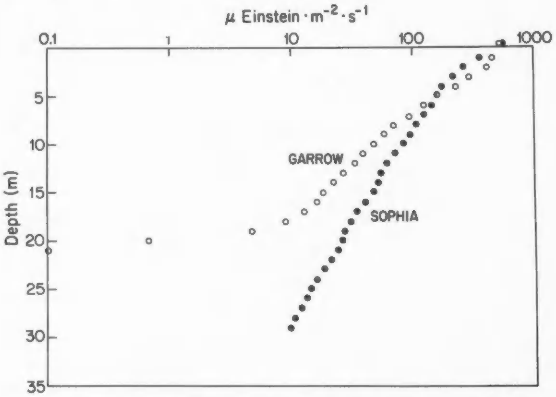

FIG. 3. Decay of PAR irradiance in Sophia (26 August 1982) and Garrow (28 August 1982) lakes. Note the rapid decrease in transmission in Garrow, at about 18–21 m, probably associated with a photosynthetic bacterial layer.

(man's) influence. If so, it will be interesting to see if the anthropogenic inputs (slurry tailings from a lead–zinc mine), being discharged into Garrow Lake since November 1981, will impact the carbon fractions in the future.

A weighted mean salinity was calculated for each lake by a summation of the products of salinities and volume fractions at ≤5 m intervals and assuming horizontal uniformity. Mean salinities were 26–29 for Sophia Lake and 37 for Garrow Lake. These salinities are close to the salinity of the surrounding seawater (~32) and suggest an isolation from the surrounding sea some time in the past.

Stability

As might be expected, in spite of the obvious thermal in-

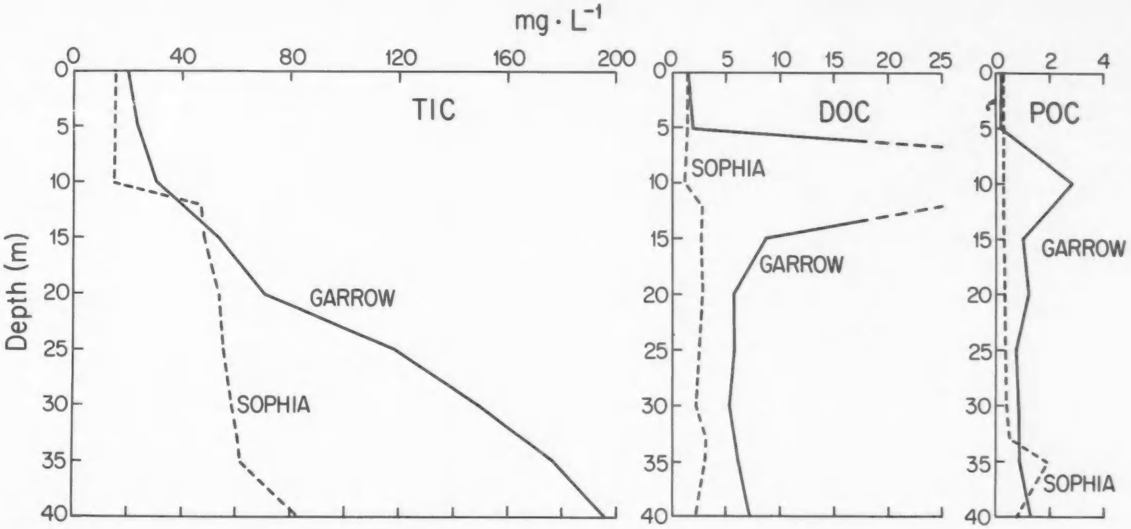

FIG. 4. Profiles of TIC, DOC, and POC in Sophia (26 August 1982) and Garrow (28 August 1982) lakes. The unknown value of DOC at 10 m reflects a single limited sample that was above the instrumental range.

stability (Fig. 2), the hypersaline chemical gradients (Table 2; Fig. 2) prevent complete vertical mixing in either lake and produce a marked hydrostatic stability. Stability here refers to the amount of work required to mix the lake completely without loss or gain of heat. When defined in terms of a unit area (A) at depths (z), acceleration of gravity (g), and center of mass (z_g), stability (S_t) can be calculated from

$$S_t = g\,A_0^{-1}\int_0^{zm}(z - z_g)A_z(\bar{e} - e_z)dz.$$

The equation and symbols are equivalent to those in Hutchinson (1957, p. 510, equation 37) except that we calculated a mean density ($\bar{e}$) for the dates of sampling and then substituted that $\bar{e}$ for the 1 of Hutchinson. This substitution makes the equation more universally applicable and is important when lake water densities exceed 1 $g \cdot cm^{-3}$, as is the case for Sophia and Garrow lakes.

From the salinity relationships discussed earlier, stabilities were calculated from two separate sets of density determinations (Table 4). Other than the differences in numerical stability between the lakes, both approaches give similar results, thus illustrating the overwhelming chemical component to the stability of the lakes. The stabilities are among the highest known and exceed those of some saline lakes in the Antarctic (Burton 1981), as well as some tropical (Lewis 1984) and temperate (Hutchinson 1957) lakes.

Interpretation of Chemical Results

The major ion data (Table 2) can be most simply summarized by comparing them with seawater data. The surface waters (above the chemocline) in either lake appear to be diluted seawater; the waters below the chemocline appear to be concentrated seawater, with no major alteration in the ionic ratios such as would have resulted from differential mineral precipitation or intrusion of saline groundwater.

As a specific check, we compared the similarity of cation milliequivalents in the Arctic lakes with the ocean and with two Antarctic lakes (Table 5). The similarities are of course most obvious in the lower waters of both Sophia and Garrow (also noted in the latter by Fallis and Harbicht 1980). In detail, upper water calcium, especially in Sophia, shows the greatest difference from that of mean seawater. Given the somewhat calcareous nature of surficial material on Cornwallis Island (Cruickshank 1971), runoff contributions from the catchment basin could enhance those mixolimnetic differences over time.

TABLE 4. Stabilities ($ergs \cdot cm^{-2}$) of lakes from two separate sets of density determinations (corrected for in situ temperature).

Lake	Density from relationship to salinty (as in Ichiye 1966)	Density from pycnometer
Sophia	40 800	40 990
Garrow	64 790	59 300

In contrast, milliequivalent percentages in the Antartic lakes Vanda (particularly) and the two basins of Bonney suggest an older or more complicated history (Table 5). Combinations of evaporation, freshwater flooding, and differential precipitation of sodium (first as mirabilite at about four times and then has hydrohalite at around eight times seawater concentration) are believed to be responsible (Thompson and Nelson 1956; Matsubaya et al. 1979).

Heavy Metals (Garrow Lake)

The bottom waters of Garrow Lake contain up to 150 mg dissolved $H_2S \cdot L^{-1}$. At the pH of the lake (7–8) the sulfide concentration should be about 10^{-9} M (Stumm and Morgan 1970). The heavy metal concentrations (Table 3) correspond to $>10^{-7}$ M for lead, zinc, and iron. The solubility products for the sulfides are about 10^{-27}, 10^{-20}, and 10^{-19}, respectively (Vogel 1951), so that the water is enormously oversaturated with the three sulfides. The Polaris mine, located roughly 3 km

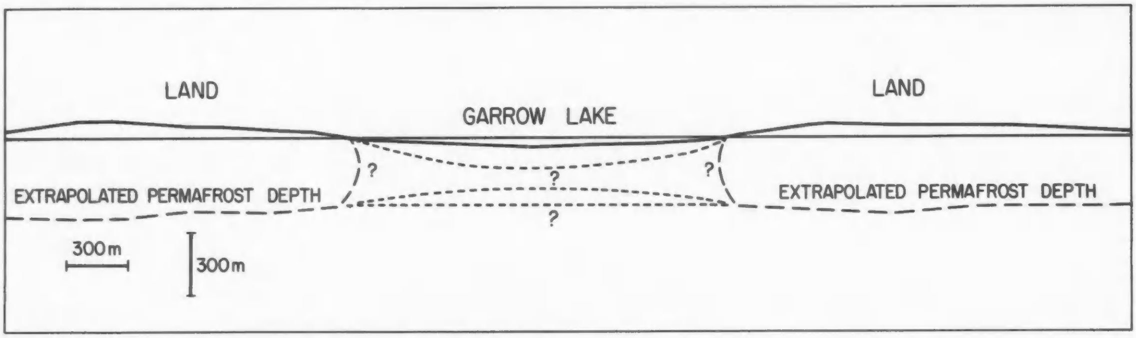

FIG. 5. Schematic representation of possible permafrost distribution along a hypothetical east–west transect through the middle of Garrow Lake. Vertical and horizontal scales are identical.

TABLE 5. Comparative milliequivalent percentages of dominant cations in the ocean and upper and lower waters of four hypersaline polar lakes. Determined from chemical data in (1) Broecker (1974), (2) this paper (1982 data), and (3) Matsubaya et al. (1979) Sophia and Garrow lakes are in the Arctic and Lakes Bonney and Vanda are in the Antarctic (Bonney W and Bonney E = west and east basins of Lake Bonney).

Water body	Depth (m)	Milliequivalent percentages				Reference
		Na^+	Mg^{2+}	Ca^{2+}	K^+	
Ocean		77.7	17.2	3.4	1.6	1
Sophia	5	71.3	18.1	9.4	1.2	2
	40	76.8	18.0	3.6	1.5	2
Garrow	5	74.2	18.4	6.2	1.3	2
	40	77.0	18.1	3.5	1.4	2
Bonney W	5	65.2	22.3	11.1	1.4	3
Bonney W	29.5	63.6	31.3	3.4	1.7	3
Bonney E	5	52.1	22.2	23.9	1.8	3
Bonney E	29.5	47.7	49.2	1.4	1.7	3
Vanda	8	30.1	20.2	46.0	3.7	3
	60	11.5	27.8	60.0	0.6	3

west of Garrow Lake, lies on one of the richest lead–zinc surface deposits in the world (Scales 1982). Therefore, it would not be surprising to find particulate galena, sphalerite, and pyrite in the bottom waters. An inspection of the vertical distribution of the heavy metals and sulfide in the water columns of the sampling site indicates that the water could become unsaturated with heavy metal sulfides above about 15–20 m of depth, which is near the chemocline.

Permafrost and Thermal Chimney

On the basis of earlier temperature profiles, made through the deep permafrost by Cominco Ltd. at the Polaris lead-zinc mine on Little Cornwallis Island, we prepared Fig. 5. Temperatures were measured in three (200–300 m) thermistor-rigged drill holes located in the mine area ~3 km west of Garrow Lake (Burns and Hamilton 1974) and in two shallower drilled holes (54 m, of which only thermistors from 12 m upward functioned properly, and 91 m) located ~0.9 and 0.2 km, respectively, from the south and southeast seaward side of the lake (J. K. Gowans, Cominco Ltd., Polaris, N.W.T. X0A 0Y0). Considerable uncertainties in the extrapolated permafrost depth (Fig. 5) reflect both the limited number of profiles available and the difficulty of instrumenting holes much beyond depths at which drill hole fluid is lost (from >200–300 m) and where temperatures have risen to ~−2°C. Drill hole fluid was lost in two of the three instrumented holes in the mine region. Because they are shallower, the loss of such fluid in the holes on the seaward side of Garrow had not yet been encountered. Linear extrapolation of the temperature profiles with depth provides an approximate 0°C permafrost depth.

Because the depth at which drill hole fluid is lost is reduced significantly as the sea coast is approached (Burns and Hamilton 1974), it is interesting to speculate on whether there is permafrost beneath Sophia and Garrow lakes. Lachenbruch (1968, p. 836) suggested that "if the minimum horizontal dimension of the water body is more than about twice as great as the local undisturbed permafrost depth, an unfrozen *chimney* generally occurs beneath the body of water... unless it was very recently formed." Some support for this rule of thumb comes from a study of two small lakes (roughly 6 ha, 1 m maximum depth and 3 ha, 6 m maximum depth) in the Mackenzie River delta region of the Northwest Territories (Johnson and Brown 1961, 1966). The latter authors found no permafrost beneath the lakes proper to the depth of their drilling (~73 m in the shallower and ~98 m in the deeper lake) whereas permafrost was encountered within a few metres of the landward side of the lake edge and its thickness increased rapidly with distance from shore.

Owing to their greater size, depth, and unusually warm lower waters, it would seem that Sophia and Garrow lakes should have an unfrozen thermal chimney also. However, seismic and drilling data reveal that subsea permafrost from earlier times may extend many kilometres off shore in some Arctic regions (Hunter et al. 1976; Neave and Sellman 1982). This might be expected given the fairly rapid transgression of Arctic seas onto the land in some regions, thus causing a slow degradation of the cold terrestrial permafrost (Lachenbruch et al. 1982). Granted, the temperature of the seawater (−1.7 ± 0.1°C, Burns and Hamilton 1974) surrounding the Cornwallis Islands is markedly less than that of the lower lake waters, but it seems unlikely that permafrost would extend laterally well below the mud–water interface and effectively seal the hypersaline lakes. The age and rate of expanding (aggrading) or contracting (degrading) of deep permafrost on the Cornwallis Islands are uncertain, as is specific knowledge of possible earlier glacial and isostatic episodes. Consequently, until seismic or drill hole data are available from beneath the lakes proper, it will be difficult to confirm the presence or absence of permafrost beneath Sophia and Garrow. Interestingly, as

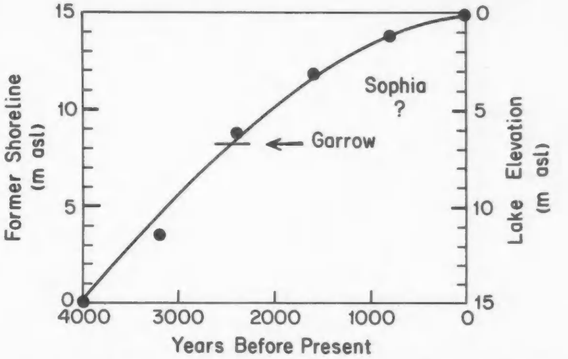

FIG. 6. Elevation of the former shoreline near Resolute on Cornwallis Island during 800-yr stages (solid circles along curve) of the past 4000 yr (from estimates of Andrews et al. 1971) in comparison with present lake surface elevations.

part of some initial geophysical exploration by the Cominco Ltd. lead–zinc mine, plans were made one year to drill through the center of Garrow Lake to check for permafrost beneath the lake. The lake ice became unsafe unexpectedly early that year and the project was never pursued (R. Burns, P.O. Box 519, Pine Point, N.W.T. X0E 0W0).

Evolution of Hypersalinity

Based on the estimates of Andrews et al. (1971), shorelines that formed 4000 yr before present (B.P.) near Resolute on Cornwallis Island are now about 15 m above sea level (asl) (Fig. 6). This time and elevation estimate also fits within the emergence-curve envelopes of Washburn and Stuvier (1985, their fig. 2). Washburn and Stuvier (1985) also showed that the uplift on Cornwallis Island has slowed dramatically from an initial rate of emergence of $8.3\ \mathrm{m}\cdot(100\ \mathrm{yr})^{-1}$ for the first 75 m to about $0.5\ \mathrm{m}\cdot(100\ \mathrm{yr})^{-1}$ for the last 40 m. Consequently, given the relative proximity of the lakes to Resolute, the current lake surface elevations (Table 1), and the shoreline thresholds near the outlet within 1 m of the lake elevation, we could estimate roughly that Garrow Lake separated from the sea ~2500–3000 yr ago (Fig. 6). This period encompasses the estimates of 2600 B.P. (Fallis and Harbicht 1980), 3000 B.P. (Dickman and Ouellet 1983), and 2580 ± 260 B.P. (Pagé et al. 1984, carbon-dated sample of 1982 from 35 m in Garrow Lake) for the age of Garrow Lake. Though not available for this paper, the surface elevation of Sophia Lake is known (M. Dickman, Biological Sciences, Brock University, St. Catharines, Ont. L2S 3A1) to be substantially less than that of Garrow Lake. Therefore, if the curve drawn from the data of Andrews et al. (1971) in Fig. 6 is valid, Sophia Lake should have separated from the sea more recently and be younger. No ^{14}C dates were included by Pagé et al. (1984) for Sophia, but a higher percentage of modern carbon was found in its lower waters.

Although the uper water values of the δ^{18}O isotope are fairly similar in both lakes, as are comparative lower water values, Pagé et al. (1984) attributed the higher percent of modern carbon in the lower brines of Sophia Lake to recent seepage of seawater into the lake through taliks or seasonally unfrozen zones or underlake chimneys.

Further, Pagé et al. (1984) have recently suggested, on the basis of isotopic studies, that meromixis in Garrow Lake developed crenogenically. Specifically, they felt that the high salinity of the lower waters developed from brine production (i.e. solute rejection from the surrounding ground to the lake during uplift and permafrost growth). As evidence, they cited the lower (more negative) values of the heavier δ^{18}O isotope in the mixolimnion and higher (less negative) values in the monimolimnion.

The Case for Hypersaline Gradients by Permafrost

The argument of Pagé et al. (1984) seems initially plausible because there is some slight enrichment (~3%) of the δ^{18}O isotope in the ice during freezing (Matsubaya et al. 1979; Pagé et al. 1984). Consequently, ice forming at the lake surface would tend to have less negative values than the saline water descending from brine exclusion during freeze out. Of course, isotopic enrichment in ice could gradually become isotopic impoverishment, as laboratory studies of Souchez and Jouzel (1984) have shown, if a huge volume fraction of a water body were to freeze. However, although the early details of the glacial climatic history of Cornwallis Islands are unknown, it seems unlikely that the present depth of freezing (roughly 2–2.5 m, ≥10% of the lake volume) would at one time have been great enough (say 35 m, >90% of the lake volume) to significantly alter the present isotopic profile.

Further, if the land were once covered by seawater, the groundwater, at least near the sediment–water interface, should have a composition closer to that of the sea than groundwater from land not so covered. Finally, although many salts besides those of seawater will lower the freezing point, the fact that some bore hole fluid was lost in the drill holes when a temperature of ~−2.0°C was reached at least attests to some salts being present.

The Case for Hypersaline Gradients by Freeze Out

The concentration of brines from seawater (Thompson and Nelson 1956) and development of hypersaline gradients in saline polar lakes (Goldman et al. 1967) have been attributed to the freezing out of salts and gases from the ice cover. Indeed, a much lower but significant increase in salts and gases during freeze out has been documented from freshwater lakes as well (Welch 1974; Barica 1977; Rigler 1978; Canfield et al. 1983).

The descent of brines excluded from sea ice does not take place merely by slow downward molecular diffusion because, even if one assumed an instantaneous uplift and separation (instead of a much more likely and slower separation during uplift) after the first or a few annual cycles in the two closed Arctic lakes, subsequent less dense saline layers would have to move against a density gradient. In fact, slow upward diffusion would be more likely from the more saline lower waters (Toth and Lerman 1975). However, hypersaline profiles could develop rapidly, even with a climate and ice thickness similar to the present, if there was a mechanism by which the brines formed during freeze out were concentrated. Such a mechanism occurs naturally and is well documented in mechanics, heat transfer, and oceanographic literature.

During the freezing of sea ice, there is rejection of concentrated brines in the form of narrow "salt fingers" (Lake and Lewis 1970; Fedorov 1972; Farhadieh and Tankin 1975) which easily lead to thermohaline convection (Grange et al. 1977). The salt is rejected through narrow brine channels in the ice matrix as the ice thickens. The salinity and density of the descending salt fingers vary with initial salinity and rate of sea ice growth. Generally, the salinity increases at reduced rates of ice growth. Starting with a seawater salinity of 33, Wakatsuchi and Ono (1983) found that the salinity of the excluded brines, collected by positioning funnels within a few centimetres of the descending ice front, ranged from 42.3 to 92.7. It is noteworthy that the salinity of the seawater and that of the excluded brines is similar to the seawater surrounding the Cornwallis Islands and the monimolimnetic brines of the lakes, respectively. Wakatsuchi and Ono (1983) and Wakatsuchi (1977) observed relatively little diffusion of the descending salt fingers into the seawater just below the ice. Whether or not the integrity of these long and relatively dense salt fingers could be maintained for several metres as they descend, either individually or in aggregated plumes to the bottom or to an equilibrium density, is unknown. However, the fact that hypersaline brines can be formed in one season, merely by freeze out from above, was documented by Schell (1973) and Coyle (1974) when they found salinities of ~40−72 in water below sea ice in some shallow (≤2.5 m) and restricted coastal waters of the Alaskan Beaufort Sea. In two extreme cases, Schell (1973) found salinities of ~126−183 where the ice was within a few centimetres of (or on) the bottom.

Following some interesting dye studies in small (2−10 ha) freshwater Arctic lakes, Welch and Bergmann (1985) hypothesized that the normal convective pattern in winter was for water immediately below the ice to move laterally toward the shore, picking up cryoconcentrated salts enroute, and then sink downslope. Upward displacement in the central region of the lake would theoretically complete the cycle. Whether such conclusions apply to much larger and saline lakes is open to further investigation. Obviously, however, if a descending saline plume hits a bottom slope before it finds an equilibrium density, it will flow down the slope.

Prior to the time of lake−sea separation on the Cornwallis Islands, there should have been lower δ^{18}O values throughout the lakes more similar to those of the connecting sea. During uplift and isolation, freeze out from above would have made the lower waters somewhat more negative than they were originally while at the same time making them rapidly more saline and increasingly resistant to vertical mixing. Indeed, the ^{14}C value of 2580 ± 260 B.P. of Pagé et al. (1984) suggests that the lower stable waters of Garrow Lake have mixed relatively little with the upper water since separation. As far as the more negative (δ^{18}O) upper mixed waters are concerned, they are more simply explained by meteoric contributions over time which can be added (by runoff and direct precipitation) or lost (outflow).

We feel that the interpretation of Pagé et al. (1984) unnecessarily stresses bottom (permafrost) and lateral (talik) contributions to explain the hypersalinity. We do not discount all such possible contributions during the course of an unknown and complex history. However, we feel that freeze out from the surface is a more likely and dominant factor in the evolution of the hypersaline gradients in Sophia and Garrow lakes. If freeze out were the process, it should be expected to impact every lake on either island. *It does* — but would tend to cause permanent hypersaline gradients in those very few lakes that were saline relicts (or cutoff fjords) initially. In contrast, if permafrost growth were the process by which salts were pushed into the lakes from below or laterally, it should also impact all the lakes on both islands and generate numerous hypersaline bodies above and beyond those that might have been saline relicts. However, *this is not the case*. Therefore, freeze out leading to the development of a cryogenic meromixis (as in Goldman et al. 1967), not crenogenic meromixis (as in Pagé et al. 1984), is the most plausible mechanism.

The possible role of double-diffusive convection in either the early structuring or the present maintenance of thermal−salinity gradients in Sophia and Garrow lakes is unknown. However, double-diffusive convection, i.e. where salt (diffusing about 100 times more slowly than heat, Terwilliger and Dizio 1970) and temperature make opposing contributions to the density, is known to play a role in the microstratification of the oceans (Gregg 1973; Huppert and Turner 1981) and in the density gradients of Lake Vanda in the Antarctic (Huppert and Turner 1972). Future measurements with greater spatial and temporal resolution may provide new insights into the possible significance of this intriguing phenomenon on density gradients in Sophia and Garrow lakes.

Acknowledgments

We acknowledge the aid of the staff and pilots of Polar Shelf in Resolute on Cornwallis Island and cooperation of J. Gowan and C. Bennett at Cominco Ltd. on Little Cornwallis Island, N.W.T. All helicopter and twin Otter flights to Sophia and Garrow lakes, and all logistical support at Resolute, N.W.T., were supplied by the Energy, Mines and Resources Polar Continental Shelf Program through a research grant to Dr. Mike Dickman, Biological Sciences Department, Brock University, St. Catharines, Ont. L2S 3A1. We are grateful for this financial support. The Water Quality Laboratory at the NWRI in Burlington, Ont., determined major ions and heavy metals. M. Pendl and R. Rumer from SUNY/Buffalo aided in the determination of carbon fractions and calculations of stability, respectively. H. Welch from the Freshwater Institute in Winnipeg, Man., kindly provided some morphometric data. P. Sellman of the CRREL in Hanover, NH, and T. Coplen of the USGS in Reston, VA, contributed helpful discussions on permafrost.

References

American Public Health Association, American Water Works Association, and Water Pollution Control Federation. 1971. Standard methods for the examination of water and wastewater. 13th ed. Washington, DC. 874 p.

Andrews, J. T., R. McGhee, and L. McKenzie-Pollock. 1971. Comparison of elevations of archeological sites and calculated sea levels in Arctic Canada. Arctic 24: 210−228.

Barica, J. 1977. Effects of freeze-up on major ion and nutrient content of a prairie winterkill lake. J. Fish. Res. Board Can. 34: 2210−2215.

Blake, W. 1964. Preliminary account of the glacial history of Bathurst Island, Arctic Archipeligo. Geol. Surv. Can. Pap. 64-30: 8 p.

Broecker, W. S. 1974. Chemical oceanography. Harcourt Brace Jovanovich, Inc., New York, NY. 214 p.

Burns, R., and J. M. Hamilton. 1974. Some geophysical and hydrological aspects of permafrost in the Cornwallis Island area, N.W.T., p. 80−91. *In* National Research Council of Canada Tech. Memo. 113. NRC, Ottawa, Ont.

Burton, H. R. 1981. Chemistry, physics, and evolution of Antarctic saline lakes. Hydrobiologia 82: 339−362.

Canfield, D. E., R. W. Bachmann, and M. W. Hoyer. 1983. Freeze-out of salts in hard-water lakes. Limnol. Oceanogr. 28: 970−977.

Coyle, K. O. 1974. The ecology of the phytoplankton of Prudhoe Bay, Alaska, and the surrounding waters. M.S. thesis, University of Alaska, Fairbanks, AK. 106 p.

Cruickshank, J. G. 1971. Soils and terrain units around Resolute, Cornwallis Island. Arctic 24: 195−209.

Dickman, M., and M. Ouellet. 1983. Limnological aspects of meromictic Lake Garrow. Que. Univ. (INRS-Eau) Rep. 73: 25 p.

Fallis, B. W., and S. M. Harbicht. 1980. A preliminary study of the limnology and biology of Garrow Lake, N.W.T. Tech. Rep. Fish. Aquat. Sci. Department of Fisheries and Oceans, Winnipeg, Man. 76 p.

Farhadieh, R., and R. S. Tankin. 1975. A study of freezing of sea water. J. Fluid Mech. 71: 293−304.

Fedorov, K. N. 1972. Thermohaline convection in the form of salt fingers and its possible manifestations in the ocean. Izv. Acad. Sci. USSR Atmos. Oceanic Phys. 8: 122−130. (English edition)

Goldman, C. R., D. T. Mason, and J. E. Hobbie. 1967. Two Antarctic desert lakes. Limnol. Oceanogr. 12: 295−310.

Grange, B. W., R. Viskanta, and W. H. Stevenson. 1977. Interferometric observation of thermohaline convection during freezing of saline solution. Lett. Heat Mass Transfer 4: 85−92.

Gregg, M. C. 1973. The microstructure of the ocean. Sci. Am. 228(2): 64−77.

Hattersley-Smith, G., J. E. Keys, H. Serson, and J. E. Mielke. 1970. Density stratified lakes in northern Ellesmere Island. Nature (Lond.) 225: 55−56.

Hoare, R. A., K. B. Popplewell, D. A. House, R. A. Henderson, W. M. Prebble, and A. T. Wilson. 1964. Lake Bonney, Taylor Valley, Antarctica: a natural solar energy trap. Nature (Lond.) 202: 886−888.

Hunter, J. A. M., A. S. Judge, H. A. Macauly, R. L. Good, R. M. Gagne, and R. A. Burns. 1976. Permafrost and frozen sub-seabottom materials in the southern Beaufort Sea. Beaufort Sea Proj. Tech. Rep. 22, Department of the Environment, Victoria, B.C. 174 p.

Huppert, H. E., and J. S. Turner. 1972. Double-diffusive convection and its implications for the temperature and salinity structure of the ocean and Lake Vanda. J. Phys. Oceanogr. 2: 456−461.

1981. Double-diffusive convection. J. Fluid Mech. 106: 299−329.

Hutchinson, G. E. 1957. A treatise on limnology. Vol. 1. John Wiley & Sons, Inc., New York, NY. xiv + 1015 p.

Ichiye, T. 1966. Density, p. 229−230. *In* R. W. Fairbridge [ed.] The encyclopedia of oceanography. Reinhold, New York, NY.

Jeffreis, M. O., H. R. Krouse, M. A. Shakur, and S. A. Harris. 1984. Isotope geochemistry of stratified Lake "A", Ellesmere Island, N.W.T., Canada. Can. J. Earth Sci. 21: 1008−1017.

Johnson, G. H., and R. J. Brown. 1961. Effect of a lake on distribution of permafrost in the Mackenzie River delta. Nature (Lond.) 192: 251−252.

1966. Occurrence of permafrost at an Arctic Lake. Nature (Lond.) 211: 952−953.

Kirkland, D. W., J. P. Bradbury, and W. E. Dean. 1983. The heliothermic lake — a direct method of collecting and storing solar energy. Arch. Hydrobiol. (Suppl.) 65, 1: 1−60.

Lachenbruch, A. H. 1968. Permafrost, p. 833−839. *In* R. W. Fairbridge [ed.] The encyclopedia of geomorphology. Reinhold, New York, NY.

Lachenbruch, A. H., J. H. Sass, B. V. Marshall, and T. H. Moses Jr. 1982. Permafrost, heat flow, and the geothermal regime at Prudhoe Bay, Alaska. J. Geophys. Res. 87: 9301−9316.

Lake, R. A., and E. L. Lewis. 1970. Salt rejection by sea ice during growth. J. Geophys. Res. 75: 583−597.

Lewis, W. M. 1984. A five-year record of temperature, mixing and stability for a tropical lake (Lake Valencia, Venezuela). Arch. Hydrobiol. 99: 340−346.

Matsubaya, O., H. Sakai, T. Torii, H. Burton, and K. Kerry. 1979. Antarctic saline lakes — stable isotopic ratios, chemical compositions and evolution. Geochim. Cosmochim. Acta 43: 7−25.

Millero, F. J., A. Gonzalez, and G. K. Ward. 1976. The density of seawater solutions at one atmosphere as a function of temperature and salinity. J. Mar. Res. 34: 61−93.

Neave, K. G., and P. V. Sellman. 1982. Subsea permafrost in Harrison Bay, Alaska: an interpretation from seismic data. U.S. Army Cold Regions Research and Engineering Report 82-24, Hanover, NH. 62 p.

Oceanography International Corporation. 1978. Operating procedures manual for 0524B total carbon system. College Station, TX. 74 p.

Pagé, P., M. Ouellet, C. Hillaire-Marcel, and M. Dickman. 1984. Isotopic analyses (^{18}O, ^{13}C, ^{14}C) of two meromictic lakes in the Canadian Arctic Archipelago. Limnol. Oceanogr. 29: 564−573.

Ragotzkie, R. A., and G. E. Likens. 1964. The heat balance of two Antarctic lakes. Limnol. Oceanogr. 9: 412−425.

Remmert, H. 1980. Arctic animal ecology. Springer-Verlag New York, Inc., Secaucus, NJ. 250 p.

Rigler, F. H. 1978. Limnology in the high Arctic: a case study of Char Lake. Int. Ver. Theor. Angew. Limnol. Verh. 20: 127−140.

Scales, M. 1982. High Arctic wizardry: Polaris mine on stream. Can. Min. J. 103(7): 24−41.

Schell, D. M. 1973. Seasonal variation in the nutrient chemistry and conservative constituents in coastal Alaskan Beaufort sea waters, p. 217−281. *In* V. Alexander et al. (16 authors). Sea Grant Report 73-16, IMS Report R-74-1, University of Alaska, Fairbanks, AK.

Shirtcliffe, T. G. L., and R. F. Benseman. 1964. A sun-heated Antarctic lake. J. Geophys. Res. 69: 3355−3359.

Sonnenfeld, P., and P. P. Hudec. 1980. Heliothermal lakes, p. 93−100. *In* A. Nissenbaum [ed.] Hypersaline brines and evaporitic environments. Developments in sedimentology. 28. Elsevier Scientific Publishing Company, New York, NY.

Souchez, R. A., and J. Jouzel. 1984. On the isotopic composition in D and ^{18}O of water and ice during freezing. J. Glaciol. 30: 369−372.

Stumm, W., and J. J. Morgan. 1970. Aquatic chemistry. Wiley-Interscience, New York, NY. 583 p.

Takahashi, M., and S. Ichimura. 1968. Vertical distribution and organic matter production of photosynthetic sulfur bacteria in Japanese lakes. Limnol. Oceanogr. 13: 644−655.

Terwilliger, J. P., and S. F. Dizio. 1970. Salt rejection phenomena in the freezing of saline solutions. Chem. Eng. Sci. 25: 1331−1349.

Thompson, T. G., and K. H. Nelson. 1956. Concentration of brines and deposition of salts from sea water under frigid conditions. J. Sci. 254: 227−238.

Thorsteinsson, R. 1958. Cornwallis and Little Cornwallis Island, District of Franklin, Northwest Territories. Geol. Surv. Can. Memo. 294: 134 p.

Toth, D. J., and A. Lerman. 1975. Stratified lake and oceanic brines: salt movement and time limits of existence. Limnol. Oceanogr. 20: 715−728.

Vogel, A. I. 1951. A textbook of quantitative inorganic analysis. Longmans, Green, London. 918 p.

Vowinckel, E., and S. Orvig. 1970. The climate of the North Polar Basin, p. 129−252. *In* S. Orvig [ed.] World survey of climatology. 14. Climates of the polar region. Elsevier, New York, NY.

Wakatsuchi, M. 1977. Experiments on haline convection induced by freezing of sea water. Low Temp. Sci. Ser. A 35: 249−258. (In Japanese with English summary)

Wakatsuchi, M., and N. Ono. 1983. Measurements of salinity and volume of brine excluded from gowing sea ice. J. Geophys. Res. 88(C5): 2943−2951.

Washburn, A. L., and M. Stuvier. 1985. Radiocarbon dates from Cornwallis Island area, Arctic Canada — an interim report. Can. J. Earth Sci. 22: 630−637.

Weand, B. L., R. D. Fortner, R. C. Hoehn, and B. C. Parker. 1975. Subterranean flow into Lake Bonney. Antarct. J. U.S. 10: 15−19.

Welch, H. E. 1974. Metabolic rates of arctic lakes. Limnol. Oceanogr. 19: 65−73.

Welch, H. E., and M. A. Bergmann. 1985. Water circulation in small arctic lakes in winter. Can. J. Fish. Aquat. Sci. 42: 506−520.

Wetzel, R. G. 1983. Limnology. Saunders College Publishing, Philadelphia, PA. 767 p. + R81 + I10.

Yoshida, W., T. Torii, Y. Yusa, S. Nakaya, and K. Moriwaki. 1975. A limnological study of some lakes in the Antarctica. Bull. R. Soc. N.Z. 13: 311−320.

Analysis of the Phytoplankton Composition of 95 Labrador Lakes, with Special Reference to Natural and Anthropogenic Acidification

J. Chris Earle and Hamish C. Duthie

Department of Biology, University of Waterloo, Waterloo, Ont. N2L 3G1

and David A. Scruton

Department of Fisheries and Oceans, Fisheries Research Branch, P.O. Box 5667, St. John's, Nfld. A1C 5X1

Earle, J. C., H. C. Duthie, and D. A. Scruton. 1986. Analysis of the phytoplankton composition of 95 Labrador lakes, with special reference to natural and anthropogenic acidification. Can. J. Fish. Aquat. Sci. 43: 1804–1811.

Phytoplankton abundances and accompanying morphometric, physical, and chemical data from 95 Labrador lakes were subjected to statistical analysis to determine the structure of the phytoplankton communities and to relate environmental factors to the patterns observed. Factor analysis of the 22 measured physical and chemical variables reduced the data to six derived environmental factors: hardness, dystrophy, lake size, salinity, oligotrophy, and seasonality. The analysis showed that the low-pH lakes are associated with dystrophy and hence are likely to be naturally acidic. There was no evidence of anthropogenic acidification. Eight groups of co-occurring taxa were recognized from the data set, and all but two exhibited relatively consistent habitat preferences. It was suggested that the groups represent "species associations" in the sense that each group contains taxa that occur together because of similar requirements for a specific set of environmental conditions. Several lake types were identified as potentially influencing the distribution of phytoplankton in Labrador: small, dystrophic lakes; clear, softwater lakes; clear, hardwater lakes; large, hardwater lakes; and coloured, hardwater lakes.

Des données relatives à l'abondance du phytoplancton dans 95 lacs du Labrador de même que des données relatives à des paramètres morphométriques, physiques et chimiques connexes ont fait l'objet d'une analyse statistique visant à déterminer la structure des communautés phytoplanctoniques et à établir des relations entre les facteurs environnementaux et les tendances observées. L'analyse par facteurs des 22 variables physiques et chimiques mesurées a permis de réduire les données en six facteurs environnementaux : la dureté, le caractère dystrophe, la taille du lac, la salinité, le caractère oligotrophe et la saisonnalité. L'analyse a montré l'existence d'une corrélation entre l'état dystrophe et les lacs à faible pH qui ont donc tendance à être naturellement acides. Il n'y avait aucun indice d'acidification anthropogène. Huit groupes de taxons simultanément présents ont été identifiés à partir de l'ensemble des données et, à l'exception de deux, ces groupes présentaient des préférences d'habitat relativement constantes. On a émis l'hypothèse que ces groupes formaient des « associations d'espèces » en se sens que chacun d'eux était formé de taxons présents ensemble à cause d'exigences semblables quant à un ensemble précis de conditions environnementales. Les auteurs ont identifié plusieurs types de lacs pouvant influer sur la distribution du phytoplancton au Labrador. Ce sont les petits lacs dystrophes, les lacs à eau douce et transparente, les lacs à eau dure et transparente, les lacs à eau dure de grande dimension et les lacs à eau dure et colorée.

Received January 20, 1986
Accepted May 22, 1986
(J8650)

Reçu le 20 janvier 1986
Accepté le 22 mai 1986

Although the freshwater algae of Labrador have been investigated both taxonomically and ecologically, a comprehensive study of the phytoplankton is lacking. Early taxonomic work was carried out by Cedercreutz (1944), Gardner (1949), and Croasdale and Grönblad (1964); more recently, Duthie et al. (1975, 1976, 1978) published several annotated lists of freshwater algal taxa from western Labrador. The first major ecological study was conducted by Duthie and Ostrofsky (1974), and the first estimates of phytoplankton primary productivity in Labrador lakes are in Ostrofsky and Duthie (1975). Information on phytoplankton biomass and seasonality is given in Ostrofsky and Duthie (1980), and limnological research on Labrador lakes and reservoirs is summarized in Duthie (1979) and Duthie and Ostrofsky (1982).

A limnological and fisheries survey of 95 Labrador lakes has recently been carried out (Scruton 1984) with the purpose of obtaining a reference source of information against which any future changes resulting from acidic precipitation could be evaluated. The survey, which included phytoplankton, made it possible to investigate relationships among phytoplankton communities and their physical and chemical environments throughout Labrador.

Our major objectives are to identify the structure of the freshwater phytoplankton communities of Labrador using cluster analysis, to characterize the structure of the abiotic environment using factor analysis, and then to determine the critical environmental variables related to the phycological organization observed from a correlation of the species abundances and the factor scores.

Methods

Field and Laboratory Analyses

Ninety-five headwater lakes situated throughout Labrador (Fig. 1) were sampled by floatplane and helicopter in August through October 1982 for phytoplankton and a suite of morphometric, physical, and chemical variables (Scruton 1984). The sampling procedures and protocol were established by the Scientific Advisory Committee for National Inventory Survey of the effects of long range transport of atmospheric pollutants (LRTAP). An overview of the LRTAP program is provided in Kelso et al. (1986).

Phytoplankton samples were collected by dipping a wide-mouth bottle below the water surface. The samples were then preserved immediately with Lugol's iodine. Morphometric data were collected at the site from echo-sounding transects, and watershed data were derived from maps and airphotos.

Measurements for alkalinity, free carbon dioxide, and dissolved oxygen were made in a mobile field laboratory. The pH of the surface waters was measured at the site using a combination glass and reference electrode pH meter (Radiometric model 26). Samples for chemical analysis were kept cool and in the dark until analysed. Alkalinity determinations were made by gram titration within 24 h of collection, and free carbon dioxide was determined by potentiometric titration within 12 h of collection. Determinations of dissolved oxygen content were carried out using the Winkler titration method. The other physical and chemical analyses, major ions, orthophosphate, sulphate, nitrate, colour, and turbidity, were performed at the Environmental Chemistry Laboratory of the Victoria Public Hospital in Halifax, Nova Scotia. A detailed account of the methodology of all the physical and chemical analyses is provided in Kendaris (1982).

Phytoplankton Enumeration

The phytoplankton were identified and enumerated using the methods described in Ostrofsky and Duthie (1980). A combined minimum of 500 cells, colonies, and filaments were counted per sample. Counts were expressed as cells per litre and milligrams per cubic metre. Biomass was estimated from calculations of cell volume based on seven geometric shapes selected to approximate the different shapes exhibited by freshwater algae (Janus and Duthie 1979).

Statistical Methods

The statistical approach used to help interpret the data involved a series of cluster, factor, and correlation analyses. The biological data matrix was first reduced to a smaller subset of 80 species based on Orlóci's (1978) sum of squares variance procedure. The algorithm calculates the individual proportion of the total variance accounted for by each of the species. To reduce the data set, species that failed to explain any independant share of the total variance were eliminated. This criterion was adopted because such species can provide no new information about the structure of the phytoplankton communities. The reduced data set was then transformed ($\ln(X + 1)$) in an effort to achieve a normal distribution of the variables and homoscedasticity. The Kolmogorov–Smirnov–Lilliefors test indicated that all but the rarest species, amounting to 8% of the total taxa, were reasonably normalized by the transformation ($\alpha = 0.10$). The morphometric, physical, and chemical data were standardized ($X - \bar{X}/\text{SD}$) to reduce the variables to a common scale because many had either incompatible units or large numeric differences.

A complete-linkage cluster procedure was then used to examine the phytoplankton data for evidence of species associations. The term "association" in this study is used in the context of a group of co-occurring species having similar reactions to properties of the environment. The cluster analysis was based on a matrix of Spearman correlation coefficients calculated from the abundances of the 80 selected species.

Finally, an attempt was made to correlate the algal taxa comprising these associations with the morphometric, physical, and chemical variables thought to regulate their distributions in lakes. Correlations of species abundances with individual variables are, however, difficult to interpret because many environmental variables are highly correlated with one another. However, such interdependence is often caused by underlying factors which cannot be accounted for by any single variable. Exploratory factor analysis simplifies the relationship between interdependent variables by creating a smaller number of synthesized variables or factors. Each factor represents the portion of the original variables that relate to the same environmental parameter. As a result, factor analysis represents the covariance structure of the original variables in terms of a hypothetical causal model. Factor analysis was performed on a correlation matrix among the morphometric, physical, and chemical variables from the 95 Labrador lakes, and the principal-axes factoring solution was then rotated using an orthogonal rotation method (VARIMAX) to simplify the factor structure. The correlation coefficients between the six derived factors and the original 22 variables were computed. Lastly, the scores from the six factors were correlated with the abundances of the phytoplankton species by a Spearman correlation analysis to interpret the intraspecific preferences of the phytoplankton. Therefore, each factor potentially represents an environmental property influencing phytoplankton growth and distribution in the lakes. The general environmental preferences of the groups of co-occurring algae were interpreted by a comparison of results for each species association.

Results

The phytoplankton identified from the 95 lakes in this study consisted of 389 taxa. The mean number of taxa per lake was 61, ranging from 29 to 106. A species list including nomenclatural authorities has been provided in Earle et al. (1986).

The dendrogram from the complete-linkage cluster analysis (Fig. 2) indicates that the Labrador phytoplankton can be partitioned into eight different species associations. There were two reasons for selecting this level. First, the eight-group level is the last with a statistically reasonable number of species (>90%) that exhibit significant differences between the cluster groups, significance ($\alpha = 0.10$) having been determined by analysis of variance. Second, the eight-group solution roughly corresponds to the structure of the physical and chemical environment of the lakes described in the factor analysis. The level of environmental structure discerned is primarily dependent on sampling frequency and seasonal differences at the time of sampling. In this study, six factors were derived from the original 22 physical and chemical variables (Table 1). Factor 1, which explains 27% of the total variance, is highly correlated with alkalinity, calcium, magnesium, potassium, and pH. It may be considered a hardness factor. Factor 2, which explains

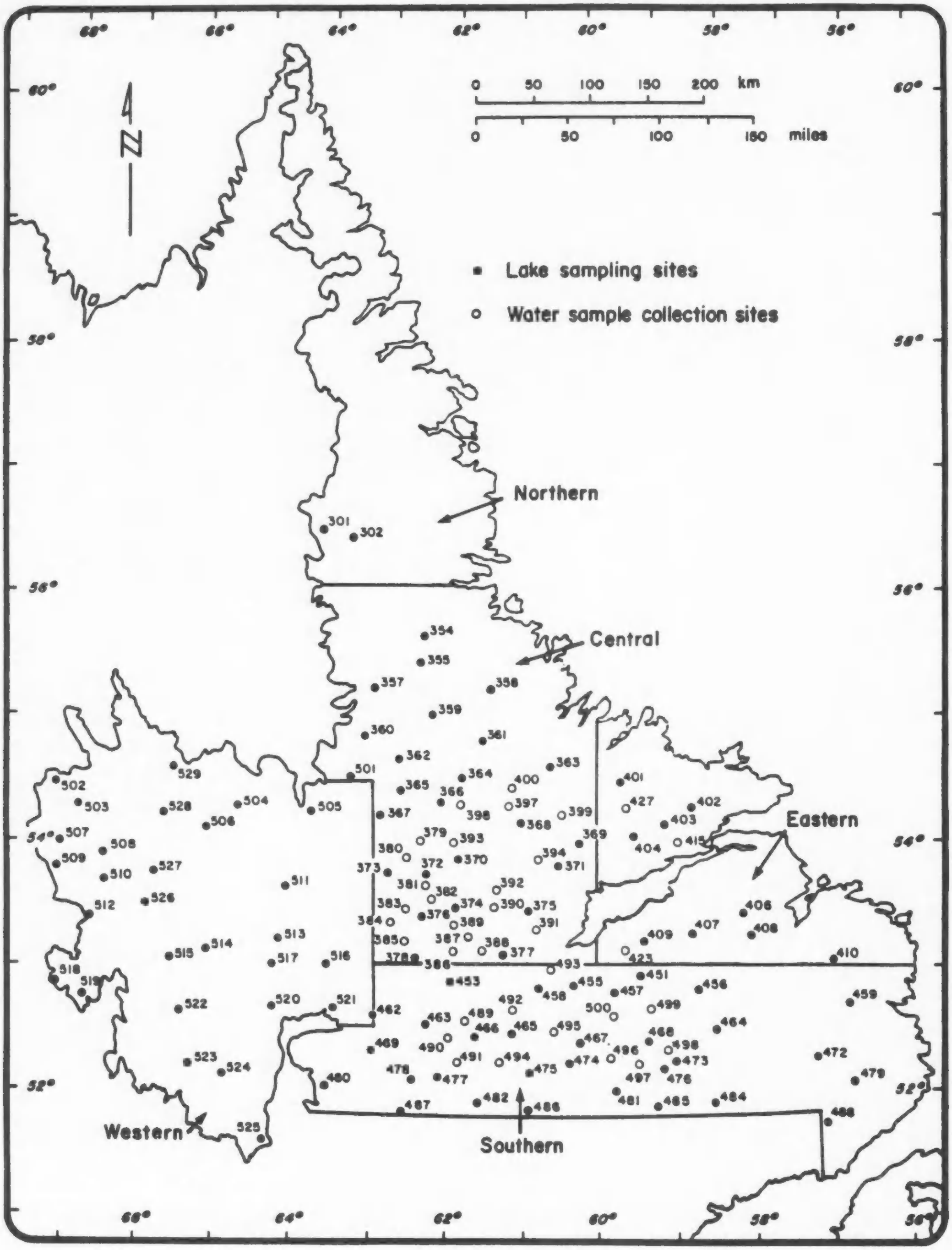
68°
66°
64°
62°
60°
58°
56°
60°
58°
56°
54°
52°
N
0 50 100 150 200 km
0 50 100 150 miles
Lake sampling sites
Water sample collection sites
Northern
Central
Eastern
Western
Southern
301
302
354
355
357
358
359
360
361
362
363
364
365
366
367
368
369
370
371
372
373
374
375
376
377
378
379
380
381
382
383
384
385
386
387
388
389
390
391
392
393
394
397
398
399
400
401
402
403
404
406
407
408
409
410
415
423
427
451
453
455
456
457
458
459
460
462
463
464
465
466
467
468
469
472
473
474
475
476
477
478
479
481
482
484
485
486
487
488
489
490
491
492
493
494
495
496
497
498
499
500
501
502
503
504
505
506
507
508
509
510
511
512
513
514
515
516
517
518
519
520
521
522
523
524
525
526
527
528
529

FIG. 1. Location of lakes sampled in Labrador.

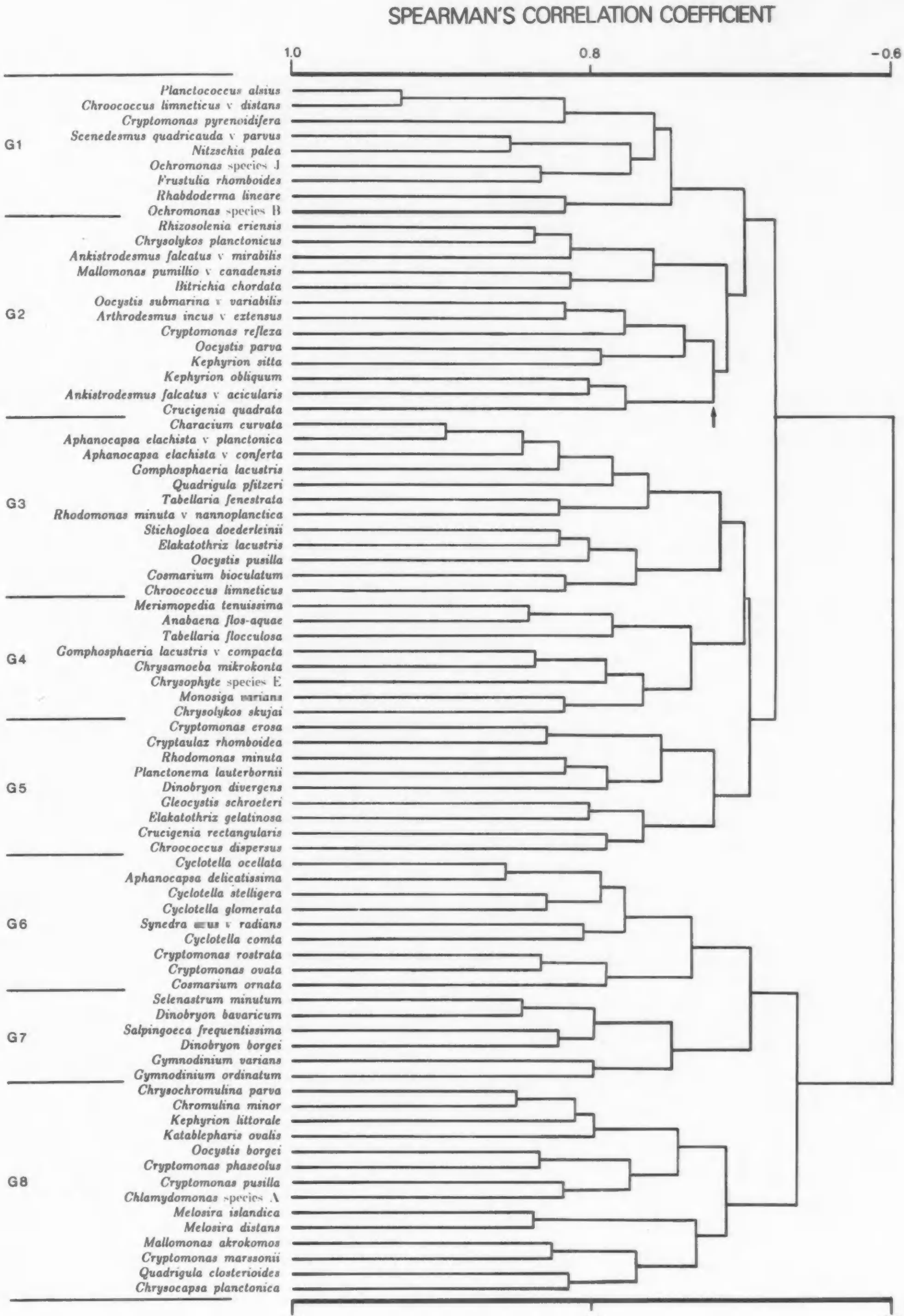

FIG. 2. Results of a complete-linkage cluster analysis of 80 selected phytoplankton taxa based on their abundance in 95 Labrador lakes. Arrow indicates the eight cluster-group level.

TABLE 1. Factor analysis of 22 physical, chemical, and morphometric variables. Correlation coefficients are between the six derived factors and the original 22 variables. Nonsignificant coefficients (i.e. <0.250) have been omitted.

	Factor					
Variable[a]	1 Hardness	2 Dystrophy	3 Lake Size	4 Salinity	5 Oligotrophy	6 Seasonality
Alkalinity	0.961					
Calcium	0.972					
Magnesium	0.954					
Potassium	0.724					
pH	0.628	−0.419				
Colour		0.902				
DOC		0.880			−0.384	
TDS	0.407	0.753				
Turbidity		0.703				
Sulphate	0.471	0.633				
LSA			0.832			
DA			0.816	0.307		
Sodium				0.855		
Chloride		0.374		0.645		
Secchi depth		−0.464			0.742	
Max. depth		−0.247			0.708	
Water temp.						0.726
CO_2		0.396				−0.410
DO				0.286		−0.583
Nitrate						
SLD						
Orthophosphate						
% variance explained	27.0	25.1	10.3	9.8	9.5	8.3

[a] DOC = dissolved organic carbon, TDS = total dissolved solids, LSA = lake surface area, DA = drainage area, DO = dissolved oxygen, SLD = shoreline development.

25% of the variance, is highly correlated with colour, dissolved organic carbon, total dissolved solids, turbidity, and sulfate and can be considered a dystrophy factor. Factor 3 is correlated with two variables reflecting overall lake size and explains 10.3% of the total variance in the data set. High loading by sodium and chloride on Factor 4 indicates that it represents salinity. Factor 5, which is positively correlated with Secchi depth and maximum depth and negatively correlated with dissolved organic carbon, may represent clear-water oligotrophic conditions. Factor 6, which is associated with water temperature, free carbon dioxide, and dissolved oxygen, probably reflects seasonal differences in water chemistry more than differences between lakes.

Table 2 indicates that a large number of phytoplankton species were strongly correlated with Factor 1 (hardness). This group included *Rhodomonas minuta*, *R. minuta* var. *nannoplanctica*, *Gomphosphaeria lacustris*, *Cryptomonas erosa*, and *Chrysolykos skujai*. Representatives of these positively correlated species occurred in all but Groups 1 and 2. There were only three species negatively correlated with Factor 1: *Kephyrion obliquum*, *Gymnodinium varians*, and *Ankistrodesmus falcatus* var. *mirabilis*. Two of these belong to Group 2, which has only four members.

Both species of *Melosira* found commonly in Labrador, *M. distans* and *M. islandica*, along with several other species, including *Cryptomonas pyrenoidifera*, *Cryptomonas ovata*, and *Nitzschia palea*, are highly correlated with Factor 2, dystrophy. Except for *C. ovata*, which belongs to Group 6, all the species positively correlated with dystrophy belong to either Group 1 or 8. Many more species, including *Cyclotella comta*, *Cyclotella ocellata*, *Selenastrum minutum*, *Dinobryon bavaricum*, and *Aphanocapsa delicatissima*, are negatively associated with dystrophy. They occur in Groups 2 through 7 but are most prevalent in Group 3 where they comprise about 60% of the association.

Many species are associated with lake size (Factor 3) including *Anabaena flos-aquae*, *Tabellaria fenestrata*, *Chrysamoeba mikrokonta*, and *Chrysochromulina parva*. Only four species are negatively correlated with this factor: *Cryptomonas pyrenoidifera*, *Chroococcus limneticus* var. *distans*, *Frustulia rhomboides*, and an unidentified species of *Ochromonas* (species J). All four species occur in Group 1.

Species positively associated with salinity (Factor 4) include *Synedra acus* var. *radians*, *Gomphosphaeria lacustris*, *Chrysolykos planctonicus*, and *Rhodomonas minuta*. Negative correlations are observed for *Oocystis pusilla*, *Merismopedia tenuissima*, and *Cryptomonas phaseolus*. The only trend readily evident is that Group 8 contains three negatively correlated taxa and none that are positively correlated.

Factor 5, oligotrophy, shows significant correlation with *Ankistrodesmus falcatus* var. *mirabilis*, *Kephyrion obliquum*, *Cryptaulax rhomboides*, *Cyclotella comta*, *Cyclotella ocellata*, and *Selenastrum minutum*. Only three species showed a negative correlation with oligotrophy: *Mallomonas akrokomos*, *Scenedesmus quadricauda* var. *parvus*, and *Nitzschia palea*. With the exception of Group 2, none of the other associations are consistently positive or negative for this factor. Within Group 2, however, two of the four species are nonsignificantly

TABLE 2. Spearman correlation coefficients and associated probabilities between seven derived factors and the abundance of selected species. Nonsignificant correlations (<0.18; prob. >0.10) have been omitted. Other critical values are 0.20 (prob. = 0.05) and 0.25 (prob. = 0.01). Species having no significant correlation with any of the six factors were eliminated from the table.

	Factor					
Species	1 Hardness	2 Dystrophy	3 Lake Size	4 Salinity	5 Oligotrophy	6 Seasonality
Group 1						
Chroococcus limneticus var. *distans*			−0.21			
Cryptomonas pyrenoidifera		0.32	−0.27			
Frustulia rhomboides		0.18	−0.21			
Nitzschia palea		0.25	0.21			
Ochromonas species J			−0.30			
Scenedesmus quadricauda var. *parvus*		0.21			−0.29	
Group 2						
Ankistrodesmus falcatus var. *mirabilis*	−0.19				0.31	
Chrysolykos planctonicus				0.22		
Kephyrion obliquum	−0.23	−0.20			0.33	
Oocystis submarina var. *variabilis*		−0.18				
Group 3						
Aphanocapsa elachista var. *planctonica*	0.20	−0.25		0.18		0.24
Aphanocapsa elachista var. *conferta*		−0.23				0.17
Characium curvata		−0.20				0.20
Chroococcus limneticus		−0.20				
Cosmarium bioculatum					−0.30	−0.30
Gomphosphaeria lacustris	0.43	−0.24		0.25		
Oocystis pusilla				−0.33		
Quadrigula pfitzeri	0.25					
Rhodomonas minuta var. *nannoplanctica*	0.27					
Stichogloea doederleinii		−0.21				
Tabellaria fenestrata	0.25		0.31			
Group 4						
Anabaena flos-aquae			0.32			0.20
Chrysamoeba mikrokonta	0.18		0.27			
Chrysolykos skujai	0.27		0.21			
Gomphosphaeria lacustris var. *compacta*			0.18			
Merismopedia tenuissima				−0.24		
Monosiga varians	0.18		0.23			
Group 5						
Crucigenia rectangularis		−0.20				
Cryptaulax rhomboidea					0.18	
Cryptomonas erosa	0.33					
Dinobryon divergens	0.19	−0.20	0.21			
Elakatothrix gelatinosa		−0.19				
Planctonema lauterbornii	0.19					
Rhodomonas minuta	0.52		0.19	0.21		−0.28
Group 6						
Aphanocapsa delicatissima		−0.29				
Cryptomonas ovata		0.24				
Cyclotella comta	0.27	−0.28	0.26		0.26	
Cyclotella ocellata		−0.17			0.21	−0.20
Synedra acus var. *radians*			0.22	0.30		
Group 7						
Dinobryon bavaricum		−0.33				−0.29
Dinobryon borgei			0.18			
Gymnodinium varians	−0.22					
Salpingoeca frequentissima	0.18					
Selenastrum minutum		−0.33			0.22	
Group 8						
Chrysocapsa planctonica	0.18					
Chrysochromulina parva	0.17		0.23			

TABLE 2. (*Concluded*)

Species	Factor 1 Hardness	 2 Dystrophy	 3 Lake Size	 4 Salinity	 5 Oligotrophy	 6 Seasonality
Cryptomonas marssonii				−0.18		
Cryptomonas phaseolus				−0.19		
Cryptomonas pusilla		0.19		−0.33		
Mallomonas akrokomos					−0.33	
Melosira distans		0.42	0.19			−0.26
Melosira islandica	0.18	0.35	0.18			
Oocystis borgei	0.19					

correlated.

Several species are correlated with Factor 6, which has a strong loading on water temperature, carbon dioxide, and dissolved oxygen. Group 3 was the only association that had more than a single member correlated with this factor. In Group 3, three species were positively correlated with Factor 6, and one species, *Cosmarium bioculatum*, was negatively correlated.

Discussion

Lake Chemistry and Phytoplankton Ecology

Clustering and ordination analysis suggest that the Labrador phytoplankton may consist of at least eight different species associations. The size of these associations appears to vary greatly, and not all members of an association are highly similar to one another. Many species that join a cluster at low similarity levels appear to be relatively cosmopolitan in their distribution, possibly as a result of adapting to a wide range of environmental conditions. Species that are not correlated with any of the factors (i.e. the 27 species excluded from Table 2) are obvious examples.

Correlations between individual species and the seven synthersized factors should be interpreted with care. Furthermore, the ecological literature should be consulted routinely to ensure that the interpretation is realistic. The abundances of the two species of *Melosira* in our samples, *M. distans* and *M. islandica*, were highly correlated with dystrophy. Although the former is common in acidic and dystrophic lakes (Hudon et al. 1986), the latter species is usually considered to favour circumneutral oligotrophic waters (Davis and Anderson 1985). Two other planktonic diatoms, *Cyclotella comta* and *Cyclotella ocellata*, are often considered to be oligotrophic taxa, and this agrees with their apparent distribution in Labrador.

Most planktonic diatoms are significantly correlated with Factor 3, lake size, possibly as a consequence of wind-driven circulation, which tends to keep these "heavy" algae from sinking out. The strong negative correlation of *Frustulia rhomboides* with Factor 3 is expected, since this is a benthic diatom favouring dystrophic lakes. It is more difficult to explain the positive correlation of lake size with several other taxa, e.g. *Anabaena flos-aquae*, *Chrysochromulinas parva*, and *Chrysamoeba mikrokonta*, although all three are common in the Laurentian Great Lakes (Munawar and Munawar 1981).

The sodium chloride content of lakes (Factor 4) appears to correlate highly with the abundances of a number of species, which suggests that it may influence their distributions. These species may be regarded as halophiles because they appear to be stimulated by small amounts of salts. Species associated with salinity appear to be most abundant in lakes closest to the sea where oceanic spray can significantly influence the ionic character of the lake water. A discussion of the influence of ionic balance on the phytoplankton of Labrador lakes may be found in Duthie and Ostrofsky (1974). Only a few species (e.g. *Mallomonas akrokomos* and *Scenedesmus quadricauda* var. *parvus*) show a strong negative correlation with oligotrophy (Factor 5), suggesting that most species respond to the increased nutrients found in lakes with higher productivity.

Several species are negatively associated with water temperature and positively associated with free carbon dioxide and dissolved oxygen (Factor 6). Initially this observation might suggest that many species prefer cool water. If this explanation were valid, depth should also have contributed significantly on Factor 6 because deep lakes are usually cooler than shallow lakes. However, this was not observed. As an alternative explanation, significant correlations between species abundances and Factor 6 are probably a consequence of the time of year in which the samples were collected. Species sampled in midsummer tend to demonstrate a positive correlation with temperature when the cool-water spring and fall forms are less abundant. This interpretation reveals a problem inherent in much of the data. Different sampling periods introduce seasonal variability that can mask relationships between the biological and the physical and chemical variables. Conservative variables, such as sodium and chloride, and the broadly based synthesized factors, such as dystrophy, may be more valuable in this sort of analysis.

Comparisons of the results of the Spearman correlation analysis for the eight phytoplankton associations suggest that the environmental conditions represented by the six synthesized factors substantially influence species distribution. Many of the eight associations of co-occurring taxa appear to require a distinct set of environmental conditions. For example, Group 1 probably prefers small dystrophic lakes whereas Group 3 appears to require clear, hard waters. Group 4 appears to favour large lakes with high mineral content, and Group 5 may require either hard water or extremely clear-water conditions. This also suggests that groups of algae do indeed co-occur because of similar requirements for specific environmental conditions. Such a phenomenon, although expected on theoretical grounds, has not previously been adequately demonstrated for freshwater phytoplankton. Part of the reason for this has been that, until now, large comprehensive data sets for specific regions were scarce.

Despite the demonstrated affiliations with measured environmental conditions, many associations display a considerable amount of heterogeneity. All eight associations contain at least one species with environmental preferences different from those of most species in the association. This suggests that the six synthesized factors fail to account fully for the observed species distributions. Additional factors not revealed in this study are probably responsible for this heterogeneity. Indeed, an entire realm of biological factors, such as competition, parasitism, and selective grazing, are not considered at all.

Lake Acidification

The existing and potential effects of acidic precipitation on Canadian lakes are a problem of national concern. It is worthwhile, therefore, to consider the possible effect that anthropogenic acidification may have had on Labrador lakes and the usefulness of multivariate analyses to detect it. As a variable in the factor analysis, pH has significant negative loadings on only one of the six derived factors. In Factor 2, low pH is associated naturally with highly coloured dystrophic water. The factor analysis demonstrates that atmospheric deposition of acids has not resulted in a substantial reduction of the pH of Labrador lakes. There are a sufficient number of clear unbuffered lakes, which, if they had received acid from anthropogenic sources, would have diverged from the nonaffected lakes in the factor analysis. Under these conditions, one would expect to find a factor with a significant loading on pH as well as on other variables that represent susceptible (i.e. unbuffered) clear-water lakes. The data show no evidence of a negative loading on pH other than in association with naturally acidic dystrophic water. Indeed, Factor 5, which represents the clear-water, poorly buffered lakes of Labrador, had negligible loading on pH (−0.004). We conclude that there is no evidence for anthropogenic acidification. It is noteworthy that in the Sept-Îles region of northeast Quebec, Hudon et al. (1985) found evidence for recent lake acidification from recorded pH measurements and from sedimentary diatom analysis.

Acknowledgements

N. MacNeill assisted in the phytoplankton enumeration and in the preparation of the manuscript. Funds were provided by a contract from the Department of Fisheries and Oceans and from an NSERC operating grant to H.C.D.

References

Cedercreutz, C. 1944. Freshwater algae from Labrador. Mem. Soc. Fauna Flora Fenn. 19: 216−222.

Croasdale, H., and R. Grönblad. 1964. Desmids of Labrador 1. Desmids of the southeastern coastal area. Trans. Am. Microsc. Soc. 83: 142−212.

Davis, R. B., and D. S. Anderson. 1985. Methods of pH calibration of sedimentary diatom remains for reconstructing history of pH in lakes. Hydrobiologia 120: 69−87.

Duthie, H. C. 1979. Limnology of subarctic Canadian lakes and some effects of impoundment. Arct. Alp. Res. 11: 145−158.

Duthie, H. C., and M. L. Ostrofsky. 1974. Plankton, chemistry, and physics of lakes in the Churchill Falls region of Labrador. J. Fish. Res. Board Can. 31: 1105−1117.

1982. Use of phosphorus budget models in reservoir management. Can. Water Res. J. 7: 337−348.

Duthie, H. C., M. L. Ostrofsky, M. R. Screenivasa, and D. J. Brown. 1975. Freshwater algae from western Labrador. Nova Hedwigia 26: 17−31, 253−268, 555−560.

1976. Freshwater algae from western Labrador. Nova Hedwigia 27: 909−917.

1978. Freshwater algae from western Labrador. Nova Hedwigia 29: 237−242.

Earle, J. C., H. C. Duthie, and D. A. Scruton. 1986. A statistical analysis of the phytoplankton composition of selected Labrador lakes, with special reference to natural and anthropogenic acidification. Can. Techn. Rep. Fish. Aquat. Sci. In press.

Gardner, G. 1949. Algues, lichens, mousses, hepatiques recoltées au Labrador à la Baie d'Hudson. Mem. Soc. Bot. France 32: 74−94.

Hudon, C., H. C. Duthie, S. M. Smith, and S. A. Ditner. 1986. Relationships between lakewater pH and sedimentary diatoms in the Matamek watershed, northeastern Quebec, Canada. Hydrobiologia (In press)

Janus, L. L., and H. C. Duthie. 1979. Phytoplankton and primary production of lakes in the Matamek Watershed, Quebec. Int. Rev. Gesamten Hydrobiol. 64: 89−98.

Kelso, J. R. M., C. K. Minns, J. E. Gray, and M. L. Jones. 1986. Acidification of surface waters in eastern Canada and its relationship to aquatic biota. Can. Spec. Publ. Fish. Aquat. Sci. 87: 42 p.

Kendaris, T. A. 1982. An acid rain inventory survey of selected Labrador Lakes. Technical report, Department of Fisheries and Oceans, DSS File No. 07SC.FP001-2-1168: 52 p.

Munawar, M., and I. F. Munawar. 1981. A general comparison of the taxonomic composition and size analyses of the phytoplankton of the North American Great Lakes. Verh. Int. Ver. Limnol. 21: 1695−1716.

Orlóci, L. 1978. Multivariate analysis in vegetation research. 2nd ed. Dr. W. Junk, Publishers, Boston, MA. 451. p.

Ostrofsky, M. L., and H. C. Duthie. 1975. Primary productivity and phytoplankton of lakes on the eastern Canadian Shield. Verh. Int. Ver. Limnol. 19: 732−738.

1980. Trophic upsurge and the relationship between phytoplankton biomass and productivity in Smallwood Reservoir, Canada. Can. J. Bot. 58: 1174−1180.

Scruton, D. A. 1984. A survey of selected lakes in Labrador, with an assessment of lake status and sensitivity in relation to acid precipitation. Can. Tech. Rep. Fish. Aquat. Sci. 1296: v + 115 p.

Three-Dimensional Distribution of Winter Stonefly Nymphs, *Allocapnia pygmaea*, within the Substrate of a Southern Ontario River

C. W. Pugsley[1] and H. B. N. Hynes[2]

Department of Biology, University of Waterloo, Waterloo, Ont N2L 3G1

Pugsley, C. W., and H. B. N. Hynes. 1986. Three-dimensional distribution of winter stonefly nymphs, *Allocapnia pygmaea*, within the substrate of a southern Ontario river. Can. J. Fish. Aquat. Sci. 43: 1812–1817.

Changes in the three-dimensional distribution patterns of stonefly nymphs, *Allocapnia pygmaea*, beneath the streambed in the Speed River, southern Ontario, were monitored throughout their 1-yr life cycle using 270 colonization chambers. These were filled with organism-free, sieved stream gravel and buried in vertical groups of three, at three depth intervals, in three trenches positioned across a riffle. Nymphs were present throughout the year. Seasonal changes in the distribution pattern of nymphs indicated that they were able to move beneath the streambed in both the horizontal and vertical planes. Nymphs were most abundant at depth during the summer diapause, but moved up to the surface once diapause had been broken in the autumn. There was no evidence of any bankwards migration of nymphs prior to emergence. We have therefore confirmed in detail previous suggestions that stream insects move freely into and out of the hyporheic, using it as a refuge from adverse conditions on the streambed. Stream ecologists should therefore be aware of the possibilities of movement to and from the hyporheic when working with benthic invertebrates.

Les variations de la distribution tridimensionnelle de nymphes de plécoptères, *Allocapnia pygmaea*, dans le lit de la rivière Speed, du sud de l'Ontario, ont été contrôlées tout au long du cycle vital d'une année de ces organismes. Les auteurs ont utilisé 270 enceintes de colonisation remplies de gravier du cours d'eau tamisé et exempt d'organismes. Les enceintes ont été enfouies à la verticale par groupes de trois, à trois profondeurs différentes. Elles ont été placées dans trois failles traversant un haut-fond. Des nymphes ont été décelées tout au long de l'année. Les variations saisonnières des distributions ont montré que les nymphes pouvaient se déplacer à l'intérieur du lit, tant à l'horizontale qu'à la verticale. Elles étaient plus abondantes en profondeur au cours de la diapause d'été, mais se déplacaient vers la surface après la fin de la diapause, en automne. Il n'y avait aucun indice d'une migration des nymphes vers les rives avant l'émergence. Les auteurs ont donc confirmé de façon détaillée des hypothèses selon lesquelles les insectes des cours d'eau se déplacaient librement ou sortaient de la zone hyporhéique qu'ils utilisaient comme refuge lorsque les conditions sur le lit devenaient mauvaises. Les écologistes spécialistes de ce domaine devraient donc prendre note des possibilités de déplacement tant à l'intérieur que vers l'extérieur de la zone hyporhéique au cours de leurs études des invertébrés benthiques.

Received May 14, 1985
Accepted May 7, 1986
(J8241)

Reçu le 14 mai 1985
Accepté le 7 mai 1986

Many studies of stream invertebrates concentrate entirely on what happens in the top 10 cm of streambed; however, the presence of a hyporheic zone populated by both stream and groundwater faunas has now been widely documented (e.g. Danielpol 1980; Hynes 1983; Pugsley and Hynes 1983). In the traditional two-dimensional approach to stream ecology, variables are measured along the horizontal plane of the stream channel, while spatial variability in the third, or depth, dimension is ignored. Godbout and Hynes (1982) established the value of the three-dimensional approach. For example, they found that even within a small section of apparently uniform riffle the depth distribution of fauna was highly variable. In addition, they discovered effects on insect distribution which were related to variations in the flow rate of upwelling groundwater, a parameter rarely measured in benthic studies.

The free movement of many stream insects into and out of the deeper levels of the streambed has wide-ranging implications for our understanding of their ecology. For example, it may help to explain the following phenomena: (1) the temporary disappearance of species from streams at certain times of their life cycle (Hynes 1970); (2) the rapid recolonization of streams after the surface benthos has been destroyed (Williams and Hynes 1974) by pollution (Sterba 1978), spates (Bishop 1973; Hynes 1968, 1974; Poole and Stewart 1976), drought (Bishop 1973; Williams 1977), or drawdown of upstream reservoirs (Kaster and Jacobs 1978); (3) the diurnal fluctuation in stream drift resulting from changes in the density of fauna on the surface of the streambed (Campbell 1980; Kovalak 1978); and (4) the seasonal change that occurs in the vertical distribution of stream benthos (Bretschko 1981; Godbout and Hynes 1982; Morris and Brooker 1979; Poole and Stewart 1976;

---

[1] Present address: Flat 2, 47a Shakespeare St., Greymouth, New Zealand.

[2] Author to whom reprint requests should be addressed.

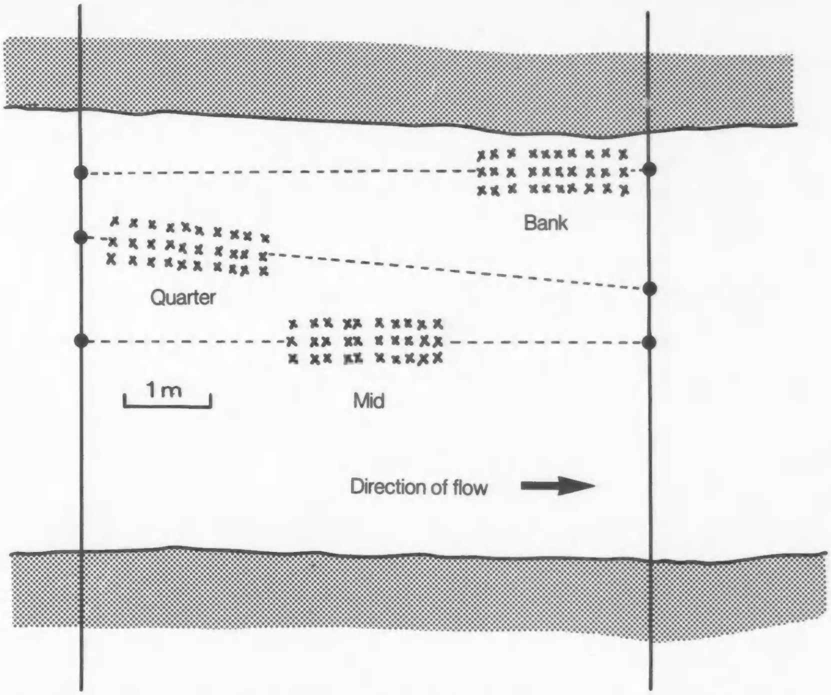

FIG. 1. Plan of the Speed River study site (banks stippled) showing the actual mapped positions of each set of three colonization chambers (crosses) buried at depths of 10, 30, and 50 cm. Steel cables (solid lines) and sliding rope positions (broken lines) used in the mapping and relocation of the buried chambers are also shown.

Williams and Hynes 1974).

The aim of this study was to record in detail the movement of stream insects to and from the hyporheic zone. This was considered necessary in order to confirm what had previously been only a suggestion: that the hyporheic functions as an extension of the benthic habitat, offering a convenient refuge from adverse conditions on the streambed. We focused on the winter stonefly *Allocapnia pygmaea* (Burmeister) (Plecoptera, Capniidae) because diapausing nymphs of this species had previously been found in the hyporheic and were abundant at the study site (Harper and Hynes 1970, 1972).

Methods

Colonization chambers ($n = 270$) containing organism-free, uniform-sized stream gravels were buried on 28 April 1981 in three trenches dug in the bed of the Speed River, southern Ontario (43°43′50″N, 80°15′50″W). We used chambers rather than a freeze-core sampler (Pugsley and Hynes 1983) to eliminate the effect of substrate variability (Mestrov et al. 1976) on the distribution of nymphs. The sampling site was previously described by Bishop and Hynes (1969) and Williams and Hynes (1974). The chambers were plastic cylinders, 9 cm long and 7.6 cm in diameter, closed at each end with 1.5-mm-mesh fibreglass flyscreen. Each chamber was labelled conspicuously for ease of identification.

Chambers were laid in the bottom of each trench (2 × 1 × 0.5 m deep), in a grid pattern (Fig. 1), with the long axis of each chamber aligned with the stream flow. Yellow plastic pegs were used to mark their position before the trench was refilled to a depth of 30 cm with excavated material. A second tier of chambers was then laid out directly above the first. The marker pegs were raised and the trench backfilled until it was 10 cm deep. A third tier of chambers was then positioned directly above the other two. Before the trench was completely refilled, a map of the position of each vertical set of three chambers was prepared so that they could be recovered even in winter from below the ice. The mapping was done as follows. Two steel cables were stretched across the width of the stream, one upstream and the other downstream of the three trenches. These cables were removable, each being attached by tensioning hooks to two stout cedar trees on either side of the stream. A rope was tied between these two cables, i.e. parallel with the stream flow, in such a way that it could be moved freely to any position (Fig. 1). For each of the three trenches, the rope was aligned with the center line of the 10 chambers in each trench and the position at both ends was marked on the cables. A plumb line was then suspended over each of the chambers in turn, starting at the upstream end. The horizontal distance between the plumb line (directly above the chamber) and the upstream steel cable was then measured for each chamber. The two outer rows of chambers in each trench were located 30 cm from, and at 90° to, the centre line on either side of it (Fig. 1). Once mapped, the chambers and markers were completely buried and the surface boulders replaced.

On 10 sampling dates between 31 May 1981 and 10 June 1982, three randomly selected vertical sets of three chambers were lifted from each of the three trenches (i.e. $n = 27$ per

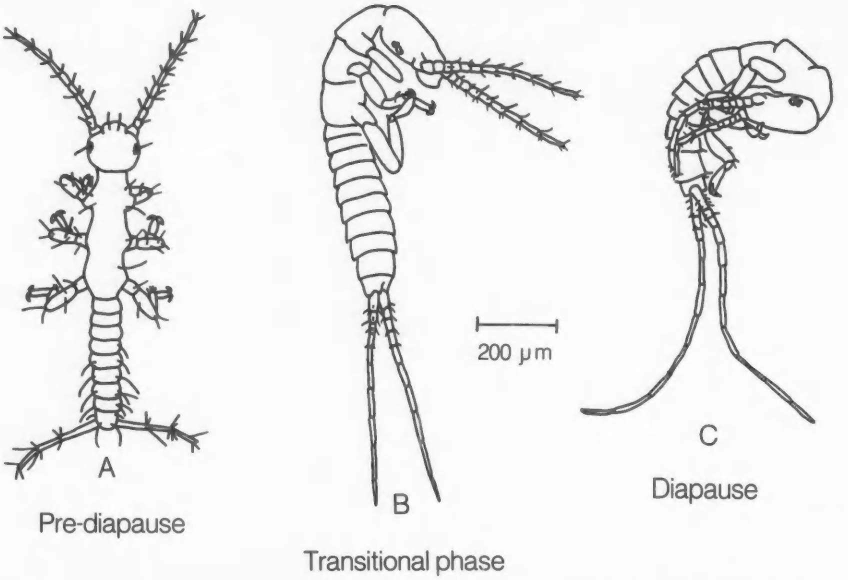

FIG. 2. Diagnostic stages (post-diapause stage not shown) in the early nymphal development of *Allocapnia pygmaea*. The transitional phase occurs twice, i.e. as nymphs enter and leave diapause.

sampling date). For this, a stovepipe corer (Merritt and Cummins 1978), 20 cm in diameter and 60 cm long, was used. The corer was twisted into the streambed, substrate within the cylinder removed, and the corer twisted deeper into the streambed. This process was repeated until each chamber was located and removed. The stovepipe corer was then backfilled with the excavated material before being withdrawn from the streambed. This prevented the disturbance of adjacent chambers that were buried in the trench. To prevent substrate loss as the chambers were lifted from the streambed, we slipped a plastic bag over each before it was raised through the center of the corer. Once recovered, the flyscreen mesh was removed from one end of the chamber and the entire contents placed in a resealable plastic container. This plastic container contained sufficient 40% formaldehyde to give a 4% solution once it became diluted with the water from within the chamber.

In the laboratory, substrate from each chamber was elutriated (Stewart 1975); the elutriate was passed through a 160-μm-mesh net and stained with Rose Bengal. After storage in 70% ethanol, the nymphs were picked and later classified and enumerated into three developmental stages: pre-diapause, diapause, and post-diapause. A transitional diapause phase that occurred twice, i.e. as nymphs entered and left diapause, was also identified (Fig. 2). The post-diapause stage differed from the transitional diapause phase (Fig. 2) in being active and in reacquiring its full complement of cercal bristles.

Results and Discussion

Nymphs were present in the chambers on all 10 sampling dates (Fig. 3D). The total number varied erratically. Some of these fluctuations (Fig. 3D) coincided with developmental phases; for example: the decline in numbers during December, and January, a period when post-diapause nymphs were growing rapidly (Pugsley and Hynes 1985); the static midwinter numbers in January and February prior to emergence; and the rapid build-up in numbers between May and June 1982 as a new generation of hatchlings (Fig. 3A) entered diapause. However, further discussion is warranted to explain why the total number of nymphs collected by the chambers varied between 185 and 43 over the first five sampling dates, i.e. 31 May to 23 November 1981 (Fig. 3D). First, the fact that similarly high numbers of nymphs were extracted from the 27 chambers (nine chambers at each of the three depths) on three of the first five sampling dates may indicate a carrying capacity for the chambers of between 149 and 185. Second, the low number of nymphs found in the August sample, almost all of which were in diapause (Fig. 3B, 3D), suggests that any pre-diapause nymphs moved away from the trenches to diapause, perhaps to depths below 50 cm or to areas beneath the stream bank. In September a similarly low number of diapausing nymphs, now in the transitional diapause phase (Fig. 3B, 3D), was collected (Fig. 3B). However, the dramatic September increase in the number of post-diapause nymphs (Fig. 3C, 3D) was perhaps caused by nymphs moving back into the sampling area once diapause had been broken. Third, the low numbers of post-diapause nymphs in October (Fig. 3C, 3D) may reflect avoidance of the chambers, perhaps caused by movement of the post-diapause nymphs onto surface boulders to feed.

Spatial distribution of nymphs is illustrated by means of three-dimensional plots (Fig. 4, 5), generated from the natural or Naperian logarithmic transformation of the abundance data. These plots show changes in distributional patterns as the nymphs mature. In describing these changes, we will deal with each developmental stage separately, and for each stage describe its distribution with depth before describing changes in its horizontal (positional) distribution patterns.

Pre-diapause nymphs were most numerous near the surface of the streambed, and rapidly became scarce with increased depth (Fig. 4A). In the horizontal plane, the quarter-stream

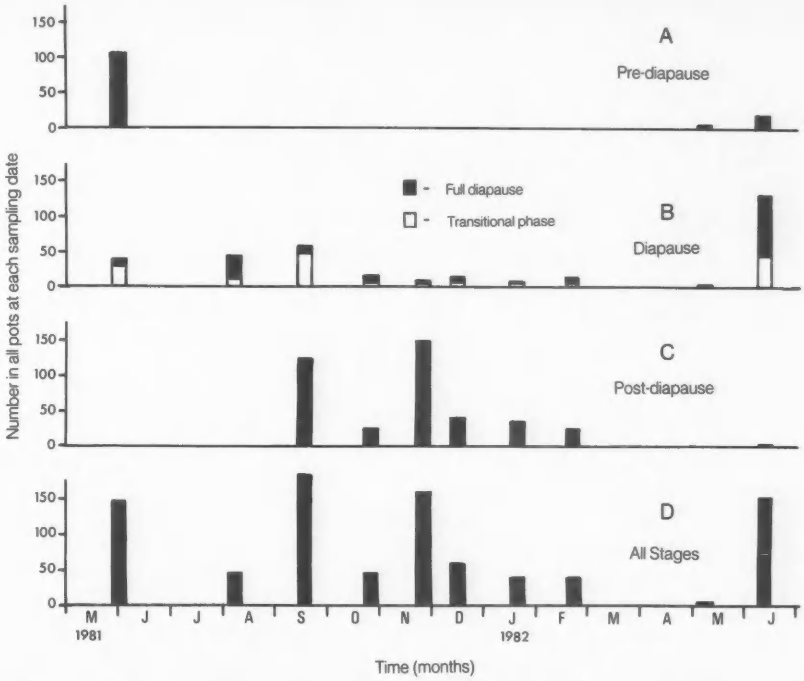

FIG. 3. Actual numbers of *Allocapnia pygmaea* nymphs extracted from all 27 chambers at each sampling date to illustrate seasonal changes in the structure of the population.

chambers (Fig. 1) contained few pre-diapause nymphs (Fig. 4D).

Diapause nymphs predominated in the deeper chambers; however, the high number collected from shallow chambers near the bank in May 1982 was an anomaly (Fig. 4B), perhaps caused by the early diapausing of nymphs in this area. As with the pre-diapause nymphs, the diapause nymphs also avoided the quarter-stream area (Fig. 4E); however, nymphs that remained in diapause throughout winter were more evenly distributed across the stream.

In September, when post-diapause nymphs first appeared, they were most frequent at depth near the bank (Fig. 4C, 4F). The early breaking of diapause in the bank area (Fig. 4F) corresponds with the equally early start of diapause that occurred there (Fig. 4E). However, by November, post-diapause nymphs predominated at the surface of the streambed (Fig. 4C), with many in the quarter-stream position (Fig. 4F), an area where pre-diapause and diapause nymphs were scarce (Fig. 4D, 4E). This shift in abundance in favor of the chambers at the surface (−10 cm) of the streambed in the quarter-stream area coincides with a period of intense nymphal growth (Pugsley and Hynes 1985). The apparent upward movement of nymphs was probably a response to the greater availability of food and oxygen near the surface of the streambed. In January, and to a lesser extent in February, the now fully grown nymphs (Pugsley and Hynes 1985) were more evenly distributed as regards both depth and position in the streambed (Fig. 4C, 4F). The increase in the proportion of nymphs found at depth during midwinter could have resulted from downward movement of nymphs as they sought warmer upwelling groundwater (Hynes 1983). This downward movement would also have helped nymphs avoid predators during the period of slow growth that precedes emergence (Pugsley and Hynes 1985).

There was no obvious movement of mature nymphs toward the stream bank during winter. Such movement had been anticipated because freshly emerged adults were thought to congregate under the ice near the stream bank to await warm weather, whereupon they could crawl up onto the snow surface through holes formed as riparian vegetation was released from the ice. This behavior was observed. However, adults were also seen walking along the undersurface of the ice in midstream areas, taking advantage of the air gap present above the water. Therefore, it seems that it is the adults, rather than the nymphs, that move toward the bank beneath the ice.

If, to further clarify this discussion of spatial distribution patterns, the time component is now removed from the abundance data, the pre-diapause and diapause stages are clearly most frequent near the bank, with very few in the quarter-stream area (Fig. 5A, 5B). It also becomes clear that nymphs moved to greater depths to diapause, but came back to the surface once diapause had been broken (Fig. 5B, 5C). Pre-diapause and diapause nymphs were found at depth most often in bank rather than midstream positions (Fig. 5A, 5B). By contrast, the post-diapause nymphs were much more evenly distributed across the stream (Fig. 5C).

The presence of a large number and variety of benthic stream invertebrates at depth below the streambed is widely reported. However, prior to this study there was little detailed documentation on when, or why, species that normally live on the streambed were found in the hyporheic. Our study carefully follows the movement of *Allocapnia pygmaea* to and from the hyporheic to diapause, confirming suggestions that the hypo-

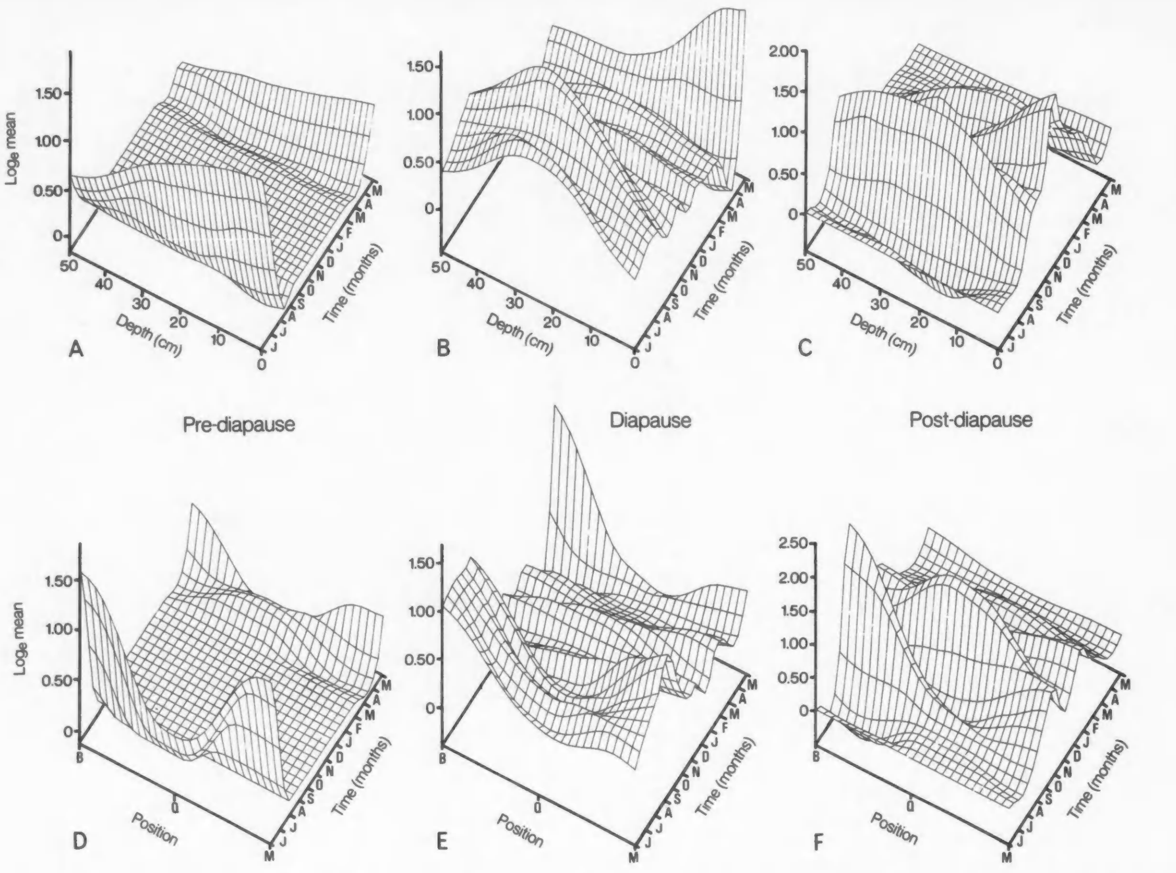

FIG. 4. Three-dimensional plots, generated from curve-fitting procedures using the transformed data, showing spatial and temporal distributions (1981–82) of each nymphal stage of *Allocapnia pygmaea* extracted from the colonization chambers. Population densities (log$_e$ mean) are the means of the natural or Naperian logarithmic transformation of the data ($X' = \log_e (X + 1)$). (A–C) Changes in population density with depth (10, 30, and 50 cm); (D–F) changes in population density at three positions across the width of the streambed (B = Bank, Q = quarter-stream, M = midstream; see Fig. 1).

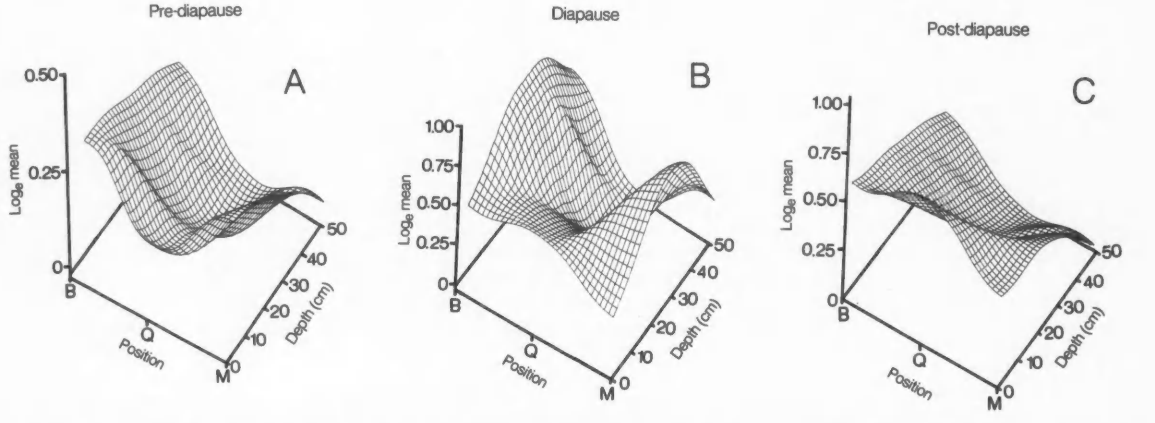

FIG. 5. Spatial distribution (1981–82) of pre-diapause, diapause, and post-diapause nymphs of *Allocapnia pygmaea* extracted from colonization chambers. See Fig. 4 for explanation of procedures and axes.

rheic offers refuge from adverse conditions on the surface.

It is understandable that many have treated the benthic habitat as an uneven two-dimensional surface. The hyporheic is invisible and requires specialist sampling equipment for its study. However, to many benthic insects the streambed and banks, if penetrable, are three-dimensional, their indefinite boundaries linking lotic, terrestial, and groundwater environments. Therefore, wherever it can physically exist, the hyporheic adds a vast spacial extension to the traditional two-dimensional view of the benthic habitat. Its exploitation by stream insects is incompletely documented, particularly the movement in space and time of individual species. Therefore, in this study, we have concentrated on the detailed documentation of movement to and from the hyporheic. Further work like this is needed to validate suggestions that benthic invertebrates move down into the hyporheic as a temporary escape from adverse conditions on the streambed explaining phenomena previously listed in the introduction.

Although loss or redistribution of stream insects into or through surface waters is usually acknowledged, implicit in many sampling designs is the assumption that the bank and streambed are inpenetrable. In the light of this study, we should be cautious in treating streambed and banks as if they were sealed from the terrestial and groundwater environments by some imaginary plastic liner.

Acknowledgments

This work was supported by Natural Sciences and Engineering Research Council of Canada grants to H. B. N. Hynes for which we express our thanks. We are also grateful to Dr. W. Zielonko for allowing unrestricted access to the Speed River.

References

BISHOP, J. E. 1973. Observations on the vertical distribution of the benthos in a Malaysian stream. Freshwater Biol. 3: 147–156.

BISHOP, J. E., AND H. B. N. HYNES. 1969. Upstream movements of the benthic invertebrates in the Speed River, Ontario. J. Fish. Res. Board Can. 26: 279–298.

BRETSCHKO, G. 1981. Vertical distribution of zoobenthos in an alpine brook of the Ritrodat–Lunz study area. Verh. Int. Ver. Limnol. 21: 873–876.

CAMPBELL, I. C. 1980. Diurnal variations in the activity of *Mirawara purpurea* Riek. (Ephemeroptera, Siphlonuridae) in the Aberfeldy River, Victoria, Australia, p. 297–308. *In* J. F. Flannagan and K. E. Marshall [ed.] Advances in Ephemeroptera biology. Plenum Press, New York, NY.

DANIELPOL, D. L. 1980. The role of the limnologist in ground water studies. Int. Rev. Gesamten Hydobiol. 65: 777–791.

GODBOUT, L., AND H. B. N. HYNES. 1982. The three dimensional distribution of the fauna in a single riffle in a stream in Ontario. Hydrobiologia 97: 87–96.

HARPER, P. P., AND H. B. N. HYNES. 1970. Diapause in the nymphs of Canadian winter stoneflies. Ecology 51: 925–927.

1972. Life histories of Capniidae and Taeniopterygidae (Plecoptera) in southern Ontario. Arch. Hydrobiol. Suppl. 40: 274–314.

HYNES, H. B. N. 1968. Further studies on the invertebrate fauna of a Welsh mountain stream. Arch. Hydrobiol. 65: 360–379.

1970. The ecology of running waters. Liverpool University Press, Liverpool. 555 p.

1974. Further studies on the distribution of stream insects within the substratum. Limnol. Oceanogr. 19: 92–99.

1983. Groundwater and stream ecology. Hydrobiologia 100: 93–99.

KASTER, J. L., AND G. Z. JACOBS. 1978. Benthic macroinvertebrates of a fluctuating reservoir. Freshwater Biol. 8: 283–290.

KOVALAK, W. P. 1978. Diel changes in stream benthos density on stones and artificial substrates. Hydrobiologia 58: 7–16.

MERRITT, R. W., AND K. W. CUMMINS. 1978. An introduction to the aquatic insects of North America. Kendall-Hunt Publishing Company, Dubuque, IA. 441 p.

MESTROV, M., R. LATTINGER-PENKO, AND V. TAVCAR. 1976. La dynamique de population de l'isopode *Proasellus slavus* ssp.n. et les larves de chironomides dans l'hyporhéique de la Drave du point de vue de la pollution. Int. J. Speleol. 8: 157–166.

MORRIS, D. L., AND M. P. BROOKER. 1979. The vertical distribution of macroinvertebrates in the substratum of the upper reaches of the River Wye, Wales. Freshwater Biol. 9: 573–583.

POOLE, W. C., AND K. W. STEWART. 1976. The vertical distribution of macrobenthos within the substratum of the Brazos River, Texas. Hydrobiologia 50: 151–160.

PUGSLEY, C. W., AND H. B. N. HYNES. 1983. A modified freeze-core technique to quantify the depth distribution of fauna in stony streambeds. Can. J. Fish. Aquat. Sci. 40: 637–643.

1985. Summer diapause and nymphal development in *Allocapnia pygmaea* (Burmeister) (Plecoptera: Capniidae), in the Speed River, southern Ontario. Aquat. Insects 7: 53–63.

STERBA, O. 1978. Stratifikation der Organismen in der Oberschicht der Sandkiessedimente unter der aktiven Strömung der Flüsse. Věst. Cesk. Spol. Zool. 42: 60–68.

STEWART, K. W. 1975. An improved elutriator for separating stream insects from stony substrates. Trans. Am. Fish. Soc. 104: 821–823.

WILLIAMS, D. D. 1977. Movements of benthos during recolonization of temporary streams. Oikos 29: 306–312.

WILLIAMS, D. D., AND H. B. N. HYNES. 1974. The occurrence of benthos deep in the substratum of a stream. Freshwater Biol. 4: 233–256.

NOTES

Relationships Between Stream and Intragravel Temperatures in Coastal Drainages, and Some Implications for Fisheries Workers

Bruce G. Shepherd

Department of Fisheries and Oceans, Salmonid Enhancement Program, 1090 West Pender Street, Vancouver, B.C. V6E 2P1

Gordon F. Hartman

Department of Fisheries and Oceans, Fisheries Research Branch, Pacific Biological Station, Nanaimo, B.C. V9R 5K6

and William J. Wilson

University of Alaska, Fairbanks Arctic Environmental Information and Data Center, 707 'A' Street, Anchorage, AK 99501, USA

Shepherd, B. G., G. F. Hartman, and W. J. Wilson. 1986. Relationships between stream and intragravel temperatures in coastal drainages, and some implications for fisheries workers. Can. J. Fish. Aquat. Sci. 43: 1818–1822.

By a depth of 10 cm into the streambed, water temperatures are likely to be different from those in the open water of the stream. Combined results from three independent studies on disparate streams on the Pacific Northwest coast indicated that there are widespread similarities in the thermal behavior of intragravel water. In general, the thermal mass of the substrate causes parallel but lagged and buffered heating and cooling trends in infiltration-source intragravel water compared with surface water. Intragravel mean daily temperatures were generally 0.5–1.0°C warmer in winter and 0.5–1.5°C cooler in summer, with cross-overs around March and October; intragravel daily maximum temperatures could be up to 6°C different in summer (a difference of 4°C was common). The degree of difference showed considerable site-specific variation, and potentially can be affected by several factors. Such intragravel temperature differences have implications for those involved in salmonid egg incubation and fry emergence studies, enhancement projects, benthic invertebrate research, and environmental impact assessments.

La température de l'eau se trouvant à 10 cm sous la surface du lit d'un cours d'eau tend à être différente de celle de l'eau du cours d'eau lui-même. Les résultats de trois études indépendantes portant sur trois cours d'eau distincts de la côte nord-ouest du Pacifique ont montré l'existence de similitudes généralisées quant au comportement thermique de l'eau occupant les interstices du gravier. De façon générale, la masse thermique du substrat provoque des réchauffements ou des refroidissements, décalés et amoindris, de l'eau intersticielle d'infiltration comparativement à l'eau de surface. La température moyenne quotidienne dans le gravier était généralement de 0,5 à 1,0°C plus chaude en hiver et de 0,5 à 1,5°C plus froide en été, les inversions se produisant vers mars et octobre. La température maximale quotidienne dans le gravier pouvait différer de 6°C de la température des eaux de surface en été (une différence de 4°C était courante). L'écart variait de façon considérable en fonction du site et était sans doute fonction de plusieurs facteurs. Ces écarts de température de l'eau présentent un grand intérêt pour les études de l'incubation des oeufs de salmonidés et de l'émergence des alevins, les projets de mise en valeur, les recherches sur les invertébrés benthiques et les évaluations d'incidences environnementales.

Received January 20, 1986
Accepted May 13, 1986
(J8651)

Reçu le 20 janvier 1986
Accepté le 13 mai 1986

The purpose of this paper is to alert resource managers to the importance of determining the relationship between intragravel and surface water temperatures. Some examples of the consequences of not correcting for such a difference are discussed.

It often has been observed during field surveys that certain species of Pacific salmon, especially chum (*Oncorhynchus keta*), are attracted to groundwater-fed areas for spawning (Kogl 1965; ADFG 1985). The sensory basis of groundwater detection is not clear. However, the advantages of using such locations would include exposure of the eggs to cleaner water, more stable flows, and a better incubation temperature regime. With respect to the latter factor, several studies suggest that water temperature is a driving factor in determining the progress of incubation and emergence of Pacific salmon fry (e.g. Leitritz and Lewis 1976). Other workers have noted that

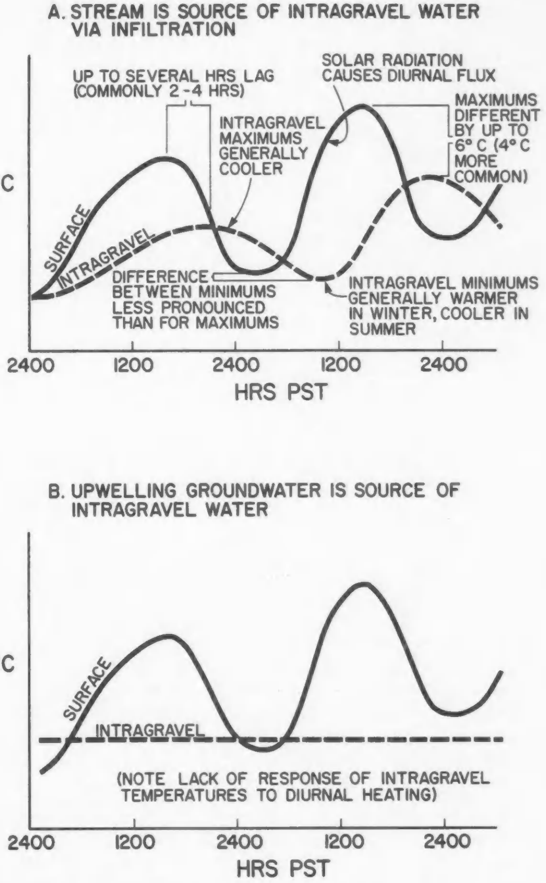
A. STREAM IS SOURCE OF INTRAGRAVEL WATER VIA INFILTRATION
UP TO SEVERAL HRS LAG (COMMONLY 2-4 HRS)
SOLAR RADIATION CAUSES DIURNAL FLUX
MAXIMUMS DIFFERENT BY UP TO 6° C (4° C MORE COMMON)
INTRAGRAVEL MAXIMUMS GENERALLY COOLER
°C
SURFACE
INTRAGRAVEL
DIFFERENCE BETWEEN MINIMUMS LESS PRONOUNCED THAN FOR MAXIMUMS
INTRAGRAVEL MINIMUMS GENERALLY WARMER IN WINTER, COOLER IN SUMMER
2400
1200
2400
1200
2400
HRS PST
B. UPWELLING GROUNDWATER IS SOURCE OF INTRAGRAVEL WATER
°C
SURFACE
INTRAGRAVEL
(NOTE LACK OF RESPONSE OF INTRAGRAVEL TEMPERATURES TO DIURNAL HEATING)
2400
1200
2400
1200
2400
HRS PST

FIG. 1. General summer diurnal surface and intragravel water temperature patterns.

intragravel water temperatures can differ from surface water temperatures (e.g. Sheridan 1962). What has not been obvious until recently is how widespread intragravel temperature differences might be and how they might vary over time.

Each of the coauthors independently compared intragravel and surface water temperature regimes of coastal streams in the Pacific Northwest. The three studies were done with different objectives in mind, using differing methodologies, and were widely separated geographically. Nevertheless, the combined results balance the strengths and weaknesses of the individual studies and allow a more general overview of the behavior of intragravel water temperatures.

Materials and Methods

The reader is referred to the individual reports (Hartman and Leahy 1983, for Carnation Creek; Shepherd 1984, for Glendale Creek; and Wilson et al. 1980, for the Terror and Kizhuyak rivers) for full details on the methods and results of the three studies. The following sections highlight the different approaches of each study.

Carnation Creek — This system flows into Barkley Sound on the west coast of Vancouver Island, British Columbia. This small (~10 km^2) watershed has been the subject of a 15-yr multidisciplinary study on the effects of logging (see Hartman 1982 for a recent review of results). Since 1970, monthly discharges have ranged 0.03−63 m$^3\cdot$s^{-1}. Surface water temperatures have ranged 1.5−17.0°C seasonally. Intragravel and surface temperatures were measured with a calibration thermometer or with a Fenwell Electronics 1000 OHM thermistor probe coupled to a Beckman voltmeter and calibrated to the thermometer (accuracy ± 0.1°C). For each intragravel measurement, a 2.5-cm pipe 90 cm long was fitted around a pointed steel core and both were driven 10−30 cm into the streambed. The lower 8−10 cm of the pipe was perforated to allow entry of intragravel water when the driving rod was removed. Throughout 1981−82, 20 series of intragravel and stream temperatures were recorded. Each series consisted of paired readings at a minimum of 10 sites. It is emphasized that these were instantaneous samples; measurement of diel variations was not done, beyond comparison of "morning" and "afternoon" results.

Glendale Creek — This lake-headed system flows into Knight Inlet, located on the central coast of British Columbia. Water temperature studies were done between 1981 and 1983 as part of a program determining the feasibility of constructing a spawning channel for pink salmon (*Oncorhynchus gorbuscha*). Glendale Creek drains a total of 136 km^2; average monthly flows have ranged 4−11 m$^3\cdot$s^{-1} since 1971. Surface water temperature ranged 2−19°C over the 1983 study period. Intragravel and surface temperatures were measured in two ways. During February, April, and May of 1983, point sampling was done using a calibrated YSI model 43TD thermistor (accuracy ± 0.5°C) and a heavy pointed steel pipe (3 mm wall thickness, 25 mm ID, and 120 cm long) perforated over the lower 12 cm. The pipe was driven to a depth of 30 cm and the temperature immediately measured at the bottom of the pipe. From one to five sites were sampled within each of five cross-sections. Also, two Peabody−Ryan J-90 submersible thermographs were calibrated and installed at a site having a representative temperature difference during the January survey. One thermograph was buried at about 30 cm depth, and the other was cabled to the bottom nearby. Although these machines were maintained through to November of 1983, malfunctions resulted in loss of intragravel data for the first half of May and most of November and surface data for the last half of August through the first half of September of that year. No data were collected for the months of December and January.

Terror and Kizhuyak rivers — These two systems are located on Kodiak Island, Alaska. Temperature studies were undertaken as part of an environmental assessment of a proposed hydroelectric project which would divert Terror River water via a reservoir and tunnel into the Kizhuyak River. The Kizhuyak and Terror watersheds are 141 and 126 km^2, respectively; average monthly flows have ranged 1.1−17 and 1.4−23 m$^3\cdot$s^{-1}. Surface water temperatures ranged 1−12.5°C during the 1980 study period. Three sites in the Kizhuyak and two in the Terror were selected on the basis of egg or alevin presence. Three armored temperature probes were installed at each site: at the streambed surface, at 10−25 cm depth, and at 25−50 cm depth. Each probe was attached to a YSI model 42SC telethermometer (accuracy ±0.2°C), which could be read directly or connected to a Linear model 142 strip chart recorder. Instantaneous measurements were taken between early April and late August, and at least one continuous 24-h cycle was recorded

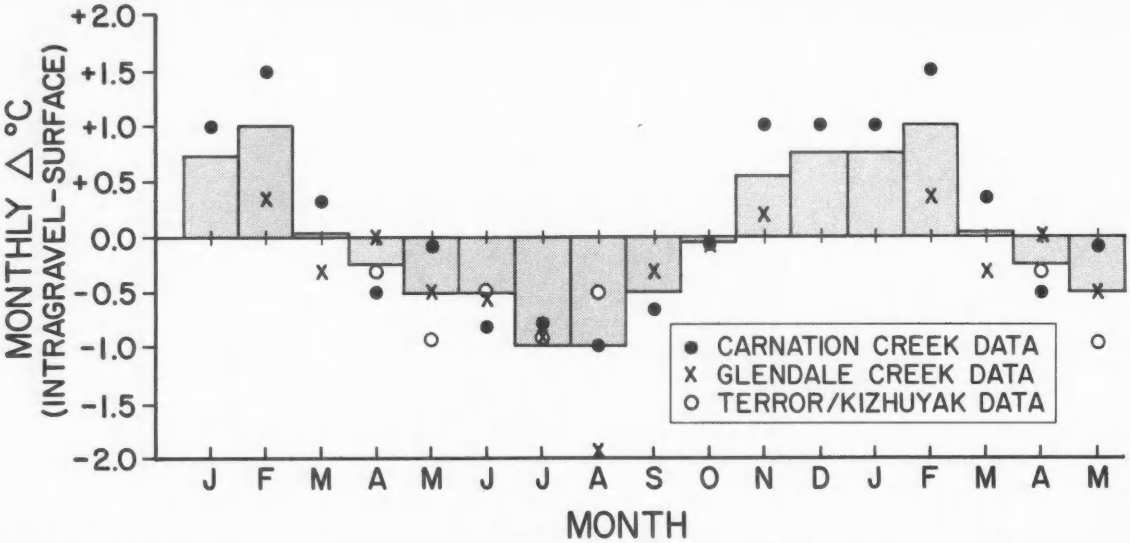

FIG. 2. Monthly differences between surface and intragravel water temperatures, presuming stream is the primary source of intragravel water. Actual average monthly differences from the three studies (points) were used to derive approximations (bars) by eye.

for all but one site in May, July, and August of 1980. This study provided the best diurnal data for the spring and summer period, when differences were greatest.

Results

The combined results of the three studies confirm that intragravel water temperatures can be expected to differ regularly from surface water temperatures. In general, one can expect intragravel water temperatures to be buffered by the thermal mass of the substrate. This buffering effect seems to be complete at a depth of 10 cm. Where intragravel flows are maintained primarily by infiltration of diurnally heated surface water into the substrate (which is seen as the common situation in the mainstem of larger streams), one can expect parallel, but lagged and buffered, heating/cooling trends in the intragravel versus the surface water (Fig. 1A).

A general predictive model of the differences in water temperatures that might be expected for infiltration-source intragravel water is shown in Fig. 2. The reader is cautioned not to derive precise monthly correction factors from this figure, as site-specific factors can result in considerable variation. One extreme example is shown in Fig. 1B, where the dominant source of intragravel water is upwelling groundwater. In this case, the intragravel temperature is highly buffered and will show little or no response to diurnal heating of the surface water. At such sites, intragravel temperatures will show only slow changes, on a seasonal rather than a diel scale. Such strong groundwater influence will tend to increase the amplitude of the curve shown in Fig. 2. For example, one section of Carnation Creek was heavily influenced by groundwater, and intragravel temperatures were as much as 3°C cooler in summer and over 5°C warmer in winter (Hartman and Leahy 1983).

Discussion

Several factors can affect the intragravel thermal regime. Hewlett and Fortson (1982) and Hartman et al. (1982) independently speculated that when groundwater is an important source of intragravel flows, logging of the areas where percolation from the surface occurs can increase groundwater temperatures by increasing solar heating effects. In winter, ice dams can develop on a river mainstem, forcing cold river water down side channels and sloughs normally fed solely by groundwater upwelling. Infiltration of 0°C water into these areas can dramatically alter the thermal regime and delay the development of, or even kill, incubating embryos (e.g. ADFG 1983). The degree of interchange between surface and intragravel water may depend on the stream's physical characteristics, including flow rate and turbulence, gradient, how even the streambed is, and the coarseness of the substrate (Pollard 1955; Vaux 1968; Sowden and Power 1985). In areas of tidal influence at Carnation Creek, diel intragravel temperatures appear to be warmer than surface temperatures in summer and colder in winter. This is the reverse of what is generally experienced in upstream areas, and probably is due to percolation of incoming water through beach and bank areas that have been exposed to the more extreme atmospheric heating or cooling during low tide.

There are many implications of the above phenomena for fisheries workers. Where intragravel temperatures differ, the use of surface temperatures in accumulated thermal unit (ATU, degrees Celsius) calculations of hatch and emergence timings will throw such predictions off. This could lead the life history researcher to incorrectly hypothesize stock-specific biological adaptations or additional physical factors such as temperature "triggers," stage of freshet, or phase of moon, where none in fact actually exist. In the construction of artificial spawning channels, a lack of recognition of this potential for different thermal regimes could result in actual fry emergence timings that are significantly skewed from the desired situation. Before committing to the site, one should consider the degree of groundwater contribution, both at natural spawning areas and at the proposed channel site.

In both field studies and the operation of spawning channels,

TABLE 1. Calculated ATU values to emergence for 1984 brood sockeye in Fulton Spawning Channel 2.

	ATU (surface temp.)	Difference	ATU (intragravel temp.)[a]	Difference
50% spawning to 50% emergence dates[b]	793	−44	890	+2
MAWW[c]	837		888	

[a] Adjusted using values shown in Fig. 2 (there is no groundwater input to Channel 2).

[b] Taken from spawner counts and fry trapping data.

[c] MAWW = maximum alevin wet weight; calculated per Belehradec model (Alderdice and Velsen 1978) using parameter values recently developed for sockeye (F. Velsen, J. Jensen, and D. Alderdice, unpubl. data).

the planning and coverage of fry counts might be improved if fry migrations were predicted using intragravel temperatures. Taking the Fulton sockeye (*Oncorhynchus nerka*) Spawning Channel 2 on Babine Lake, British Columbia, as an example, the 1984−85 interval between the 50% spawning and 50% emergence dates worked out to 793 ATU using surface temperature data, but was 97 ATU higher when the surface temperatures were adjusted to reflect intragravel conditions (Table 1). Maximum alevin wet weight (MAWW) and thus emergence were predicted to occur 9 d later than actual fry emigration data would have suggested (emergence has been related to attainment of MAWW by Heming 1982). When surface temperatures were corrected to reflect the intragravel situation, MAWW and emergence were predicted to occur on the same day as the actual date of migration. Although such accuracy is perhaps fortuitous given the many assumptions used in the calculation sequence, it does demonstrate the potential for improving the precision with which incubation timings can be predicted.

Where workers are planting eggs into streams, variations in intragravel temperatures along the stream's length should be considered. "Hotspots" could be used or avoided for egg planting, depending on the species and purpose. For instance, coho (*Oncorhynchus kisutch*) that emerge early tend to achieve a larger size by fall, although this advantage might be offset by their higher probability of experiencing freshets and being flushed seaward (Scrivener and Andersen 1984); species such as pink, chum, and sockeye can be quite sensitive to premature emergence in that prey levels could be low enough to cause mortality through starvation (Bilton and Robins 1973). For the researcher examining distributional behavior of benthos, vertical and horizontal variations in intragravel temperatures may be an important environmental influence.

Intragravel water temperatures can be modified by other activities in the watershed. A prime example is changes in water temperatures with logging. It may be possible for management workers to map areas of groundwater influence and to plan clearcuts either to take advantage of heated input water or to ensure maintenance of cool water input to the groundwater aquifer. Furthermore, it is possible that where large river diversion projects result in high spring−summer flows being diverted or stored, recharges to the downstream water table may be reduced. Such reduction could result in lower groundwater outflows into side channels on the downstream flood plain during the winter period and subsequent adverse effects on salmon spawning and incubation success. Even if flow reduction did not occur, there may be a relationship between reservoir release temperatures and downstream intragravel temperatures which would be important to examine.

We believe that the role of groundwater, and the diversity between stream and intragravel temperatures, should be considered carefully by those involved in fish enhancement and habitat management projects. These phenomena certainly deserve further investigation, particularly in areas subject to greater climatic extremes (i.e. where water temperatures fall below 1°C or exceed 19°C). Some very useful information on the complexities and significance of groundwater influences could result from cooperative research done by groundwater hydrologists and fisheries biologists. A related area worth further study is that of intragravel dissolved gases. Groundwater often is supersaturated in nitrogen and undersaturated in oxygen. Spawning success may be questionable in some cases; certainly, low oxygen levels are known to slow development (Doudoroff and Shumway 1970; Davis 1975) and could affect the precision of ATU predictions.

In summary, our studies show clearly that the fisheries worker cannot assume that stream temperatures are identical to those experienced by the egg in the intragravel environment.

Acknowledgements

The three studies resulting in this overview were funded by the Salmonid Enhancement Program (Glendale) and the Fisheries Research Branch (Carnation Creek Watershed Project) of the Department of Fisheries and Oceans and the Kodiak Electric Association Inc. (Terror Lake Hydroelectric Project). D. Alderdice, J. Jensen, and F. Velsen of the Pacific Biological Station at Nanaimo are thanked for allowing the use of their unpublished sockeye development data. M. D. Kelly, C. N. MacKinnon, P. R. Meyer, W. J. Schouwenburg, R. L. Beschta, and an anonymous referee reviewed the manuscript and provided helpful suggestions.

References

ALASKA DEPARTMENT OF FISH AND GAME (ADFG). 1983. Susitna hydro aquatic studies. Phase II data report, winter aquatic studies (October 1982 − May 1983). Report for Alaska Power Authority. 137 p. (Available from Alaska Power Authority, 334 W. 5th Ave., Anchorage, AK, 99501).

1985. An evaluation of the incubation life phase of chum salmon in the Middle Susitna River. Winter aquatic investigations, September 1983 − May 1984. 1985 Reports, Vol. 1. Report for Alaska Power Authority. 157 p. (Available from Alaska Power Authority, 334 W. 5th Ave., Anchorage, AK, 99501).

ALDERDICE, D. F., AND F. P. J. VELSEN. 1978. Relation between temperature and incubation time for eggs of chinook salmon (*Oncorhynchus tshawytscha*). J. Fish. Res. Board Can. 35: 69−75.

BILTON, H. T., AND G. L. ROBINS. 1973. The effects of starvation and subsequent feeding on survival and growth of Fulton Channel sockeye salmon fry (*Oncorhynchus nerka*). J. Fish. Res. Board Can. 30: 1–5.

DAVIS, J. C. 1975. Minimal dissolved oxygen requirements of aquatic life with emphasis on Canadian species: a review. J. Fish. Res. Board Can. 32: 2295–2332.

DOUDOROFF, P., AND D. L. SHUMWAY. 1970. Dissolved oxygen requirements of freshwater fishes. FAO Fish. Tech. Pap. FIRI/T86.

HARTMAN, G. F. [ED.]. 1982. Proceedings of the Carnation Creek Workshop, a 10 year review. 404 p. (Available from the Pacific Biological Station, Nanaimo, B.C. V9R 5K6)

HARTMAN, G. F., B. C. ANDERSEN, AND J. C. SCRIVENER. 1982. Seaward movement of coho salmon (*Oncorhynchus kisutch*) fry in Carnation Creek, an unstable coastal stream in British Columbia. Can. J. Fish. Aquat. Sci. 39: 588–597.

HARTMAN, G. F., AND R. M. LEAHY. 1983. Some temperature characteristics of stream and intra-gravel water in Carnation Creek, British Columbia. Can. MS Rep. Fish. Aquat. Sci. 1731: 36 p.

HEMING, T. A. 1982. Effects of temperature on utilization of yolk by chinook salmon (*Oncorhynchus tshawytscha*) eggs and alevins. Can. J. Fish. Aquat. Sci. 39: 184–190.

HEWLETT, J. D., AND J. C. FORTSON. 1982. Stream temperature under an inadequate buffer strip in the southeast Piedmont. Water Resour. Bull. 18: 983–988.

KOGL, D. R. 1965. Springs and groundwater as factors affecting survival of chum salmon spawn in a subarctic stream. M.Sc. thesis, University of Alaska, Fairbanks, AK. 59 p.

LEITRITZ, E., AND R. C. LEWIS. 1976. Trout and salmon culture (hatchery methods). Calif. Dep. Fish Game Fish Bull. 164: 197 p.

POLLARD, R. A. 1955. Measuring seepage through salmon spawning gravel. J. Fish. Res. Board Can. 12: 706–741.

SCRIVENER, J. C., AND B. C. ANDERSEN. 1984. Logging impacts and some mechanisms that determine the size of spring and summer populations of coho salmon fry (*Oncorhynchus kisutch*) in Carnation Creek, British Columbia. Can. J. Fish. Aquat. Sci. 41: 1097–1105.

SHEPHERD, B. G. 1984. Predicted impacts of altered water temperature regime on Glendale Creek pink (*Oncorhynchus gorbuscha*) fry. Can. MS Rep. Fish. Aquat. Sci. 1782: 55 p.

SHERIDAN, W. L. 1962. Waterflow through a salmon spawning riffle in southeastern Alaska. U.S. Fish Wildl. Serv. Spec. Sci. Rep. Fish. No. 407: 20 p.

SOWDEN, T. K., AND G. POWER. 1985. Prediction of rainbow trout embryo survival in relation to groundwater seepage and particle size of spawning substrates. Trans. Am. Fish. Soc. 114: 804–812.

VAUX, W. G. 1968. Intragravel flow and interchange of water in a streambed. U.S. Natl. Mar. Fish. Serv. Fish. Bull. 66: 479–489.

WILSON, W. J., C. D. EVANS, M. S. WILSON, AND D. E. TRUDGEN. 1980. An assessment of environmental effects of construction and operation of the proposed Terror Lake hydroelectric facility, Kodiak, Alaska. Report for Kodiak Electric Association Inc. by Arctic Environmental Information Data Center, University of Alaska. (Available from Arctic Environmental Information Data Center, 707 'A' St., Anchorage, AK 99501)

ANNOUNCEMENTS/AVIS

C.C.F.F.R. – C.C.R.P.
Vancouver, 5–6 January, 1987

Preliminary Program and Call for Papers

This year's program will begin on Monday, January 5, with the Stevenson lecture, to be presented by Dr. Bill Leggett of McGill University. The Stevenson lecture will be followed by two contributed papers sessions organized around specific themes: (1) Climate and Oceanography and its Effects on Fisheries and (2) Ecology and Population Dynamics of Forage Species. Tuesday, January 6, will begin with an invited papers session: The Biology of Little Known and Unusual Canadian Fishes. This session is being convened by M. C. Healey. The invited papers session will be followed by a poster session, and in the afternoon by a contributed papers session without theme. M. C. Healey is in charge of the overall scientific program, Jake Schweigert is coordinating the contributed papers sessions (all three), and Laura Richards is coordinating the poster session.

This is a ***Call for Abstracts*** for the three contributed papers sessions and the poster session. Type your abstract (maximum 200 words, single spaced). In particular, we want to hear from those of you who want to contribute to one of the sessions having a particular theme. Depending on the number of papers received, we may have to rearrange the sessions. Please forward abstracts for the contributed papers sessions to Jake Schweigert and indicate on your abstract in which session you think the paper belongs. Abstracts for the poster session should be forwarded to Laura Richards. General enquiries should be sent to Mike Healey. Jake, Laura, and Mike are all at the Department of Fisheries and Ocean, Pacific Biological Station, Nanaimo, B.C. V9R 5K6. Deadline for abstracts is November 30, 1986. Earlier submission would, however, be appreciated.

The meetings will be held at the Delta River Inn in Richmond. Dr. G. Geen, Biology Department, Simon Fraser University, is in charge of local arrangements. Contact him for further information about hotel rates, etc.

Conférence canadienne relative à la recherche sur les pêches
Vancouver, les 5 et 6 janvier 1987

Programme préliminaire et appel de documents

Le programme de cette année débutera le lundi 5 janvier avec la conférence Stevenson, qui sera présentée par le Dr Bill Leggett de l'Université McGill. La conférence Stevenson sera suivie de deux séances de présentation de documents organisées autour de thèmes précis : (1) le climat et l'océanographie et ses effets sur les pêches et (2) écologie et dynamique de population d'espèces fourrage. Le mardi 6 janvier débutera avec une séance d'exposés de conférenciers invités : la biologie de poissons du Canada inhabituels et peu connus. Cette séance est convoquée par M. C. Healey et sera suivie par après d'une séance d'affichage et dans l'après-midi d'une séance de présentation de documents sans thème. M. C. Healey est la personne responsable de l'ensemble du programme scientifique, Jake Schweigert coordonne les séances de présentation de documents (les trois), tandis que Laura Richards coordonne la séance d'affichage.

Par la présente, on ***demande des résumés*** pour les trois séances de présentation de documents et pour la séance d'affichage. Veuillez dactylographier votre résumé (maximum de 200 mots à simple interligne). En particulier, nous désirons avoir des nouvelles de ceux d'entre vous qui veulent participer à l'une des séances ayant un thème donné. Selon le nombre de documents reçus, il est possible que nous devions remanier les séances. Veuillez faire parvenir les résumés pour les séances de présentation de documents à Jake Schweigert et indiquer sur votre résumé à quelle séance vous pensez que le document se rattache. Les résumés pour la séance d'affichage doivent être envoyés à Laura Richards. Les demandes de renseignements généraux doivent être adressées à Mike Healey. Jake, Laura et Mike travaillent tous pour le ministère des Pêches et des Océans, à la Station de biologie du Pacifique, Nanaimo (C.-B.) V9R 5K6. La date limite pour les résumés est le 30 novembre 1986. Cependant, nous aimerions les recevoir plus tôt.

Les réunions auront lieu au Delta River Inn, à Richmond. Le Dr G. Geen, département de biologie, Université Simon Fraser, est chargé de faire les arrangements au niveau local. Communiquez avec lui si vous désirez de plus amples informations au sujet des tarifs d'hôtel, etc.

COMING NEXT MONTH / À PARAÎTRE LE MOIS PROCHAIN

Articles

Growth and genetic variation of Atlantic salmon (*Salmo salar*) from different sections of the River Alta, North Norway **T. G. Heggberget, R. A. Lund, N. Ryman, and G. Ståhl**

Spatial variability in sedimentary algal microfossils and its bearing on diatom-inferred pH reconstructions **S. S. Dixit and R. D. Evans**

Effect of stream acidification on periphyton composition, chlorophyll, and productivity **P. J. Mulholland, J. W. Elwood, A. V. Palumbo, and R. J. Stevenson**

Metabolic changes during the reproductive migration of two sympatric coregonines, *Coregonus artedii* and *Coregonus clupeaformis* **H. Guderley, P. Blier, and L. Richard**

Characterization of cloned mitochondrial DNA from the teleost *Fundulus heteroclitus* and its usefulness as an interspecies hybridization probe **L. I. González-Villaseñor, A. M. Burkhoff, V. Corces, and D. A. Powers**

Methyl mercury levels in a polluted prairie river–lake system: seasonal and site-specific variations, and the dominant influence of trophic conditions **T. A. Jackson**

Limestone slurry reduces physiological stress and increases survival of Atlantic salmon (*Salmo salar*) in an acidic Norwegian river **B. O. Rosseland, O. K. Skogheim, H. Abrahamsen, and D. Matzow**

A new view of the predation cycle of a planktivorous fish, white crappie (*Pomoxis annularis*) **W. J. O'Brien, B. I. Evans, and G. L. Howick**

Patterns in biomass and cover of aquatic macrophytes in lakes **C. M. Duarte, J. Kalff, and R. H. Peters**

Environmental factors regulating the seaward migration of European silver eels (*Anguilla anguilla*) **L. A. Vøllestad, B. Jonsson, N. A. Hvidsten, T. F. Næsje, Ø. Haraldstad, and J. Ruud-Hansen**

Impact of atrazine on periphyton in freshwater enclosures and some ecological consequences **D. Herman, N. K. Kaushik, and K. R. Solomon**

Biomass and production of fishes in natural and channelized streams **C. B. Portt, E. K. Balon, and D. L. G. Noakes**

Effects of flooding on dissolved and suspended nutrients in small diked marshes **J. A. Kadlec**

Input–output nutrient budgets for small diked marshes **J. A. Kadlec**

Experimental analysis of the direct and indirect effects of an omnivorous filter-feeding clupeid on plankton community structure **R. W. Drenner, S. T. Threlkeld, and M. D. McCracken**

Estimating the abundance of stone-dwelling organisms: a new method **F. J. Wrona, P. Calow, I. Ford, D. J. Baird, and L. Maltby**

Selection for adult size in female coho salmon (*Oncorhynchus kisutch*) **L. B. Holtby and M. C. Healey**

Photosynthetic characteristics of lotic periphyton **S. Jasper and M. L. Bothwell**

Habitat utilization and behavioral interaction of juvenile Atlantic salmon (*Salmo salar*) and rainbow trout (*S. gairdneri*) in tributaries of the White River of Vermont **W. E. Hearn and B. E. Kynard**

Population estimates of white whale, *Delphinapterus leucas*, in James Bay, eastern Hudson Bay, and Ungava Bay **T. G. Smith and M. O. Hammill**

Winter habitat utilization by stream resident brook trout (*Salvelinus fontinalis*) and brown trout (*Salmo trutta*) **R. A. Cunjak and G. Power**

Investigation sur la toxicodynamique du cyanure et sur sa biotransformation chez la truite arc-en-ciel (*Salmo gairdneri*) **P. Raymond, G. Leduc et J. A. Kornblatt**

Notes

Comparison of continuous and episodic exposure to acidic, aluminum-contaminated waters of brook trout (*Salvelinus fontinalis*) **L. K. Siddens, W. K. Seim, L. R. Curtis, and G. A. Chapman**

Retardation and recovery of growth in brook trout fry (*Salvelinus fontinalis*) exposed for various durations to acidified water **W. H. Tam, P. D. Payson, and R. J. J. Roy**

Variation in major ion concentration of *Cambarus robustus* and *Orconectes rusticus* following exposure to low pH **L. Hollett, M. Berrill, and L. Rowe**

High precision microcomputer based measuring system for ecological research **J. C. Roff and R. R. Hopcroft**

Letters and comments / Lettres et commentaires

Generalizing fisheries models: an unfortunate illusion **R. Bodell**

Illusion and reality in fisheries models **N. Roy, E. Tsoa, and W. E. Schrank**

Announcements / Avis

ESTUARINE, COASTAL AND SHELF SCIENCE

EDITORS

N. C. Flemming
Institute of Oceanographic Sciences, Wormley, Godalming, Surrey, U.K.

E. Naylor
School of Animal Biology, University College of North Wales, U.K.

M. Grant Gross
Baltimore, Maryland, U.S.A.

Estuarine, Coastal and Shelf Science is an international multidisciplinary journal devoted to the analysis of saline water phenomena ranging from the outer edge of the continental shelf to the upper limits of the tidal zone.

The journal provides a unique forum, unifying the multidisciplinary approaches to the study of the oceanography of estuaries, coastal zones, and continental shelf seas. It features original papers and short communications treating such disciplines as zoology, botany, geology, sedimentology, physical oceanography, numerical models, and chemical processes.

The journal also publishes articles on brackish water and lagoon phenomena, subjects frequently neglected by journals specializing in either freshwater or marine sciences.

Research Areas Covered

Analysis of species distribution in relation to varying environments, effects of waste disposal, groundwater run off, estuarine and fjord circulation patterns, and meteorological forcing of semi-enclosed and continental shelf water masses.

Recent Papers Published in 1986 Include

Pakulski, J. D., The release of reducing sugars and dissolved organic carbon from *Spartina alterniflora* Loisel in a Georgia salt marsh.

Topliss, B. J., Spectral variations in upwelling radiant intensity in turbid coastal waters.

Wolanski, E., An evaporation-driven salinity maximum zone in Australian tropical estuaries.

Degobbis, D., Homme-Maslowska, E., Orio, A. A., Donazzolo, R. and **Pavoni, B.,** The role of alkaline phosphatase in the sediments of Venice Lagoon on nutrient regeneration.

Uncles, R. J., Elliott, R. C. A. and **Weston, S. A.,** Observed and computed lateral circulation patterns in a partly mixed estuary.

Published by Academic Press, Inc. (London) Limited
in association with the Estuarine and Brackish-water Sciences Association

ORDER FORM

ESTUARINE, COASTAL AND SHELF SCIENCE

Publication: Monthly
Subscription: Volumes 22-23, 1986, $315.00

To: Journal Marketing Department,
Academic Press, Inc. (London) Ltd.,
24-28 Oval Road,
London NW1 7DX

or to: Journal Promotion Department,
Academic Press, Inc.,
1250 Sixth Avenue,
San Diego, CA 92101, U.S.A.

Please send me:
A free sample copy ☐
Subscription details ☐
Instructions to Authors ☐

NAME .... ADDRESS ....

....

.... DATE ....

ACADEMIC PRESS

Harcourt Brace Jovanovich, Publishers

London Orlando San Diego New York Austin Boston Sydney Tokyo Toronto

Canadian Journal of Fisheries and Aquatic Sciences

Journal canadien des sciences halieutiques et aquatiques

Volume 43, No. 9, September 1986 **Volume 43, nº 9, septembre 1986**

Articles

A general multivariate dose–response model J. Schnute and J. O. T. Jensen **1684–1693**

Assessing juvenile salmonid response to gas supersaturation using a general multivariate dose–response model J. O. T. Jensen, J. Schnute, and D. F. Alderdice **1694–1709**

Functional maturity and terminal molt of male snow crab, *Chionoecetes opilio* G. Y. Conan and M. Comeau **1710–1719**

Food limitation of larval dragonflies: a field test of spacing behaviour R. L. Baker **1720–1725**

Zinc and cadmium transport by the vertically migrating opossum shrimp, *Mysis relicta* J. A. Van Duyn-Henderson and D. C. Lasenby **1726–1732**

Dynamics of unexploited and lightly exploited populations of rainbow trout (*Salmo gairdneri*) from coastal, montane, and subalpine lakes in western Canada D. B. Donald and D. J. Alger **1733–1741**

Functional regression and correlation analysis A. L. Jensen **1742–1745**

Dependence of exploitation rates for maximum yield and stock collapse on age and sex structure of chinook salmon (*Oncorhynchus tshawytscha*) stocks D. G. Hankin and M. C. Healey **1746–1759**

Apex predation by yellowfin tuna (*Thunnus albacares*): independent estimates from gastric evacuation and stomach contents, bioenergetics, and cesium concentrations R. J. Olson and C. H. Boggs **1760–1775**

Application of dual-beam acoustic survey techniques to limnetic populations of juvenile sockeye salmon (*Oncorhynchus nerka*) J. J. Burczynski and R. L. Johnson **1776–1788**

Plankton size spectra in relation to ecosystem productivity, size, and perturbation W. G. Sprules and M. Munawar **1789–1794**

Hypersaline gradients in two Canadian High Arctic lakes K. M. Stewart and R. F. Platford **1795–1803**

Analysis of the phytoplankton composition of 95 Labrador lakes, with special reference to natural and anthropogenic acidification J. C. Earle, H. C. Duthie, and D. A. Scruton **1804–1811**

Three-dimensional distribution of winter stonefly nymphs, *Allocapnia pygmaea*, within the substrate of a southern Ontario river C. W. Pugsley and H. B. N. Hynes **1812–1817**

Notes

Relationships between stream and intragravel temperatures in coastal drainages, and some implications for fisheries workers B. G. Shepherd, G. F. Hartman, and W. J. Wilson **1818–1822**

Announcements / Avis **1823**

Coming next month / À paraître le mois prochain **1824–1825**

(continued inside back)

©Minister of Supply and Services Canada 1986
Ministre des Approvisionnements et Services Canada 1986

CJFSDX43(9) 1683–1825 (1986)
ISSN 0706-652X

Subscription rates / Abonnements

Canada: Institutional / Collectif $150; Personal / Personnel $50
Other countries / Autres pays: Institutional / Collectif $180; Personal / Personnel $60
Single issue / Par numéro: $11.95 (Canada); $14.35 (Other countries / Autres pays)